The Biomechanical and Biological Pathways of Tibiofemoral Focal Cartilage Defect Pathogenesis and Shortfalls of Microfracture Surgery

Thesis submitted in fulfilment of the requirement for the degree of Doctor of Philosophy in Biomedical Engineering

Nidal Khatib

School of Engineering - Cardiff University

UK

October 2018

DECLARATION AND STATEMENTS

DECLARATION

This work has not previously been accepted in substance for any degree and is not concurrently submitted in candidature for any degree.

Signed …….. (**Nidal Khatib**) Date……..

STATEMENT 1

This thesis is being submitted in partial fulfilment of the requirements for the degree of Doctor of Philosophy (PhD).

Signed …….. (**Nidal Khatib**) Date……..

STATEMENT 2

This thesis is the result of my own independent work/investigation, except where otherwise stated. Other sources are acknowledged by explicit references.

Signed …….. (**Nidal Khatib**) Date……..

STATEMENT 3

I hereby give consent for my thesis, if accepted, to be available for photocopying and inter-library loan, and for the title and summary to be made available to outside organisations.

Signed …….. (**Nidal Khatib**) Date……..

ABSTRACT

Tibiofemoral focal cartilage defects (FCDs) are lesions of the smooth articular surface of the knee caused by maladaptive overload and predispose the knee to osteoarthritis (OA), a major clinical issue. However, the pathways involved in their pathophysiology and progression, particularly in humans, are not well understood. It is clinically useful to characterise this since the outcomes of conventional treatments such as microfracture surgery which aim to repair the lost or damaged cartilage are heterogeneous and less than adequate. This study investigates mechanical and biological pathways of FCD pathogenesis that could be useful in the development of comprehensive treatment strategies, as well as to address the shortfalls of microfracture surgery.

Lower limb biomechanical and neuromuscular function was investigated using gait analysis techniques including 3D motion capture analysis, electromyography and principal component analysis of waveforms in a cohort of tibiofemoral medial and lateral compartment FCD subjects relative to healthy control subjects during the performance of level gait. Both medial and lateral knee FCD subjects exhibited biomechanical indicators of increased dynamic loading of the respective affected knee compartment, which was concomitant with dynamic frontal plane knee malalignment. A proportion of FCD subjects, notably medial knee affected types presented adaptive biomechanical gait strategies reflective of pain avoidance that appears to be related to loading of the chondral defect site during gait. Differences in the activation of lower limb muscles during gait was also found, most prominently in medial FCD subjects who abnormally co-contracted their thigh muscles during load bearing, reflective of compensation for knee instability. Longitudinal assessment of biomechanical and neuromuscular function was also carried out six-months following microfracture surgery, which revealed heterogeneous functional outcomes that were independent of subject-perceived outcomes (reduced pain, symptoms and increased functional ability). Some improvement in function was experienced by lateral knee FCD subjects, in contrast to overall worsening function in medial FCD subjects.

A total of seventeen biomarkers of bone remodelling, cartilage degradation, bone mechanical loading and inflammation were examined using immunoassays in knee FCD synovial fluid and serum samples relative to knee OA and healthy control samples, respectively. Many synovial fluid biomarkers were reflected poorly in serum, however high levels of bone resorption (CTX-I) and glutamate were found in FCD serum relative to controls, as well as decreasing anti-inflammatory cytokine IL-10 levels concomitant with advancing disease state (i.e. control > FCD > OA). In synovial fluid analysis, inflammatory dysregulation (increased IL-6 and IL-8 and decreased IL-10 and IL-13) and high osteoprotegerin (OPG) levels were found in OA relative to FCD subject joint fluids. Discrete principal component analysis identified distinct phenotypes of FCD and OA fluids relating to sclerostin and anti-inflammatory cytokine levels. Furthermore, follow-up analysis of serum biomarkers six-months following microfracture surgery revealed decreased CTX-I and glutamate, as well as increased anti-inflammatory cytokine levels associated with positive patient-reported outcomes, in contrast to decreased IL-10 and IFN-γ with negative reported outcomes.

Finally, associations between biomechanical indicators of altered knee biomechanical loading and synovial fluid biomarkers relating to previous objectives were explored in FCD and OA subjects, whilst controlling for demographic factors. The magnitude of knee peak loading, cumulative loading or degree of knee malalignment significantly predicted pro-inflammatory cytokine and bone resorption activity when combining FCD and OA data. However, in FCD knees alone, dynamic joint malalignment associated with increased bone remodelling (CTX-I and ALP). Furthermore, discrete PCA identified high knee loaders from each group that were associated with high pro-inflammatory activity, increased osteoclast activation (RANKL-OPG) and reduced symptoms.

This study provides new evidence of aberrant biomechanical and biological factors associated with FCD pathogenesis and progression, as well as the association between them, that improves our understanding of the heterogeneity of the condition and outcomes to microfracture surgery. The failure of microfracture surgery to address functional and biological deficiencies in some subjects is a critical factor that needs to be addressed in future areas of treatment for optimum outcomes.

ACKNOWLEDGEMENTS

First and foremost, I would like to express my sincere gratitude to my supervisors, Prof Cathy Holt and Dr Deborah Mason, for giving me the opportunity to embark on this exciting project and providing me with invaluable technical and emotional support throughout. My curiosity, developing interest and knowledge in our research field has been driven by their enthusiasm and constructive supervision.

I consider myself very lucky to have worked with such an engaging multidisciplinary research team of whom became close friends and companions during my time at Cardiff. A special thanks to David Williams, Dr Paul Biggs, Sam Woodgate, Dr Philippa Jones, Dr Wayne Ayre, Dr Aseel Ghazwan, Dr Cleo Bonnet and Dr Sophie Gilbert, who made it feel like not a single challenge was tackled alone as they selflessly gave up their time to help with the research and retaining my sanity through this journey.

My appreciation goes to the funders, Cardiff University, the Sêr Cymru National Research Network for Advanced Engineering and Materials, as well as Hospital Innovations our industrial collaborator, who rescued this project during early issues with funding and thus without I wouldn't be submitting this thesis today. I am also indebted to the support of the Arthritis Research UK Centre for providing a strong interdisciplinary network of fellow researchers, as well as the clinical liaison at the Cardiff & Vale Orthopaedic Centre, particularly Mr Christopher Wilson, Mr Rhys Williams, Cheryl Cleary and Jessica Whiteman for their instrumental support with patient recruitment.

Finally, a massive thank you to my incredible family and partner, Kirsty Griffiths, who were patient during my absence in writing this thesis and who shared unconditional joy, love and warmth that has kept me afloat in the most difficult times.

Table of Contents

LIST OF ABBREVIATIONS

µCT	micro-Computed Tomography
3D	Three Dimensional
ACI	Autologous Chondrocyte Implantation
ACL	Anterior Cruciate Ligament
ADAMTS	A Disintegrin and Metalloproteinase with a Thrombospondin Type 1 motif
ADP	Adenosine diphosphate
AIA	Antigen Induced Arthritis
ALP	Alkaline Phosphatase
AMPA	α-amino-3-hydroxyl-5-methyl-4-isoxazoleproprionic acid
AMPK	AMP-activated protein kinase
ANCOVA	Analysis of Covariance
ANOVA	Analysis of Variance
AP-5	DL-2-Amino-5-phosphonopentanoic acid
ARUK BBC	Arthritis Research UK Biomechanics & Bioengineering Centre
ATP	Adenosine Triphosphate
BCAAs	Branched-Chain Amino Acids
BD	Becton Dickinson
BIOSI	School of Biosciences
BMI	Body Mass Index
BML	Bone Marrow Lesions
BM-MSCs	Bone Marrow-Mesenchymal Stem Cells
BMP-2	Bone Morphogenic Protein-2
BMP-6	Bone Morphogenic Protein-6
BSA	Bovine Serum Albumin
Ca^{2+}	Calcium
CAVOC	Cardiff and Vale Orthopaedic Centre
cbfa1	core-binding factor subunit alpha-1
CD40L	Cluster of Differentiation 40
CHECK	Cohort Hip and Cohort Knee
CoM	Centre of Mass
COMP	Cartilage Oligomeric Matrix Protein
CoP	Centre of Pressure
COX-2	Cyclo-oxygenase-2
CTX-I	C-telopeptide of Type-I Collagen
CTX-II	C-telopeptide of Type-II Collagen
CV	Coefficient of Variance
CXCLR1	Chemokine (C-X-C motif) ligand receptor 1
CXCLR2	Chemokine (C-X-C motif) ligand receptor 2
DNA	Deoxyribonucleic Acid

E2	Estradiol
EAATs	Excitatory Amino Acid Transporter
ECM	Extracellular Matrix
EDTA	Ethylenediaminetetraacetic acid
ELISAs	Enzyme-Linked Immunosorbent Assay
EMG	Electromyography
ERK-1/2	Extracellular signal-Regulated Kinase 1/2
FCD	Focal Cartilage Defect
F_{cir}	Tensile hoop stress
FN-f	Fibronectin fragments
F_{rad}	Radial reaction force
GCS	Global Co-ordinate System
GLAST	Glutamate Aspartate Transporter
GluR	Glutamate Receptor
GM-CSF	Granulocyte-macrophage colony-stimulating factor
GRF	Ground Reaction Force
HA	Hyaluronic Acid
HAM	Hip Adduction Moment
HCA	Hierarchical Cluster Analysis
HKA	Hip-Knee-Angle
HMDB	Human Metabolome Database
HOCI	Hypochlorous Acid
HSP70	Heat-Shock Protein 70
HTO	High Tibial Osteotomy
IFN-γ	Interferon-gamma
iGluR	ionotropic Glutamate Receptor
IkB-1/2	Inhibitor of kinase B-1/2
IL-10	Interleukin-10
IL-12p70	Interleukin-12p70
IL-13	Interleukin-13
IL-1β	Interleukin-1-beta
IL-2	Interleukin-2
IL-4	Interleukin-4
IL-6	Interleukin-6
IL-8	Interleukin-8
iNOS	Nitric Oxide Synthase
IR	Infra-Red
ISB	International Society of Biomechanics
JAK	Janus Kinases
JNK	c-Jun N-terminal kinases
JSN	Joint Space Narrowing
KA	Kainate
KAA	Knee Adduction Angle
KAAI	Knee Adduction Angular Impulse
KAM	Knee Adduction Moment

KANON	Knee Anterior Cruciate Ligament, Non-surgical versus Surgical Treatment
KFA	Knee Flexion Angle
KICK	Knee Injury Cohort at the Kennedy
KL	Kellgren-Lawrence
KOOS	Knee Osteoarthritis Outcome Survey
LCL	Lateral Collateral Ligament
LRP5/6	Low-density lipoprotein receptor-related protein 5
MAPK	Mitogen-activated Protein Kinase
MCL	Medial Collateral Ligament
mGluRs	metabotropic Glutamate Receptor
MK-801	Dizocilpine
MMP	Matrix Metalloproteinase
MMP-3	Matrix Metalloproteinase-3
MRI	Magnetic Resonance Imaging
mRNA	messenger Ribonucleic Acid
MSD	Mesoscale Discovery
mTOR	mechanistic Target Of Rapamycin
mV	millivolts
NBQX	2,3-dihydroxy-6-Nitro-7-sulfamoyl-Benzo-Quinoxaline
NF-κB	Nuclear Factor Kappa-light-chain enhancer of activated B cells
NHS	National Health Service
NMDA	N-methyl-D-aspartate
NMDAR	N-methyl-D-aspartate Receptor
NO	Nitric Oxide
NRN	National Research Network
NSAID	Non-Steroidal Anti-Inflammatory Drug
OA	Osteoarthritis
OARSI	Osteoarthritis Research Society International
OPG	Osteoprotegerin
P13-L/Akt	Phosphoinositide 3-kinase
PBS	Phosphate Buffered Saline
PC	Principle Component
PCA	Principal Component Analysis
PGE_2	Prostoglandins E2
PLS	Partial Least Squares
PPR	Pathophysiology and Repair
PTOA	Post Traumatic Osteoarthritis
RA	Rheumatoid Arthritis
RANKL	Receptor Activator of Nuclear Factor Kappa-B ligand
RelA	transcription factor p65
RNA	Ribonucleic Acid
ROS	Reactive Oxygen Species
Runx2	Runt-related transcription factor 2
SD	Standard Deviation

SENIAM	Surface Electromyography for the Non-Invasive Assessment of Muscles
SF	Synovial Fluid
SIRT-1	Sirtuin 1
SMURF1	Specific E3 Ubiquitin Protein Ligase 1
SMURF2	Specific E3 Ubiquitin Protein Ligase 2
SNR	Signal-to-Noise Ratio
SOST	Sclerostin
sPINP	serum Procollagen type I N Propeptide
STAT	Signal Transducer and Activator of Transcription
TIMP	Tissue Inhibitor of Metalloproteinase
TKR	Total Knee Replacement
TNF-α	Tumor Necrosis Factor-alpha
TSG-6	TNF-stimulated gene 6 protein
TTL	Totem-pole
uNTX-1	urinary N-terminal telopeptide
uOA	unilateral OA
VGLUTs	Vesicular Glutamate Transporters
VGSCs	Voltage-Gate Sodium Channel
Wnt	Wingless/Integrated
α5β1	fibronectin receptor

Chapter 1

Introduction and Background

Motivation

With the ever-increasing age population of our world, degenerative knee diseases such as osteoarthritis (OA) are becoming increasingly relevant. Joint arthritis conditions are collectively the most common causes of long-term disability, with OA affecting 15% people worldwide and accounting for 2.4% of all years lived with disability worldwide, affecting at least 242 million people of multiple at-risk groups including the elderly, sedentary or athletic lifestyle types (Osteoarthritis Research Society International White Paper, 2016). The cause or set of causes of OA are complex and mounting evidence has suggested that OA is best described as a set of diseases at varying stages with distinct etiologic characteristics that have a common end-point, that is, total joint dysfunction and the requirement for knee replacement surgery (Dell'Isola et al., 2016, Driban et al., 2010). Identifying and characterising at-risk groups of etiological phenotypes may improve our ability to prevent or treat individuals predisposed to OA, to lower the clinical burden the end-stage of disease has on our healthcare systems and population quality of life.

Focal cartilage defects (FCDs) of the knee are a degenerative condition defined as chondral lesions of the articulating cartilage surface, which predispose the joint to OA in their natural course (Brittberg et al., 1994, Spahn and Hofmann, 2014, Davies-Tuck et al., 2008b). Unlike with knee OA, the cause of FCDs can most likely be attributed to mechanical insult of joint tissues, whether it be an injury or prolonged overload, due to the focal nature of the cartilage damage typically found in the tibiofemoral weight-bearing region of the knee. However, very little is understood about the progressive mechanisms of FCD pathogenesis, which is concerning, since it has been shown approximately 30% of individuals that bear them go on to require knee replacements within 10 years (Spahn and Hofmann, 2014). FCDs are conventionally treated with cartilage repair techniques such as microfracture surgery and autologous chondrocyte implantation (ACI) which aim to halt chondral damage progression by replacing lost cartilage. However long-term outcomes are poor since many go on to require revision surgery and total knee replacements (Knutsen et al., 2016, Solheim et al., 2016).

The poor outcomes of treatment may be related to the complex and multiscale pathology of knee degenerative conditions such as FCDs and OA, which involves mechanical (e.g. joint overloading), biological (e.g. joint inflammation) and structural (e.g. bone remodelling) pathways (Andriacchi and Favre, 2014). Knee OA gait analysis studies have importantly evidenced the altered knee loading patterns resultant of aberrant lower

limb biomechanical function that correlate with disease progression (Felson, 2013). Whereas clinical OA studies have identified changes in biomarker concentrations reflective of dysregulated homeostatic mechanisms and cell metabolism in the joint (Kraus et al., 2017, Mobasheri et al., 2017, Attur et al., 2013). Although crucial advances have been made in elucidating these pathways in patients with established OA, there is a deficit of evidence characterising them in individuals with symptomatic FCDs at risk of OA development. Advancing our knowledge of aberrant knee biomechanics and tissue biology in individuals with symptomatic FCDs, as well as the poorly understood association between them, may reveal new pathways of disease and improve our approach to treatment strategies. Furthermore, identification of diagnostic and prognostic markers of FCD presence and progression could be useful in the comparison of the increasing number of conventional and future treatments, to aid clinical decision making for the most effective treatment choices.

This PhD studentship was funded by the Sêr Cymru National Research Network (NRN) for Advanced Engineering and Materials, Cardiff University and our collaborating industrial partner Hospital Innovations, an orthopaedic product specialist and distributer. One of the goals from this studentship was to bridge the gap between bench and bedside, by working alongside researchers, clinicians and industrial collaborators and sharing information with the collective goal of solving translational research needs of the engineering discipline. Secondly, to take a multidisciplinary approach to the research challenge by working across the Cardiff University Schools of Engineering and Biosciences which permitted access to interdisciplinary facilities, alongside the Arthritis Research UK Biomechanics and Bioengineering centre (ARUK BBC) and Cardiff & Vale Orthopaedic Centre (CAVOC) which provided access to clinical liaison, NHS patients and data required to carry out this research project.

1.1 Aims and Objectives

This PhD thesis aims to advance our understanding of the characteristic features and etiologic factors of progressive knee FCDs, as well as the shortfalls of current surgical practice, such as microfracture surgery, to aid clinical decision making in the choice of effective treatments.

The body of work intends to achieve this by satisfying three overarching objectives:

Objective 1 (Chapter 3) - *To identify biomechanical and neuromuscular pathways of tibiofemoral FCD pathogenesis in patients and assess longitudinal functional outcomes of microfracture surgery*

Chapter 3 utilises 3D motion analysis combined with electromyography techniques to identify the pathomechanic features of tibiofemoral FCD lower limb function by cross-sectional comparison to healthy function. Secondly, to assess functional outcomes of microfracture surgery that could reveal mechanical pathways of long-term failure and generate predictive functional markers of positive or poor outcomes. Finally, to identify knee FCD functional groups which exhibit distinct biomechanical and neuromuscular characteristics that may benefit from targeted intervention.

Objective 2 (Chapter 4) - *To identify biological pathways and biomarkers of tibiofemoral FCD pathogenesis and outcomes by investigating molecules relating to OA pathology in synovial fluid and serum of tibiofemoral FCD subjects undergoing microfracture surgery*

Chapter 4 firstly utilizes immunoassays to quantify and compare a range of biomarkers associated with bone and cartilage remodelling, degradation, mechano-biology and inflammation in synovial fluid and serum of tibiofemoral FCD subjects relative to established OA and control groups (respectively), to reveal biological pathways and biomarkers of pathogenesis. Secondly, to investigate longitudinal changes and biomarker patterns reflective of positive or poor outcomes of microfracture surgery, which may be informative of long-term failure mechanisms. Finally, to investigate inter- and intra-disease group variances by combining linear combinations of biomarkers, to identify phenotypic groups that may benefit from targeted therapy.

Objective 3 (Chapter 5) - *To characterise the effect of altered knee mechanical loading on joint biology in tibiofemoral FCD and OA pathogenesis*

Chapter 5 explores the association between indicators of altered tibiofemoral FCD and OA knee biomechanical loading and synovial fluid biomarkers relating to previous objectives, to elucidate mechanisms of pathogenesis and progression as well as address the shortfalls of microfracture surgery.

1.2 Background and Literature Review

1.2.1 Function of articular tissues of the knee joint

The human knee joint is a complex structure whose function is to permit smooth and stable ambulation, whilst efficiently managing up to 3.5 times body weight on a day-to-day basis (Kutzner et al., 2010). In order to achieve this, the musculoskeletal tissue that comprises the knee joint is highly adapted to ensure longevity of the joint through a lifetime of mechanical insult (MacKinnon, 2005).

Osteochondral tissue found on the femoral, tibial and patellar surfaces are one set of structures that are organised to deal with transmission of high stresses and strains (Ulrich-Vinther et al., 2003). Cartilage is made up of a series of extracellular matrix (ECM) layers, which are differentiated by the alignment of type-II collagen fibres, aggrecans and cartilage cells (chondrocytes) throughout the tissue (Figure 1.2-1). These elements are organised to direct the force across the entire surface area of the contact regions between the femur and tibia, thus reducing focal areas of stress (MacKinnon, 2005). The surface is composed of hyaline cartilage, a very low friction gliding surface aided by the lubrication of synovial fluid to maximally reduce wear. This is a crucial property due to the avascular nature of cartilage, resulting in slow tissue turnover rates and very limited regenerating potential. Its hydrophilic properties aided by the high abundance of embedded proteoglycans gives cartilage its viscoelasticity, and therefore it's shock absorbing properties (Ulrich-Vinther et al., 2003).

Beyond the deeper regions of cartilage approaching bone resides the calcified cartilage – a stiffer tissue found to be a compromise between bone and cartilage which permits a smooth transition of the load between these tissues of very different mechanical and biochemical properties. Finally, the subchondral bone; a dense plate of high trabecular bone volume which lines the ends of bones, separating and protecting the mechanically inferior cancellous bone from joint stresses (MacKinnon, 2005). Subchondral bone consists of mineralised matrix, composed of predominantly of type-I collagen fibres,

hydroxyapatite, calcium and phosphate with embedded bone cells, including osteocytes within in the matrix and osteoblasts and osteoclasts on the surfaces.

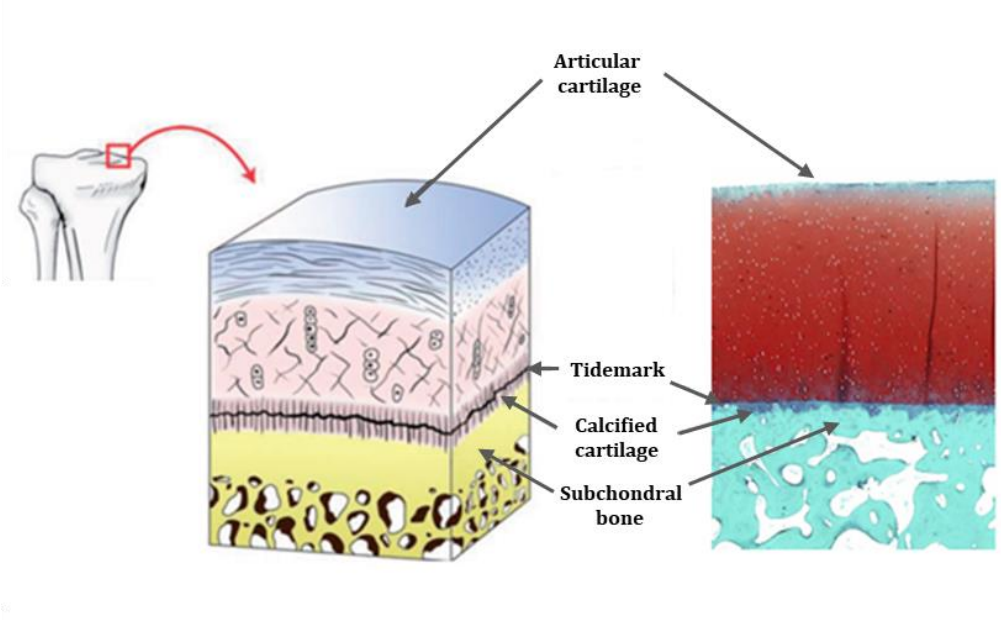

Figure 1.2-1 - Illustration (left) and histological cross-section (right) of the osteochondral interface at the joint surface.

The knee is stabilized by several structures that permit constrained articulation of the joint to provide stability. Of those are ligaments, which are comprised of bundles of dense connective tissues of collagenous fibres and sheaths (Flandry and Hommel, 2011). There are four major ligaments, the anterior and posterior cruciate ligaments (ACL and PCL), and the medial and lateral collateral ligaments (MCL and LCL), as well as capsular ligaments that line the joint capsule. In addition to preventing unwanted rotation of the joint, they add to the important proprioceptive function of joint tissues, generating feedback in response to strain that allow identification of knee position (Frank, 2004). The menisci are two 'horse-shoe' shaped tissues also involved in knee stability, guiding the rotation of the femur over the tibia during articulation. However, the primary role of the menisci involves the dispersion of joint loads across the wide surface of the knee to aid cartilaginous structures in reducing focal forces (Makris et al., 2011, Buckwalter and Mankin, 1998).

1.2.1 Knee osteoarthritis

Knee osteoarthritis (OA) is a multifactorial degenerative whole-joint disease in which the function of the knee is impaired, due to degradation of articular cartilage in the joint that protects the underlying subchondral bone, from intra-articular inflammation, bone marrow lesions, and changes in peri-articular subchondral bone (Goldring and Goldring, 2007). These physiological changes result in debilitating symptoms such as acute and chronic knee pain, swelling and stiffening of the joint, consequently resulting in complete knee dysfunction and reduced quality of life. In the UK, around 18.2% over the age of 45 years are currently affected with osteoarthritis (OA), a major clinical issue and burden on the NHS (Arthritis Research UK, 2017).

OA is classically diagnosed using weight-bearing radiographs of the knee with identification of characteristic features including joint space narrowing (JSN), osteophyte lipping, sclerosis and bony deformations (Figure 1.2-2).

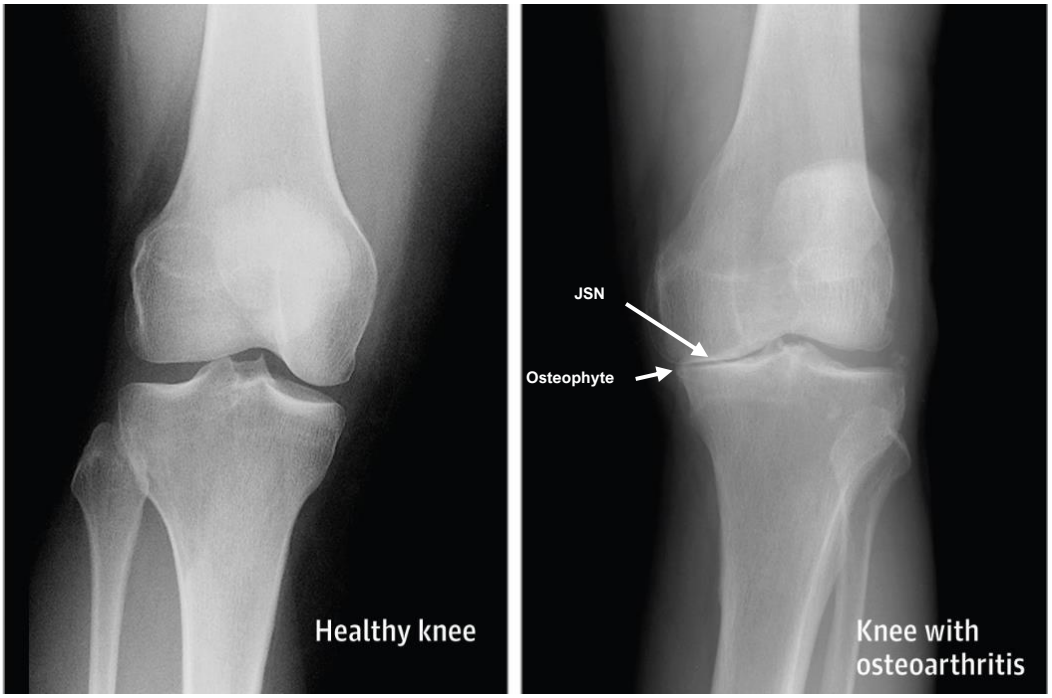

Figure 1.2-2 - Weight-bearing radiograph of healthy knee and OA knee with joint space narrowing (JSN) and osteophyte lipping

Once known as 'wear and tear' arthritis due to its high prevalence in the overused joint, we now understand that a there is large range of risk factors that lead to the initiation and progression of OA; blunt trauma from injury, malalignment of the mechanical joint axis, simple overuse of the joint, as well as morphological abnormalities resultant of genetic traits are some of the causes commonly reported (Goldring and Goldring, 2007,

Loeser et al., 2012). OA is referred to as the 'silent disease', as it is often the case that accumulating musculoskeletal derangements can occur undetected until the damage become irreversible. This is primarily because cartilage is not innervated, thus affected subjects experience very limited or intermittent pain in the early stages which permits damage to progress unattended (Ulrich-Vinther et al., 2003, Heijink et al., 2012). It appears that only when other factors such as acute joint inflammation or exposure of subchondral bone due to excessive loss of cartilage occurs, that severe pain is experienced, which for a large number of cases is only experienced towards the irrevocable end stage of the disease.

There are multiple available treatments for relieving OA, however the current gold standard treatment for 'end-stage' OA is total knee replacement (TKR) surgery or knee arthroplasty– a costly, non-tissue preserving, invasive and joint altering procedure, which requires months of post-operative recovery and rehabilitation with unsatisfying outcomes (Goldring and Goldring, 2007). Furthermore, the survival rate for TKR implants appears to decline rapidly beyond 10 years due to implant loosening, wearing, reoccurring inflammation and pain, which means they are only appropriate for the older population if the increasingly destructive revision surgeries are to be avoided (Murray et al., 1993, Civinini et al., 2017). When projecting forwards from historical data in the US alone, the demand for TKRs is expected to grow by 673% by the year 2030 due to our increasing age population, therefore there is a demand for newer advancements for screening, diagnosing and preventing this condition from an earlier stage (Kurtz et al., 2007). Identifying and characterising at-risk groups of etiological phenotypes may improve our ability to prevent or treat individuals predisposed to OA, to lower the clinical burden the end-stage of disease has on our healthcare systems and population quality of life.

1.2.1 Knee focal cartilage defects

FCDs are defined as focal loss of the smooth articular cartilage that spans the femoral condyle, tibial plateau or patella, often associated with OA-like symptoms including acute joint pain during weight-bearing activities, joint stiffening and inflammation (Spahn and Hofmann, 2014, Heir et al., 2010). The presence of FCDs is concomitant with tissue damage all the way down to the underlying subchondral bone, evident by their associations with bone marrow lesions detected by magnetic resonance imaging (Dore et al., 2010, Muratovic et al., 2016). However, the clinical definitions which involve grading systems for FCDs are more representative of the degree of visible chondral damage in the joint (Lasmar et al., 2011). The general consensus is that visible damage down to, but not breaching subchondral bone is referred to as a cartilage defect, whereas additional visible degradation (loss) of subchondral bone tissue is referred to as an osteochondral defect (Bhosale and Richardson, 2008, Davies-Tuck et al., 2008b). There are several clinical grading systems used clinically to define FCD stage, which are used as a guide for clinical decision making as the most appropriate choice of treatment. Of them, the Outerbridge system (Figure 1.2-3) is most commonly used today (Slattery and Kweon, 2018).

Outerbridge grade 0 – normal articular cartilage

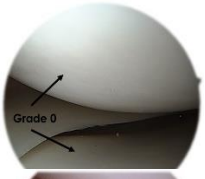

Outerbridge grade I – articular cartilage with softening and swelling

Outerbridge grade II – partial-thickness articular cartilage defect with fissures on the surface that do not breach subchondral bone or exceed 1.5cm in diameter

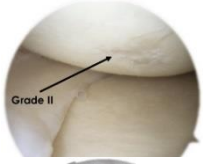

Outerbridge grade III – articular cartilage fissuring to the level of subchondral bone in an area with a diameter more than 1.5cm

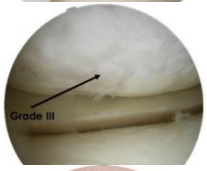

Outerbridge grade IV – articular cartilage with exposed subchondral bone

Figure 1.2-3: Outerbridge grading system (Slattery and Kweon, 2018, Lasmar et al., 2011).

The knee FCD population is heterogeneous. Chondral damage is found on either the medial or lateral compartment of the knee, in weight-bearing or non-weight bearing regions and appears to be etiologically diverse. However, a common ground of their presence is their relation to an event or set of events relating to mechanical insult of the joint. Such events can include blunt trauma (such as a sporting injury), repetitive increased loading (obesity, marathon running) or ageing of the joint cartilage (Davies-Tuck et al., 2008b, Magnussen et al., 2008). This is particularly the case in joint injury subjects, where the site of the lesion is often reflective of the injury that has taken place (Mithoefer et al., 2006). Although these risk factors may be related to their initial induction, they are not necessarily explanatory of their long-term pathogenesis or natural progression in severity and size, since this seems to occur inconsistently

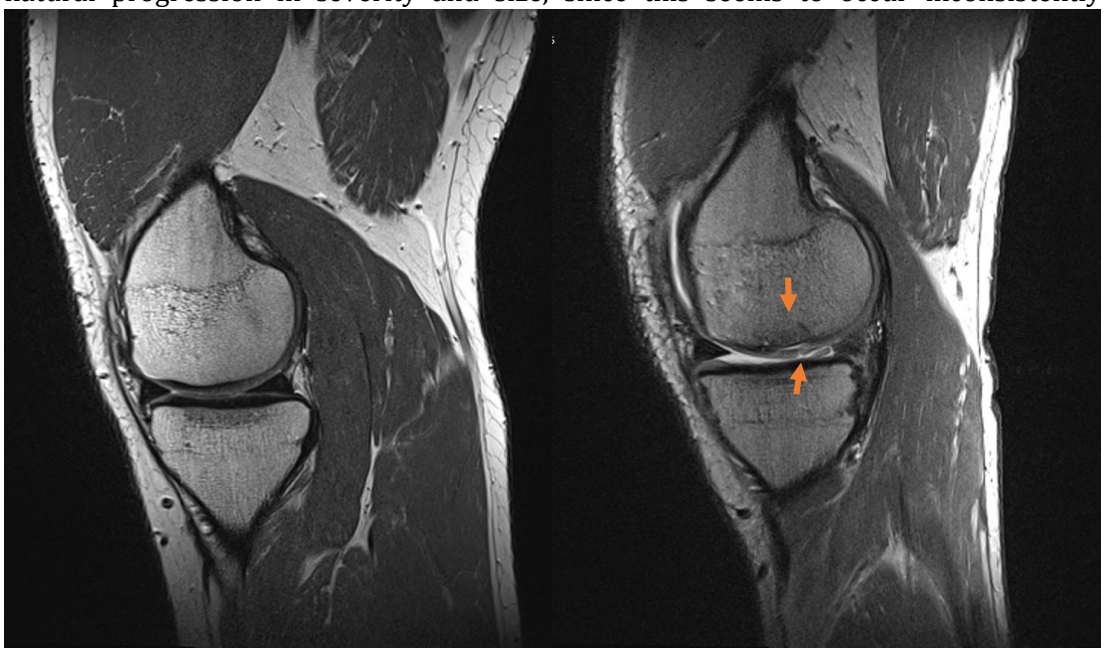

Figure 1.2-4 – Turbo Spin Echo (TSE) Magnetic Resonance Imaging (MRI) scan of a healthy knee (left) and a typical tibiofemoral Outerbridge grade III knee FCD of a subject from this thesis (right).

throughout the affected population (Tetteh et al., 2012, Spahn and Hofmann, 2014).

In longitudinal studies of FCD progression in the joint using MRI methods (Figure 1.2-4), it is found that they progress in severity. One study of 84 subjects with medial and lateral tibiofemoral or patellofemoral FCDs revealed between 38-70% of the population experienced increased Outerbridge cartilage defect scores over two years, whereas 27-46% experienced no change at all, and 2-18% showed regression of the defect score (Wang et al., 2006). Although age, gender, BMI, physical activity, bone size and baseline cartilage defect score were all tested for associations with progression/regression of lesions, only baseline score was found to be associated. In another similar study

investigating the same factors in 117 subjects over the course of two years, it was found that 81% of FCDs progressed at any site in the knee, 15% remained stable and 4% decreased, which appeared to associate with bone size and increasing age (Davies-Tuck et al., 2008b). The clear heterogeneous long-term pathogenesis of FCDs infers that more complex underlying pathways exist that introduce risk to the population, which may not always be explained by demographics and lifestyle characteristics alone.

It is uncommon that knee FCDs exist in isolation of other knee co-morbidities. In large multicentre study of 684 males and 80 females investigating the presence of focal lesions in subjects who have had ACL tears, Tandogan and colleagues reported that nineteen percent of the knees had one or more chondral lesions, sixty percent of which were located in the medial tibiofemoral compartment (Tandogan et al., 2004). This association has been further substantiated by a prospective study of 541 patients undergoing ACL reconstruction, where it was found that increased time from initial ACL injury predicted the presence of meniscal tears and chondral damage in the joint (Kluczynski et al., 2013). Whereas a more recent prospective study of 764 knee injury patients showed an increased incidence of chondral defects with time since both meniscal injury and ACL injury individually (de Campos et al., 2016). Aside from articular tissues, the presence of underlying bone marrow lesions (BMLs), which are defined as focal areas of bone edema and disorganised tissue, have shown to strongly correlate with the presence and severity of FCDs (Dore et al., 2010, Muratovic et al., 2016). These findings suggest the likely involvement of knee co-morbidities in FCD pathogenesis, each of which have been suggested by others to be large risk factors for OA progression (Felson et al., 2000, Andriacchi and Favre, 2014).

The presence of knee FCDs in the joint are thought to be clinically problematic in that they may also predispose the joint to OA. Spahn and Hofmann reported that in 115 patients with isolated FCDs of the medial knee compartment, around 30% went on to undergo total knee replacement surgery within 10 years (Spahn and Hofmann, 2014). Furthermore, in a review of 374 knee compartments affected with pre-OA or OA radiographic classification, it was demonstrated that the presence of chondral or full-thickness defects in the joint appeared to significantly increase the risk of developing more focal regions of chondral damage and predicted radiographic OA severity (Guermazi et al., 2017). This evidence is suggestive that altered joint physiology of the joint involved with the presence of FCDs may be a driving factor for knee damage following FCD induction. However, the mechanisms involved in their development are

poorly understood, with very limited literature describing the suspected mechanical, biological and structural pathways involved in their pathogenesis.

1.2.1 Surgical treatment of FCDs and microfracture surgery

Surgical intervention for the treatment of knee FCDs is very common and often reported to be more effective than conservative management alone. Conservative management largely involves the use of analgesic and non-steroidal anti-inflammatory drugs (NSAIDS) to reduce pain, since currently there are no approved drugs that can prevent or even restrain progression of degenerative knee pathologies (Osteoarthritis Research Society International White Paper, 2016). Surgical intervention is usually limited to cartilage repair techniques, which aims to replace the lost cartilage on the joint surfaces (Bhosale and Richardson, 2008, Magnussen et al., 2008). These procedures are suggested to negate pain and halt progression of chondral or osteochondral progressive damage. Current strategies range from stimulating the body's own repair response, to insertion of bio-active materials intended to replicate the mechanical function of the replaced tissue (Magnussen et al., 2008, Pascual-Garrido et al., 2017). However, these strategies are not curative, but only fixative and do not restore full function of the joint (Pascual-Garrido et al., 2017).

The ideal surgical intervention for chondral injuries would restore the high weight-bearing organised hyaline-type cartilage with similar properties to the surrounding tissue. However, the two most common treatment options, microfracture and autologous chondrocyte implantation (ACI), generate fibro-cartilage, a highly disorganised and mechanically inferior tissue that lacks the biomechanical properties necessary to withstand forces surrounding the knee (Brittberg et al., 1994). This makes the neocartilage susceptible to dissociation from surrounding tissue, functional loss and mechanical deterioration, which leads to relatively high revision surgery rates (Magnussen et al., 2008, Falah et al., 2010).

Microfracture surgery, a method once referred to as 'Pridie drilling' due to its initial application by K. Pridie and G. Gordon in 1959, is a conventional surgical technique aimed at resurfacing knee chondral lesions by means of drilling into the subchondral bone to repopulate the hyaline surface with bone marrow-derived mesenchymal stem cells (BM-MSCs) and blood (Pridie and Gordon, 1959). With formation of a blood clot within the lesion and controlled weight-bearing, BM-MSCs will yield a fibrocartilage to protect the underlying subchondral bone and remaining surround cartilage from further

degeneration (Pridie and Gordon, 1959, Mithoefer, 2013). However, the long-term benefits are commonly reported to be less than desired (Magnussen et al., 2008, Falah et al., 2010). In a study of 3,498 patients undergoing microfracture surgery, 9-18% patients required revision surgery within 1 year, 18-30% within 3 years and 32-41% within 5 years. Of those, 22% went on to require total knee arthroplasties (Layton et al., 2015). These statistics importantly highlight the demand for investigating current shortfalls of cartilage repair strategies such as microfracture surgery and identification of treatment groups that may benefit from alternative treatments.

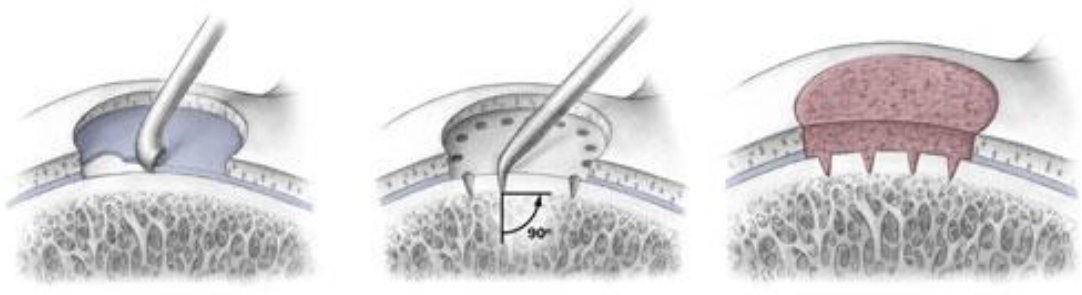

Figure 1.2-5 - Illustration of the microfracture surgical technique (Seo et al., 2011). Debridement of existing damaged cartilage (left), creation of microfractures breaching into subchondral bone to release blood and bone marrow (middle), formation of blood clot and stable fibro-cartilage tissue (right).

The heterogeneous nature of FCD pathogenesis and treatment outcomes infers that clinical groups exist that may exhibit distinct etiological or progressive mechanisms of FCD pathogenesis. Despite its evident shortcomings, microfracture surgery serves a good model for exploring the response to treatment, since it is a commonly used, repeatable procedure with limited variation in technique between surgeons (Seo et al., 2011, Pascual-Garrido et al., 2017). Furthermore, as it is a minimally invasive method, it allows exploration of the longitudinal response to cartilage repair without the major influence surgical wounds may have on the outcomes.

1.2.2 The role of mechanical loading in joint homeostasis and disease

In the healthy knee, bone and cartilage are continually adapting to load distributions in the joint by reshaping, or 'remodelling' their structures, and are dependent on physiological mechanical signals to maintain these mechanisms and retain normal tissue functions (Arokoski et al., 2000, Robling and Turner, 2009). There are a number of external mechanical signals of different origin and type (e.g. compression or shear) acting at the knee during ambulation, including structural loading generated by gravitational forces that create ground reaction forces (GRFs) in response to body weight, forces produced by contraction of muscles, strains caused by the mechanical properties of tissue structures, as well as inertial forces (Andriacchi and Muendermann, 2006). Together, these forces create the mechanical environment that tissues and cells in the joint require to remodel structures and maintain homeostatic conditions, permitting effective functioning of the knee.

In order for tissues to respond to knee forces, most cell types of the joint tissues including cartilage cells (chondrocytes), bone cells (osteocytes, osteoblasts and osteoclasts), as well as ligament fibroblasts respond to mechanical changes in their environment through signalling pathways in a process called 'mechanotransduction' (Salter et al., 2002, Liedert et al., 2006, Millward-Sadler and Salter, 2004, Robling and Turner, 2009, Sanchez-Adams et al., 2014). These cells possess the proteins necessary for transduction of mechanical signals, or 'biomechanical' signals, that act on the cell through deformation of the extracellular matrix (ECM) or shear fluid stress, including stretch-activated calcium (Ca^{2+}) channels, cadherins and integrins, which regulate homeostatic signalling processes in health and disease (Liedert et al., 2006). These proteins transmit signals through the activation of a network of intra-cellular components including enzymes and transcription factor to the nucleus, that eventually results in the expression of genes that regulate the cells adaptive behaviour (Figure 1.2-6).

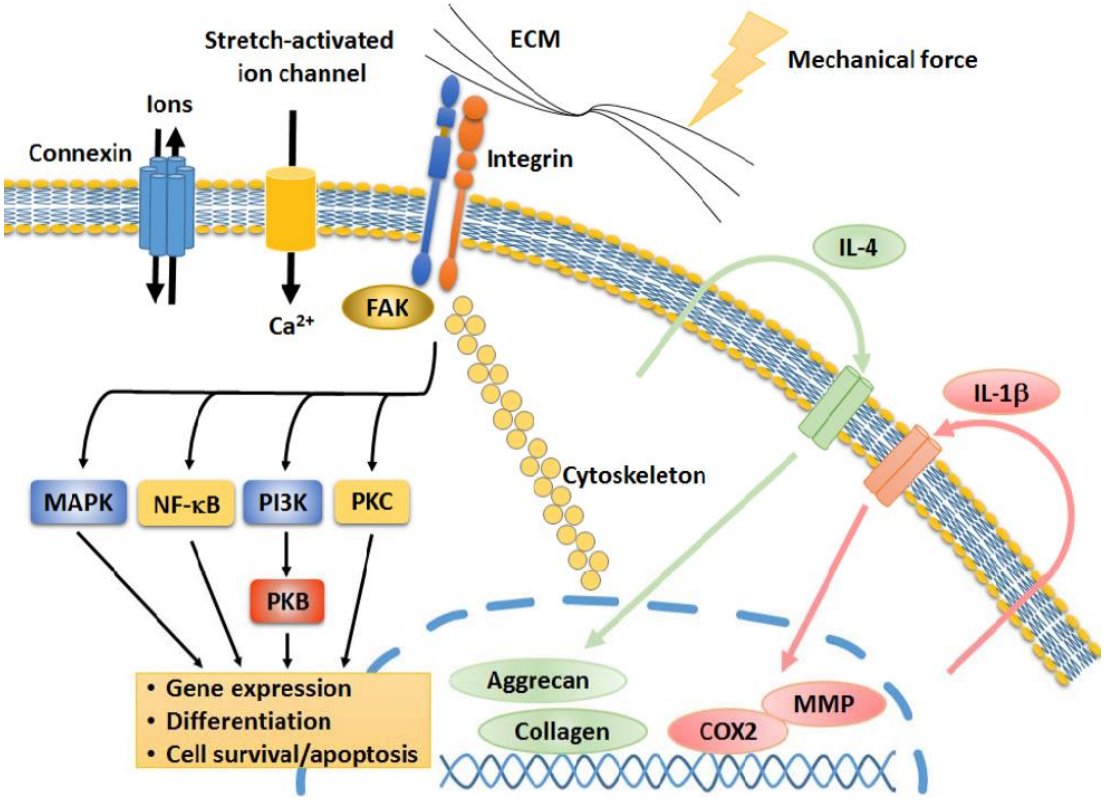

Figure 1.2-6 – Schematic depicting commonly studied mechanotransduction pathways in chondrocytes. Adapted from (Lee and Salter, 2015). External mechanical forces derived from lower limb joint loading cause deformation of the extracellular matrix (ECM), stimulating integrin, connexin, and stretch-activated ion channel mechanoreceptors at the cell surface, or intracellular cytoskeletal filaments, all of which transduce external forces into intracellular signalling pathways by activating a series of signalling molecules or permitting ions (such as calcium) to pass through the membrane. Mechanotransduction pathways include the focal adhesion kinase (FAK), mitogen-activated protein kinases (MAPK), nuclear factor kappa-light-chain-enhancer of activated B cells (NF-κB), phosphatidylinositol 3-kinase (PI3K) and protein kinace C (PKC), which act to regulate homeostatic processes through gene expression, and are responsible for cell functioning and differentiation. Interleukin-4 (IL-4) and IL-1β are auto- and paracrine inflammatory signalling cytokines which have also been shown to be regulated by integrin-dependent mechanotransduction cascade of chondrocytes and bone cells in response to mechanical stimulation. Anti-inflammatory cytokine IL-4 has beneficial effects in activating anabolic responses by upregulating expression of aggrecan and collagen, as well as inhibiting matrix metalloproteinase (MMP) expression. On the other hand, production of IL-1β, as seen in OA, stimulates a catabolic response with activation of pathways resulting in increased expression of Cyclooxygenase-2 and MMPs, resulting in tissue degradation and destruction, as well as activation of pain pathways through the production of prostaglandins E2.

In the healthy joint, it has been reported in several studies that spatial thicknesses and structural composition of cartilage and bone in the knee correspond to regions of weight-bearing (Van Rossom et al., 2017, Day et al., 2004, Andriacchi et al., 2009). It is the general

consensus that thicker and stiffer tissues are able to better manage higher loads and therefore cartilage and bone structurally adapt to suit the mechanical environment they are subjected to. Interestingly, *in vitro* studies have shown that there appears to be a physiological range of strains that leads to optimal healthy biosynthetic responses of cells, and higher or normal (pathophysiological) strains leads to abnormal cell behaviour, reflective of biological differences measures in the disease joint (Goldring and Goldring, 2007, Loeser et al., 2012, Bader et al., 2011, Buckwalter and Mankin, 1998). These studies involve 2D or 3D (e.g. hydrogel-based) cell culture systems, as well as tissue explant studies, which induce a mechanical load of a given frequency and magnitude on the cultured cells or tissues, and output in the form of molecular biomarkers or changes in the extracellular environment resultant from cell activity is measured. It has been demonstrated in chondrocyte cultures that high (0.1-1Hz) frequencies of loading and low amplitudes strains (in the range of 0.6-10.5%) results in increased proteoglycan production, whereas low frequencies showed very little biosynthetic activity (Sah et al., 1989, Thomas et al., 2011). These observations suggest that cartilage and bone become conditioned to daily cyclic load distribution patterns and as long as normal patterns are maintained, healthy joint homeostasis is maintained (Seedhom, 2006, Andriacchi et al., 2009).

It is well-recognised that in people that suffer knee injuries, damage to joint structures results in changes of the normal kinematics of the joint during ambulation (Andriacchi and Muendermann, 2006). These functional changes are considered a major risk factor for joint degeneration, since many injury patients go on to develop post-traumatic OA (PTOA), a fast progressing phenotype of degenerative disease of the knee. Furthermore, it has been shown in animal models that destabilising the joint results in structural and biological changes similar to that in progressive OA (Legrand et al., 2017, Gilbert et al., 2018). The leading consensus is that altered cyclic loading distributions and patterns of non-adapted regions of tissue due to the changed kinematics of the knee may be responsible, since measures of knee loading in humans are strongly associated with and predictors of the progression of knee damage and treatment outcomes (Felson et al., 2000).

It is also relevant to note that in most degenerative joint pathologies such as FCDs and OA, the most progressive damage is often focal in nature, typically affecting one compartment (medial or lateral side) of the knee in the weight-bearing region with little to no damage of the other (Felson, 2013, Goldring and Goldring, 2007). These progressive structural changes are concomitant with significantly elevated or decreased

levels of molecules representative of biological processes such as cartilage metabolism (breaking down and recycling of ECM components such as COMP), bone remodelling (degradation and rebuilding of new bone) and inflammation, which are in more recent years shown to be implicated in joint tissue destruction during the course of disease (Hunter et al., 2014, Kraus et al., 2017).

In vitro biological research has aimed to understand the disparity of cellular responses to physiological and pathophysiological mechanical stimulation, where it is evident that enhanced loading conditions elicit dysregulated inflammatory gene expression, aberrant activation of catabolic pathways in chondrocytes and remodelling pathways in bone cells (Goldring and Otero, 2011, Kapoor et al., 2011). Whereas animal studies have taught us through the use of post-traumatic OA (PTOA) joint destabilization models of the early initiating factors and subsequent stages post-injury, driven by both inflammation and mechanics, such as leukocyte infiltration, synovitis and tissue architectural changes that lead to eventual joint dysfunction (Scanzello, 2017, Legrand et al., 2017, Gilbert et al., 2000). Finally, human functional studies have evidenced the link between altered patterns of knee biomechanical loading and OA disease progression, which appears to be consistent with structural tissue changes detected by MRI methods (Van Rossom et al., 2017, Andriacchi and Favre, 2014). Taken together, it is clearly evident that mechanical, biological and structural pathways are involved in the pathogenesis of degenerative joint disease.

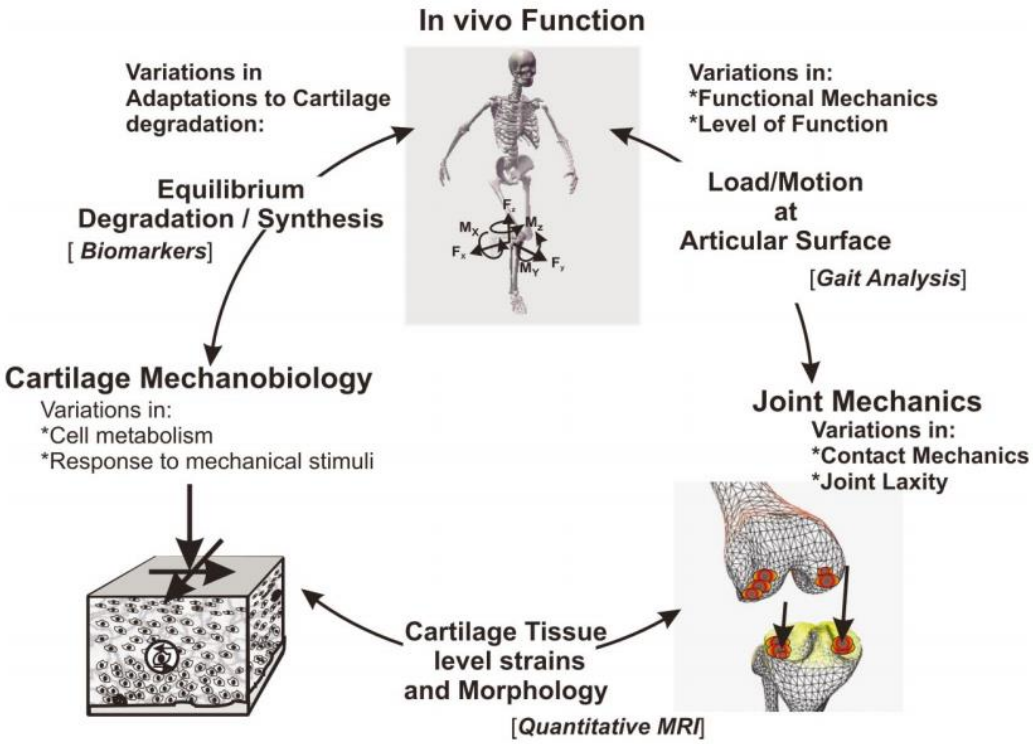

Figure 1.2-7 – The multiple considerations proposed for understanding of the adaptative and maladaptive response of joint tissues such as cartilage in health and disease (Andriacchi and Favre, 2014)

Despite these critical advances, there is very little evidence elucidating the relationship between altered biomechanical loading and aberrant biology particularly in *in vivo* studies of the human knee. A demonstration of these links would validate previous findings from *in vitro* studies and widen the scope for comprehensive therapeutic strategies to enhance the efficacy and longevity of intervention (Kraus et al., 2011). This is particularly the case for tibiofemoral FCD subjects, who as to reiterate are exposed to higher risks for developing knee OA, as well as high failure rates for current conventional treatments. Individuals with symptomatic, progressive knee FCDs are a valid human *in vivo* model for studying the link between joint loading and biology, since progressing tissue damage in the joint is unicompartmental and focal in nature. Furthermore, their incidence is highly correlated to the morbidity of tissues that provide stability of the knee during ambulation. An important focus over the course of this thesis is to further characterise mechanical and biological pathways involved in FCD pathogenesis, as well as the important link between them, to further understand the heterogeneous progression and treatment outcomes in this population.

1.2.3 The study of lower limb function in OA research

The initiation and progression of progressive joint pathologies such as knee OA have been related to the biomechanical function of the joint during ambulation (Andriacchi and Favre, 2014). There is growing evidence to suggest that functional alterations of the mechanical kinematic and loading patterns the knee is subjected to on a daily basis, particularly in activities of cyclic loading such as walking, have a profound influence on the initiation, progression, severity and therapeutic outcomes for degenerative knee pathology (Chen et al., 2017, Felson, 2013, Andriacchi and Favre, 2014). 3-dimensional motion analysis has been widely adopted for investigating biomechanical pathways in disease, by calculating the disparity in dynamic measures representative of movement or loading of the knee that may be explanatory of changes in joint tissue structures during the course of the disease (Andriacchi and Muendermann, 2006). This involves the use of gait laboratories equipped with motion capture systems involving infra-red (IR) optoelectric cameras and floor-embedded force plates (Favre and Jolles, 2016). The measurement of marker trajectories attached to the subjects lower limbs of the subject combined with ground reaction force data from the force plates allows for non-invasive estimation of joint kinematics (i.e. joint angles and translations) and kinetics (i.e. joint moments), used to estimate loading patterns at the knee during activities such as walking (Figure 1.2-8).

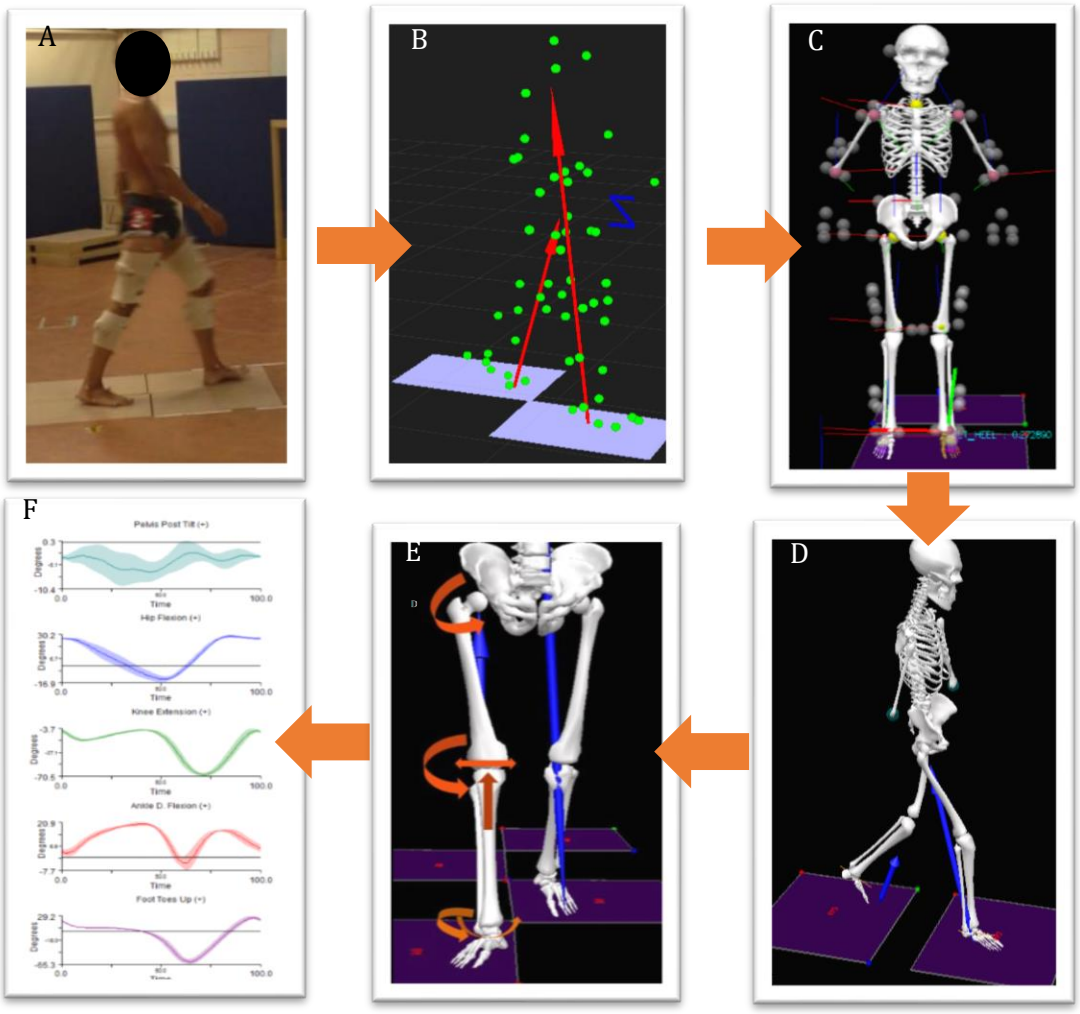

Figure 1.2-8 – Typical pipeline for gait analysis methods. Retro-reflective markers are attached to the various anatomical landmarks of the subject. A series of gait trials across the laboratory is performed whilst marker trajectory and ground reaction force (GRF) data is collected (A & B). A static calibration procedure is used to generate subject-specific models based on the marker positions and anthropometric data (C). Data is processed using the musculoskeletal model to calculate the positions and orientations of examined segments (i.e. foot, shank, thigh, pelvis) which allows estimations of joint angles (D & E), whereas an inverse dynamics calculation is performed using angle data and GRFs to estimate joint kinetics such as moments or powers. Joint angle or moment waveforms are extracted and used for biomechanical analysis of gait (F).

Biomechanical waveform data representing ground reaction forces (GRFs), joint angles and joint moments from the frontal plane (adduction/abduction) and sagittal plane (flexion-extension) are typically assessed. Joint moments are commonly examined in biomechanics literature which are calculated as a product of the GRF vector and the distance between the centre of joint rotation and the vector (moment arm) to generate measures of the rotational forces applied at the joints. Due to the known geometry of the knee, it is possible to interpret how the calculated rotational forces may be associated

with the altered loading of joint tissues (Favre and Jolles, 2016). These features are useful to consider since as previously noted, altered joint mechanics that occurs over large number of cycles during daily activities is likely responsible for aberrant joint biological changes (Andriacchi and Favre, 2014, Felson, 2013).

For example, the dynamic external knee adduction moment (KAM) is one such parameter commonly investigated (Figure 1.2-9), which describes the frontal plane dynamic 'bending' forces at the knee resulting from knee alignment and weight-bearing (Heiden et al., 2009). Patient gait analysis studies utilising instrumented knee implants that directly measured forces in the knee have shown strong correlations between medial-to-lateral knee compartmental force distributions and magnitudes of the KAM waveform, which validates its use as a surrogate measure of compartmental knee loading (Zhao et al., 2007, Kutzner et al., 2013). The KAM has shown to be increased in the knee OA population, which is consistent with the medial compartmental damage commonly associated.

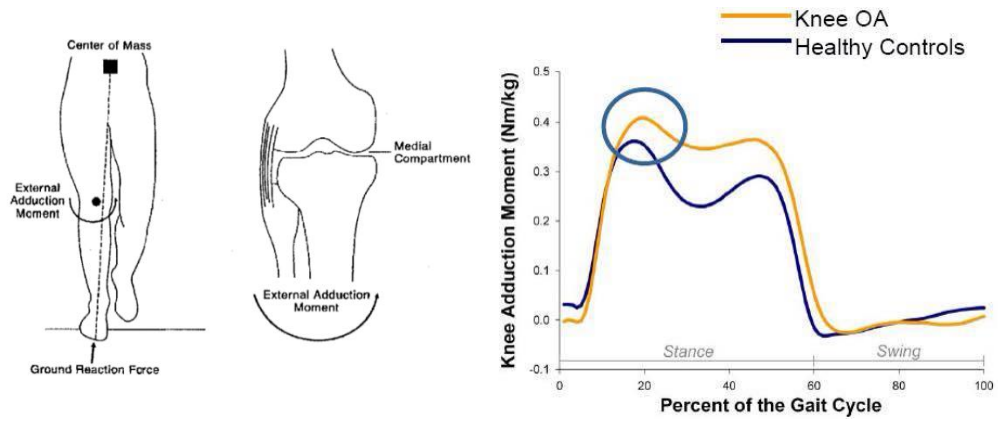

Figure 1.2-9 - The knee adduction moment (KAM) waveform is calculated from the GRF that passes medially to the knee and the distance between the centre of knee rotation and the GRF vector (moment arm). Knee OA subjects typically experience higher KAMs than normal.

Currently there are many research groups including our own aiming to characterise lower limb biomechanical function in knee patient groups, to understand progressive biomechanical pathways of pathogenesis and assess longitudinal outcomes of interventions aiming to restore joint function. Assessment of biomechanical waveform parameters of gait have revealed meaningful differences in disease groups such as OA or ACL-injury relative to controls, that has provided evidence of altered joint loading patterns and thus identified possible risk factors of progression (Felson et al., 2000, Mundermann et al., 2005a, Deluzio and Astephen, 2007, Astephen et al., 2008). Furthermore, longitudinal gait analysis studies have been used to assess the load altering

effects of interventions targeted at changing the kinematics and forces at the knee (Mundermann et al., 2004). For example, the KAM has been extensively used to assess the efficacy of high tibial osteotomy (HTO) surgery, a surgery aimed at realigning the frontal plane knee joint axis, for offloading the medial compartment in medial knee OA subjects (Favre and Jolles, 2016). Within our research group, lower limb function of patients with progressive knee OA undergoing high tibial osteotomy (HTO) total knee replacement (TKR) surgery has been investigated (Jones et al., 2006, Whatling, 2009, Watling, 2014). These studies have revealed distinct biomechanical features of moderate to severe OA patients during gait reflective of knee overloading and pain adaptations, which have proven to be useful predictors of outcomes to HTO and TKR surgery. The high heterogeneity of treatment outcomes to these surgeries appears to be related to biomechanical function prior to surgery.

Aside from biomechanical measures, there has also been interest in investigating the neuromuscular function of knee pathology subjects, which involves investigating the sensory (proprioceptive) and motor impairments affecting muscle contraction (activation) patterning during ambulation. Using electromyography (EMG) techniques which measure the electrical signals generated by contracting muscles, several studies have evidenced abnormal recruitment and co-contraction activity of lower limb flexor and extensor muscles during gait in patients with knee OA (Hubley-Kozey et al., 2008, Lewek et al., 2005, Takacs et al., 2013). This has revealed possible alterations in postural control and gait adaptations to knee pain and instability, which could be relevant to functioning of the knee related to disease (Duffell et al., 2014). It has been hypothesised that abnormal co-contraction patterns of the quadriceps and hamstrings may contribute to increased compressive forces at the knee, implicating neuromuscular function with mechanical pathways of pathogenesis (Lewek et al., 2005). Furthermore, long-term changes in postural control in compensatory mechanisms of pain avoidance is thought to contribute to muscle activation imbalances or weakening due to over- or underactivity of important stabilising muscles, which is thought to be a critical risk factor for OA development (Hortobagyi et al., 2005, Takacs et al., 2013).

In gait analysis studies, biomechanical and muscle activation waveforms are usually truncated to be representative of features during events of the gait cycle. Since the features of interest are typically during weight-bearing of the affected knee, moment waveforms are reported in a time-series normalised to percentage of stance phase (Figure 1.2-10), whereas joint angles and muscle activation waveforms are expressed for the whole gait cycle (heel-strike to heel-strike) which includes swing phase (not included

in the figure). The magnitude of the waveforms on the other hand are expressed as relevant units (i.e. joint angles in degrees, joint moments as %bodyweight*height and muscle activation as %maximum contraction) to permit comparison of the waveforms between subjects or between groups. Ultimately, it is the magnitude and shape differences of these waveforms that allows for a meaningful interpretation of group differences.

There is clear evidence of the value of gait analysis in elucidating the role of

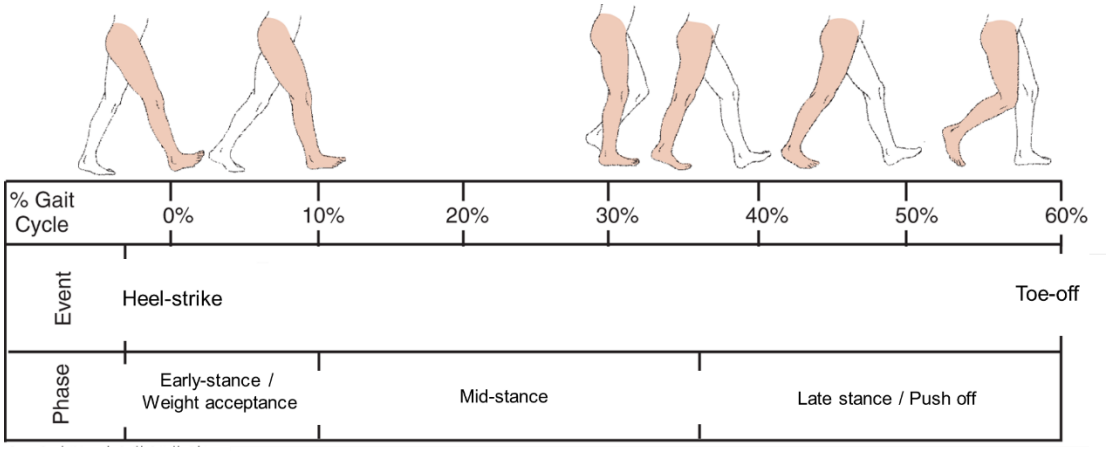

Figure 1.2-10 – Events of the gait cycle during stance-phase

biomechanical in knee OA, however this has not been characterised in subjects with knee FCDs, a condition where mechanical pathways are likely involved. Within this thesis, gait analysis techniques combined with EMG will be used for the first time to assess lower limb kinematic, kinetic and neuromuscular function in subjects bearing medial or lateral knee FCDs in relation to healthy subjects, to identify mechanical pathways of FCD pathogenesis that could explain disease progression or treatment outcomes of microfracture surgery.

1.2.4 The study of biological molecules in degenerative knee disease research

The pathogenesis of OA is characterised by successive stages of molecular derangements initiated by micro- and macro-injuries that results in the activation of maladaptive repair responses, followed by larger anatomical changes that culminate in full joint dysfunction. Within our research group, the longitudinal joint tissue response to knee injury by non-invasive ACL rupture has been characterised in mice revealed distinct biological events. This includes a time-dependent increase in the number of inflammatory-activated macrophage populations in the intra-articular space and upregulated gene expression of

pro-inflammatory cytokines, nitric oxide synthase and tissue matrix degrading enzymes consistent with bone remodelling and tissue architectural changes such as cartilage damage (Gilbert et al., 2018).

Organisations such as the Osteoarthritis Biomarkers Network (OBN), the Biomarkers Working Group (BWG), as well as the Osteoarthritis research Society International (OARSI) initiative aim to define a set of reliable biomarkers of normal or pathogenic processes associated with pre-OA and OA phenotypes in humans (Attur et al., 2013, Kraus et al., 2011, Lotz et al., 2013). Within these large multicentre projects, biological fluids such as synovial fluid, peripheral blood and urine are commonly explored for molecules reflective of the tissue response to injury, disease progression as well as therapeutic outcomes (Hunter et al., 2014, Kraus et al., 2017). Ultimately, biomarkers of OA could be used as either exploratory tools for investigative research, or as clinical tools such as for the diagnosis and prognosis of disease stage or surrogates for clinical trial end-points.

Although a few promising candidates exist, there is no single biomarker that can reliably and repeatably diagnose or prognose pre-OA or OA in humans (Lotz et al., 2013, Watt, 2018, Kraus et al., 2017). The validation of robust biomarkers for clinical research is becoming increasingly important due to the growing number of available treatments for early stages of disease. Most interventional studies use clinical end-points based on patient-reported (e.g., pain and symptoms) and imaging (X-ray and MRI) criteria. Although such assessments are valuable, they not sensitive to the molecular derangements that occur during early stages of the disease or in response to treatments, making it difficult to distinguish between them to identify those of highest efficacy (Lotz et al., 2013, Kraus et al., 2011, Kraus et al., 2017). For this reason, identification of valid biomarkers may generate more rapid therapeutic outcomes to treatments than is currently used in interventional studies (Kraus et al., 2011). Furthermore, although current hard clinical end-points provide information about the point-of-failure, they do not provide information for reasons of failure. Relating alterations of biological pathways with positive or poor outcomes to intervention may aid in the development and optimisation of future treatments.

Animal and clinical observations have taught us that the structural changes in joint tissues such as subchondral bone and cartilage during the course of OA are associated with changes in biological molecules that are thought to either facilitate and/or are resultant of cell metabolic or anabolic processes (remodelling), structural tissue degradation or inflammation (Scanzello et al., 2008, Karsdal et al., 2010). The

quantification of such molecules allows for investigating biological pathways of disease, to further characterise the etiological or progressive factors involved in dysregulated homeostatic functions which may aid to develop biomarkers or new target pathways for new biological treatments including Disease Modifying Osteoarthritis Drugs (DMOADs). In more recent years *in vitro* biological research has highlighted the cross-talk between functions of the immune system, cartilage and bone biology, therefore it may be increasingly relevant to investigate them together for this purpose (Legrand et al., 2017). Furthermore, although pre-clinical and clinical research has revealed potential biological mechanisms, targets and biomarkers of OA disease progression, there is little evidence for FCD specific pathology.

1.2.4.1 Biomarkers of cartilage and bone turnover and degradation

Products of bone and cartilage extra-cellular matrix (ECM) changes related to tissue remodelling and degradation are the most commonly examined biomarkers in animal and human OA studies and have been recognised as promising diagnostic and prognostic biomarkers by multi-centre organisations such as the OBN, BWG and the OARSI initiative, particularly for their utility in serum and urine (Attur et al., 2013, Kraus et al., 2011, Lotz et al., 2013). This is not surprising considering cartilage degradation as well as alterations in bone mineralisation and structure are hallmarks of OA (Goldring and Goldring, 2007).

A plethora of evidence has revealed disease group specific alterations in biomarkers of bone remodelling pathways, which describes the signals orchestrating turnover of skeletal tissue. Bone remodels continuously, an important process in repair and adaptation of bone to daily physiological loading (Day et al., 2004). It is thought this occurs through mechanotransduction pathways as well as the repair response to micro-fractures generated from tissue strain, resultant of structural compression. There are two cell types known to be directly active in bone remodelling - osteoblasts which synthesise new mineralised bone (formation) and osteoclasts which break it down (resorption) as illustrated in Figure 1.2-11. Studies of OA often quantify the concentrations of alkaline phosphatase (ALP) and C-terminal telopeptide of collagen type-I (CTX-I) in synovial fluid or serum, which are representative of osteoblastic bone formation activity and osteoclastic bone resorption activity, respectively (Burr and Gallant, 2012). Changes in the concentrations of these biomarkers could be reflective of the many observed changes in bone surrounding the joint, such as bone marrow lesions (BMLs), osteophyte formation and sclerosis of subchondral bone (Hunter et al., 2014).

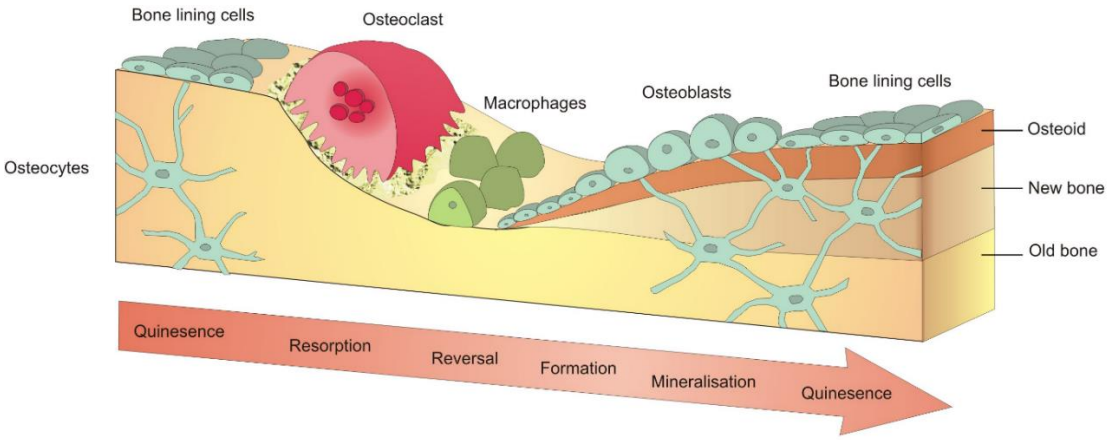

Figure 1.2-11 – Illustration of the bone remodelling process. Bone resorption activity involves the recruitment and activation of mature osteoclasts that release matrix degrading enzyme to remove old bone. Bone formation involves the recruitment and maturation of osteoblasts which secrete new matrix components to replace lost old bone with new mineralised bone (Burr and Gallant, 2012).

Interestingly, it has been shown that bone remodelling activity variably changes in early to late-stages of OA. However, the mechanisms of this are complex and still unclear (Burr and Gallant, 2012, Maruotti et al., 2017). The process relies on a complex network of signalling molecules such as growth factors, inflammatory cytokines and amino acids such as glutamate produced by themselves (autocrine) from neighbouring cells (paracrine) including osteocytes, inflammatory cells and chondrocytes (Gibon et al., 2016, Galea et al., 2017). The activation of various receptors on the osteoblast and osteoclast surface then initiates intra-cellular signalling pathways such as the janus kinase (JAK)-STAT pathway, activator protein 1 (AP-1) transcription factor pathway, or the nuclear factor Kappa-light-chain-enhancer of activated B cells (NF- κB) pathway (Figure 1.2-12). One well-recognised mechanism is the canonical bone resorption pathway, which is dependent on the activation of Receptor Activator of Nuclear factor Kappa-light-chain-enhancer of activated B cells (RANK) found on the surface of osteoclasts, which when activated by RANK ligand (RANKL) located on activated osteoblasts and some immune cells stimulates osteoclast maturity (osteoclastogenesis) and osteoclast resorption activity through multiple intracellular mechanisms, including the NF-κB and AP-1 pathways. However, osteoprotegerin (OPG), a signalling molecule also secreted by osteoblasts can inhibit the activation of the canonical resorption pathway binding to and deactivating RANKL. Thus, the relative quantities of RANKL and OPG in the joint as a ratio (RANKL-OPG) can be a useful biomarker of the net activation of canonical bone resorption of subchondral bone (Tat et al., 2009). Is has been suggested by previous authors that abnormal regulation of RANKL-OPG by osteoblasts is one of the

largest contributors to bone abnormal bone remodelling and mineralisation (Maruotti et al., 2017).

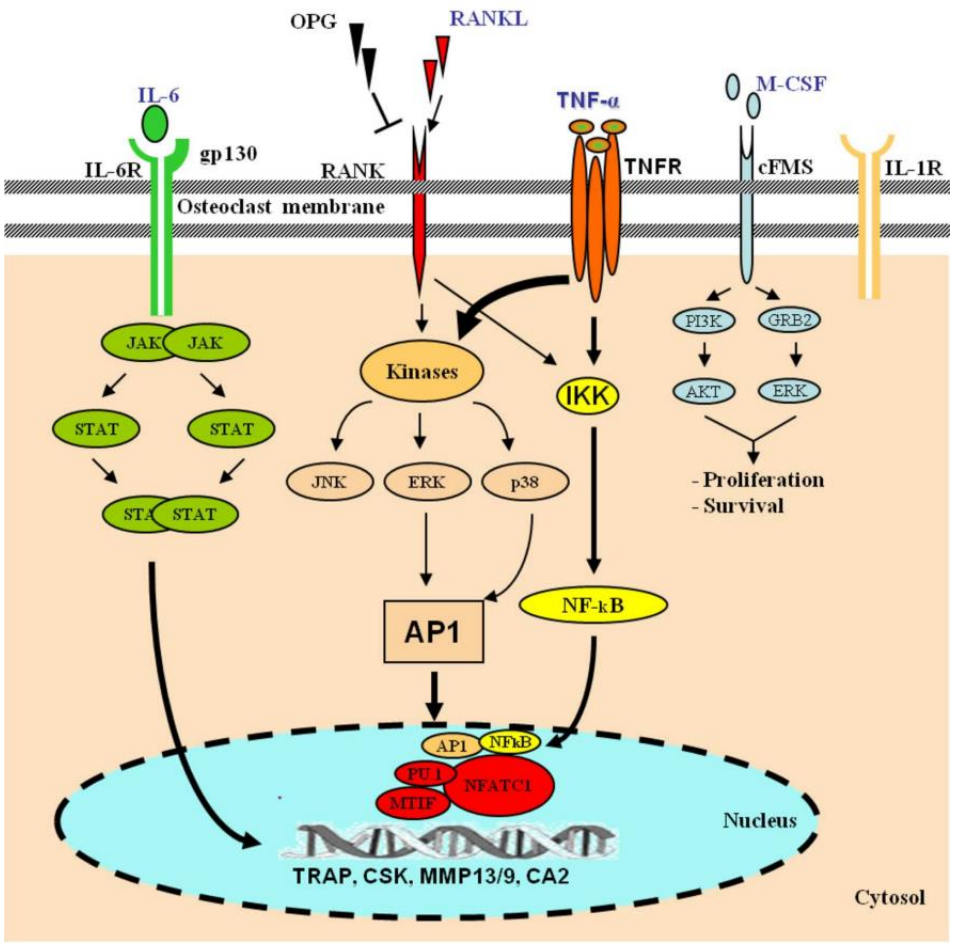

Figure 1.2-12 - Schematic of common pathways involved in activating bone resorption including the JAK-STAT, NF-κB and AP-1 transcription pathways. RANKL expression by osteoblasts activates the canonical signalling pathway in osteoclasts leading to up-regulated gene expression of matrix degrading enzymes including matrix-metalloproteinases (MMPs), Tartrate-resistant acid phosphatase (TRAP), C-terminal c-Src kinase (Csk), but is inhibited by OPG activity (Osta et al., 2014).

Structural degradation of cartilage during the course of OA was once thought to be due to 'wear and tear' of the joint, however it has become much clearer that biological mechanisms of degradation are involved in the process. When chondrocytes are stimulated by chondral damage, inflammatory cytokines or pathophysiological mechanical signals due to altered loading of the joint, they shift towards a catabolic state, producing inflammatory cytokines, matrix degrading enzymes including MMPs that degrade structural collagens as well as aggrecanases such a disintegrin and metalloproteinase with a thrombospondins (ADAMTS) which cleave the important

aggrecan chains that give cartilage its hydrophilic properties (Bader et al., 2011, Gilbert et al., 2018, Chen et al., 2017). For this reason, cartilage matrix molecules resultant of metabolism such as C-terminal telopeptide of collagen type-II (CTX-II) and hyaluronan (HA) are arguably of the most commonly explored OA-related molecules in serum (Lotz et al., 2013, Kraus et al., 2017).

Cartilage oligomeric matrix protein (COMP) is a structural component of cartilage that is thought to be involved with organisation of the fibrils that give cartilage its mechanical properties, thus making it a good indicator of structural cartilage degradation (Attur et al., 2013). Since COMP is produced by chondrocytes, it is also a valid indicator of anabolic activities in a reparative state (Clark et al., 1999). Interestingly, cartilage matrix components including COMP have been shown to stimulate chondrocyte catabolic pathway activation through interacting with integrins on the chondrocyte cell surface, stimulating a catabolic feedback loop involving the perpetual breakdown of cartilage (Recklies et al., 1998, Bader et al., 2011, Chowdhury et al., 2010). Together, this suggests COMP is a good indicator of pathogenic processes of cartilage during the course of degenerative knee pathologies.

1.2.4.2 Biomarkers of mechanical loading of bone

Bone is thought to be the fastest and most responsive tissue to mechanical loading in the body, exhibiting the earliest changes following initiation of OA in animal models (Goldring and Goldring, 2007). As previously detailed, the adaptative response to local stresses is a repair response, but also ensures the mechanical properties of bone underlying regions of high mechanical loading is adequate for its supportive function in the joint (Burr and Gallant, 2012). Structural changes in subchondral bone as detected by imaging methods such as X-ray and MRI have reported to involved both thinning in the early stages of OA to thickening and stiffening (sclerosis) in the later stages (Garnero et al., 2001, Hayami et al., 2004), as well as site specific bone marrow lesions composed of disorganised bone formation and attrition (Lo et al., 2005). Therefore, there is a desire to understand how bone is loaded in the joint, particularly in relation to changes in cartilage. It is thought that sclerostin and glutamate are importantly involved in the adaptive response mechanism, acting as mechano-tropic agents linking cell mechanotransduction pathways and bone cell maturity and activity (Galea et al., 2017, Brakspear and Mason, 2012, Mason et al., 1997, Robling et al., 2008).

Activation of the Wingless/integrated (Wnt) signalling pathway in bone is responsible for the upregulated activity of Runt-related transcription factor 2 (Runx2), which orchestrates expression of bone formation genes in osteoblasts, including those for the synthesis of ALP, OPG, osteocalcin, collagen type-I, bone sialoprotein (BSP) and osteopontin. Therefore, as a potent Wnt/β-catenin pathway inhibitor, sclerostin has control over important osteogenic pathways in bone (Sebastian and Loots, 2017, Raggatt and Partridge, 2010). Sclerostin is produced by osteocytes in resting conditions. However, when bone is loaded sclerostin expression is down-regulated due to the activation of strain-sensitive surface receptors, ultimately permitting bone formation activity by osteoblasts to occur (Lewiecki, 2014, Sebastian and Loots, 2017). This mechanism therefore describes a direct feedback mechanism in which bone repair is stimulated by mechanical loading with sclerostin as the key regulator (Galea et al., 2017). For this reason, sclerostin could be a good biological indicator of subchondral bone loading in the healthy and degenerative joint, whereby reduced sclerostin would represent higher loads.

Interestingly, it has been recognised that chondrocytes from sheep and mouse joint destabilization post-traumatic OA models exhibit expression of sclerostin in regions of focal cartilage damage, whilst reduced sclerostin expression was detected in regions of sclerotic subchondral bone (Chan et al., 2011, Lewiecki, 2014). Sclerostin is biologically active in chondrocytes, inhibiting Wnt/β-catenin activation responsible for catabolic MMP and ADAMTS expression, but also decreasing expression of collagen type-II and aggrecan. Due to these contrasting effects which have been verified more recently, this response has sparked controversy over whether or not up-regulated sclerostin it is a chondro-protective mechanism (Chang et al., 2018)). The emerging consensus is that extracellular release could be an auto- and paracrine signalling response to the high mechanical stress and/or pro-inflammatory conditions to protect local regions of cartilage from excess degradation.

Although the sclerostin pathway is well-established, the role of glutamate and glutamatergic signalling in the response to loading still requires further clarification, however there is early evidence of its involvement in OA (Brakspear and Mason, 2012). An earlier study by Mason and colleagues (1997) showed that an osteogenic load externally applied (10 N, 10Hz) to rat ulna resulted in a down-regulation of glutamate aspartate transporter (EAAT) expression in bone. This is suggestive of a mechano-regulatory mechanism involving glutamate signalling, since EAATs terminate glutamate signalling by removing it from the extracellular space in the synapse. Since later

discoveries of functional components such as proteins required for calcium-mediated exocytosis of glutamate, it has been hypothesised that opening of osteocyte stretch- and voltage-sensitive calcium channels as a result of mechanical loading may result in Ca^{2+}-mediated release of glutamate into the extracellular space (Mason, 2004). Combined with the down-regulation of glutamate transporters, the evidence supports the accumulation of glutamate within the joint following continued response to load – a possible mechano-regulatory signalling system.

Other studies including from our research group have evidenced the possible role of glutamate signalling in most joint tissues, since functional components of glutamate signalling including ionotropic (iGluRs) and metabotropic (mGluR) glutamate receptors have been found on the surface of osteoblasts, osteoclasts, osteocytes, chondrocytes and fibroblasts (Cowan et al., 2012, Bonnet et al., 2015, Wen et al., 2015, Brakspear and Mason, 2012). Collectively, several studies have proven by the use of glutamate receptor antagonists that glutamatergic signalling is important in the regulation of osteoblastic bone formation activities (Ho et al., 2005, Lin et al., 2009), osteoclast differentiation and resorption activity (Merle et al., 2003, Mentaverri et al., 2003), nociceptive pathways (Bonnet et al., 2015, Wen et al., 2015) as well as inflammatory pathways (Flood et al., 2007). Furthermore, inhibiting glutamatergic signalling in mouse models of inflammatory arthritis inhibits histological cartilage, bone and synovium OA-related changes, as well as pain-related behaviour (Bonnet et al., 2015), suggesting glutamate may be a key player in the pathogenesis and pain experienced during OA.

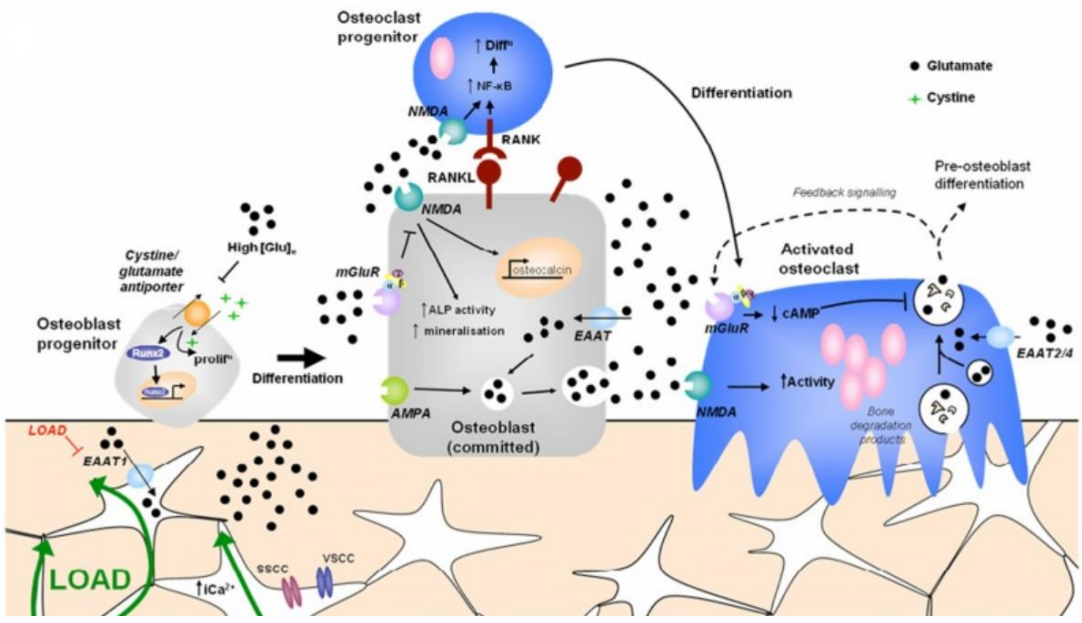

Figure 1.2-13 - Proposed glutamate signalling interactions in bone based on previous evidence by Brakspear and Mason (2012). Opening of osteocyte stretch-sensitive

calcium (Ca^{2+}) channels in response to mechanical load results in release of glutamate (black circles) into the extra-cellular space. Mechanical loading down-regulates glutamate transporter (EAAT) expression (Mason et al., 1997), resulting in increased net extracellular glutamate. High glutamate levels activate iGluRs (NMDA/AMPA) on the surface of osteoblasts and osteoclasts (Wen et al., 2015), which activate intracellular bone formation (Ho et al., 2005, Hinoi et al., 2003) and resorption (Merle et al., 2003, Mentaverri et al., 2003) pathways. Therefore, glutamatergic signalling may act as a mechano-tropic mechanism of transduction of mechanical cues and coupling of bone remodelling.

1.2.4.3 Biomarkers of inflammation

All tissues in the joint play a role in the pathophysiology of OA through the mediation of inflammatory cytokines and chemokines, a complex network of influential regulators of which the dysregulation many investigators claim drives the pathogenesis of OA (Wojdasiewicz et al., 2014, Mobasheri et al., 2017, Kapoor et al., 2011, Mobasheri, 2013). Increased presence of pro-inflammatory mediators such as interleukin-1β (IL-1β), IL-6, IL-8, tissue necrosis factor-α (TNF-α) and interferon- γ (IFN-γ) have consistently been linked to self-propagation of inflammatory factors, joint tissue structural alterations through the promotion of tissue turnover pathways (Figure 1.2-12), upregulation of matrix-degrading enzymes such as MMPs and ADAMTSs, production of destructive and pain inducing molecules such as prostaglandins E2 (PGE_2) and nitric oxide (NO), as well as worsening of clinical factors such as joint pain and OA-related symptoms (Fernandes et al., 2002, Lotz et al., 2013). These molecules arise from specific inflammatory tissues such as the synovium, infiltrating leukocytes, or traumatised bone and cartilage cells, and facilitate autocrine and paracrine signalling to stimulate the production of themselves in a destructive positive feedback loop in the course of OA (Wojdasiewicz et al., 2014, Lotz et al., 2013).

Anti-inflammatory mediators such as IL-4, IL-10 and IL-13 on the other hand play an antagonistic role to disease progression, through the inhibition of pro-inflammatory cytokine activity, direct downregulation of tissue turnover pathways (such as the RANK/RANKL/OPG canonical pathway in bone), and suppression of destructive factors (Wojdasiewicz et al., 2014, Onoe et al., 1996, Scanzello, 2017). Aside from utility as useful biomarkers of disease pathogenesis, a better understanding of individual functions and roles of inflammatory mediators in disease is of interest for the development of effective anti-cytokine therapies (Kapoor et al., 2011).

Pro-inflammatory mediators have been widely acknowledged for their diagnostic and prognostic potential for clinical knee OA (Fernandes et al., 2002, Kapoor et al., 2011, Liu-Bryan and Terkeltaub, 2015), as well as progression of knee FCDs (Cuellar et al., 2016, Tsuchida et al., 2012, Streich et al., 2011). There has been a particular interest in the involvement of inflammation in the acute response to injury, since the up-regulation of pro-inflammatory cytokine expression and release appears to be the earliest reported response following injury in PTOA animal models or injured human subjects, preceding degenerative changes (Scanzello, 2017, Gilbert et al., 2018). Several large multi-centre cohort studies involving the Knee Injury Cohort at the Kennedy (KICK) cohort of 150 subjects (Watt et al., 2016) and the Knee Anterior Cruciate Ligament, Non-surgical versus Surgical Treatment (KANON) cohort of over 121 subjects (Struglics et al., 2015) have reported that pro-inflammatory cytokines including IL-1β, IL-6, TNF-α and chemokines such as IL-8 and monocyte chemotactic protein-1 (MCP-1), are elevated following injury up to five years in synovial fluid and correlate with patient-reported outcomes such as pain and symptoms, making them strong candidate biomarkers for early disease pathogeneses.

1.2.5 Joint homeostasis in health and osteoarthritis

Joint homeostasis is dependent on intra-scale biomechanical signalling, which ranges from full body ambulatory mechanics to the local mechanical environment of the cell (Andriacchi and Favre, 2014, Felson, 2013). Most cell types in joint tissues including chondrocytes, osteocytes, osteoblasts and osteoclasts respond to mechanical load as a means of regulating growth, cellular differentiation, and metabolism in the joint tissue extracellular matrix (Sanchez-Adams et al., 2014, Blain et al., 2001, Bader et al., 2011, Sah et al., 1989). Maintenance of a balanced synthesis and degradation cycle is essential for normal morphology and thus function of the knee. In the microenvironment, physiological ranges of matrix deformation, hydrostatic and osmotic pressure, altered matrix water content and oscillatory fluid flow are all capable of individually stimulating a cell signalling response (Hoey et al., 2012, Fitzgerald et al., 2006, Liedert et al., 2006, Robling and Turner, 2009). In a state of rest (no joint loading), catabolic activity signalling is dominant, which is required to remove damaged tissues exposed to loading that may have lost structural function (Figure 1.3-14). Whereas activated signalling pathways following loading are reflective of biosynthetic anabolic responses, which are thought to be responsible for the repair and replacement of damaged tissues caused by joint use (Figure 1.3-15). The overall resulting turnover process allows for repair,

growth and remodelling of skeletal tissues (Loeser, 2014). The following figures represent some of the major pathways involved in these distinct phases of homeostasis.

1.2.5.1 Effect of loading on joint homeostatic mechanisms

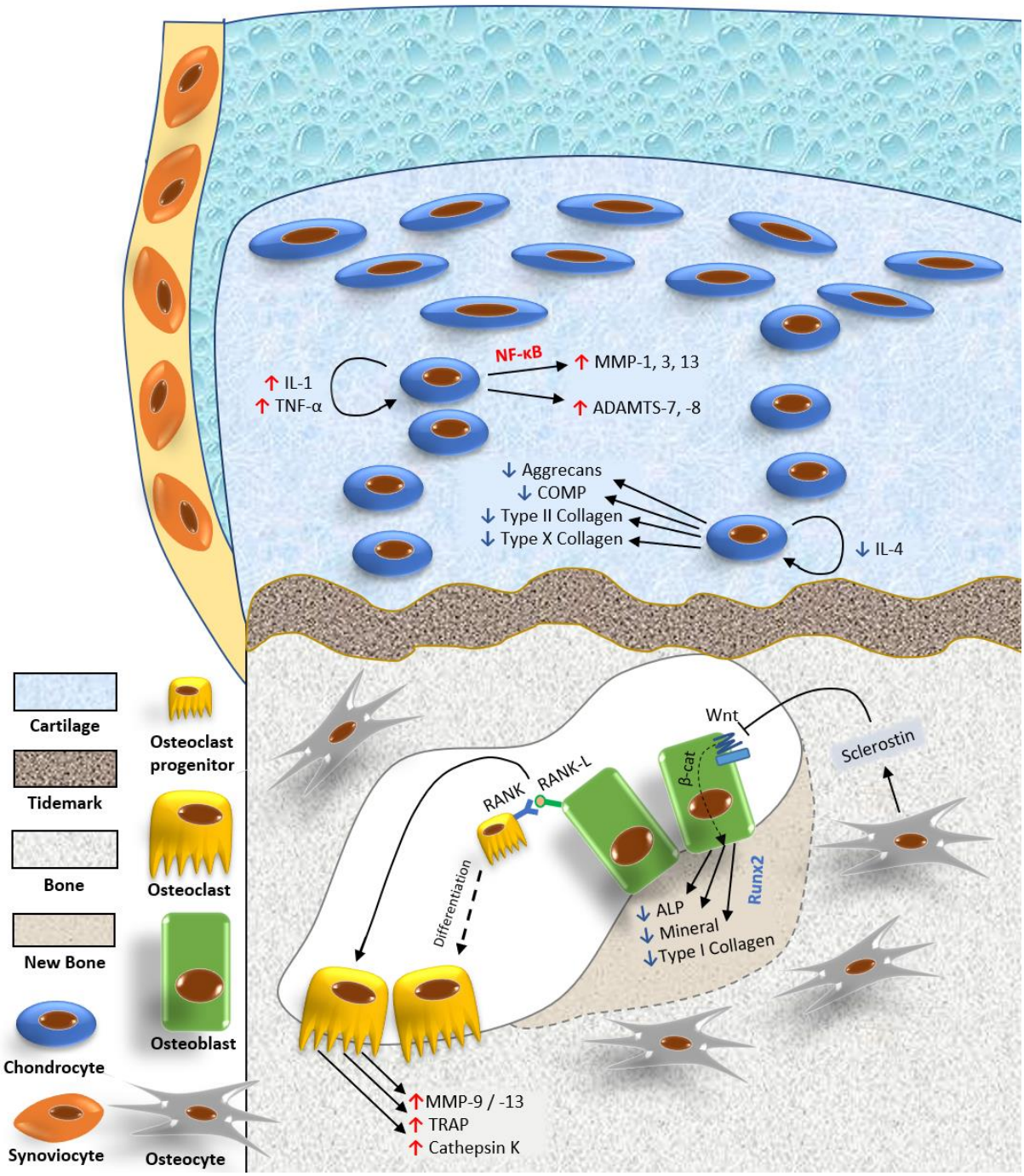

Figure 1.3-14 – Schematic representing homeostatic mechanisms during resting conditions. Chondrocytic anti-inflammatory cytokine (e.g. IL-4) expression and intra-cellular calcium signalling is down-regulated due to lack of mechanical stimulation, permitting activity of the NF-κB intracellular signalling pathway (Sanchez-Adams et al., 2014, Salter et al., 2001). This results in the upregulation of chondrocytic catabolic expression of matrix degrading proteases (MMPs) and aggrecanases (ADAMTS), as well

as increased pro-inflammatory cytokine (IL-1β and TNF-α) synthesis, which promote catabolism in an autocrine and paracrine manner (Leong et al., 2010, Loeser, 2014). In subchondral bone, resting osteocytes release sclerostin, which binds to low-density lipoprotein receptor-related protein 5 or 6 (LRP5/6) and Frizzled co-receptors on the osteoblastic surface and potently inhibits the Wnt/β-catenin pathway, interrupting osteogenesis and osteoblastic bone formation activity, including via activity of the osteogenic transcription factor Runx2 (Robling et al., 2008, Li et al., 2005). Due to the activity of parathyroid hormone (PTH), vitamin D and pro-inflammatory cytokines (IL-1 and IL-6), osteoblasts express RANKL, which binds to RANK on the surface of premature osteoclasts and stimulates osteoclastogenesis and increased bone resorption activity (Lewiecki, 2014, Sebastian and Loots, 2017). Bone resorption by osteoclasts involves the secretion of proteases (MMP-9, -13 and Cathepsin K) and tartrate-resistant acid phosphatase (TRAP), which break down old bone.

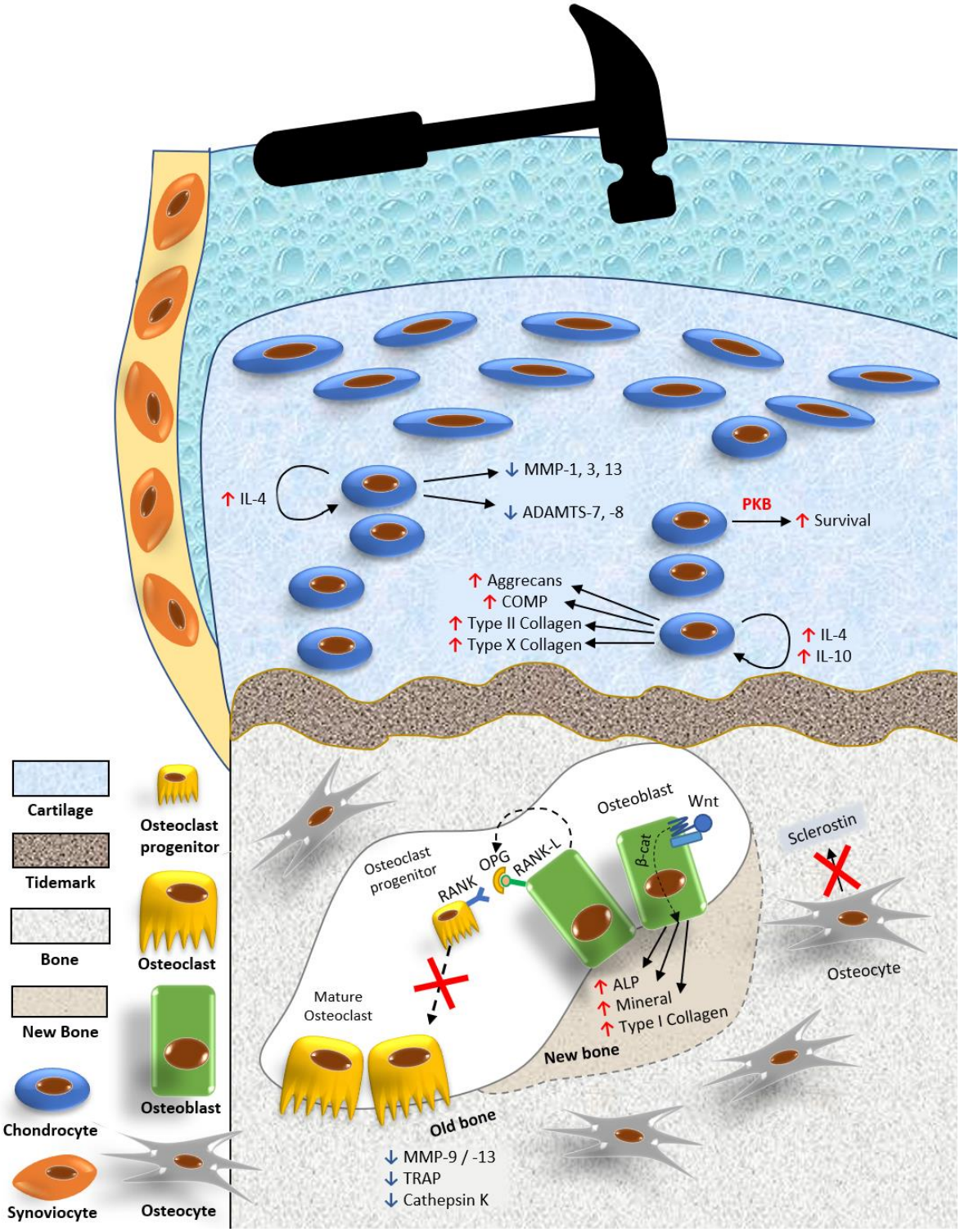

Figure 1.3-15 – Schematic representing homeostatic mechanisms in response to physiological loading. The stimulation of stretch-activated ion channels (e.g. Transient receptor potential cation channel subfamily V member 4) and integrins (e.g. α5β1) on the chondrocyte surface leads increased intracellular Ca^{2+} levels and the release of anti-inflammatory cytokines (e.g. IL-4), which in an autocrine and paracrine (cytokines only) manner, upregulate gene expression for the synthesis of matrix components (e.g. collagen type II and aggrecans), and counteracts protease (MMP-3) expression and the synthesis of pro-inflammatory mediators including PGE2, IL-1β and TNF-α (Millward-

Sadler and Salter, 2004, Wong and Carter, 2003, Bader et al., 2011). Activation of these surface molecules is also thought to play a role in many aspects of chondrocyte function, including proliferation, chondrocyte adhesion, chondrogenesis and survival through intracellular calcium and cytoskeletal signalling pathways (Hirsch et al., 1997, Sanchez-Adams et al., 2014). For example, integrin-dependent activation of phosphoinositide3 kinase (P13k) regulates PKB/Akt activity which has multiple roles such as the inhibition of apoptosis and pro-apoptotic molecules (Guan et al., 2014). In bone, osteocytes downregulate sclerostin expression, a potent inhibitor of Wnt signalling, leading to heightened activity of the canonical Wnt (β-catenin) signalling pathway in osteoblasts, responsible for stimulating Runx2-dependent expression of anabolic genes (e.g. type I collagen and ALP) responsible for the formation of new mineralised bone (Osta et al., 2014, Sebastian and Loots, 2017). Loaded osteoblasts release osteoprotegerin (OPG), an autocrine and paracrine inhibitor of the osteoblastic RANKL-dependent NF-κB pathway in osteoclasts, leading to reduced osteoclast maturation and resorption activity (Tat et al., 2009, Sanchez et al., 2009). This results in an overall increase in bone remodelling with a bias toward new bone formation.

1.2.5.2 Homeostatic mechanisms during different stages of the OA process

Biological homeostasis is disrupted in osteoarthritis due to mechanical and biochemical changes in the joint that bias the synthesis-degradation balance. When the extracellular matrix is damaged, chondrocytes and bone cells show a distinct repair response in an attempt to recover, but due to the extent of damage and complexity of these tissues, anabolic activities cannot effectively restore functional tissue (Karsdal et al., 2014, Zhu et al., 2009). Histological studies have provided a plethora of evidence of joint tidemark advancement (the boundary between bone and cartilage) in OA tissues, and thus it is recognised that re-establishment of the endochondral ossification process is likely a key contributor to the process of OA progression (Burr and Gallant, 2012). As this development process is rekindled, the thickness of calcified tissue advances into the cartilage matrix in a process called tidemark duplication, reducing the thickness of tissue with functional hyaline properties. The biomechanical changes in hyaline cartilage due to these changes is thought to play an important part in the accelerated deterioration of cartilage (Andriacchi and Favre, 2014)

The association of bone remodelling and cartilage thinning throughout the course of OA is a dynamic process initiated by maladaptive overloading (e.g. blunt trauma or prolonged) that aberrant activation of mechanotransduction pathways in the affected cells, eventually changing the molecular composition of tissues (Lee & Salter, 2015). It is well recognised that joint cells respond differently to physiological versus

pathophysiological ranges of load stimulus, which drive differential mechanisms of homeostasis which often become increasingly unbalanced in the overloaded joint during the course of OA (Martel-Pelletier, 1999, Arokoski et al., 2000). Subchondral bone exhibits differences in tissue remodelling rates within the tissue concomitant with the altered loading patterns experienced, which can lead to regions of bone sclerosis and attrition often found in the form of bone marrow lesions (Burr, 2004). These paradoxical observations are consistent with the spatial separation of these processes in the affected joint (Burr and Gallant, 2012). The consequential changes in thickness or stiffness of the subchondral bone plate can further contribute to altered biomechanical and compositional properties of the tissues, which ultimately alter the cellular response to joint loading. Aside from mechanical factors, biochemical factors such as inflammatory mediators, stress-response factors as well as matrix components released resultant of increased loading can further drive pathogenesis through aberrant stimulation of cell receptor-ligand interactions (Day et al., 2004). This leads to perpetual catabolic feedback loops that synergistically with altered loading patterns throughout the course of OA contribute to the eventual destruction and dysfunction of the joint.

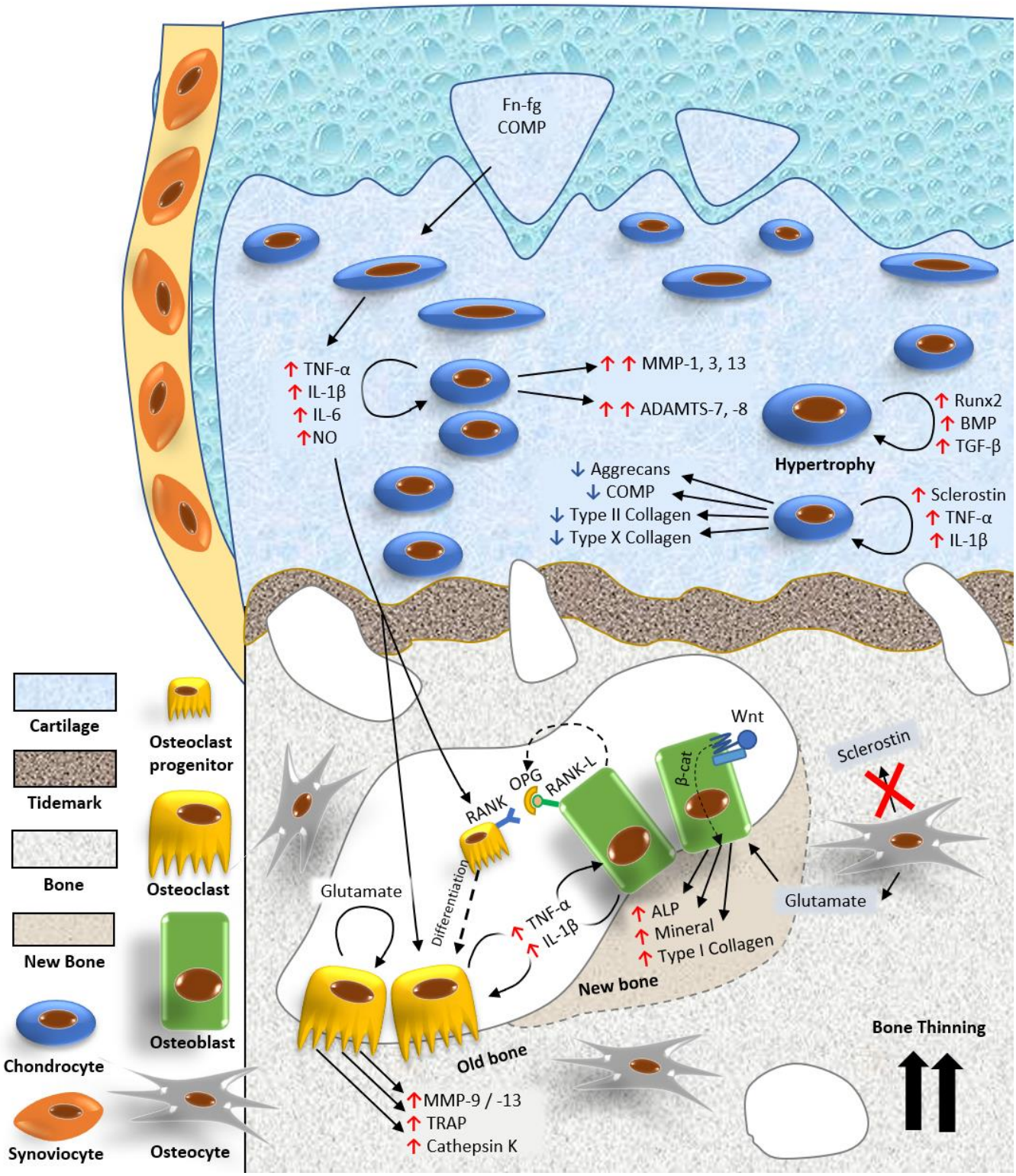

Figure 1.3-16 - Schematic representing currently hypothesised mechanisms of early OA pathogenesis. The superficial layer of cartilage first degrades due to abnormal mechanical insult, and eventually changes are seen in the internal structural and cell organisation. The increased forces experienced by chondrocytes and exposure to ECM breakdown components (e.g. fibronectin, collagen and COMP fragments) overstimulates the toll-like-receptor (TLR) and integrin-dependent (e.g. α5β1) pathways in chondrocytes and synovial cells, which are involved in the activation of NF-κB and MAPK

p38 intracellular signalling pathways (Bader et al., 2011, Martel-Pelletier, 1999, Loeser et al., 2012). This leads to enhanced synthesis of stress-response factors (e.g. PGE2 and NO), pro-inflammatory mediators (e.g. IL-1β, IL-6 and TNF-α) and proteolytic enzymes (MMP-1, MMP-3, MMP-8, MMP-13) and ADAMTS-4 and 5 (Chowdhury et al., 2010, Kim et al., 2006b, Fernandes et al., 2002, Hwang et al., 2015). These external and autocrine factors in combination stimulate a hypertrophic repair phase, whereby chondrocytes exhibit accelerated proliferation and anabolic activity in the form of matrix component synthesis (e.g. collagen type II, collagen type X and aggrecan). This is partially influenced by the release of anabolic factors including insulin-like growth factor (IGF-1) and TGF-β by stimulated chondrocytes, a staple trait for early OA (Favero et al., 2015, Goldring and Otero, 2011). However, due to the loss of the superficial layer, glycosaminoglycans is eventually lost from the matrix and replaced with water, leading to softening of the hyaline tissue (Favero et al., 2015, Blaker et al., 2017). Release of pro-inflammatory mediators (e.g. IL-1β and TNF-α) and TGF-β from the deteriorating cartilage also stimulates bone remodelling, due to the heightened activation of the NF-κB, SMAD-dependent and MAPK pathways in osteoblasts and osteoclasts (Osta et al., 2014). Pro-inflammatory cytokines IL-1β and IL-6 influence the expression of RANKL by osteoblasts, activating RANK on the surface of osteoclasts which increases osteoclast maturation and resorption activity through the NF-κB-dependent pathway (Steeve et al., 2004). Aberrant bone remodelling is also influenced by the pathophysiological subchondral bone loading experienced due to loss of cartilage. Sclerostin is heavily downregulated by osteocytes, increasing osteogenic activity (Robling et al., 2008, Robling and Turner, 2009). Increased release of intracellular glutamate stores and down-regulation of glutamate transporters leads to high extracellular glutamate, which acts on bone cell ionotropic glutamate (NMDA/AMPA) receptors to stimulate pro-inflammatory activity, osteoclast maturation and resorption activity, as well as osteoblast activity (Brakspear and Mason, 2012, Flood et al., 2007, Mason, 2004). This enhanced bone remodelling activity leads to increased porosity and eventual thinning of the subchondral plate, resulting in mechanically inferior bone, altering biomechanical factors such as stiffness and further catalysing destruction through abnormal biomechanical cues.

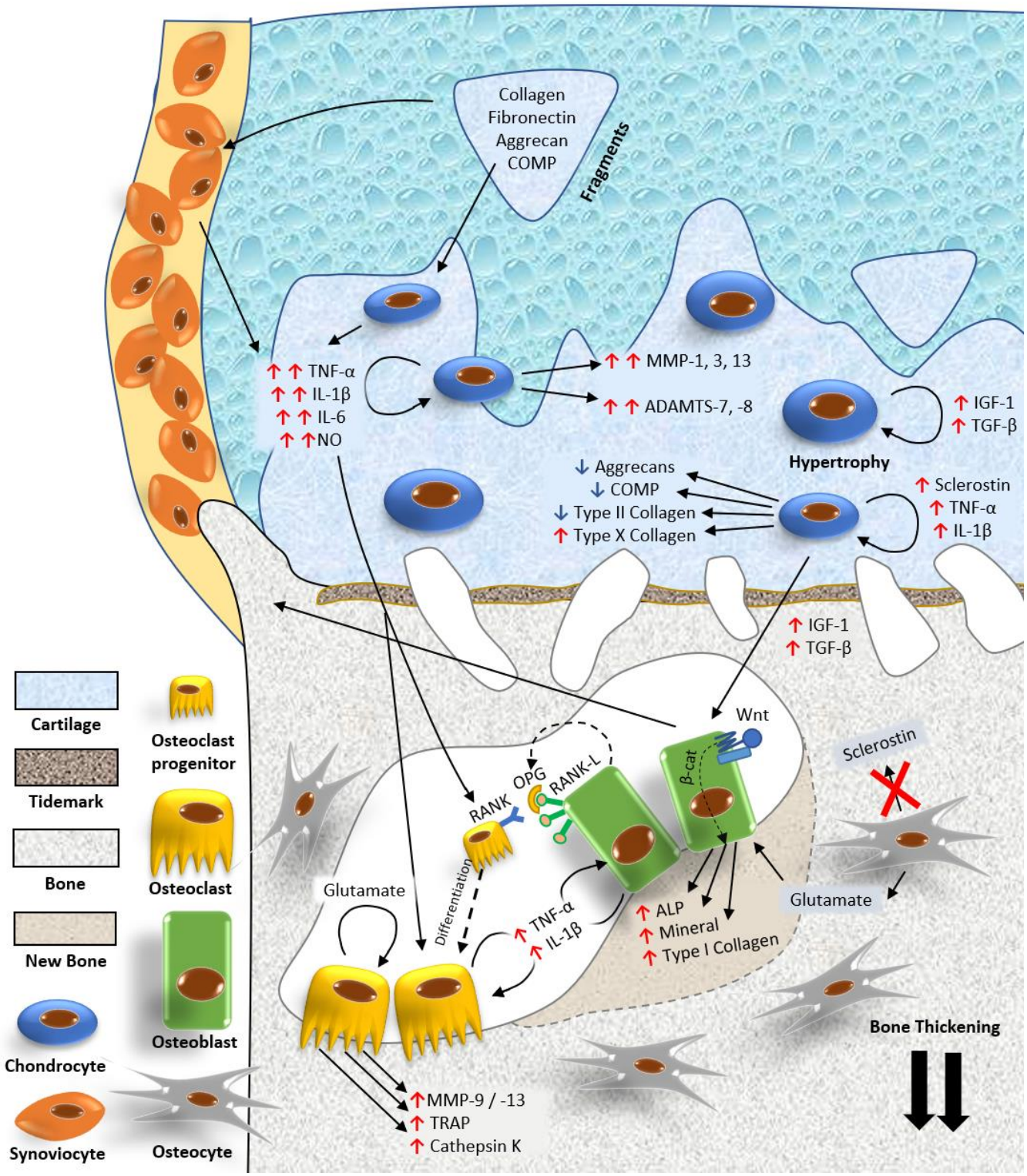

Figure 1.3-17 - In the later stages of OA, most of the cartilaginous structure of the hyaline surface is lost, with heavy denudation of the osteochondral tidemark and thus increased cross-talk between cartilage and bone (Karsdal et al., 2014, Findlay and Kuliwaba, 2016). The stimulation of synoviocytes by heightened pro-inflammatory cytokine (e.g. IL-1 and TNF-α) production leads to the development of synovitis, synovial tissue hyperplasia and thus heavy involvement in the amplification of catabolic signalling via production of pro-

inflammatory cytokines, and pro-inflammatory mediators (e.g. PGE2 and NO). The remaining hypertrophic chondrocytes produce mainly collagen type X instead of type II, but otherwise reducing synthetic activity to a minimum (Attur et al., 1998, Pelletier et al., 2001). This is partially due to the expression and release of local sclerostin in response to damage, a possible chondroprotective mechanism that paradoxically inhibits Wnt/β-catenin-dependent expression of anabolic (e.g. Col II) and catabolic (MMP, ADAMTS) genes, to avoid further destruction of cartilage (Chang et al., 2018). Abnormal stresses across subchondral bone and increased movement of growth factors (e.g. TGFβ and IGF-1) into bone due to the increased cartilage-bone crosstalk from the cartilage repair response results in renewing of the endochondral ossification process (van der Kraan and van den Berg, 2007). This leads to the growth of new bone at the joint extremeties and entheseal sites in the form of osteophytes.

1.2.6 Conclusion

The involvement of mechanical, biological and structural pathways in degenerative joint conditions such as FCDs and OA are undoubtedly involved, however the interaction between these pathways require further investigation. The knee FCD population are a good human disease model of joint overload, given that the aetiology or progression of the condition is often attributed to joint injury or morbidity of tissues that provide stability of the knee during ambulation. Furthermore, we possess the tools to investigate *in vivo* kinematics and mechanical loading of the joint and lower limb function, as well as cross-sectional and longitudinal biological differences in the joint that may reveal new pathways or indicators of FCD pathogenesis that have not previously been described. A new approach investigating these areas both independently and relatively may reveal new pathways that could lead to the development of more comprehensive treatment strategies.

Chapter 2

Methodology for the biomechanical and biological assessment of clinical cohorts

Overview

This chapter aims to outline the experimental design and methodology for:

- The objective assessment of lower function during gait using 3D motion analysis
- Synovial fluid and serum biomarker quantification using immunoassay
- Collection of clinical data

For each of these aspects, methods for data collection and generation of variables for analysis will be outlined. Study design and methodology described in this chapter are common to multiple chapters within this thesis, however specific chapter data analysis methods will be outlined within the chapter methods sections.

2.1 Study Design

2.1.1 Study approval

The identification, recruitment and analysis of healthy volunteers, NHS patients with knee FCDs undergoing microfracture surgery and unilateral OA undergoing high tibial osteotomy (HTO) surgery was approved by the Research Ethics Committee for Wales and Cardiff & Vale University Health Board under the Arthritis Research UK Biomechanics and Bioengineering Centre (ARUK BBC) umbrella approval (REC: 12-OAE-4976-9). This permitted the collection and assessment of clinical data surgical and access to historical patient records regarding the involved condition, assessment of patient gait using approved 3D motion analysis protocols, as well as the collection and analysis of synovial fluid and serum of removed genetic data. The following courses were attended/documents were obtained for the approval of all methodology carried out with NHS patients during the course of this study:

- Good clinical practice training and certificate
- Informed consent training and certificate
- Disclosure and Barring Service (DBS) check
- Honorary research contract issued by Cardiff and Vale University Health Board
- Phlebotomy Training Level 2 certificate

2.1.2 Cohorts and study criteria

This study was designed to evaluate cross-sectional and longitudinal differences in biomechanical, biological and clinical variables of a single FCD cohort in relation to healthy volunteers as controls and established OA subjects as a disease comparator group representing higher disease advancement/severity.

Although a single FCD group was maintained throughout the study, it was not possible to maintain consistent comparator cohorts due to limitations of data collection and accessibility to fluid samples (section 7.2). This led to a total of four overall cohorts assessed throughout the thesis:

2.1.2.1 FCD Subjects

The FCD cohort were the primary cohort assessed within this thesis that remained consistent among all chapters. These were NHS patients in line for microfracture surgery, who presented single, isolated Outerbridge grade II chondral lesions in the weight-bearing region of the tibiofemoral joint. Subjects included had long-term pathology and progressive symptoms thought to be resultant of a past injury (10 subjects; mean time since injury (SD) = 4.9 (3.1) years) or from non-specific causes of an unknown time (3 subjects), however no subjects were thought to be experiencing acute phase inflammation from recent injury/impact. Injuries reported included: sports injuries (rugby/football), ultra-marathon running, martial arts and accidental impact from falling. Subjects with minor meniscal loss/injury or ACL tears/injury were included, but those of total meniscal loss of the affected compartment or complete ACL rupture were discounted from the study as they were considered major confounding co-morbidities in the analysis. Furthermore, subjects with confirmed clinical osteoarthritis (KL grade II - IV) were excluded.

Initial assessments for the diagnosis of tibiofemoral FCDs consisted of clinical 1.5 tesla MRI scans, which confirmed chondral damage in the joint. Patients with identified grade II tibiofemoral lesions were listed on the orthopaedic surgery list as ‘arthroscopy and microfracture surgery’, of which were shortlisted for recruitment. Following initial contact from clinical liaison at the Cardiff & Vale Orthopaedic Centre (CAVOC), the candidate was recruited via telephone with by the following criteria:

- Ability to understand the study information sheets and give informed consent
- An ability to walk 10m without a walking aid

- No history of, or planned major surgery on the hip, ankle or back
- No subject-reported pain or impaired function of the hip, ankle or back
- No other condition including neurological, musculoskeletal or visual condition that may alter the way subjects perform activities of daily living; walking, stair ascent/decent, sitting-to-standing
- Within the age range of 18 – 75

Suitable candidates were sent the 'ARUK Patient Information Sheet' to read, outlining the study protocol and additional ethical considerations, and given at least 24 hours before making the decision to take part in the study. Willing candidates were then consented using the 'ARUK MOCAP Consent Form' (Appendix B.1) and the 'ARUK SAMPLES Consent form' (Appendix B.2) during the day of study prior to assessment or fluid collection.

2.1.2.2 Control subjects

Control subjects were involved in both gait analysis and serum biomarker quantification aspects of this thesis. Inclusion of subjects in the comparator analyses involved outlier identification methods for both biomechanical and biological variables, since it was not possible to assess for potential undiagnosed joint damage using MRI. Recruitment of non-pathological controls was done through study advertisement in the form of posters, university-wide email promotion and word of mouth. When volunteers showed interest in the study, they were first screened using the following inclusion criteria:

- Ability to understand the study information sheets and give informed consent
- No history of major traumatic lower limb joint injury, or lower back injury
- No history of lower limb joint surgery, or lower back surgery
- No subject-reported pain or impaired function of the knee, hip, ankle or back
- No other condition including neurological, musculoskeletal or visual condition that may alter the way subjects perform activities of daily living; walking, stair ascent/decent, sitting-to-standing
- Within the age range of 18 - 80

Suitable volunteers were given the ARUK 'Healthy Volunteer' information sheets for Motion Capture Analysis to read, outlining the study protocol and additional ethical considerations, before agreeing to take part in the study. Willing candidates were then consented using the ARUK Healthy Volunteer Consent form.

2.1.2.3 OA subjects

The unicompartmental OA (uOA) cohort presented KL grade II – IV knee osteoarthritis in the medial knee compartment and were diagnosed with radiographic static knee malalignment (1.9° – 15.4°). KL grading is defined as (Brandt et al., 1991):

KL grade II – 'definite joint space narrowing (JSN) and possible osteophytic lipping'
KL grade III – 'multiple osteophytes, definite JSN, sclerosis, possible bony deformity'
KL grade IV – 'large osteophytes, marked JSN, severe sclerosis and definite bone deformity'

The uOA group were chosen as a comparator representative of disease advancement/severity rather than severe total joint OA since knee FCDs have been commonly reported to predispose to unilateral OA on their natural course, rather than total joint OA which may occur in much later stages (Davies-Tuck et al., 2008b, Carnes et al., 2012, Spahn and Hofmann, 2014). Unilateral OA joint tissue damage, similarly to tibiofemoral FCD damage, is focal in nature, typically isolated to a single compartment of the knee. Therefore, it is likely they experience similar pathophysiological and etiological characteristics. Finally, unilateral OA subjects are generally younger with lower BMIs relative to severe OA subjects, which means they are more demographically matched. This was an important consideration for analysis since age and BMI are thought to be confounding factors due to their influence on biomechanical gait measures (Loeser et al., 2016, Felson et al., 2000, Andriacchi and Muendermann, 2006) and biomarkers of tissue turnover, degradation and inflammation (Chung et al., 2009, Dore et al., 2010, Gibon et al., 2016).

Patients with symptomatic joint OA confirmed by clinical radiographic assessment were referred to CAVOC and recruited by other researchers through the clinical pipeline. uOA subjects were listed on the orthopaedic surgery list for high tibial osteotomy (HTO) surgery to realign the mechanical joint axis. Following initial contact from clinical liaison, the patient was contacted by a researcher and the following recruitment criteria were applied:

- Ability to understand the study information sheets and give informed consent
- Ability to walk 15m without a walking aid
- No history of, or planned major surgery on the hip, ankle or back
- No other condition including neurological, musculoskeletal or visual condition that may alter the way subjects perform activities of daily living; walking, stair ascent/decent, sitting-to-standing

- Within the age range of 18 – 75

Suitable candidates were sent the 'ARUK Patient Information Sheet' to read, outlining the study protocol and additional ethical considerations, and given at least 24 hours before making the decision to take part in the study. Willing candidates were then consented using the 'ARUK MOCAP Consent Form' (Appendix B.1) and the 'ARUK SAMPLES Consent form' (Appendix B.2) during the day of study prior to assessment or fluid collection.

2.1.3 Cohort assignments

These final cohort assignments to each subsequent chapter is presented in Table 2.1-1:

Table 2.1-1 – Cohort chapter assignments

Chapter	Analysis type	FCD	Control	Unilateral OA
3	Gait analysis	✔	✔	
4	Synovial fluid biomarker analysis	✔		✔
	Serum biomarker analysis	✔	✔	
5	Combined gait analysis & synovial fluid biomarker analysis	✔		✔

2.1.4 Time points for longitudinal assessment of FCD subjects undergoing microfracture surgery

A secondary objective of chapters 3 and 4 were to assess functional, biological and clinical longitudinal outcomes of microfracture surgery utilizing indicators of FCD pathogenesis identified from cross-section analyses. To meet these objectives, two time-points were decided (Figure 2-1). Gait analysis was carried out once prior to surgery (Time-point 1) and again six-months following surgery (Time-point 2). Whereas synovial fluid and serum were collected at time of surgery and again at Time-point 2. Time-point 1 was typically within 1 week prior to surgery (mean (SD): 3.5(±3.4) days), which depended on the date of the pre-administration prior to surgery and availability of the subject. The six-month time point was decided based on several factors including:

(1) The limitation of the data collection period – The time period for data collection was initially limited to 1.5 years post-study approval, to allow time for data-processing and analysis of the full dataset.

(2) The rarity of the subjects for analysis – Due to the low number of subjects diagnosed with knee FCDs in the NHS patient lists, it was not possible to recruit the required number of subjects within a short time-frame. A six-month time-point ensured a higher number of subjects could return for follow-up assessments within the given time frame.

(3) The willingness of participants to return for follow up assessments – Due to the demand of time required from each subject involved in the study (up to four hours of gait analysis), it was not possible to recruit subjects for multiple time-points.

(4) The minimum number of months post-surgery when clinical factors including pain, symptoms and self-perceived function were found to indicate post-operative outcome. – This was recommended by the consultant orthopaedic surgeon involved in the study, where it was believed a 6-month time point was most commonly when differing response to treatment is reported.

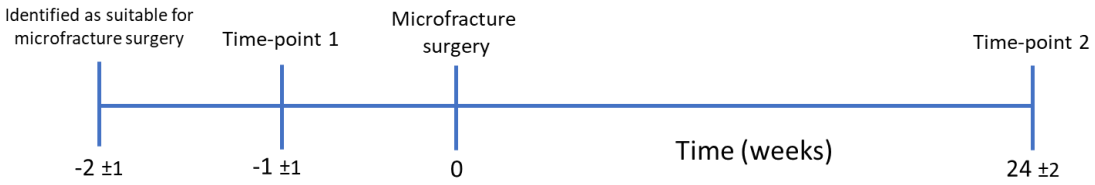

Figure 2-1 - Timeline for assessment of FCD subjects. At time-point 1, gait analysis was carried out subjects were recruited for assessment of biomechanical function

2.2 Clinical data collection

2.2.1 Subject-reported questionnaires (clinical scores)

Subject-reported questionnaires used in OA research are designed to capture relevant clinical information regarding disease related factors such as symptoms and pain. Due to the score-based system (most commonly Likert scales) often employed, this allows the generation of semi-quantitative data representative of these factors that can be used in standard statistical analyses as continuous or categorical variables to investigate associations to biomechanical, biological or other quantitative variables.

The Knee Osteoarthritis Outcome Score (KOOS) is one more commonly used in the knee pathology field and has been validated for measuring the patient-reported outcomes of several orthopaedic surgeries including ACL reconstruction, meniscectomy and total knee replacement (Rodriguez-Merchan, 2012). It was designed to be used for knee injury patients that are at risk of PTOA following ACL injury, meniscal loss or chondral damage, therefore making it fitting for this thesis' objectives (Roos et al., 1998, Roos and Lohmander, 2003). The KOOS is now also commonly used in advanced disease stage research including severe OA, which makes it an ideal candidate considering the comparator groups within this study. A broad range of clinical factors are evaluated over five subscales and forty-two individual Likert-based questions (Appendix C.1), including:

- Symptoms – e.g. knee stiffness, locking, instability)
- Pain – e.g. acute pain, resting pain, pain during various daily activities
- Ability to perform activities of daily living - e.g. walking and stair ascent/descent
- Ability to perform sports and exercises - e.g. squatting, running, jumping
- Quality of life – e.g. mood, affected lifestyle

Each question is scored, and then total scores are converted into composite scores for each subscale with a range of 0 – 100 (100 being the best possible condition and 0 being the worst possible condition). Within this study, the KOOS was used cross-sectionally to evaluate test group differences at baseline as well as longitudinally to assess the six-month outcomes of microfracture surgery. KOOS scores were also used as continuous variables in chapters 4 and 5 to relate to biological variables and in multivariate analysis models.

All individual FCD and OA subject KOOS scores are found in Appendix A.2

2.2.2 Clinical notes

To aid interpretations or explore explanatory causes of biomechanical and biological differences between individuals or groups, relevant clinical information was collected from patient clinical and surgical notes reported by clinical liaison including consultant orthopaedic surgeons and general practitioners. These included:

- Disease severity scores – i.e. Kellgren-Lawrence grades, Outerbridge scores
- Affected knee compartment
- Co-morbidities – such as ligament tears, meniscal tears, meniscal loss / extrusion
- ACL laxity (Pivot-shift) test results
- Static knee alignment – radiographs for OA subjects, clinical examination for FCD
- Prior surgical or non-surgical history of condition
- Time since initial injury
- GP and consultant notes or letters
- Analgesic or NSAID use on day of surgery
- Surgical plan
- Surgical outcomes

Height, weight, history of condition and analgesic / NSAID use within 48 hours prior to the gait session were recorded during the gait analysis sessions (at baseline and at six-month time-point). All FCD locations were recorded as in 'weight-bearing' region of medial or lateral knee compartment, however anterior or posterior locations were not reported. K-L grades were not recorded for FCD subjects due to lack of radiographs captured (this is not common in standard clinical procedures at this stage of disease) as it was deemed 'unnecessary' exposure to X-rays. Outerbridge grades were not collected for OA subjects since HTO surgery does not involve exposure of the knee surfaces to allow cartilage scoring.

Clinical findings for FCD and OA subjects are found in Appendix A.1

2.3 The objective assessment of lower limb function using 3D gait analysis

2.3.1 Laboratory hardware

All motion capture data was collected at the Musculoskeletal Biomechanics and Bioengineering Centre gait analysis laboratory at Cardiff University (). The laboratory hardware consisted of nine Qualisys Oqus 7 optoelectric infrared (IR) cameras (Qualisys, Sweden) positioned around the perimeter of the lab, six hidden floor-embedded force plates positioned along an eight-metre walkway running throughout the centre of the laboratory (Bertec Corporation, Ohio, USA), and fourteen wireless electromyography (EMG) electrodes (Delsys Inc, Massachusetts, USA).

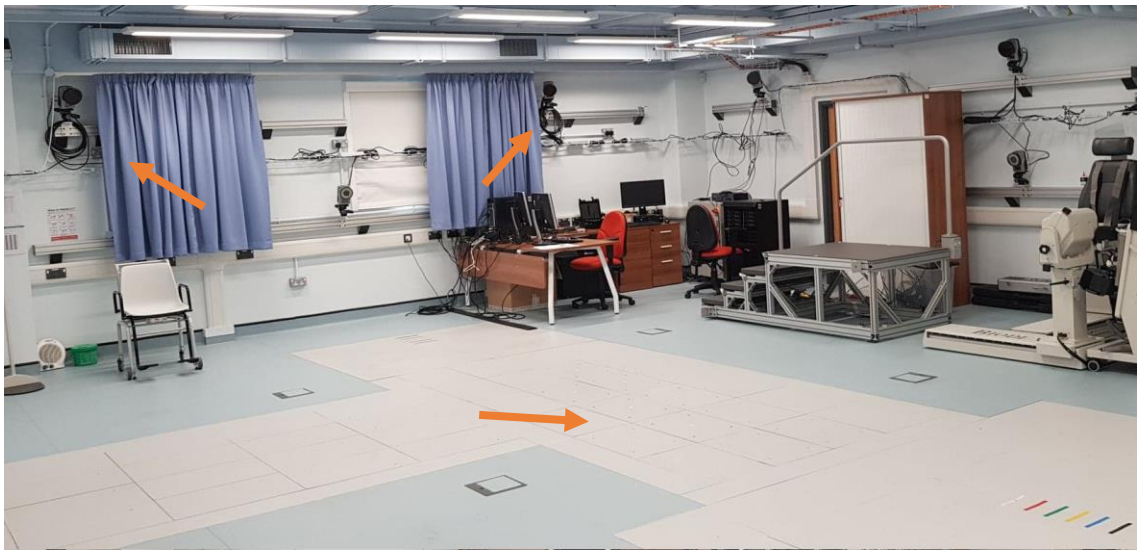

Figure 2-2 - Musculoskeletal Biomechanics Research Facility motion analysis laboratory

The IR cameras emit IR light from a set of light emitting diodes, which is reflected back to the cameras by a set of polystyrene retro-reflective markers placed on the subjects body. The reflected light is detected by sensors in the camera, which was set to capture at 120Hz. Using the reflected light, the cameras can individually generate 2D images of marker locations within its field of view, which when combined with multiple calibrated cameras can generate accurate 3D reconstructions of marker locations. The cameras were therefore positioned to optimally cover the area of the lab containing the force-plates whilst maximally increasing the likelihood of adjoining cameras viewing the same markers. This is because increasing the number of IR-cameras viewing a marker at one

time increases the accuracy of calculations of its co-ordinates due to the increased information available for reconstruction of data.

The floor embedded force plates use 4-strain gauge-based load cells to detect forces in 3 axes, allowing the measurement of vertical, frontal and sagittal plane ground reaction forces (GRFs) to floor contact at a sample rate of 1080Hz, to be synchronous with the IR cameras. The plates are of dimensions 60cm by 60cm, designed and placed optimally to account for individual subject variations in step length and foot size. The raw voltages produced by the load cells were amplified by a gain of -5 to +5 to account for the -10 to +10 operating window of the analogue board that processes its signals. Dummy force-plates (wooden blocks) were also placed alongside active force-plates with a similar vinyl coating so that subjects were not able to target them, as this would result in voluntary gait alterations.

Trigno™ EMG electrodes were wireless electrodes that are attachable to the skin surface following preparation. The electrodes record electrical activity of the muscle contraction in millivolts (mV) at a sample rate of 1000Hz. Two sets of electrodes are housed within the base of each component with a differential amplifier. Electrical signals from both electrodes are collected simultaneously and then subtraction algorithms are used eliminate noise (i.e. common frequencies caused by contact with skin and ambient electromagnetic radiation caused by surrounding electrical equipment or from the inherent noise in the EMG components themselves) from the signal output.

The IR cameras, force-plates and EMG electrodes were all connected to a 56-channel analogue board which allowed simultaneous recording of kinematic, kinetic and EMG data with synchronisation using a Delsys trigger module (Delsys Inc, USA) that sent out a TTL pulse sent via a single trigger, ultimately used to start and to stop recording.

2.3.2 3D Motion capture

2.3.2.1 Motion capture system calibration

Prior to data collection sessions, establishment of a global laboratory co-ordinate system (GCS), as well as IR-camera and force-plate calibration was carried out. This was repeated prior to every motion analysis session to account for potential changes in the camera view areas, since due to the weight of the cameras they are subject to 'drooping' over time, as well as manual adjustments by other researchers.

The establishment of an orthogonal global co-ordinate system (GCS) was achieved by aligning an L-frame in the centre of the lab, such that the long arm was facing along the length of the laboratory which defines the y-axis, and the short arm was perpendicular representing the x-axis. A vertical z-axis was generated based on the orthogonal axis to the first two, which projects from the adjoining centre of the L-frame. The marker at the adjoining corner of the frame defines the global origin (0, 0, 0), whereby all the 3D reconstructed data coordinates generated from the cameras during data capture are described relative to, based on the GCS definition.

Next, calibration of the IR-cameras was carried out using the calibration wand method. This consisted of moving a calibration wand with a fixed dimension and two rigidly connected reflective markers through the field of analysis whilst the cameras were recording – typically above the walkway area and in particular above the force-plates, where kinematic and kinetic measurements are required. Based on the wands movement relative to the statically defined L-frame during the calibration recording, a calculation is carried out to determine where the cameras locations and orientations are relative to one another and the GCS based on their 2D views of the wand markers and L-frame markers. Once the calibration recording was completed, 3D positions of the markers are reconstructed in Qualisys and errors were returned for every camera representative of the residuals between them for estimated dynamic wand marker location – typically between 0.4 to 0.8mm. If residual errors exceed 1mm, the calibration procedure was repeated to avoid poor marker tracking during the subject recordings. Finally, the calibrated volume is visually assessed to determine any major gaps in which the calibration wand was not moved through that could result in poor marker tracking for that given area in the field of analysis.

Additionally, force-plates were recalibrated due to previous session measured locations changing based on potential camera movement. This consisted of attaching metal frames that fit around the corners of the plates with markers attached in-line with the corners. 3D co-ordinates were then generated for force-plate locations and dimensions relative to the GCS, which was required for accurate calculation of the centre of pressure (CoP). Only once all the steps for motion capture system calibration were successfully completed, subject motion capture proceeded.

2.3.2.2 Patient and control group pre-preparation

All patients and control subjects were treated the same in relation to motion capture analysis, and thus the following protocol encompasses all data collection methods:

Subjects were asked to wear loose-fitting, non-reflecting clothing in order to allow full mobility and reduce false marker detection artefacts induced by undesired reflection of IR-light, respectively. Retro-reflective markers must be visible to cameras and were attached to skin, therefore clothing typically consisted of shorts for males and females, as well as a loose-fitting top or sports bra for females.

Prior to patient preparation, anthropometric measures were taken, including height and weight, which were used to calculate the body mass index (BMI) and %BW*H, a normalisation metric for the calculation of GRF and kinetic parameters.

2.3.2.3 Electromyographic capture of muscle activation

Next, placement and securing of EMG electrodes was carried out based on the protocol in Figure 2.4-2. Seven lower limb muscles targets were selected for analysis from previous recommendations of muscles with minimal cross-talk for the accurate detection of lower limb surface signals during gait (Hermens et al., 2000). Quadriceps, hamstrings and gastrocnemii were specifically chosen for analysis due to their commonly reported involvement in early- to late-stage OA function (Duffell et al., 2014, Heiden et al., 2009, Takacs et al., 2013, Hubley-Kozey et al., 2013) as discussed in more detail in chapter 1.

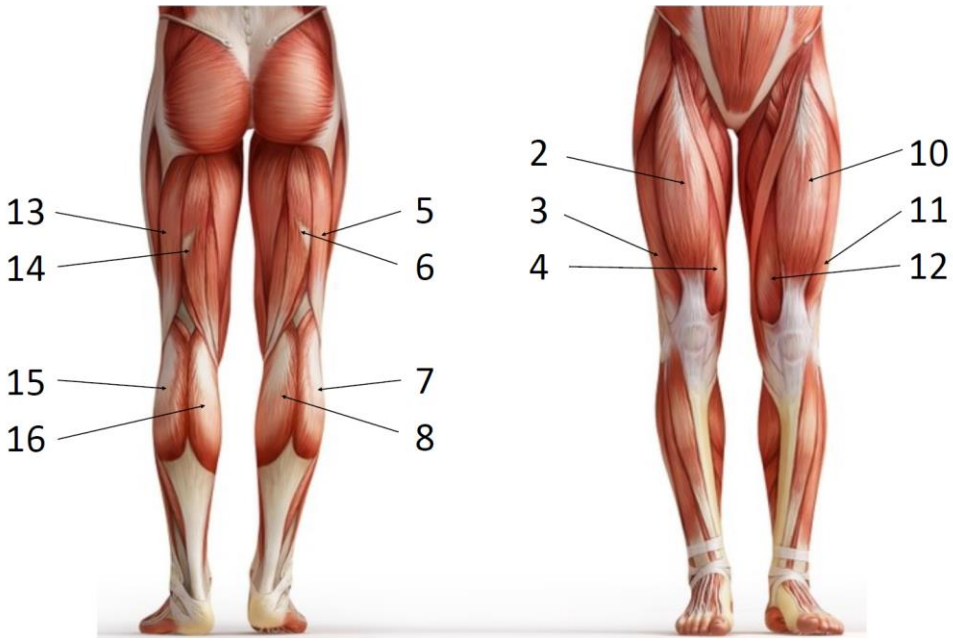

Figure 2-3 - Electromyography electrode placement protocol. Numbers represent electrode labels. Rectus femoris (2, 10); Vastus lateralis (3, 11); Vastus medialis (4, 12); Biceps femoris (5, 13); Semitendinosus (6, 14); Gastrocnemius lateral (7, 15); Gastrocnemius medial (8, 16).

Placement of EMG electrodes was based on a modified version of the Surface Electromyography for the Non-invasive Assessment of Muscles (SENIAM) guidelines (Hermans and Freriks, 1997). This firstly involved locating target muscle bellies, achieved by a combination of asking the patients to tense individual sets of muscles whilst visually inspecting, as well as palpation of the muscle region. Muscle bellies that were difficult to palpate or not visible were placed using a repeatable method using limb measurement estimations based on SENIAM guidelines (Hermans and Freriks, 1997, Hermens et al., 2000).

Skin preparation consisted of first dry shaving skin around placement area to remove hair, skin exfoliation to remove dead skin and application of electro-gel to improve the conductivity of muscle signals. Alignment of individual muscles was pre-determined based on anatomic diagrams and EMG electrodes were placed aligned with the muscle belly. To reduce inter-operator reproducibility error, all muscle belly locating, skin preparation and placement of electrodes was performed by a single researcher. Finally, electrodes were secured using elastin tubing (Tubigrip).

2.3.2.4 Retro-reflective marker placement and marker-set

55 retro-reflective markers in total were used for motion capture data collection. The markers were specifically designed for motion analysis and consisted of a plastic hollow

spherical base with a reflective coating. No preparation was required other than applying double-sided tape to the markers prior to attaching them to the skin. Placement of markers was consistent with the Helen Hayes marker-set protocol (Collins et al., 2009, Kadaba et al., 1990) which allows accurate tracking of each segment (i.e. hip, femur, tibia and foot) in six degrees-of-freedom, but has been modified to include extra markers, as illustrated in Figure 2-4 These extra markers include medial knee, medial malleolus and iliac crest which permitted improved calculation of joint centre of rotations using regression methods (section 2.4.3.2) for more accurate estimation of joint centres (Cereatti et al., 2006).

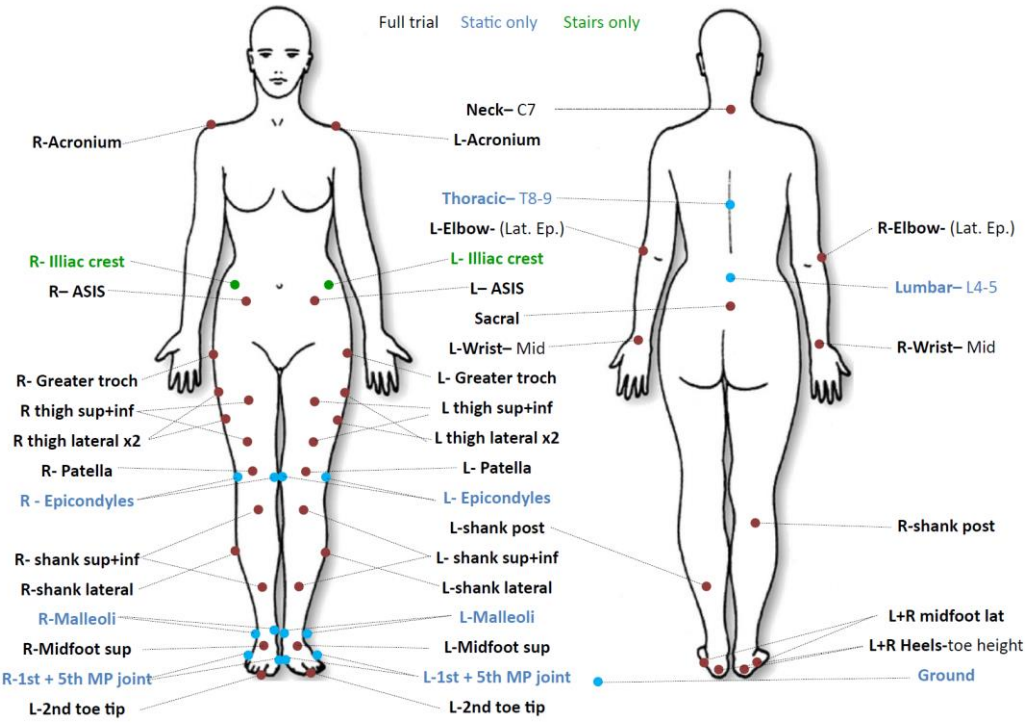

Figure 2-4 - Motion capture marker protocol. Blue markers are anatomical markers used to define 3D musculoskeletal model. Red markers are tracking markers used to measure how segments move with relation to each other to calculate angles and moments.

Anatomical markers (blue) defined in the protocol were used to define segment dimensions and centre of rotations using the static trial, whereas tracking markers (red) were used for calculations of how segments translate and rotate in relation to each other. Four tracking markers were used per segment, since at least 3 are required for calculation of rotations and translations in the three planes (i.e. sagittal, frontal and transverse) which permits for single marker drop-outs due to obstructions from clothing or equipment.

For anatomical markers, all specified bony landmarks corresponding to segment definitions were palpated to find body protrusions which were defined as the optimal location for placement for repeatability, apart from the sacral marker which was determined by surrounding visual landmarks. Tracking markers were placed around the central region of tracked segments for the thigh and shank in a consistent manner using visual cues, and foot tracking markers were located using a combination of palpation of bony landmarks, as well as visual cues.

2.3.2.5 Static calibration

Once all retro-reflective markers and EMG electrodes were placed and secured, static calibration proceeded. Static calibrations are essentially one second recorded snapshots of the placed markers, required in later stages to generate 3D models in Visual3D software. The subject remains still in view of the cameras so that Visual 3D software can accurately model where the markers are in relation to each other. In any instance where a marker had fallen off during a trial, another static calibration was captured in order that the Visual3D model be updated of the new marker locations with respect to each other.

2.3.2.6 Walking trials

The subjects were asked to walk at a self-selected speed along the force-plate walkway in bare feet towards a focal spot on the opposite side of the lab with a 3m run up prior to contact with the force-plates. Whilst recording data, two researchers were present to observe successful force-plate hits which involved the placement of all contact areas of the foot within the centre, at least ~2cm away from the edge of the plate. One researcher observed alignment of the foot along the length of the walkway, whilst the other observed foot placement perpendicular to the walkway. Walking trials commented until at least six successful force-plate hits from each limb was obtained. Walking trials were reviewed following each successful trial to ensure correct contact with the force-plates and that no data artefacts (i.e. false marker recording from light reflections, markers obscured by clothing or equipment, abnormal force or EMG signals) were present.

2.3.2.7 Sources of error in data collection

Errors in defining the location of the force-plates relative to the GCS due to incorrect placement of the L-frame or force-plate calibration frame can result in errors in reconstructions of the force vectors in relation to the applied centre of pressure. If the generated force vector is inconsistent with the relative marker location data, inaccuracies will be present in the calculations of kinetic parameters around the examined joint.

Misalignment of EMG electrodes with muscle bellies can result in poor signal from the muscle causing low signal-to-noise ratios which may increase errors in final calculation of normalised muscle activation waveforms, as well as increase cross-talk from surrounding muscles, thus reducing specificity of the signal. Whereas misplacement of retro-reflective markers on skin, particularly for anatomical landmarks, leads to inaccurate calculation of joint centres. This can lead to large errors in the calculation of joint rotations and moments from musculoskeletal models.

The goal of motion capture is to accurately record the movement of bone segments relative to each other, to allow estimations of segment rotations and joint moments. However, as a subject moves, soft tissues including muscle, fat and skin move independently of the bone due to muscle contractions and inertial effects on tissues. As markers are attached to the skin, this can lead to inaccuracies in the calculation of segment kinematics. This is a well-recognised limitation of motion analysis which has been validated by the disparity of kinematic calculations using skin markers compared to bone pins, however currently there is no solution to eliminate this in skin-marker based motion capture (Benoit et al., 2006). However, it is possible to reduce the overall influence on calculation by placement of tracking markers on differing anatomic locations of the segments including the lateral, anterior and posterior shank and thigh as demonstrated in the marker protocol Figure 2-4.

2.3.3 Generation of biomechanical variables

2.3.3.1 Visual 3D

Visual 3D (C-motion, USA) is an academic and commercial biomechanics research software that provides in-software tools used for the generation of musculoskeletal models, calculation of biomechanics data (including spatio-temporal parameters, muscle activity waveforms or kinematic and kinetic waveform data), processing of waveform

data (such as normalisation, filtering, and rectification) and parameterisation of waveform data (such as calculation of maximum or minimum values). In-software pipeline tools also allows for the generation of scripts to run a sequence of functions to eliminate the requirement of manual processing. Marker data, force data and EMG data recorded and saved within Qualisys Track Manager as a .qtm file is exported as .c3d for compatibility with Visual 3D for processing.

2.3.3.2 Musculoskeletal model generation

A six degree of freedom musculoskeletal model (three rotations, three translations for every joint) was generated for each subject, which included generation of eight segments from anatomical markers.

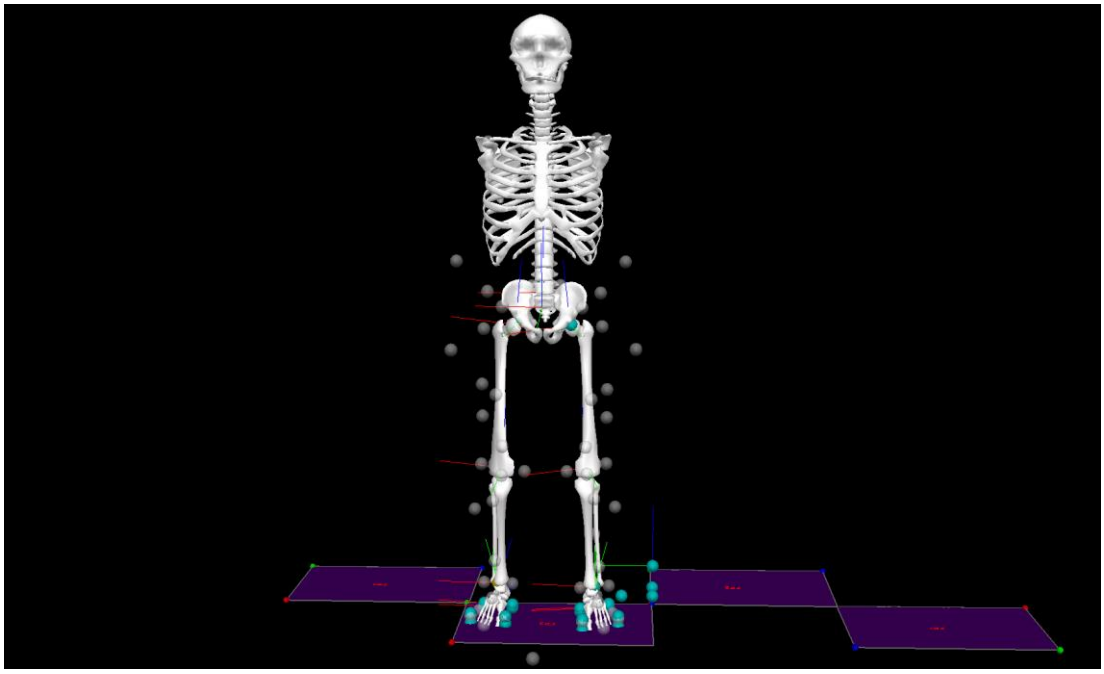

Figure 2-5 - 3D Musculoskeletal model defined using 9 segments from anatomical markers in Figure 2-4 and targets defined in

Table **2.3-1**: Thorax/spine, left and right thigh, left and right shank, left and right foot.

Each segment was defined by anatomical markers as follows:

Table 2.3-1 - Anatomical markers used to build each model segment

Segment	Proximal target	Distal target
Thorax	L R Shoulder	L R Iliac crest
Pelvis	L R ASIS	Sacral
Thigh	Hip joint centre Table 2.4-2	L R Epicondyles
Shank	L R Epicondyles	L R Malleoli
Foot	L R Malleolus	1st + 5th MP Joint

The centre of rotations were calculated for each segment in the static model based on previous recommendations (Bell et al., 1990, Collins et al., 2009, Goulermas et al., 2005) and described in terms of their mediolateral (ML), anteroposterior (AP) and axial offset coordinates relative to the segment/anatomical markers that define the segment dimensions:

Table 2.3-2 – Centre of rotation definitions. Dist (R-L #) = Distance between right and left #.

Joint Centre	Offset from	ML	AP	Axial
Right Hip	Pelvis centre	0.36*Dist (R – L ASIS)	-0.19*Dist (R – L ASIS)	-0.30*Dist (R – L ASIS)
Left Hip	Pelvis centre	-0.36*Dist (R – L ASIS)	0.19*Dist (R – L ASIS)	0.30*Dist (R – L ASIS)
Knee	R Epicondyle	0.5* Dist (R – L epicondyle)	-	-
Ankle	R Malleolus	0.5*Dist (R – L malleolus)	-	-

2.3.3.3 Calculation of kinematic data

The joint coordinate system for expression of lower limb kinematics defined by Grood and Santay (1983) is widely accepted (Wu and Cavanah 1995). The position and rotation of each segment was determined relative to either the lab coordinate system origin or relative to a reference segment, which can be either the proximal or distal segment to that joint. In motion analysis gait studies, rotations of lower limb segments (i.e. thigh,

shank and foot) are often expressed relative to either proximal or distal segments (Buczek et al., 2010). Within this study, the proximal reference system was used. For example, the rotation of shank was calculated relative to the thigh segment.

The rotations were described using the default Visual 3D Cardan sequence system, which uses the ordered sequence of rotation (x, y and z) that assumes the X axis is the medial/lateral direction (flexion-extension), Y axis is in the anterior/posterior direction (abduction/adduction) and Z is the axial direction (longitudinal rotation), which is based on ISB recommendations (Kadaba et al., 1990). The output of these rotational calculations for each joint in the motion capture recordings is in the form of x, y and z rotations in relation to the reference segment for each frame of the captured recording, which presented as a time-series makes up kinematic biomechanical waveforms.

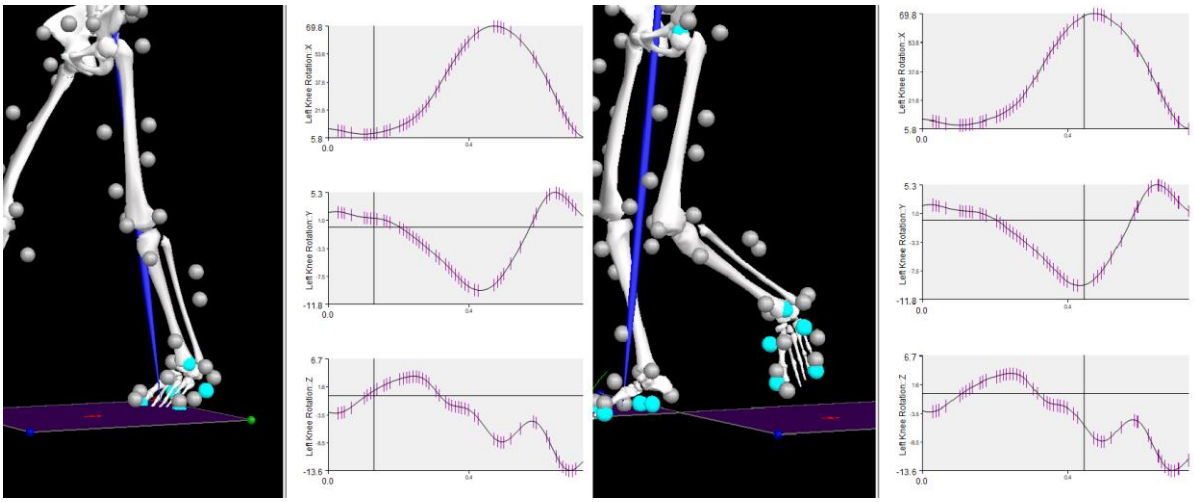

Figure 2-6 – Example of calculated dynamic angle waveform outputs from linking musculoskeletal model-based data to movement trial data

The direction (i.e. positive, negative) of the calculated angles were described such that flexion, adduction and internal rotation are positive:

- Flexion (+) / Extension (-) angles
- Adduction (+) / Abduction (-) angles
- Internal rotation (+) / external rotation (-) angles

Joint angle data used for waveform analysis were broken down into individual angle waveforms representative of rotations for a single gait cycle (heel-strike to heel-strike). The number of captured data points in the time-series was normalised to % gait cycle so that one point on the waveform was equal to a single percent.

2.3.4 Calculation of kinetic data

Ground reaction forces (GRFs) vectors in the x, y and z plane are measured within calibrated string-gauge components of the force-plates previously described which allowed the calculation of vertical, mediolateral and anteroposterior force vectors. All GRFs were normalised to bodyweight to make meaningful comparisons within inter-subject and inter-group comparisons.

The external joint moment is the rotational force acting at the joint created by the ground reaction force in each plane produced during locomotion, which is counteracted by the internal moments that are produced by muscles and ligaments to keep the joint stable. External moments are often used to describe knee function, since they can act as surrogate measures to the forces acting locally at each joint and can be used to understand the function of active and passive stabilizers (Robertson et al., 2013). Joint moments in each plane are calculated as a product of the effect of inertial forces, the planar GRF and the shortest distance (moment- or lever-arm) between the centre of joint rotation and the GRF vector (Figure 2-7), which depends on the centre of pressure, centre of mass and mechanical axis alignment of the joint.

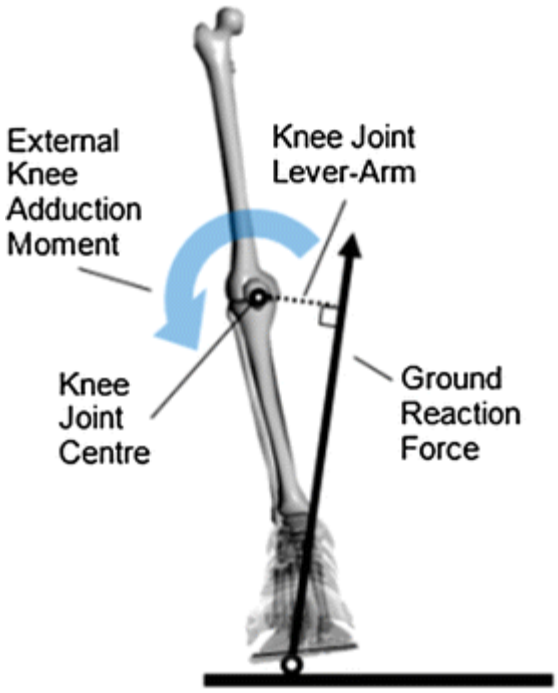

Figure 2-7 - Example of factors required for calculation of knee adduction moment (Lewinson and Stefanyshyn, 2016)

There is no standard reference frame for expression of joint moments (Schache 2008). Moments can be expressed using the distal segment coordinate system (Gok 2002, Kaufman 2001), the proximal segment coordinate system (Schache and Baker 2007), or the joint coordinate system, which is a combination of both systems (Astephen 2008, Landry 2007). Within this study, moments were calculated using the distal segment resolution co-ordinate system for resolving forces at the examined joint, in order to integrate and compare with the pool of previously collected motion analysis data in our research group. Similarly to angles, joint moments were calculated at each frame and converted into time-series data for waveform analysis. Moments were also normalised to %Bodyweight*Height, since calculations take into account GRFs and the moment lever arm which is affected by limb length. This is to allow meaningful relevant inter-subject comparisons. The direction of the moments acting at the joint were described similarly to angles, such that:

- Flexion (+) / Extension (-) moments
- Adduction (+) / Abduction (-) moments
- Internal rotation (+) / external rotation (-) moments

Joint moment data used for waveform analysis were broken into individual moment waveforms representative of a single stance-phase cycle (heel-strike to toe-off), since calculated joint moments of interest are those of when the GRF is acting at the joint (i.e. when the joint is being loaded).

2.3.5 Calculation of spatio-temporal parameters

Visual 3D pipeline tools were also used to calculate several spatio-temporal parameters:

Table 2.3-3 - Calculations for spatio-temporal measures

Parameter	Calculation
Gait speed	Distance of heel-strike to heel-strike divided by time of a single gait cycle
Stance time	Time of heel-strike to toe-off
Swing time	Time of toe-off to heel-strike
Double limb support time	Time whereby both feet at in contact with the ground

2.3.6 Generation of muscle activation waveforms

As previously mentioned, raw EMG signals are differentially amplified within the Trigno electrodes to eliminate noise from electromagnetic radiation such as from power lines, leaving the signals that make up the difference at the two electrodes from the muscle. However, differential amplification only removed a proportion of the noise that is not part of the wanted EMG signal (Chowdhury et al., 2013). Furthermore, the amplitude of EMG signals is stochastic and therefore further elimination of unwanted frequencies and further processing is required to generate a meaningful signal for comparison, particularly since waveform analysis was carried out in this thesis. The following steps were carried out in Visual 3D using pipeline tools for processing of EMG signals:

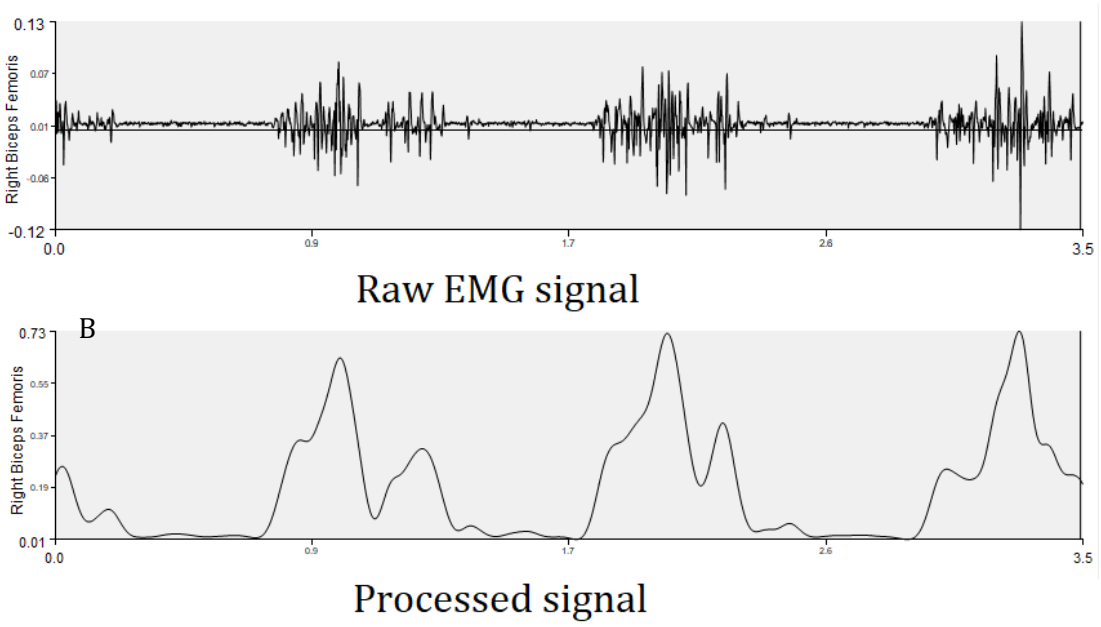

Figure 2-8 - Example of raw EMG data captured using Trigno sensors (A) and final processed muscle activation waveform signals (B)

(1) DC offset correction – Average raw EMG signal values were calculated and then subtracted from the total signal to correct for DC offset of the signal from zero

(2) Bandwidth filtering – A high-pass filter with a frequency cut-off of 20Hz followed by a low-pass filter with a cut-off of 400Hz were applied to eliminate noise contamination

(3) Signal rectification – Full-wave rectification was used to convert negative signal data into positive data by converting to the absolute value of each data point

(4) Linear envelope – The linear envelope of the signal was computed by calculating root mean square (RMS) values for 100ms moving windows, to create a smooth signal waveform

(5) Peak dynamic normalisation – The EMG signal was divided by the maximum value of the EMG signal for that trial, so that the magnitude of the waveform is expressed as muscle activity relative to the maximum activity achieved during that trial

Processed muscle activation waveforms over whole trials were broken into individual waveforms representative of single gait cycles (heel-strike to heel-strike) for inter-subject or inter-group comparisons using waveform analysis methods.

2.4 Methods for analysis of temporal waveform data

The calculated dynamic biomechanical or muscle waveform data characterising lower limb function exists as temporal waveforms of normalised magnitude of the examined parameter against percentage of stance phase or gait cycle (from 0 – 100%). There are characteristics of this data that must considered for a meaningful analysis:

Firstly, there are a large amount of data owing to biomechanical interpretation. Each waveform is composed of 101 points, each of which describes kinematic movement and kinetic information, much of which may not be useful to group comparison. Due to the high dimensionality of the data, simple comparison of variance testing is not applicable. Secondly, there is considerable variability in the data which may be related to kinematic and kinetic differences that either occur between subjects, considered inherent inter-subject variability, or that occurs between groups which is of primary interest. Extracting salient information from that which is considered noise is challenging, and so methods to retain the most important discriminatory features are often explored (Chau, 2001).

Typically, there are two approaches to evaluate temporal waveform data employed in biomechanics studies, both aimed at reducing the data into discrete summative measures for statistical testing. Parameterisation, which involves extracting discrete parameters such as waveform peaks (e.g. minimal and maximal values) and integrals (area under the curve), and multivariate methods that consider the entire waveform, such as principal component analysis (PCA) and factor analysis. Although discrete parameterisation generates an easily interpretable set of variables that describe key features of the waveform, much of the important and potentially discriminatory

temporal information is discarded. Another limitation of parameterisation is that consistent quantification of comparable features is not always possible, due to the highly variable nature of human locomotion.

As discussed previously, the calculation of joint angles and moment waveforms can be prone to offsets due to errors in marker placement and force-plate calibration (2.4.2.7). Considering the last two points discussed above, it is only possible to detect meaningful differences when the inter-group differences are much more prominent than both inter-subject differences caused by offset error and inherent inter-subject variability, rendering it unreliable for detecting group differences.

Each point of a waveform is related to adjacent points in the parameter, as well as those of other waveforms within the same point of the gait cycle. Multivariate statistical techniques such as PCA take advantage of the collinear multidimensional nature of waveform data. Both supervised (compute using prior grouping information about the variables) or unsupervised methods exist, which both serve to reduce data and highlight patterns in potentially correlated multivariate data related to common modes, or 'features' of variance. PCA has advantages over other methods. Firstly, it transforms the data into a smaller set of linearly independent unique variables which can be interpreted, of which only a few are needed to adequately explain the original data. Secondly, it generates a set of 'scores' for each subject, based on their data relative to the model, allowing further exploratory analyses such as comparison of means (e.g. t-tests), regression, clustering methods as well as discriminatory analyses. Due to advantages and the large number of gait biomechanics studies employing PCA in current literature, it was used for the primary analysis within this thesis for analysis of biomechanics data. PCA has previously been utilized more than other multivariate methods, thus allowing for better comparability to previous studies.

2.4.1 Principal component analysis of biomechanical waveforms

Mathematically, PCA takes a number ($\boldsymbol{p}$) of potentially correlated variables $\boldsymbol{X} = \boldsymbol{x_1}, \boldsymbol{x_2}, \dots, \boldsymbol{x_p}$ from $\boldsymbol{n}$ observations and converts them into a reduced number of independent, uncorrelated variables $\boldsymbol{Z} = \boldsymbol{z_1}, \boldsymbol{z_2}, \dots, \boldsymbol{z_p}$ through orthogonal transformations, which are arranged in a hierarchy of decreasing sample variances. The resulting variables, known as principal components (PCs), are summative measures related to the original shape of the examined waveform that are representative of common variances of the waveform. Within this study, PCA was applied to biomechanical

and muscle activation waveforms within Inspect 3D, software developed by C-motion, who also developed the biomechanical modelling software (Visual 3D) discussed previously. Their applied method was developed with Dr. Kevin Deluzio, who first introduced the application within the musculoskeletal biomechanics field as a data reduction tool to investigate differences between OA and control subject gait (Deluzio et al., 1997). It has since been used extensively in the field for analysis of biomechanical and muscle activation waveforms (Hubley-Kozey et al., 2008, Landry et al., 2007, Chau, 2001). A method for PCA was also adopted by Jones (2004) at Cardiff University alongside a classification method based on Dempster-Shafer Theory of Evidence, which has successfully been used to detect improvement of OA function following total knee replacement (TKR) surgery (Jones et al., 2006).

Since the method used presented within this thesis was that integrated within Inspect 3D, the methods described below are representative, and further extended and adapted from those outlined in (Robertson et al., 2013) of which Deluzio's methods are based:

Calculating principal components

Since within this study the original data exists as time-series data, it can be represented as a matrix

$$\mathbf{X} = \begin{bmatrix} \boldsymbol{x_{11}} & \cdots & \boldsymbol{x_{1p}} \\ \vdots & \ddots & \vdots \\ \boldsymbol{x_{n1}} & \cdots & \boldsymbol{x_{np}} \end{bmatrix} \tag{1.0}$$

whereby $\boldsymbol{n}$ is the number of subjects to be included in the model, and $\boldsymbol{p}$ is the number of time-points (samples), which in this study are 101 samples normalised to percentage of the gait cycle/stance phase (0 – 100%). PCA is applied to the columns of **X** so that the correlated variables are the $\boldsymbol{p}$ normalised samples observed on $\boldsymbol{n}$ subjects.

The next step is to calculate the covariance matrix **S**, in order to express the variance structure contained within the original data matrix. This is necessary to understand the variance in the waveform over time and how subject waveforms vary from each other.

$$\boldsymbol{S} = \begin{bmatrix} S_{11} & \cdots & S_{1p} \\ \vdots & \ddots & \vdots \\ S_{p1} & \cdots & S_{pp} \end{bmatrix} \tag{1.1}$$

By calculating the mean of the *i* th column of X, followed by the average squared distance between the mean and all *n* waveform values at that instantaneous point in time, the diagonal factors s_{ii} can be determined, which represent variance at each point of the waveform:

$$Sii = \frac{\sum_{k=1}^{n}(x_{ki} - \overline{x}_i)}{n-1}$$

(1.2)

Where i represents the column and n the number of subjects. The covariance between each pair of time instants are represented by off-diagonal elements, s_{ij}

$$Sij = \frac{\sum_{k=1}^{n}(x_{ki} - \overline{x}_i)(x_{kj} - \overline{x}_j)}{n-1}$$

(1.3)

where i and j are two of the columns and n is the number of subjects. There is a linear relationship between the two variables when the covariances are not 0. A correlation coefficient can then be calculated to evaluate this relationship:

$$r_{ij} = \frac{s_{ij}}{s_{ij}s_{jj}}$$

(1.4)

The covariance matrix **S** contains the variability structure from the original data, and the off-diagonal elements are non-zero in general, meaning that the columns of the original data waveforms are correlated. The PCs are extracted from this covariance matrix **S.** Since the final set of PCs are uncorrelated, they are associated with a covariance matrix that has all the off-diagonal elements equal to 0. Through a process called *diagonalization,* otherwise known as orthogonal decomposition in linear algebra, the original data covariance matrix **S** is transformed to the PC covariance matrix D.

$$\mathbf{U^tSU = D}$$

(1.5)

The matrix **U** is an orthogonal transformation that realigns the original data into a new coordinate system. The new coordinates are the PCs, which are aligned with the direction

of variation in the data matrix. The columns of **U** are the eigenvectors of **S,** often referred to as PC loading vectors. **D** is a diagonal covariance matrix whose elements, λ_i are the eigenvalues of **S**, and each eigenvalue is a measure of the variation associated with each PC. The number of nonzero diagonal elements of **D** is the maximum number of PCs. This is equal to the lesser of the number of subjects ***n***, or the length of the waveform *p*, which corresponds to the rank of *r* of **S.** Within the context of this study, the rank of **S** is 101 (samples), therefore the maximum number of PCs is 101. However, it is noteworthy that only a small number of these PCs will be retained in the practical application of the method that makes PCA a data reduction method. The last step is to use the matrix **U** to transform the zero-mean centred original data into the new uncorrelated PCs, **Z**

$$\boldsymbol{Z} = \left[\boldsymbol{X} - \overline{\boldsymbol{X}}\right] \boldsymbol{U} \tag{1.6}$$

Each column of **Z** is a PC, and the elements of the column are referred to as PC scores. After calculation, the PCs are ordered according to the amount of variance that each component explains in the original data, so that the first component explains the maximum amount, followed by second component which represents the maximum variance in the orthogonal plane to the first, and so on. The variance of each PC is given by the eigenvalues, λ_i which are diagonal elements of matrix **D.** The most commonly used measure of the total data variation is the sum of the variances of each variable, which is equal to the sum of the diagonal elements of **S**. The sum of the diagonal elements of a matrix, or the 'trace' (*tr*) of a matrix

$$\boldsymbol{tr}(\boldsymbol{S}) = \boldsymbol{tr}(\boldsymbol{D}) \tag{1.7}$$

In this way it is possible to quantify the portion of total variance explained by the PCs:

$$\text{Variance Explained by PCi} = \frac{\lambda_i}{tr(S)} = \frac{\lambda_i}{\sum \lambda} \tag{1.8}$$

When assessing variance explained by the PCs, both the shape and inter-variability of the original waveforms affect the variance captured, and therefore a method to retain the most important PCs in often employed.

2.4.2 Practical interpretation of PCA applied to waveform data

Several steps are involved in interpretation of PCA applied to biomechanical and muscle activation waveforms, however this is common between the two types. The following example given is based on the application of PCA to biomechanical data (knee flexion angle) from two groups, to determine waveform features of variance that differ. In order, these steps involve:

1. Applying PCA to the combined (group 1 + group 2) dataset
2. Selecting the number of principal components to retain
3. Interpretation of features represented by PCs by assessing loading vectors, extreme plots and reconstruction of original data using calculated PCs
4. Extraction and interpretation of subject and group PC scores
5. Summative interpretation of findings

(1) Applying PCA to combined dataset

Prior to the application of equations outlined in 1.1.3, the raw biomechanical waveforms are normalised to 101 points (Figure 2-9), then data from individual subjects of all tested groups is combined into a single matrix and formatted as described in equation 1.0. This is the case with a single, or multiple groups of data.

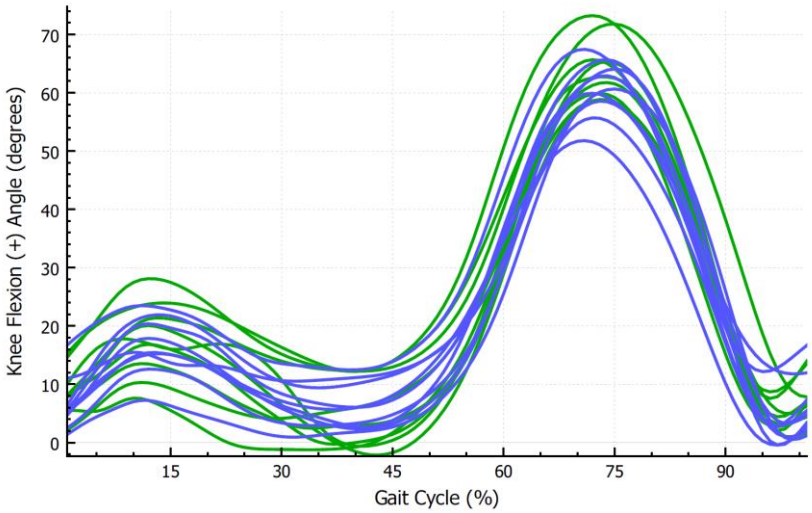

Figure 2-9 - Typical biomechanical waveform data for two test groups (green & blue) normalised to 101 points (0-100%) of the gait cycle.

(2) Selecting the number of principal components to retain

As additional PCs are calculated for a given waveform, a higher cumulative percentage of the variance from the original data is represented (Figure 2-10). The PCs representing

the highest variance that are first in order usually contain the most relevant information. However, it is notable that the highest variance components are not necessarily the most discriminatory. Ultimately, PCA is used as a data reduction tool, therefore it is desirable to select the minimum number of PCs (new discrete variables for analysis) as possible, whilst still representing salient waveform information. Therefore, it is necessary to decide on a cut-off, or stopping rule, to find the balance between informative variation and noise. In the example (Figure 2-10), it is evident that four PCs cumulatively represent over 95% of the variance in the data and with visual inspection of the scree plot, used in previous studies to decide PC retention, adding more components does not appear to substantially improve the variance explained (Robertson et al., 2013). Whilst PC4 only represents 5.19% of the variance of the original waveforms, this is still considered adequate to detect group differences over noise, however this can become subjective (Chau, 2001).

To increase objectivity of PC retention methods, previous investigators have defined cut-off rules based on eigenvalues. Kaiser's rule was one of the first and most commonly adopted, retains factors (PCs) with eigenvalues greater than 1 (Kaiser, 1960). However, this rule has been subjected to criticism, due to the high number of components it tends to retain which often have no meaningful information (Jackson, 1993). A retention rule adopted by Jones (2004, 2006) is to determine factor loadings outside the threshold eigenvalue range of -0.71 to 0.71, which are retained. This results in PCs with at least 50% of the variance from a single point in the waveform considered.

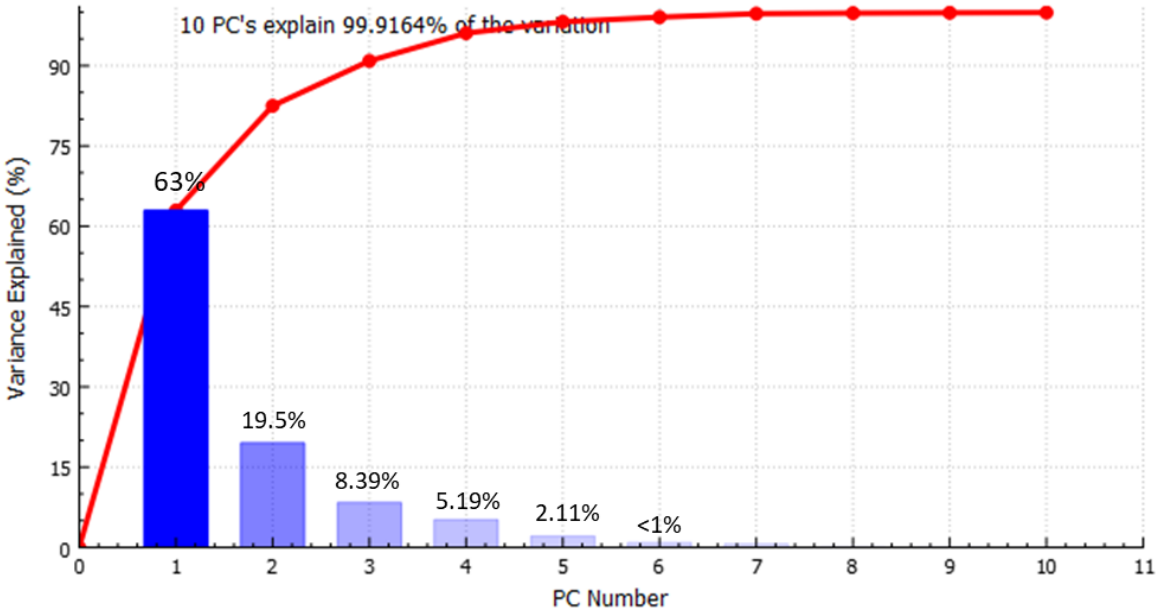

Figure 2-10 - Bar plot of variance explained (%) for each PC added to the model, with scree plot representing cumulative variance (red line). Four PCs cumulatively explain >95% variance.

Within this study, a cut-off of 95% cumulative representation of variance was used. Upon reconstructing the original waveform data using 95% of the represented variance, many of the prominent structures from the original data of most parameters can be seen (see point 3), and if meaningful group differences exist they are likely to have been picked up. Secondly, it is found particularly with biomechanical and muscle activation waveforms that between three to five PCs typically represent up to or above 95% variance per parameter. This is a suitable number of variables for downstream comparison of means testing (e.g. ANOVAs), however increasing the number of variables by increasing the cut-off will elevate the likelihood of finding a random significant difference among the data or make it very difficult to find differences due to the substantial corrections required for multiple testing.

(3) Interpretation of features represented by PCs by assessing loading vectors, extreme plots and PC reconstructions

To recap, the matrix **U** is an orthogonal transformation that realigns the original data into a new coordinate system. The new coordinates are the PCs, which are aligned with the direction of variation in the data matrix. The columns of **U** are the eigenvectors of **S,** often referred to as PC loading vectors. In the presented example, the loading vectors of the first three PCs of the knee flexion angle are shown in Figure 2-11. The loading vectors are waveforms themselves of the same number of points as the original waveforms therefore can be plotted against the same function, and the vertical axis depicts

individual sample coefficients of each vector. When the vector is close to zero, very little of the variance at that instant is represented by the PC score, and conversely the regions of the vector that are farthest from zero during the series can be interpreted as the most represented regions of variance captured by that PC.

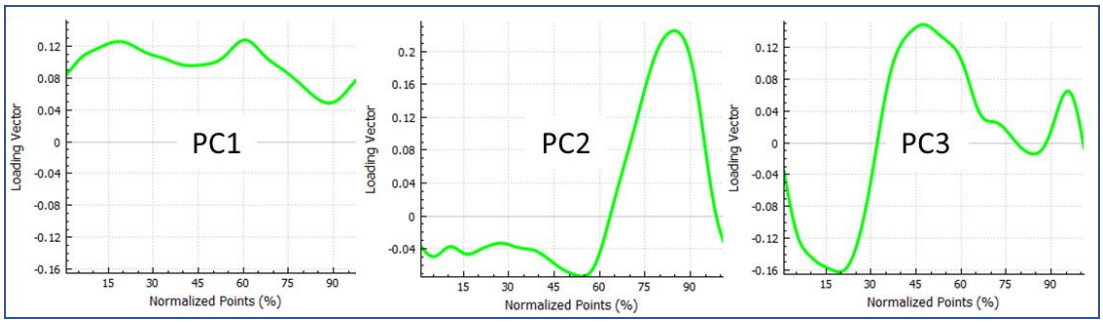

Figure 2-11 - Loading vectors for PC1, 2 and 3 of the knee flexion angle.

As explained in section 1.1.3 (equation 1.6), the PCA model is defined as $\boldsymbol{Z} = [\boldsymbol{X} - \overline{\boldsymbol{X}}]\boldsymbol{U}$. Since the eigenvector matrix is both orthogonal and normalized (orthonormal), it is possible to rearrange the equation so that $\boldsymbol{X} = \boldsymbol{Z}\boldsymbol{U}^{\boldsymbol{t}} + \overline{\boldsymbol{X}}$, allowing reconstruction of the original waveform data from the individually calculated PC loading vectors. Ultimately, these reconstructions can be used to aid interpretation of the feature of variance captured by the PC. Figure 2-12 depicts an example where all individual subject waveforms (Figure 2-9) are reconstructed using PC1, PC2 and PC3. The variance represented by the PC is visually interpreted as the shape of the overall data in regions of the waveform where the vectors do not overlap. For example, in Figure 2-12, PC1 represents the overall magnitude of the waveform, PC2 the degree of flexion during 70 – 95% of the gait cycle, and PC3 the range of knee flexion during 0 – 60% of the gait cycle.

It is also possible to aid interpretation of the PCs in a similar way by utilizing extreme plots. For an individual component, this involves plotting each point of the loading vector multiplied by the mean PC score, then also ±1 of the standard deviation (Figure 2-12). All three vectors within the same plot allows visualisation and interpretation of what the data looks like when reconstructed, with single vectors representing standard deviation of the grouped reconstructed data rather than all individual waveforms.

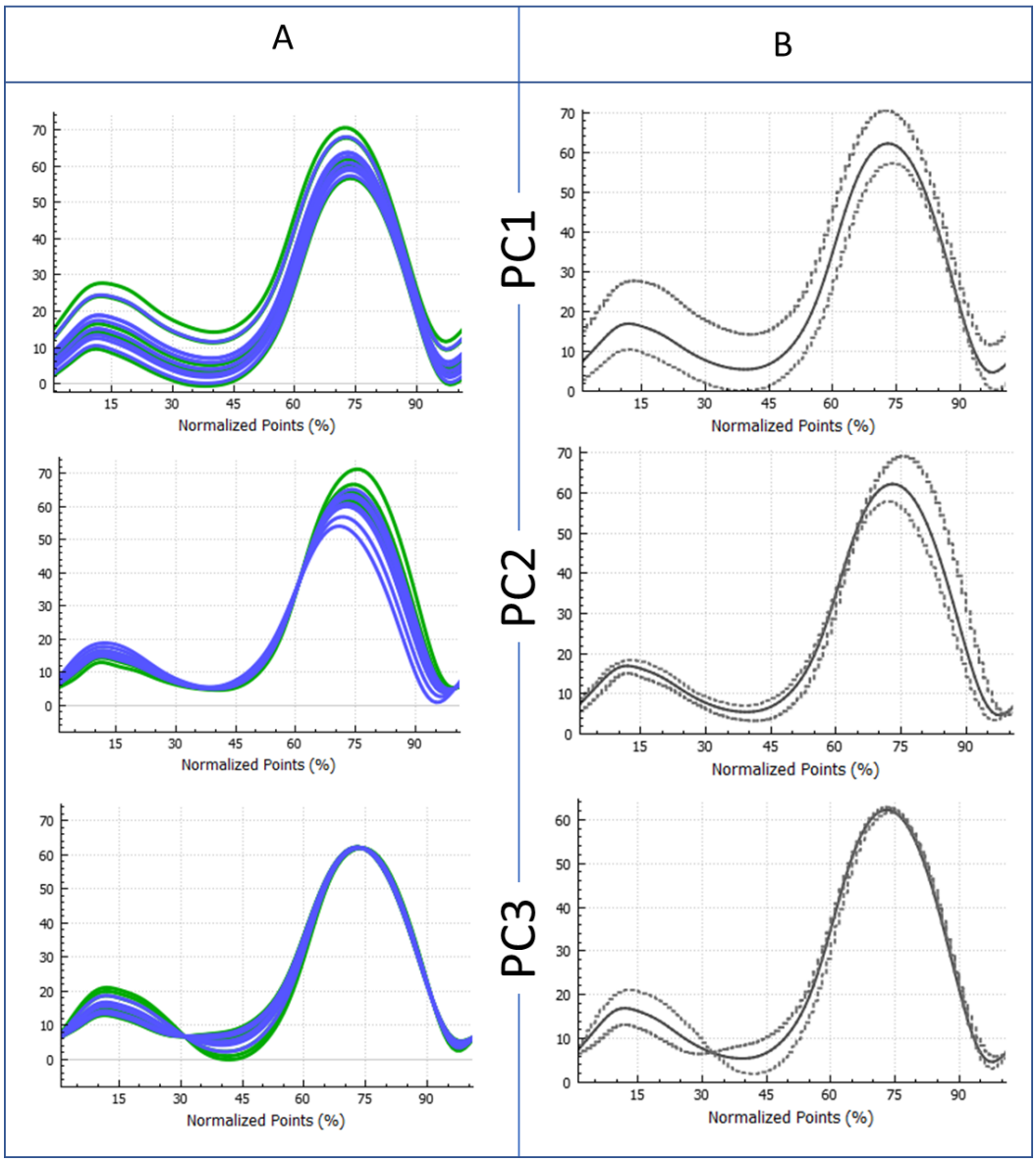

Figure 2-12 - (A) Reconstructions of individual subject waveform data using PC loading vectors. (B) Extreme plots of reconstructed data using PC loading vectors and mean (solid) and ±1 std (dotted) PC scores

(4) Extraction and interpretation of subject and group PC scores

Individual transformed observations are referred to as PC scores and are represented by the individual elements of each column of **Z.** PC scores are produced by combination of the eigenvector coefficients to the original data points. For example, to generate the first PC score for subject ***i***, the calculation is:

$$Z_{1i} = (x_{i1} - \overline{x}_1)u_{11} + (x_{i2} - \overline{x}_2)u_{21} + \cdots + (x_{1p} - \overline{x}_p)u_{p1} \quad (1.9)$$

The PC score, z_{1i} is just a linear combination of each time sample (mean corrected) of that subject's waveform and the PC loading vector coefficients. Thus, every observation (subject) included in the model is assigned a PC score per calculated PC, which is representative of the distance of the shape of that subject's waveform feature from the mean PC feature (calculated from the whole dataset). The more dissimilar the shape of the that subjects feature is from the mean, the further away both positive and negative direction their PC score is from 0, since the mean is zero-centred. This is more apparent when studying the subject waveform reconstructions, whereby the most extreme reconstructed individual waveforms are assigned the highest or lowest PC scores. The advantage of scores representative of each subject waveforms contribution to the PC is that it is possible to then use clustering analysis, regression or comparison of means testing (e.g. t-tests) to statistically compare or relate waveform features among different test groups. Once the PC scores are calculated, their class label can be elucidated, and then downstream testing applied.

(5) Summative interpretation and presentation of findings

Within this study, it was of interest to determine statistically differing features of knee FCD and control subjects biomechanical and muscle activation waveforms. Due to the low sample size, Mann-Whitney U tests were applied to the PC scores between groups to test for differences ($p \leq 0.05$). Within the biomechanics results section of chapter 2, the interpretation of the biomechanical waveform features captured by the PC alongside the Mann-Whitney U test outcome (p-values) are reported.

For features that statistically differed between groups, an extreme plot with the mean and ±1 standard deviation curves were also presented (Figure 2-13). The extreme plots are colour coded based on the determined PC score group differences. For instance, if there was a significant difference ($p \leq 0.05$) found between group A (green) who had a mean PC score of +2 and group B (blue) who had a mean PC score of -2, the +1 std curve will be colour coded blue and the -1 std curve coded green to signify how the overall group variances for the given feature differed from the mean plot. This is depicted in Figure 2-13, which represents individual subject PC3 reconstructions previously shown for the knee flexion angle, in the form of a colour coded extreme plot.

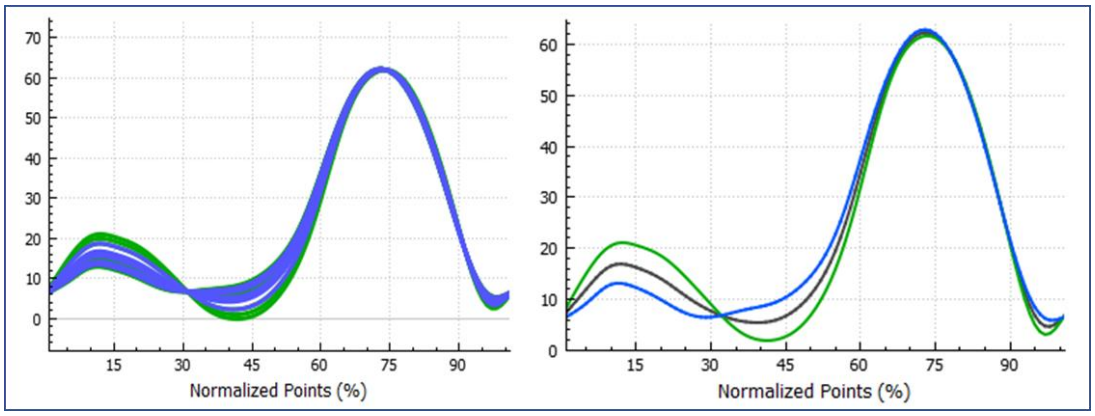

Figure 2-13 – Conversion of individual subject PC waveform reconstructions from each group (A) to extreme plots representing the mean (grey), +1 standard deviation (green) and -1 standard deviation (blue) PC waveform reconstructions colour coded to represent group differences corresponding to group mean PC scores.

2.5 Synovial fluid and serum biomarker quantification

2.5.1 Serum samples

2.5.1.1 Collection

Phlebotomy training was carried out with a UK accredited course (Phlebotomy Training Services, London UK) to carry out safe basic venepuncture on recruited adult subjects for this study (Certificate Level 2, Phlebotomy Training Services, London). Blood was collected once at day of surgery (between 7am and 5pm depending on surgery slot) prior to surgery and once again approximately six-months (±14 days) following microfracture surgery (between 10am and 1pm), prior to gait analysis.

Serum and plasma were collected via venepuncture using BD Vacutainer Safety-Lok Blood collection Sets (23g needle, 12" Tubing and Luer adaptor) (Fisher Scientific, UK) and Greiner Bio-one serum and plasma lithium heparin/EDTA collection tubes (Fisher Scientific, UK). The order of draw was conducted based on the Greiner Bio-one recommendations, which consisted of serum followed by plasma heparin and then EDTA tubes. Following successive collections, tubes were inverted five times and then kept at 4˚C before transportation to the Biosciences laboratory for processing. Serum tubes were left at room temperature to clot for 20 minutes before storing at 4˚C. Blood samples were kept no longer than 3 hours at 4˚C before transporting in a sample box with cool packs via courier to the Cardiff University School of Biosciences (BIOSI) Pathophysiology and Repair (PPR) laboratory. Care was taken not to agitate the samples during transport. Upon arrival, blood samples were processed immediately.

2.5.1.2 Processing

The protocol for processing of serum was identical to that used in the ARUK centre, permitting comparison of collected samples with pooled OA subject samples from the centre biobank. For both serum and plasma tubes, samples were first spun in their original tubes within a centrifuge at 2000G for 15 minutes, to separate serum/plasma from other blood constituents. Then, the clear fluid (plasma/serum) was carefully transferred to 1.5ml microcentrifuge tubes (Fisher-Scientific, UK) using a P1000 Gilson precision pipette, with care not to agitate the bottom layer of constituents. The clear fluids were then spun again at 3000G in a microcentrifuge for 15 minutes, to remove any

additional cells and debris. Following centrifugation, supernatants were transferred to labelled 500µl cryovials in aliquots of 100µl, with care not to disturb the cell pellet. Final aliquoted samples were stored at -80˚C until day of immunoassay.

2.5.2 Synovial fluid samples

Synovial fluid samples were obtained from the affected knee by needle aspiration prior to introduction of the arthroscope by participating orthopaedic consultant Mr C Wilson. Aspirated fluids were transferred to a 5ml falcon tube and sent via courier to the BIOSI PPR laboratory in a cool packed container within 30 minutes. The protocol for processing of serum was identical to that used in the ARUK centre, permitting comparison of collected samples with pooled OA subject samples from the centre biobank. None of the collected fluids received contained blood staining, however this information was not recorded for pooled OA samples. Immediately upon arrival, synovial fluids underwent centrifugation at 5000G for 15 minutes to remove cells. Higher centrifugal forces were required for synovial fluid processing due to the increased viscosity of the fluid. Supernatants were then gently transferred to 500µl cryovials, in aliquots of 100µl. Finally, aliquoted samples were stored at -80˚C until day of immunoassay.

2.5.3 Immunoassays

Commercially available multiplex electrochemiluminescence (ECL) or single-plex enzyme-linked immunosorbent assays (ELISAs) were utilized to measure absolute concentrations of a total of seventeen biomarkers relating to bone and cartilage turnover and degradation, mechanical loading of bone and inflammation (Table 2.5-1). Both ECL assays and ELISAs were chosen as they have been extensively by clinical studies due to their high throughput, high protein specificity and low coefficient of variance of inter- and intra-assay signal readings (Watt et al., 2016, Struglics et al., 2015, Li et al., 2016, Lequin, 2005). ELISA assays were carried out at the BIOSI PPR Laboratory, whereas MSD multiplex assays were carried out at the Central Biotechnology Services centre, Cardiff, due to the availability of the specific MSD plate reader required for chemiluminescence measurements. Where possible, each sample aliquot was freeze-thawed the minimum number of times required to cover all tests and consistently with all other test samples to avoid concentration variability caused by repeated freeze-thawed cycles. The maximum number of freeze-thaw cycles any sample was exposed to was 2x.

Table 2.5-1 – Biomarkers chosen for analysis and reference to their representation in known homeostatic processes the joint

Biomarker	Abbrev.	Representation in the joint	Reference
Cartilage Oligomeric Matrix Protein	COMP	Cartilage matrix stabiliser, chondrocyte matrix synthesis activity	(Recklies et al., 1998, Chen et al., 2007, Briggs et al., 1995, Attur et al., 2013)
C-terminal telopeptide for collagen type I	CTX-I	Bone resorption (osteoclast) activity	(Garnero et al., 2003, Nikahval et al., 2016)
Alkaline Phosphatase	ALP	Bone formation (osteoblast) activity, bone and cartilage mineralisation	(Poole et al., 1989, Burr and Gallant, 2012)
Receptor activator of nuclear factor κ-B ligand	RANKL	Canonical osteoclast pathway activation	(Odgren et al., 2003, Steeve et al., 2004, Boyce et al., 2015)
Osteoprotegerin	OPG	Canonical osteoclast pathway inhibitor	(Odgren et al., 2003, Steeve et al., 2004, Boyce et al., 2015)
RANKL:OPG ratio	RANKL/OPG	Surrogate measure of net canonical osteoclast pathway activation	(Odgren et al., 2003, Steeve et al., 2004, Boyce et al., 2015)
Glutamate	-	Glutaminergic signalling agonist, Mechanical regulator of bone physiology, inflammatory regulator	(Brakspear and Mason, 2012, Cowan et al., Wen et al., 2015)
Sclerostin	-	Wnt signalling inhibitor, mechanical regulator of bone physiology	(Robling et al., 2008, Sebastian and Loots, 2017)
Tumor necrosis factor alpha	TNF-α	Pro-inflammatory cytokine, osteoclastogenic signalling, osteoblast signalling	(Kapoor et al., 2011, Lam et al., 2000, Osta et al., 2014)
Interleukin-1β	IL-1β	Pro-inflammatory cytokine	(Attur et al., 1998, Molina-Holgado et al., 2000)
Interleukin-2	IL-2	Pro-inflammatory cytokine	(de Rham et al., 2007)
Interleukin-4	IL-4	Anti-inflammatory cytokine associated with IL-13 function	(Scanzello et al., 2008, Kapoor et al., 2011, Onoe et al., 1996)
Interleukin-6	IL-6	Pro-inflammatory cytokine, osteoclast signalling	(Wang et al., 2003, Steeve et al., 2004,

			Yoshitake et al., 2008, Tat et al., 2008a)
Interleukin-8	IL-8	Pro-inflammatory chemokine, neutrophil chemotaxis	(Merz et al., 2003, Wojdasiewicz et al., 2014)
Interleukin-10	IL-10	Anti-inflammatory cytokine, bone formation	(Wojdasiewicz et al., 2014, Jung et al., 2013, Liu et al., 2006, Zhang et al., 2016)
Interleukin-12p70	IL-12p70	T cell stimulatory factor	(Scanzello et al., 2008, Scanzello and Goldring, 2012)
Interleukin-13	IL-13	Anti-inflammatory cytokine	(Wojdasiewicz et al., 2014, Onoe et al., 1996)
Interferon-γ	IFN-γ	Pro- and anti-inflammatory cytokine, neuropathic pain pathway stimulant	(Mathieu et al., 2008, Zhang, 2007, Vikman et al., 2007)

Table 2.5-2 – Immunoassay details for analytes selected for analysis.

Target	Assay type	Assay	Catalog no. Manufact.	Dynamic range
IL-1β	ECL	U-Plex Pro-Inflam Combo 1 Human	K15049 Mesoscale Discovery	0.09 – 0.49 pg/mL
IL-2				0.52 – 1.1 pg/mL
IL-4				0.44 - 3.4 pg/mL
IL-6				0.27 – 1.3 pg/mL
IL-8				0.12 – 0.21 pg/mL
IL-10				0.13 – 0.26 pg/mL
IL-12p70				0.44 - 3.4 pg/mL
IL-13				2.2 – 6.2 pg/mL
TNF-alpha				0.36 – 0.76 pg/mL
IFN-gamma				0.70 – 1.5 pg/mL
ALP	ECL	MSD Bone Panel Kit I Human	K15146C-2 Mesoscale Discovery	0.004 – 200 ng/mL
SOST				0.004 – 100 ng/mL
OPG				1.9 – 4000 ng/mL
RANKL	ELISA	total sRANKL (human) ELISA	K 1016 Immun-Diagnostik	370-30,000 pg/ml
CTX-I	ELISA	Human CTX2 ELISA kit	E01C0071 BlueGene	0.5 – 10ng/mL
COMP	ELISA	Human COMP (Sandwich) ELISA kit	ab213764 Abcam	156 -10,000 pg/mL
Glutamate	ELISA	Human Glutamate ELISA kit	KA 1909 Abnova	0.06-12 µg/mL

2.5.3.1 Assay layout

The following immunoassay layout applied to all tests:

All assays were run on a double 96-well plate layout (Figure 2-14) from the same lot, with 8 point standard curves (7 standards and 1 blank) unless stated otherwise. Both standards and duplicates were run in adjacent duplicates on all assay plates.

STD 1	STD 1	Dilution 0	1	2	3	4	5	6	7	8	9
STD 2	STD 2	Dilution 0	1	2	3	4	5	6	7	8	9
STD 3	STD 3	Dilution 1/2									
STD 4	STD 4	Dilution 1/2									
STD 5	STD 5	Dilution 1/5									
STD 6	STD 6	Dilution 1/5									
STD 7	STD 7	Dilution 1/10									
BLANK	BLANK	Dilution 1/10									

Figure 2-14 – 96-well plate layout for immunoassays. Yellow = standard curve wells with serial dilutions. Orange = serial dilutions of unknown sample concentrations for dilution testing. Green = diluted experimental samples.

96-well assay plate layouts for all tests including both synovial fluid and serum sample testing. Yellow wells represent standard curve duplicates, orange represent dilutions (for ELISA tests only) and green wells represent test synovial fluid/serum samples.

2.5.3.2 Dilution testing and running the assay

Dilution testing of samples was carried out for each assay prior to analysis of the full set of unknown experimental samples, in order to optimise sample dilutions for fluorescence or electrochemiluminescence measurements to be within the measurable limits of the assay kit. Typically, the highest and lowest standards of known concentration provided by the assay manufacturer were representative of the maximum detection range of the assay, therefore they were used for dilution testing.

For all ELISA assays, a strip of 8 wells was removed from each plate. Duplicate wells for the highest and lowest standard provided by the manufacturer were used to define the ranges of the assay. Excess serum or synovial fluid samples from two separate knee OA (KL grade II and KL IV) subjects stored in the ARUK sample biobank were used to represent unknown sample concentrations, to conserve experimental samples.

Test samples were diluted according to the manufacturer's instructions (often using assay buffer or distilled water) in dilutions of 1x, 0.5x, 0.2x and 0.1x the original concentration in separate Eppendorf tubes. Highest and lowest standards (Figure 2-15) as well as diluted samples were allocated wells on the test strip and the full protocol was carried out according to the assay instructions (2.6.3.4.1 – 2.6.3.4.4). Absorbances were read using a spectrophotometer (BMG Labtech FLUOstar Optima plate reader, Bucks, UK) at 405 nm and recorded using the provided software (FLUOstar V2.00 R3, BMG Labtech). Absorbance readings from the test samples were compared to the high and low standard to identify optimal dilutions for samples to fit within the standard curve (2.6.3.3). Dilutions were considered optimal when the readings for the given dilution fell roughly half-way between the standards.

Following dilution testing, the assays were carried out on the full microplate with all synovial fluid and serum experimental samples of unknown concentrations diluted according to optimal dilutions for ELISA assays (2.6.3.4) or recommended dilutions for MSD assays (2.6.3.5). For each assay, a standard curve (Figure 2-15) was generated from the assay standards provided by the manufacturer which typically involved serial dilutions of the highest standard provided, however the dilution gradient varied depending on the assay. Two blank wells were assigned to assay buffer only, and were to provide a zero reading for reference. The standard curve is required to determine actual undiluted concentrations of the experimental samples in each plate (2.6.3.4), therefore the standards tested within both test plates alongside the samples for consistency. It was necessary to run standards within both plates as it was not possible to test for intra-plate variability within this study due to the funding limitations of the study.

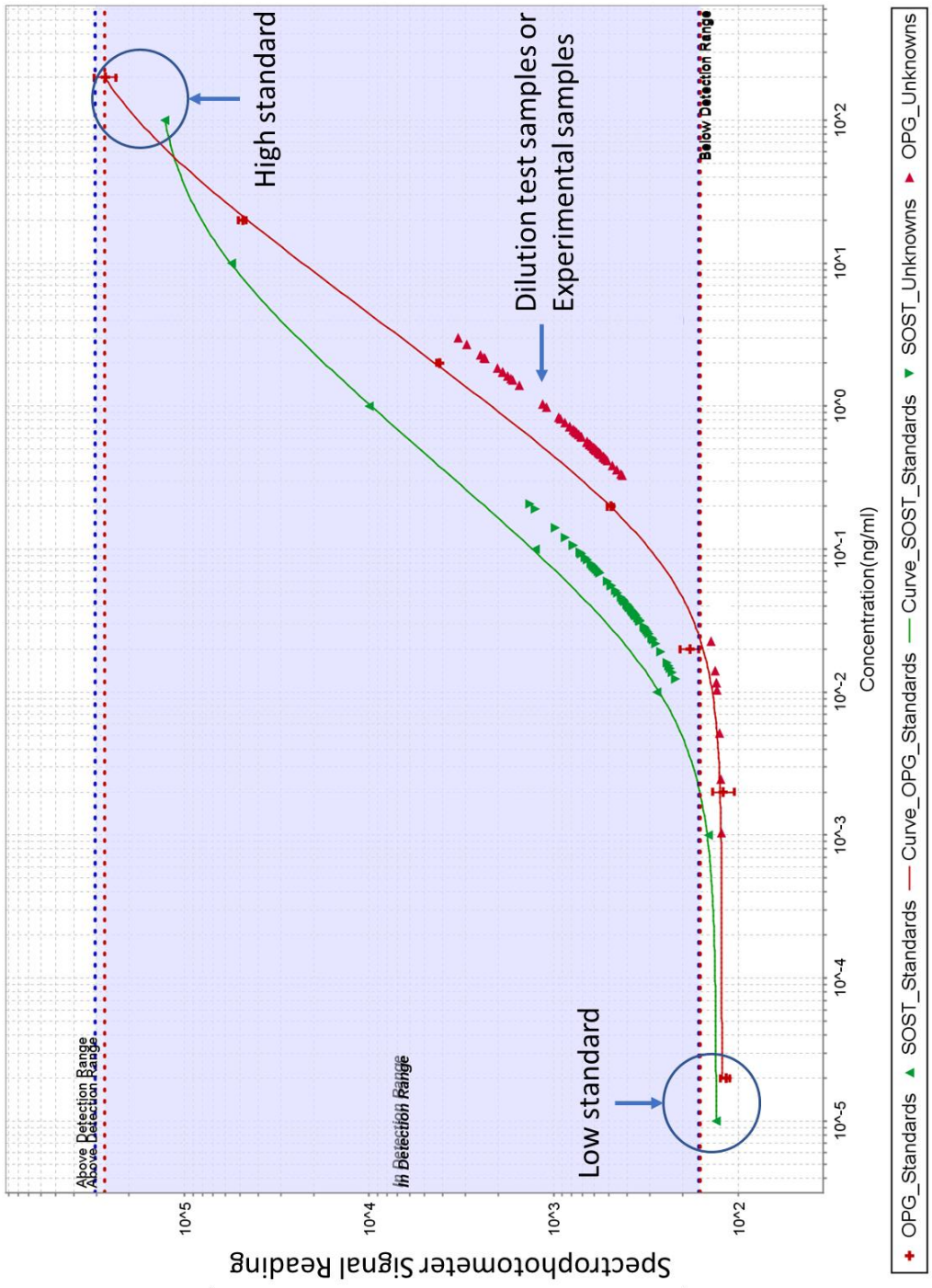

Figure 2-15 - Example of a typical standard curve (interpolated points) for sclerostin (SOST) and alkaline phosphatase (ALP) with plots of sample unknowns. A 5-parameter logistic regression curve fitting method is used to determine absolute concentrations of analytes in subject fluids.

2.5.3.3 Calculation of biomarker concentrations

5-parameters logistic (5PL) regression curve fitting with interpolation was then used to determine absolute concentrations of analytes in the FCD, established OA and control serum, plasma and synovial fluid samples. The equation for the 5PL regression is:

$$F(x) = D + \frac{A - D}{\left(1 + \left(\frac{x}{C}\right)^{B}\right)^{E}}$$

Where A is the minimum asymptote (response value at 0 standard concentration), B is Hill's slope (steepness of the curve), C is the inflection point, D is the maximum asymptote (response value for the infinite standard concentration) and E is the asymmetry factor.

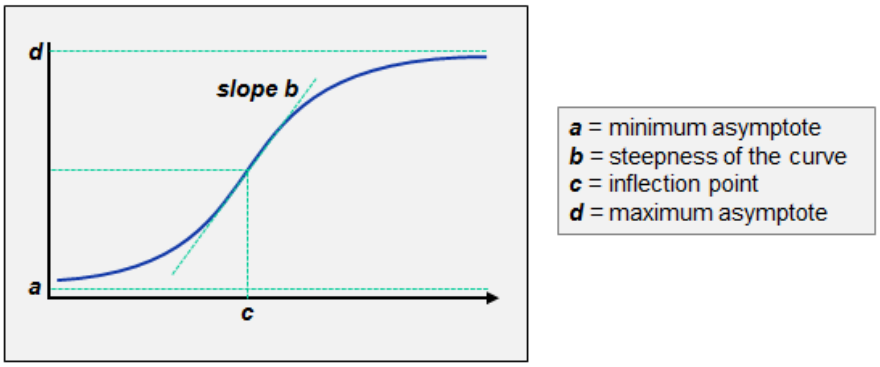

Figure 2-16 – 5-parameter logistic curve definitions

ELISA and chemiluminescence assay datasheets provide recommended maximum and minimum ranges of detection. Samples that generated signals outside this given range were only used if their coefficient of variance (CV) between the duplicate wells was below 20%. However, readings that fell outside the standard curve entirely were deemed unusable and were removed from the analysis. It is also generally recommended that signals should interpolate from the standard curve in the linear region of the curve, as most assays are less sensitive at the extremities. For this reason, prior to running ELISA assays, a test run was conducted using test synovial fluid and serum samples to optimise dilutions for the experiment before running test samples. In some cases, such as in the MSD chemiluminescence assays, it was not possible to test for dilutions due to the reaction required to read signals.

Following interpolation, determined concentrations were multiplied by the dilution factor used in the experiment to generate the true (native) concentrations of analytes. In general, dilution factors were applied to all samples of a particular sample type. Often,

synovial fluid had to be diluted more than serum and plasma due to its higher protein content.

2.5.3.4 Enzyme-linked Immunosorbent Assays

Four commercial ELISA kits were used to quantify synovial fluid and serum RANKL, CTX-I, COMP and glutamate levels (Table 2.5-2). For each of these test kits, 96-well plates came with detachable wells, therefore prior to the experimental sample testing a dilution series of test samples defined the optimum dilutions for samples to fit in the standard curves according to the plate layout (Figure 2-14). Dilution test samples were excess fluid samples from the ARUK BBC biobank sample pool that were kept in separate aliquots before testing dilutions to avoid freeze-thaw cycles. All samples were read in a standard laboratory spectrophotometer capable at measuring wavelength at 450nm. Duplicate wells that showed CVs over 50% were excluded. All ELISA assays were performed according to the manufacturer's protocols that came with the kit (all available on manufacturers websites), apart from dilutions which are stated in the next sections.

2.5.3.4.1 Soluble Human RANKL

This assay utilised a two-site sandwich method with two antibodies that bind to human soluble RANKL and OPG. Standards, controls and diluted synovial fluid and serum samples were added to the wells of the microplates pre-coated with polyclonal anti-human OPG antibody. Following the first incubation RANKL is bound to free OPG as well as the immobilised antibody. Following this, biotinylated monoclonal anti-human RANKL antibodies were added to wells and a sandwich of capture antibody-OPG-RANKL-streptavidin (peroxidase labelled) is formed. Next, a streptavidin horseradish-peroxidase (HRP) conjugate with tetramethylbenzidine (TMB) as a substrate was added that binds to biotin, causing the solution to turn from blue to yellow. The last step involved the addition of an acidic stop solution which terminates the chemical reaction, prior to reading the plate at 450nm in the spectrophotometer.

Dilution testing found that dilution of synovial fluid at 1:20 and serum at 1:10 were optimal for the standard curve. All measured experimental samples were within the standard curve range, except for two FCD synovial fluid samples, which were excluded from the analysis.

2.5.3.4.2 Glutamate

This assay utilised an extraction and derivatization step prior to a competitive sandwich ELISA. The antigen is bound within the solid phase of the plate. The glutamate concentrations in standards, samples and controls and the solid phase bound glutamate competed for antibody binding sites. Once the system reached equilibrium, excess antigen and antibody-antigen complexes were removed by washing. Then, the antibody that was bound to the solid phase was labelled using an anti-rabbit IgG-HRP conjugate with a TMB substrate, causing the solution to turn from blue to yellow. The last step involved the addition of an acidic stop solution which terminates the chemical reaction, prior to reading the plate at 450nm in the spectrophotometer. Dilution testing found that 1:5 dilution for serum and 1:10 dilution for synovial fluid was necessary to fit samples within the standard curve. All measured experimental samples fit within the standard curve, except for two FCD subject synovial fluid samples and one FCD serum samples.

2.5.3.4.3 Human CTX-I

This assay utilised a competitive sandwich technique using an anti-human-CTX-I antibody (source species not mentioned). First the samples were incubated with a CTX-I HRP conjugate in pre-coated wells. Then wells were incubated with TMB substrate causing them to turn from blue to yellow corresponding to CTX-I concentrations. The last step involved the addition of an acidic stop solution which terminates the chemical reaction, prior to reading the plate at 450nm in the spectrophotometer. Dilution testing found that 1:2 dilution for serum and 1:4 dilution for synovial fluid was necessary to fit samples within the standard curve. All measured experimental samples fit within the standard curve, except for two FCD and two HTO subject synovial fluid samples.

2.5.3.4.4 Human COMP

This ELISA was based on a standard sandwich technique. Standards and diluted synovial fluid and serum samples were added to the wells pre-coated with monoclonal mouse anti-human COMP antibody. Next, a biotinylated polyclonal goat anti-human COMP antibody was added, followed by an avidin-biotin-peroxidase complex and removal of free conjugates. Finally, TMB was added to start the HRP enzymatic reaction causing a chance in colour from blue to yellow after addition of the acidic stop solution. Dilution testing found that 1:20 dilution for serum was optimal to fit samples within the standard curve, however dilution testing for all synovial fluid was unsuccessful. All serum samples

fit within the standard curve apart from five FCD serum samples, which measured below the standard curve and were excluded from analysis. However, all synovial fluid samples were unquantifiable for unknown reasons and displayed 0 readings. It was thought that a component of the assay kit reagents may have interfered with the synovial fluid sample in the wells, causing an abnormal reaction. It is notable that this assay was only mentioned to be optimised for serum and plasma.

2.5.3.5 Electrochemiluminescence assays

Meso Scale Discovery (Meso Scale Diagnostics, USA) is a platform that is developed around multiplex ECL assays for the detection of up to 54 proteins simultaneously within the same plate with typically higher sensitivity and broader dynamic ranges relative to ELISAs and other immunoassay types (V-PLEX White Paper, MSD). Within this thesis, two V-plex MSD assays were used for the measurement of inflammatory mediators and bone markers (Table 2.5-2); one 10-plex inflammatory combo (IL-1β, IL-2, IL-4, IL-6, IL-8, IL-10, IL-12p70, IL-13, TNF-α and IFN-γ) and one 3-plex bone panel kit (ALP, SOST and OPG). MSD microplates were read using the Sector Imager 6000 MSD plate reader and analysed with Discovery Workbench v3 (Meso Scale Discovery, USA). MSD assays use high binding carbon electrodes at the bottom of multi-plot plates for capture antibodies, combined with electrochemiluminescent SULFO-TAG labels conjugated to detection antibodies. MSD plate readers then apply electricity to the plate electrodes leading to light emission by ECL labels, that is then quantified by the photometer. Within the MSD Workbench software, an automatic standard curve is generated using a 5-point parameter logistic standard curve and absolute concentrations following adjustment for dilutions is extracted using in-built algorithms. Both ECL assays were performed according to the protocols that arrived with the kit (all available on manufacturers websites), apart from dilutions which are stated in the next sections.

The multiplex assays were developed optimised for serum and plasma samples, however other research groups in the OA field have evaluated their performance on synovial fluid and serum (Struglics et al., 2015, Watt et al., 2016). Struglics et al. who evaluated the Pro-inflammatory Human 7-plex kit found an optimal serum dilution of 1:4 and synovial fluid dilution of 1:20 for detection of proteins within the assay limits. Therefore, these dilutions were employed for both the Pro-inflammatory Human 9-plex and Bone Panel Kit within this study. This was also necessary since it was not possible to test dilutions with the MSD kits, as the single fixed plate of 96 wells can only be exposed once to the

plate reader. Furthermore, duplicate wells with coefficients of variance (CV) over 20% were removed from the analysis.

2.5.3.5.1 Pro-inflammatory 10-plex kit (MSD)

For synovial fluid testing, dilutions of 1:20 were used for reasons mentioned in the previous section. Of twenty-two synovial fluid samples, >90% of IL-8, TNF-α and IFN-γ levels fit within the readable range of the standard curve of the assay, however a substantial proportion of IL-1β (18/22), IL-2 (18/22), IL-4 (21/22), IL-6 (5/22), IL-10 (7/22), IL-12p70 (11/22) and IL-13 (9/22) measurements either fell below the recommended detection limit or the readable limit of the assay. Samples that were below the recommended limit but were still quantifiable and showed low CVs (<20%) were still included in the analysis, but samples that showed 0 readings were excluded from the analysis. Furthermore, analysis of IL-1β, IL-2 and IL-4 were excluded from all analysis altogether due to very low quantifiable concentrations.

For serum testing, dilutions of 1:4 were used for reasons previously mentioned. Of twenty-one serum samples, all inflammatory analyte levels were successfully measured in all samples, except for several samples for IL-1β (18/21), IL-2 (15/21) and IL-13 (6/21), which fell below the recommended or readable detection limit of the multiplex assay. Due to the low number of measurements IL-1β and IL-2 were excluded.

It is notable that under the same conditions, both Struglics et al. and Watt et al. found a substantial proportion of IL-1β, IL-12p70 and IFN-γ concentrations fell below their lower limits of quantification and presented high CVs (>30%), therefore they also excluded IL-1β and IL-12p70 from their clinical analysis consistent with this study (Struglics et al., 2015, Watt et al., 2016).

2.5.3.5.2 Bone Panel 3-plex kit (MSD)

For synovial fluid testing, dilutions of 1:20 were used for reasons previously mentioned. Of twenty-two synovial fluid samples analysed, all samples fit within the standard curve, however 1 sclerostin and a substantial number of ALP readings (18/22) fell below the recommended readable range of the standard curve but were still included in the analysis due to low CVs (<20%). For serum testing, dilutions of 1:4 were used. Of twenty-one serum samples tested, all fit within the readable standard curve, however 3 OPG and 5 ALP readings fell below the recommended readable range of the assay but were still included in the analysis due to low CVs (<20%).

2.6 Multivariate analysis

Aside from waveform analysis, PCA has also proven to be a useful statistical procedure for exploring large complex datasets of discrete measures (Jolliffe and Cadima, 2016). In discrete PCA, the primary goal of PCA is essentially the same - to reduce dimensionality of large data in an interpretable fashion whilst still retaining as much relevant information of the original data as possible in the form of 'principal components' (PCs). To reiterate, PCs are essentially new uncorrelated (orthogonal) variables generated from mathematical linear combinations of the original data, that better represent the overall variance of the dataset as a whole. The first PC (PC1) captures the largest amount of variance with subsequent PCs progressively representing less of the data, thus, it is possible to retain the most important information very easily with substantially fewer variables.

In chapter 4 and 5, exploring linear combinations of data using PCA allowed for an integrated view of variances between observations (e.g. subject samples) and variables (e.g. biomarker concentrations), with the ultimate goal of finding variances that may be revealing or explanatory of intra- or inter-group differences. Multiple clusters of observations could represent different phenotypes of disease, since subjects within these clusters exhibit similarities in the variables they express.

PCA on discrete parameters was carried out in SIMCA (version 14.1, Umetrics, Sartorius Stedim, Sweden), which is a tool that allows for the transformation of variables using PCA into intuitive plots of the important information that could be easily interpretable. This made it possible to identify subjects that grouped together due to sharing similar characteristics in terms of the variables they express (e.g. biomarker concentrations) and find out which variables these clusters were associated with by matching spatial distributions of the observation scores and variable loadings (Figure 2-17).

The 'observations' and variables in both chapters 4 and 5 were as follows:

Chapter	Observations	Variables
4	FCD and OA subjects	Biomarker concentrations
5	FCD and OA subjects	Biomarker concentrations, discrete biomechanical parameters and KOOS scores

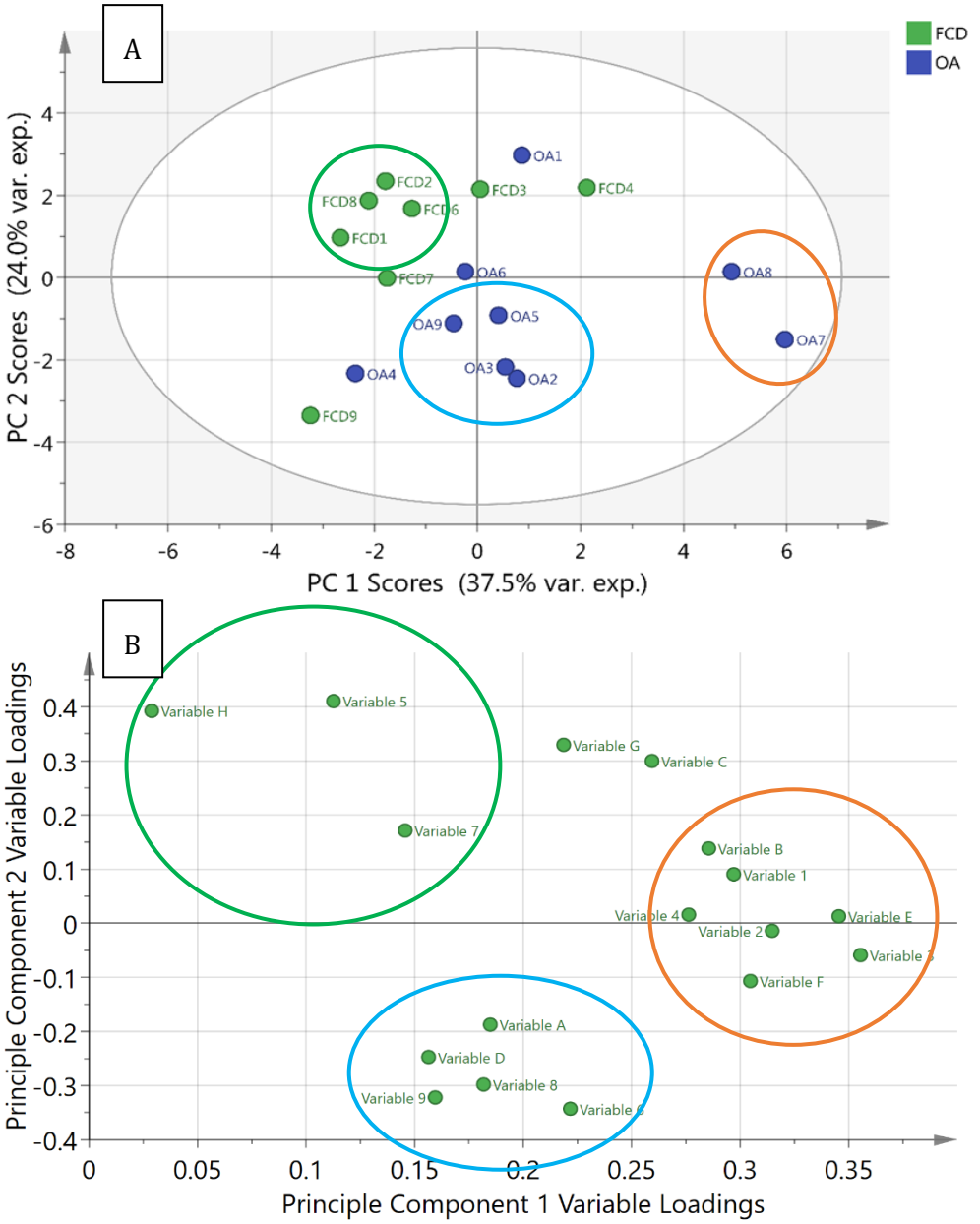

Figure 2-17 - Example of discrete PCA interpretation. The observation score plot **(A)** represents the score of each observation (i.e. subject) against the new variables (principal components) summarizing the original variables (e.g. biomarker concentrations). The first component (PC1) explains the largest variation of the original data, followed by PC 2, etc. Observations that cluster in the scores plot (score closely on the PC axes) share similar characteristics in terms of the variables they express. The variable loadings plot **(B)** represents the contributions of each variable to the principal components. High loading variables of a given principal component are therefore related to observations that scored highly on that principal component in the score space. Ultimately, the spatial distribution of variable loadings on the loadings plot can be related to the spatial distribution of the observations on the score space, making it possible to associate variables with observation groups/clusters.

Chapter 3

The characterisation and longitudinal assessment of lower limb biomechanical function in knee focal cartilage defect subjects undergoing microfracture surgery

3.1 Introduction

The link between lower limb function and established knee OA has been thoroughly investigated in human motion analysis studies, whereby an increasing body of evidence has linked altered lower limb biomechanics, notably joint loading patterns, and neuromuscular activity with OA severity (Mundermann et al., 2004, Astephen et al., 2008), disease progression (Andriacchi and Muendermann, 2006, Andriacchi and Favre, 2014), and interventional outcomes (Morin et al., 2018, Lee et al., 2017). Individuals with unicondylar OA are treated with realignment surgeries such as high tibial osteotomy (HTO), that aim to relieve the affected condyle of abnormally high loads (Roe et al., 2012). At this stage however, deterioration in the knee is substantial and, in many occasions, irreversible. It is therefore critical to identify functional deficiencies early in the disease, when interventions are effective and preventative. There is currently a scarcity of research describing functional deficits of the tibiofemoral FCD knee, which are shown to predispose the knee to OA on their natural course as damage progresses following injury (Spahn and Hofmann, 2014). The unicompartmental and isolated nature of FCDs in the joint and progression of damage suggests a mechanical component is involved in their aetiology (Carnes et al., 2012). Identifying functional deficiencies in those with progressing FCDs could improve clinical decision making with regards to treatment and post-operative rehabilitation.

It is clear from longitudinal interventional studies of the knee FCD population that treatment outcomes vary significantly amongst those treated (Randsborg et al., 2016, Quatman et al., 2012). Whilst conventional treatments such as marrow stimulation techniques (e.g. microfracture) and stem cell therapies (e.g. ACI) are effective for many cases, long-term efficacy is relatively poor for a substantial proportion whom are not able to return to sport, require revision surgeries to treat reoccurring pain, or progress toward an established OA phenotype (Layton et al., 2015, Randsborg et al., 2016, Pascual-Garrido et al., 2017). Cartilage repair techniques are shown to replace the lost or defective cartilage with fibrocartilage by stimulating bone marrow stem cell (BM-MSCs) repair, but their efficacy in restoring knee function is poorly understood. Longitudinal assessment of joint function following cartilage repair may therefore reveal mechanisms of failure in which previous MRI or patient-reported outcome studies have not (Quatman et al., 2012). Furthermore, development of predictor variables for the response to intervention or identifying phenotypic groups can help to develop targeted therapeutic strategies for distinct clinical treatment groups to further improve efficacy (Knoop et al., 2011, Driban et al., 2010).

This chapter intends to objectively define the lower limb biomechanical and neuromuscular function of individuals affected with either medial or lateral compartment tibiofemoral FCDs, to further understanding of the condition from a biomechanics standpoint with insight into development and progression of the condition. Secondly, to use this information to subsequently assess functional outcomes of a conventional intervention (i.e. microfracture surgery) aimed at repairing chondral damage in the joint six-months following surgery. This chapter aims to fulfil these objectives by using 3-dimensional motion capture technology and electromyography (EMG) in combination with multivariate statistical methods, to measure biomechanical and neuromuscular differences and longitudinal changes acting at the knee, hip and ankle during level gait relatively to healthy control subjects with no history of joint injury.

Chapter Aim: To use 3D gait analysis and electromyography techniques to identify lower limb functional differences of tibiofemoral FCD subjects relative to controls and assess longitudinal functional outcomes of microfracture surgery

> **Objective 1:** Use 3D motion capture and EMG methods to identify lower limb biomechanical and neuromuscular functional features of knee FCD subjects that differ from control subjects
>
> **Hypothesis 1:** *Patients with FCDs of the tibiofemoral joint experience biomechanical and neuromuscular differences acting at the knee, hip and ankle compared to non-pathological controls*
>
> **Objective 2:** Assess longitudinal changes in lower limb functional features of FCD pathology six-months following treatment with microfracture surgery
>
> **Hypothesis 2:** *Longitudinal assessment of lower limb functional features of FCD gait will reveal the efficacy of microfracture surgery for restoring knee function and identify mechanisms of failure*

3.2 Methods

Methodology for collection, generation, analysis and interpretation of biomechanical and muscle activation waveforms was previously described in section 2.4 and 2.5.

3.2.1 Splitting the dataset into two groups based on medial and lateral location of the lesions

Based on previous evidence investigating knee established OA gait, it is expected that biomechanical function may differ based on the mediolateral location of chondral damage in the knee (Heijink et al., 2012, Andriacchi and Muendermann, 2006, Sharma et al., 2001). Therefore, combining medial and lateral knee FCD subjects may lead to averaging out of group differences, particularly in frontal plane parameters. This is particularly relevant with focal lesions, due to the isolated nature of their pathology. It is indicated in arthroscopic surgical notes that within the entire FCD cohort, there lies a clear divide in medial and lateral-compartmental lesions and a comprehensive analysis of the arthroscopy notes for all FCD subjects indicated that only single compartments were affected. Based on these circumstances and evidence, the decision was made to divide the FCD group into medial and lateral disease groups which were individually compared to the control group for the analysis of this chapter. However, medial and lateral FCD subjects were combined in the subsequent chapters due to the advantage of increased group numbers with improving statistical power.

3.3 Results

3.3.1 Cohort characteristics and clinical data

Five medial knee FCD subjects (all male; mean (SD) age = 41.2 (16) years, BMI = 28.5 (5) kg/m2), six lateral FCD subjects (5 male, 1 female; mean (SD) age = 38.7 (10) years, BMI = 28.4 (4) kg/m2) and ten control subjects (9 male, 3 female; mean (SD) age = 33.5 (7) years, BMI = 26.1 (4) kg/m2) were recruited with consent and underwent 3D gait analysis. There was a lack of significant ($p \leq 0.05$) group differences in demographics, however trends of lower age and BMI were found in the control group relative to FCD groups (Table 3.3-1).

All FCD subjects had Outerbridge grade II tibiofemoral chondral lesions, nine out of eleven presented accompanying meniscal tears or damage in the affected compartment only (1 medial and 1 lateral subject per group had intact menisci), and three subjects presented ACL laxity (+Glide) associated with ACL-tears or damage (Appendix A.1) Furthermore, no static knee malalignment was reported for any subject. From all involved subjects, one FCD subject (KM) reported using an analgesic (Tramadol) within 3 hours prior to motion capture data collection.

3.3.2 Patient-reported clinical measures

Both medial and lateral FCD subject groups reported significantly ($p \leq 0.05$ to ≤ 0.01) higher pain levels, presence of symptoms and poorer self-perceived function relative to controls (Table 3.3-1). There was also a trend of higher pain and symptom levels and reduced function experienced by the medial relative to lateral subjects, however this did not reach significance at the $p \leq 0.05$ level.

Following microfracture surgery, medial FCD subjects experienced significantly ($p \leq 0.05$) lower self-reported pain and a trend towards improved symptoms and self-perceived function (

Table 3.3-2). Lateral FCD subjects initially reported less pain, symptoms and function than the medial group prior to surgery, but only marginally improved from pre- to post-surgery.

Table 3.3-1 – Cross-sectional cohort demographical features and patient-reported KOOS scores. Bold face p-values were considered significant (p≤0.05). Note: lower KOOS scores = worsening clinical factors (e.g. pain)

Parameter	Control	Medial FCD	Lateral FCD	*Sig. p C vs. M*	*Sig. p C vs. L*	*Sig. p M vs. L*
n =	10	5	6	-	-	-
BMI	26.1 ±4	28.5 ±5	28.4 ±4	n/s	n/s	n/s
Age (y)	33.5 ±7	41.2 ±16	38.7 ±10	n/s	n/s	n/s
Pain	96.8 ±3	66.1 ±10.7	70.8 ±21.1	**.002**	**.027**	n/s
Symptoms	93.4 ±7.3	59.3 ±23.5	66.7 ±13.9	**.032**	**.034**	n/s
Function	99.6 ±0.7	64.1 ±21.9	75.2 ±2.4	**.022**	**.032**	n/s

Table 3.3-2 – Longitudinal cohort demographical features and patient-reported KOOS scores. Bold face p-values were considered significant (p≤0.05).

Parameter	Medial FCD		*Sig. p*	Lateral FCD		*Sig. p*
	Pre	Post		Pre	Post	
n =	3	3		3	3	
BMI	28.5 ±5			28.4 ±4		
Age (y)	41.2 ±16			38.7 ±10		
Pain	68.5 ±14.3	83.3 ±16.9	**.026**	82.4 ±19.7	95.4 ±5.8	.465
Symptoms	73.8 ±7.4	85.7 ±10.7	.109	72.6 ±7.4	84.5 ±14.9	.405
Function	69.6 ±25	88.7 ±14.4	.096	80.9 ±15.9	91.7 ±10.8	.499

3.3.3 Spatio-temporal parameters

No significant (p≤0.05) differences were found for spatio-temporal parameters between disease groups and controls (

Table 3.3-3), however a trend towards slower walking speed, increased stance and swing time and decreased steps/minute were found in medial FCD subjects compared to the lateral group and controls.

Medial FCD subjects walked significantly ($p \leq 0.05$) slower after treatment, resulting in average increases in stance, swing and double limb support time, as well as reduced number of steps per minute (Table 3.3-4). In contrast, lateral FCD subjects showed an opposite effect as a result of increased walking speed, though this did not reach significance at the $p \leq 0.05$ level.

Table 3.3-3 – Cross-sectional cohort spatiotemporal parameters. Bold face p-values were considered significant (p≤0.05).

Parameter	Control	Medial FCD	Lateral FCD	*Sig. p C v M*	*Sig. p C v L*	*Sig. p M v L*
Speed (m/s)	1.16 ±0.1	1.11 ±0.18	1.18 ±0.11	.413	.637	.326
Stance time (s)	0.66 ±0.07	0.7 ±0.06	0.67 ±0.05	.259	.912	.277
Swing time (s)	0.43 ±0.02	0.46 ±0.04	0.429 ±0.01	.167	.796	.148
Steps/min	111.2	103	110	.052	.727	.087
Dbl limb support (s)	0.22 ±0.04	0.25 ±0.04	0.23 ±0.04	.234	.768	.445

Table 3.3-4 - Longitudinal cohort spatiotemporal parameters. Bold face p-values were considered significant (p≤0.05).

Parameter	Medial FCD		*Sig. p*	Lateral FCD		*Sig. p*
	Pre	Post		Pre	Post	
Speed (m/s)	1.16 ±0.19	1.10 ±0.18	**.028**	1.18 ±0.14	1.24 ±0.1	.144
Stance time (s)	0.68 ±0.07	0.70 ±0.06	.086	0.66 ±0.05	0.65 ±0.04	.135
Swing time (s)	0.44 ±0.02	0.45 ±0.03	.377	0.43 ±0.02	0.43 ±0.01	.654
Steps/min	106 ±6	104 ±5.3	.107	109.7 ±2.48	112 ±4.13	.168
Dbl limb support (s)	0.23 ±0.04	0.24 ±0.04	.151	0.23 ±0.06	0.23 ±0.04	.704

3.3.4 PCA; biomechanical waveform cross-sectional and longitudinal comparisons

From a total of 21 lower limb biomechanical features (GRFs and hip, knee and ankle rotations and moments) and 7 muscle activation features tested for significantly ($p \leq 0.05$) differing group variances (medial FCD vs controls and lateral FCDs vs controls), 11 features revealed at least one PC representative of group differences (Table 3.3-5) and were included in this chapters results.

Table 3.3-5 – Table representing biomechanical or muscle activation features that exhibited significantly ($p \leq 0.05$) differing group PC variances.

Parameter type	Plane/Muscle	Feature
Biomechanical waveform	Vertical Z	Vertical GRF
	Frontal plane	Knee adduction moment (KAM)
		Knee adduction angle (KAA)
		Hip adduction moment (HAM)
	Sagittal plane	Knee flexion-extension moment (KFM / KEM)
		Knee flexion angle (KFA)
Muscle activation waveform	Quadriceps	Rectus femoris activation
		Vastus medialis activation
		Vastus lateralis activation
	Hamstrings	Biceps femoris activation
		Semitendinosus activation

In addition to significantly differing features, two additional features (mediolateral and anteroposterior GRF) were also included to aid interpretations.

Parameter	Comparison group (versus controls)	PC	Variance explained (%)	Feature of FCD gait	*Sig. p* (FCD vs C)	Longitudinal change	*Sig. p* (Pre vs Post)
Vertical (+) reaction force	**Medial FCD**	1	68.1	↓ GRF magnitude & double-peak characteristic	**.003**	**→ Pathological**	.111
	Lateral FCD	1	70.1	↓ GRF magnitude & double-peak characteristic	**.007**	**Healthy ←**	.089
Knee Adduction (+) Moment	**Medial FCD**	1	61.9	↑ magnitude of add (+) mom	**.050**	**→ Pathological**	.371
	Lateral FCD	1	66.9	↓ overall add (+) magnitude & shape of 1st peak	**.031**	**Healthy ←**	.250
Knee Adduction (+) Angle	**Medial FCD**	3	10.9	↑ valgus at load response & ↑ varus from mid-stance to toe-off	**.032**	**→ Pathological**	.418
	Lateral FCD	1	62.6	↑ Overall magnitude of waveform	**.044**	**Healthy ←**	.747
Knee Flexion (+) Moment	**Medial FCD**	1	52.1	↓ flexion mom (early-stance) & ↓ extension mom (late-stance)	**.013**	**No change**	.999
Knee Flexion (+) Angle	**Medial FCD**	2	17.3	↑ flexion during late-stance & ↓ flexion during swing phase	**.019**	**Healthy ←**	.830
Hip Adduction (+) Moment	**Medial FCD**	2	10.8	↓ 1st : 2nd peak ratio	**.005**	**→ Pathological**	**.006**

Table 3.3-6 – Table summarising principal component variance features of biomechanical gait waveforms that significantly differed (p≤0.05) between groups (medial FCD vs control / lateral FCD vs control) and longitudinally six-months following microfracture surgery. Bold face p-values were considered significant (p≤0.05)

Parameter	Comparison group (versus controls)	PC	Variance explained (%)	Feature of FCD gait	*Sig. p* (FCD vs C)	Longitudinal change	*Sig. p* (Pre vs Post)
Rectus Femoris	**Medial FCD**	1	50.7	↑ activation (mid- to late-stance)	**.012**	**Healthy ←**	0.849
Vastus Medialis	**Medial FCD**	1	62.5	↑ activation (mid- to late-stance)	**.006**	**Healthy ←**	0.871
Vastus Lateralis	**Medial FCD**	1	51.9	↑ activation (mid- to late-stance)	**.029**	**→ Pathological**	0.557
Biceps Femoris	**Medial FCD**	1	56.6	↑ activation (heel-strike to late-stance)	**.007**	**→ Pathological**	0.152
	Lateral FCD	3	13.2	↓ pre-activation at heel-strike	**.05**	**Healthy ←**	**0.040**
Semitendinosus	**Medial FCD**	1	51.8	↑ activation (heel-strike to late-stance)	**.030**	-	-
	Lateral FCD	3	10.8	↓ pre-activation at heel-strike	**.042**	-	-

Table 3.3-7 – Table summarising principal component variance features of muscle activation waveforms that significantly differed (p≤0.05) between groups (medial FCD vs control / lateral FCD vs control) and longitudinally six-months following microfracture surgery. Bold face p-values were considered significant (p≤0.05)

3.3.4.1 Vertical GRF

PCA of the vertical GRF showed similar feature differences for both FCD groups compared to controls (Figure 3.3-1). PC1 captured variances for both comparisons represented a significant ($p \leq 0.01$) decrease in overall GRF magnitude in disease groups and lessening of the 'double-peak' characteristic indicative of reduced vertical forces. Visual assessment of the ensemble-averaged waveforms revealed that mid-stance GRFs were similar to control forces, but the first (weight-acceptance) and second (push-off) peaks were relatively reduced.

Following microfracture surgery, there were non-significant (n-s) trends towards decreased peak vertical forces and increased midstance forces in the medial FCD group representative of worsening function, in contrast to increased vertical forces in the lateral group indicating improved function, however these differences were not statistically validated at the $p \leq 0.05$ level.

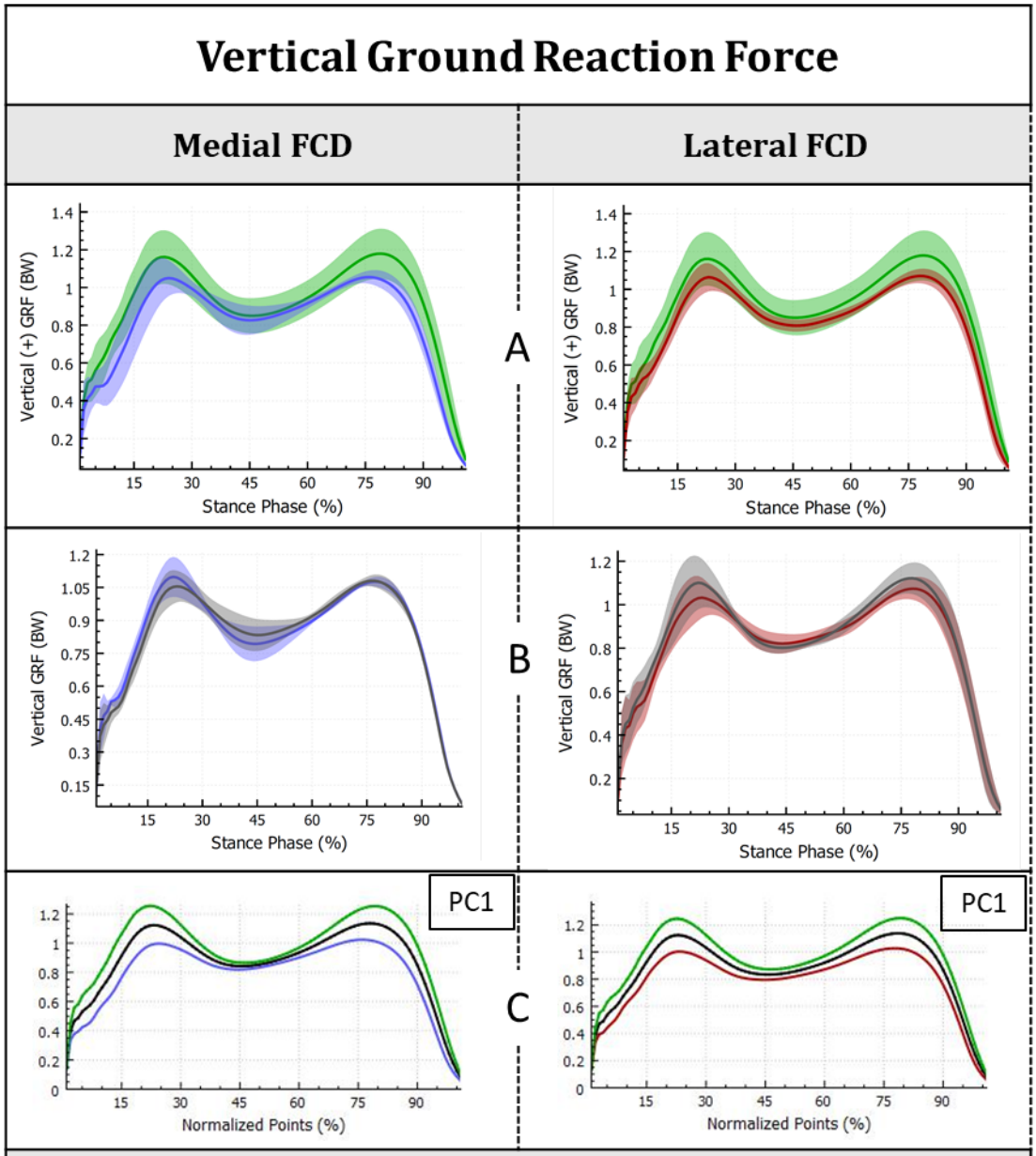

Group	PC	Var Exp. (%)	Feature of FCD patients	Sig. *p*	Δ	Sig. *p*
Medial	1	68.1	↓ GRF peak magnitude, ↓ double-peak characteristic	**.003**	→ Path	.111
Lateral	1	70.1	↓ GRF magnitude, ↓ double-peak characteristic	**.007**	Healthy ←	.089

Figure 3.3-1 - Vertical (+) ground reaction force vector ensemble-averaged waveforms (lines) and standard deviations (shaded areas) for Medial FCD and Lateral FCD subjects relative to Control subjects **(A)** and relative to Post-surgery **(B)**. Extreme plots are presented representing the mean (black) and ±1 standard deviation PC reconstructions colour coded to represent group differences corresponding to mean PC scores **(C)**.

Table 3.3-1 – Principal component features of gait waveforms that significantly differed (p≤0.05) between groups and longitudinal change in PC variance six-months following surgery.

3.3.4.2 Frontal plane features

Taking both medial and lateral FCD subjects into account, PCA captured no significant differences in mediolateral GRF force variances between the disease groups relative to controls, which was also evident by visual inspection of the ensemble-averaged waveforms (Figure 3.3-2).

The medial FCD subjects exhibited increased late-stance knee adduction moments (KAMs) relative to controls representative of increased medial knee loading, which was captured by PC1 as a significantly ($p \leq 0.05$) overall increased KAM magnitude across the whole of stance-phase (Figure 3.3-3). This was accompanied by a significantly ($p \leq 0.05$) increased varus (adduction) angles (KAA) from weight acceptance to late-stance captured by PC3 (Figure 3.3-4). Whereas at the hip, they presented reduced hip adduction moments (HAMs) during early-stance, significantly ($p \leq 0.01$) captured by PC2 as decreased 1^{st}:2^{nd} peak ratio of the waveform (Figure 3.3-5). Following microfracture, there was a n-s trend towards increased KAMs and a significantly ($p \leq 0.01$) reduced 1^{st} peak:2^{nd} peak HAM ratio at the hip, both indicative of worsening function.

In the exact opposite effect to the medial group, lateral FCD subjects presented a significantly ($p \leq 0.05$) reduced early-stance KAM representative of increased lateral knee loading significantly captured by PC1 variances, accompanied by a significant ($p \leq 0.05$) trend towards increased valgus (abduction) angles of the knee during the whole of stance captured by PC1, and a n-s trend towards a reduction of the 1^{st}:2^{nd} peak ratio of the HAM captured by PC3. Following surgery, there was n-s trend towards increased early-stance KAMs (representative of increased function), but no clear difference in KAAs or HAMs.

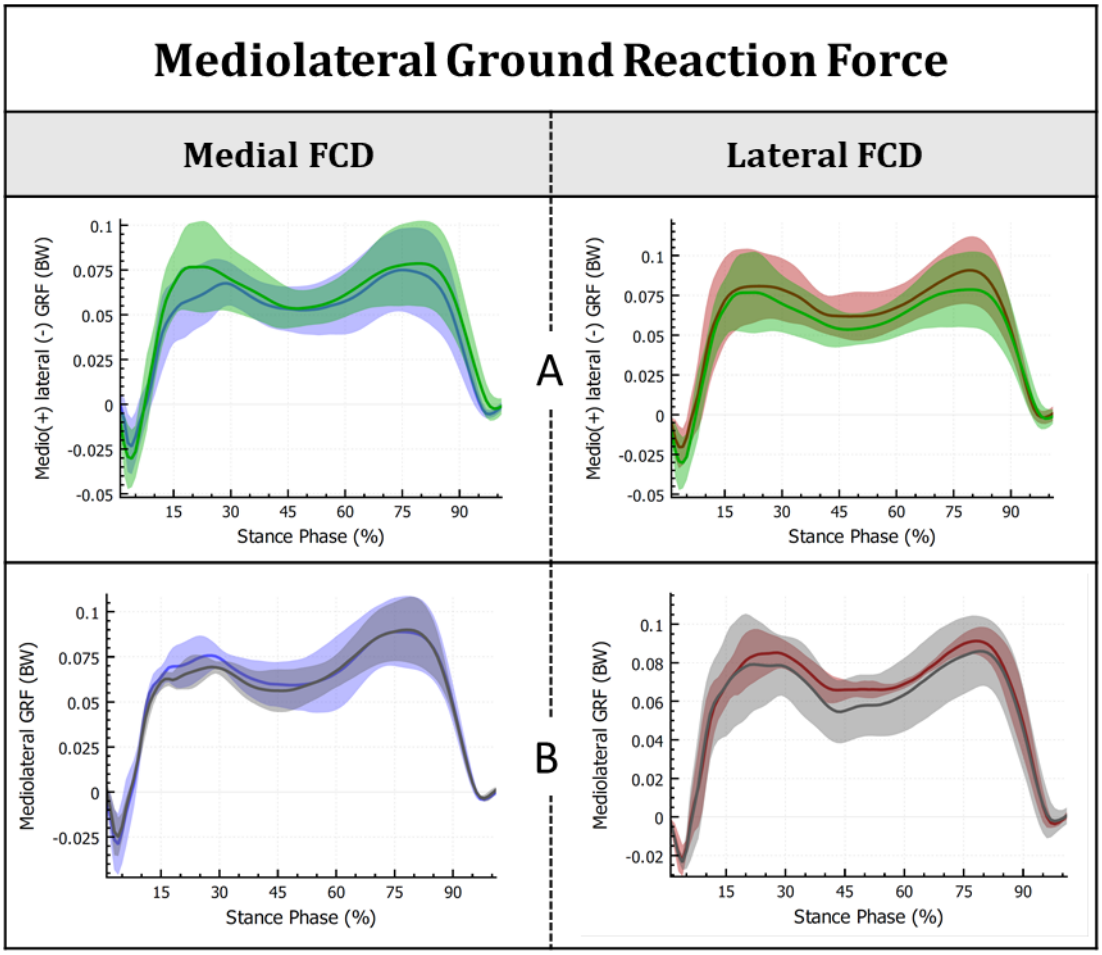

Figure 3.3-2 – Medio(+)-lateral(-) ground reaction force vector ensemble-averaged waveforms (lines) and standard deviations (shaded areas) for Medial FCD and Lateral FCD subjects relative to Control subjects **(A)** and relative to Post-surgery **(B)**. Extreme plots are presented representing the mean (black) and ±1 standard deviation PC reconstructions coded to represent group differences corresponding to mean PC scores **(C)**.

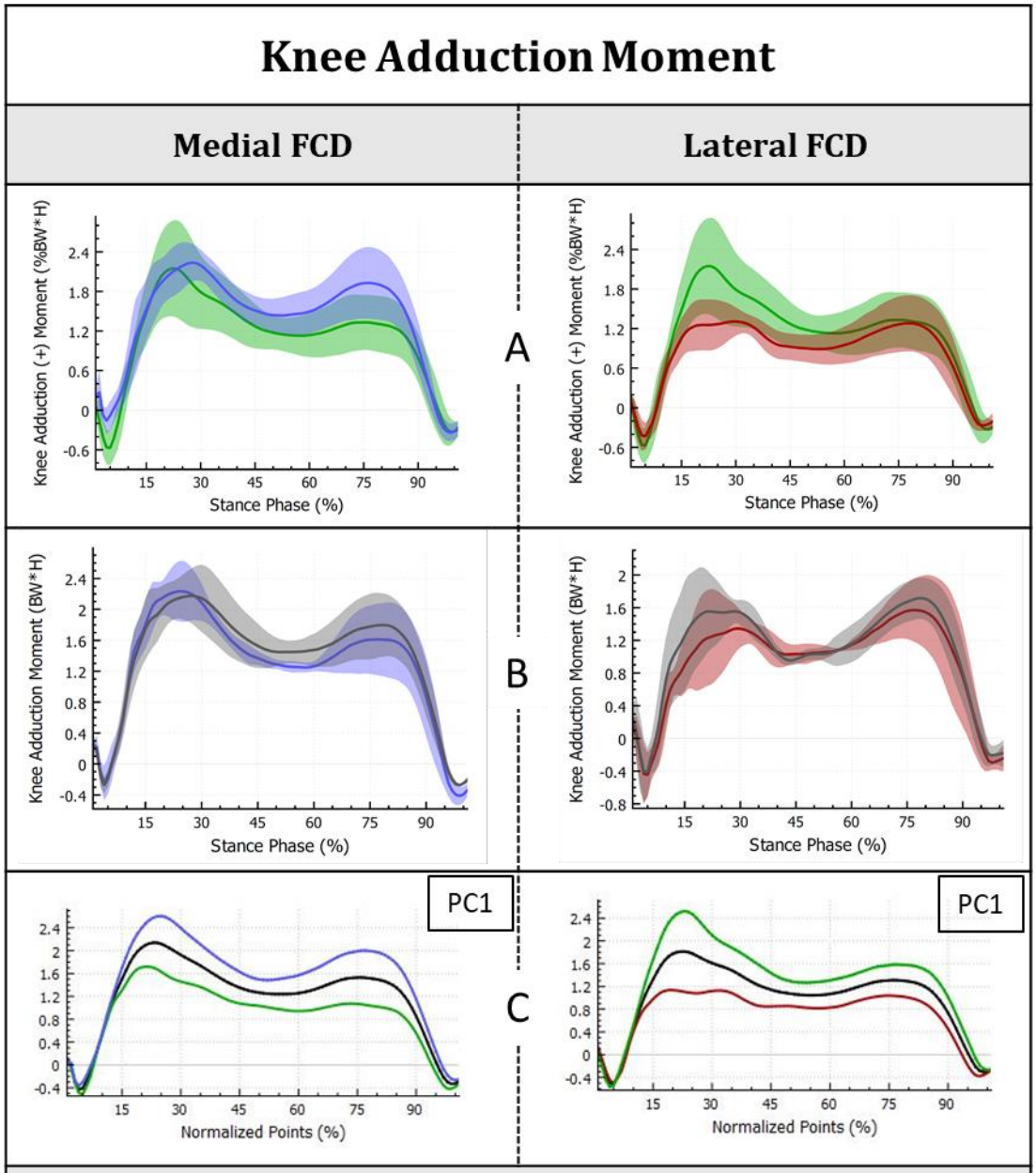

	PC	Var Exp. (%)	Feature of FCD patients	Sig. *p*	Δ	Sig. *p*
Medial	1	61.9	↑ magnitude of add (+) mom	**0.050**	→ Path	.371
Lateral	1	66.9	↓ overall add (+) magnitude & shape of 1st peak	**0.031**	Healthy ←	.250

Figure 3.3-3 – Knee adduction (+) moment ensemble-averaged waveforms (lines) and standard deviations (shaded areas) for Medial FCD and Lateral FCD subjects relative to Control subjects **(A)** and relative to Post-surgery **(B)**. Extreme plots are presented representing the mean (black) and ±1 standard deviation PC reconstructions colour coded to represent group differences corresponding to mean PC scores **(C)**.

Table 3.3-3 – Principal component features of gait waveforms that significantly differed (p≤0.05) between groups and longitudinal change in PC variance six-months following surgery.

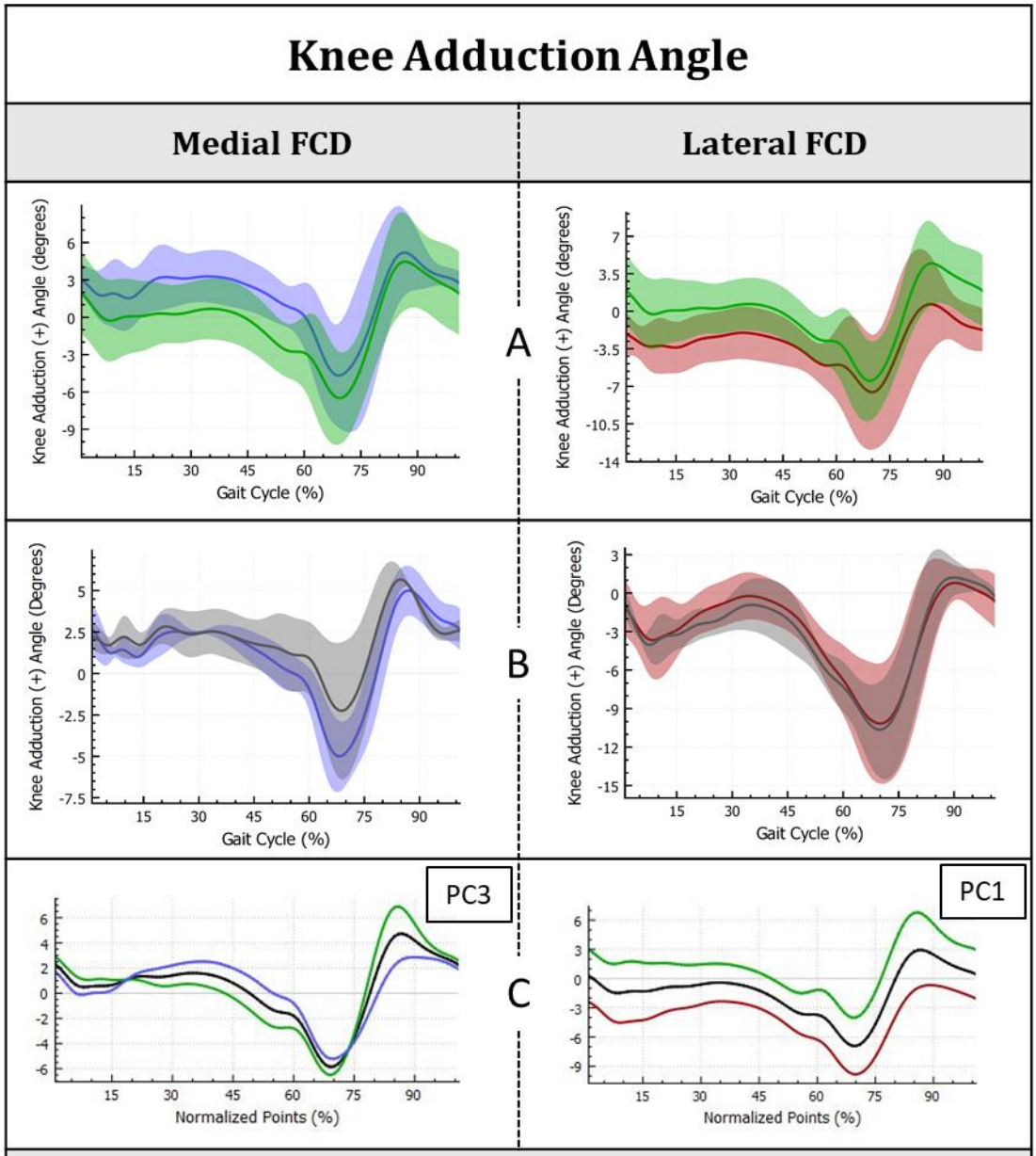

	PC	Var Exp. (%)	Feature of FCD patients	Sig. *p*	Δ	Sig. *p*
Medial	3	10.9	↑ varus from weight-acceptance to late-stance	**.032**	→ Path	.418
Lateral	1	62.6	↑ Overall valgus angle	**.044**	Healthy ←	.747

Figure 3.3-4 – Knee adduction (+) angle ensemble-averaged waveforms (lines) and standard deviations (shaded areas) for Medial FCD and Lateral FCD subjects relative Control to subjects **(A)** and relative to **(B)**. Extreme plots are presented representing the mean (black) and ±1 standard deviation Post-surgery PC reconstructions colour coded to represent group differences corresponding to mean PC scores **(C)**.

Table 3.3-4 – Principal component features of gait waveforms that significantly differed (p≤0.05) between groups and longitudinal change in PC variance six-months following surgery.

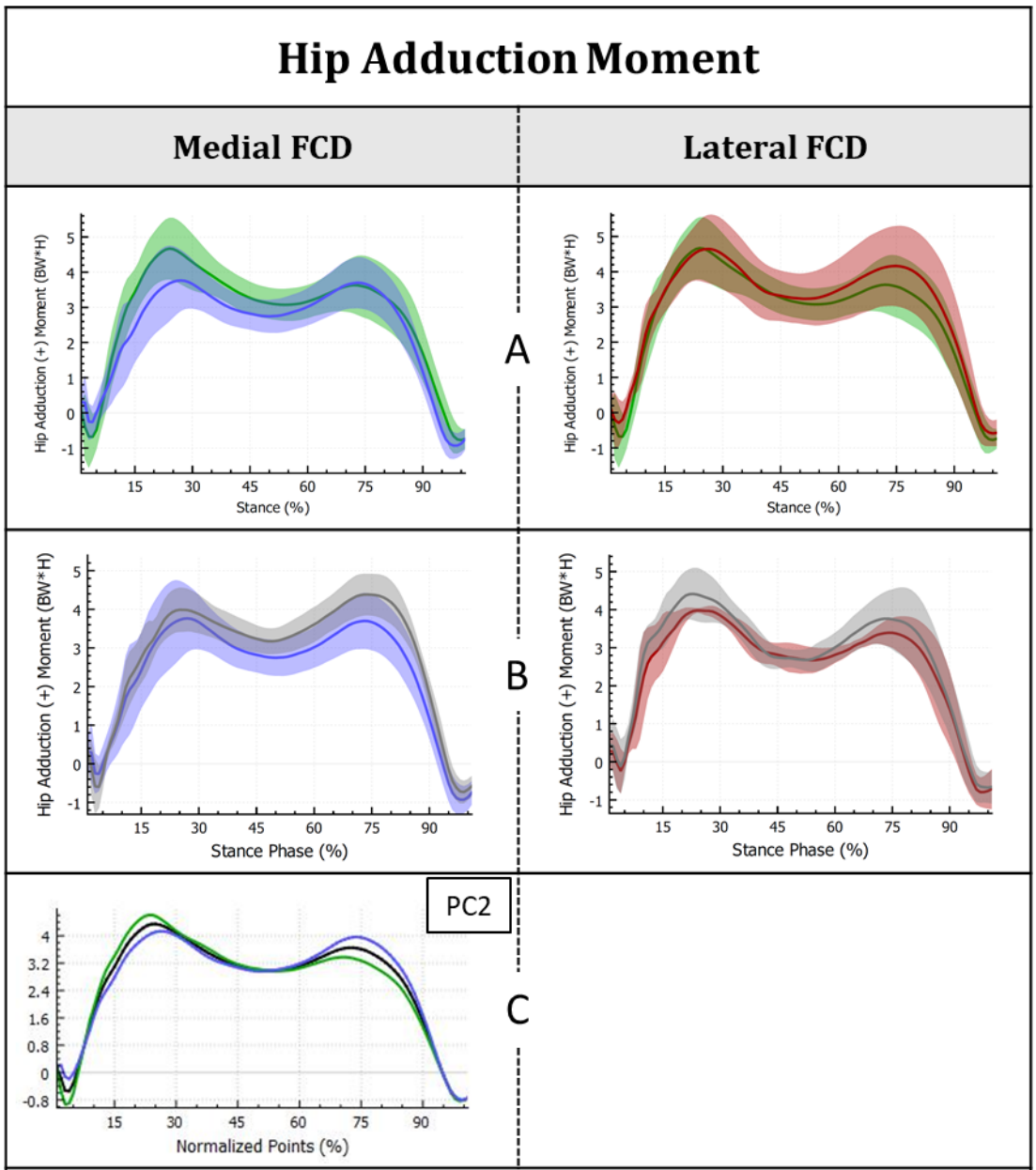

	PC	Var Exp. (%)	Feature of FCD patients	Sig. *p*	Δ	Sig. *p*
Medial	**2**	10.8	↓ 1st peak:2nd peak ratio	**.005**	→ Path	**.006**

Figure 3.3-5 – Hip adduction (+) moment ensemble-averaged waveforms (lines) and standard deviations (shaded areas) for Medial FCD and Lateral FCD subjects relative to Control subjects **(A)** and relative to Post-surgery **(B)**. Extreme plots are presented representing the mean (black) and ±1 standard deviation PC reconstructions colour coded to represent group differences corresponding to mean PC scores **(C)**.

Table 3.3-5 – Principal component features of gait waveforms that significantly differed (p≤0.05) between groups and longitudinal change in PC variance six-months following surgery.

3.3.4.3 Sagittal plane features

For the medial FCD group, sagittal plane features included a trend (n/s) towards reduced anteroposterior GRFs at early-stance and late-stance relative to controls, as captured by PC1 (Figure 3.3-6). Assessment of the knee flexion-extension moment (KFM & KEM) average waveforms (Figure 3.3-7) revealed a reduced KEM during late-stance, which was captured by PC1 as significant ($p \leq 0.05$) reduction in both the KFM and KEM waveform magnitudes compared to controls. This was accompanied by an increased knee flexion angle (KFA) during late-stance (Figure 3.3-8) representative of a reluctancy to extend the knee during push-off, which was captured by PC2 as a significantly ($p \leq 0.05$) reduced range of motion during the whole gait cycle. Following surgery, there was a trend (n/s) towards even more reduced anteroposterior forces, decreased KFM/increased KEM and no differences in the KFA, indicative of worsening knee function.

On the other hand, the lateral group showed no clear differences in anteroposterior forces relative to controls. However, there appeared to be a n-s trend towards decreased KFMs and decreased KFAs during early-stance, though these features were not captured by PC variances. In contrast to the medial group, lateral subjects did not present any biomechanical abnormalities of the KEM during late-stance. After surgery, KFM and KFA magnitudes appeared more similar to controls, indicating a change towards increased knee function.

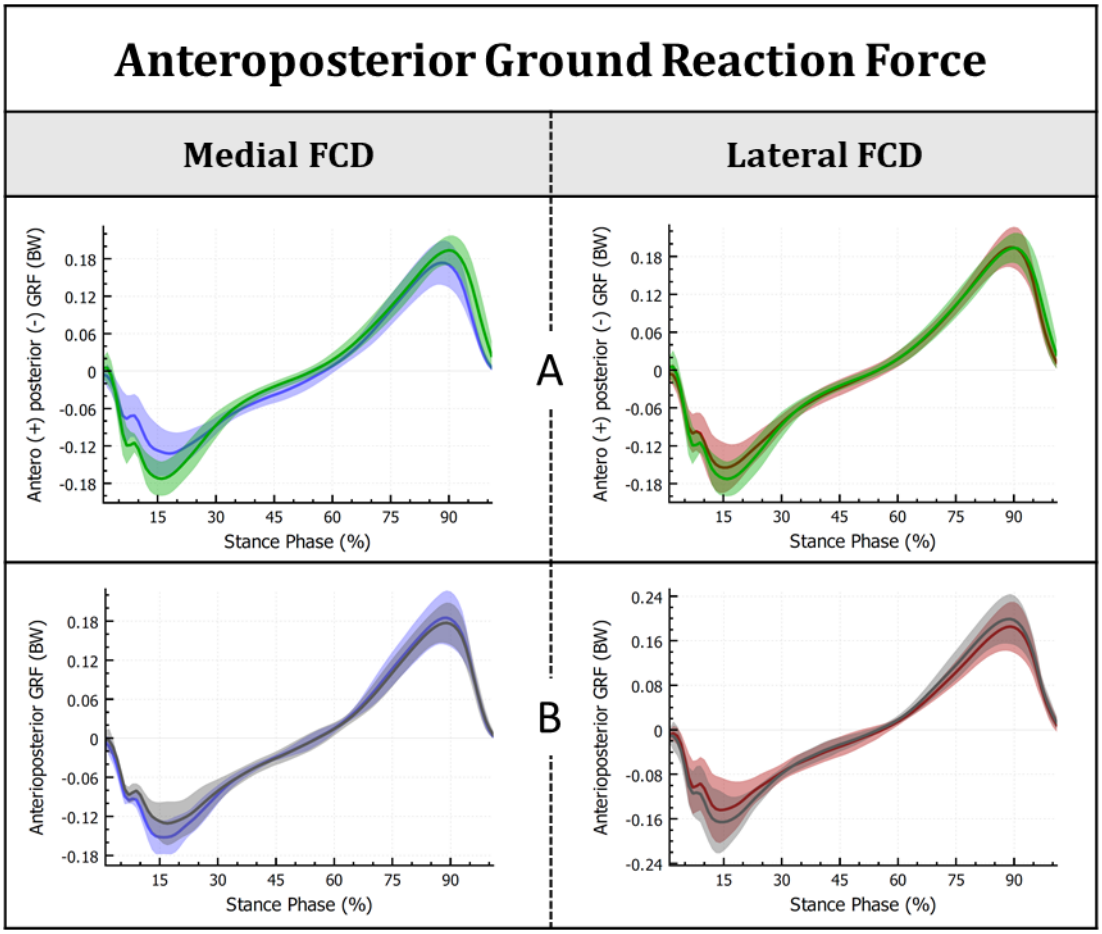

Figure 3.3-6 – Antero(+)posterior(-) ground reaction force ensemble-averaged waveforms (lines) and standard deviations (shaded areas) for Medial FCD and Lateral FCD subjects relative to Control subjects **(A)** and relative to Post-surgery **(B)**. Extreme plots are presented representing the mean (black) and ±1 standard deviation PC reconstructions coded to represent group differences corresponding to mean PC scores **(C)**.

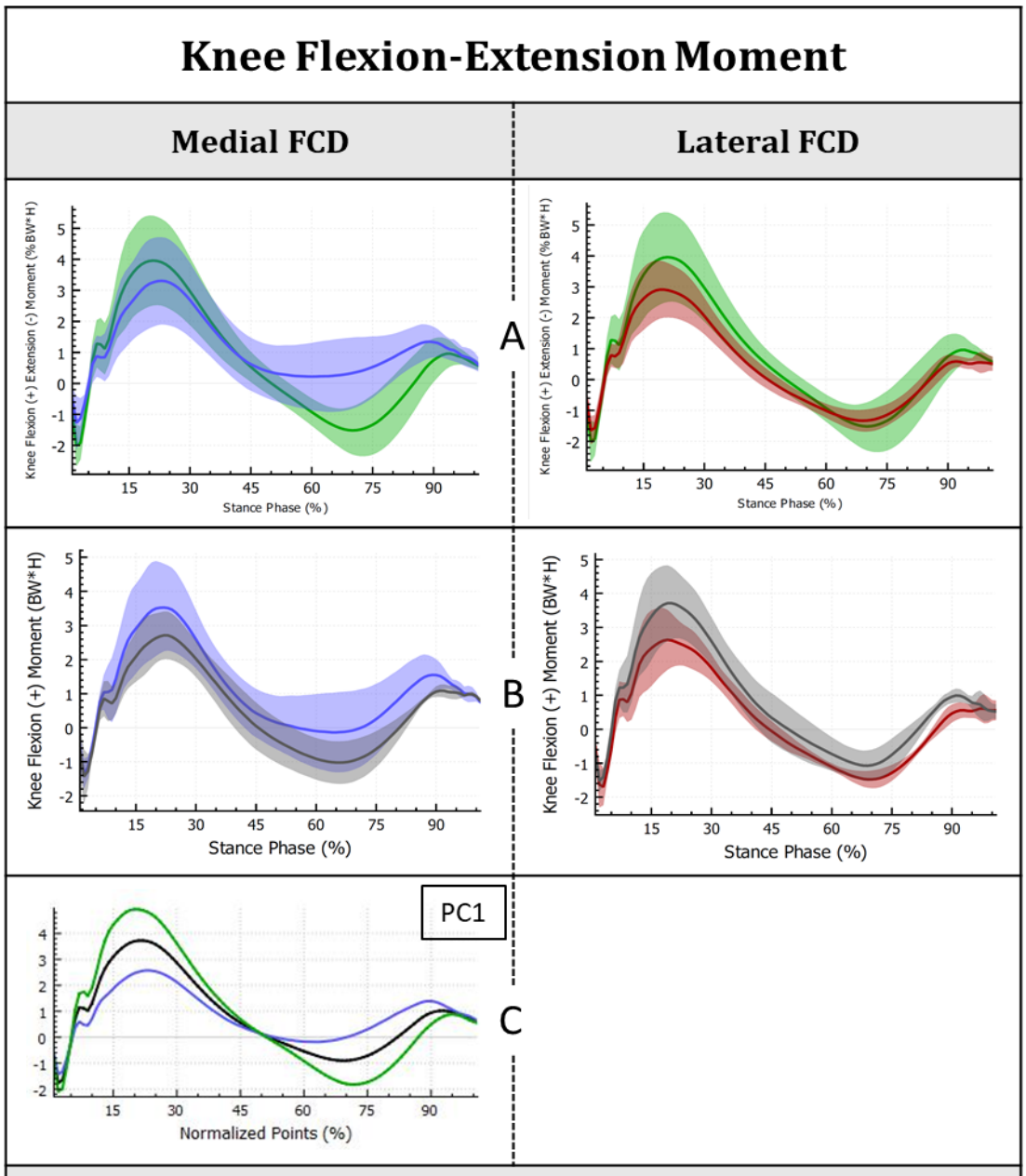

	PC	Var Exp. (%)	Feature of FCD patients	Sig. *p*	Δ	Sig. *p*
Medial	**1**	52.1	↓ flexion mom (early stance), ↓ extension mom (late stance)	**.013**	No change	.999

Figure 3.3-7 – Knee flexion(+)-extension(-) moment ensemble-averaged waveforms (lines) and standard deviations (shaded areas) for Medial FCD and Lateral FCD subjects relative to Control subjects **(A)** and relative to Post-surgery **(B)**. Extreme plots are presented representing the mean (black) and ±1 standard deviation PC reconstructions colour coded to represent group differences corresponding to mean PC scores **(C)**.

Table 3.3-7 – Principal component features of gait waveforms that significantly differed (p≤0.05) between groups and longitudinal change in PC variance six-months following surgery.

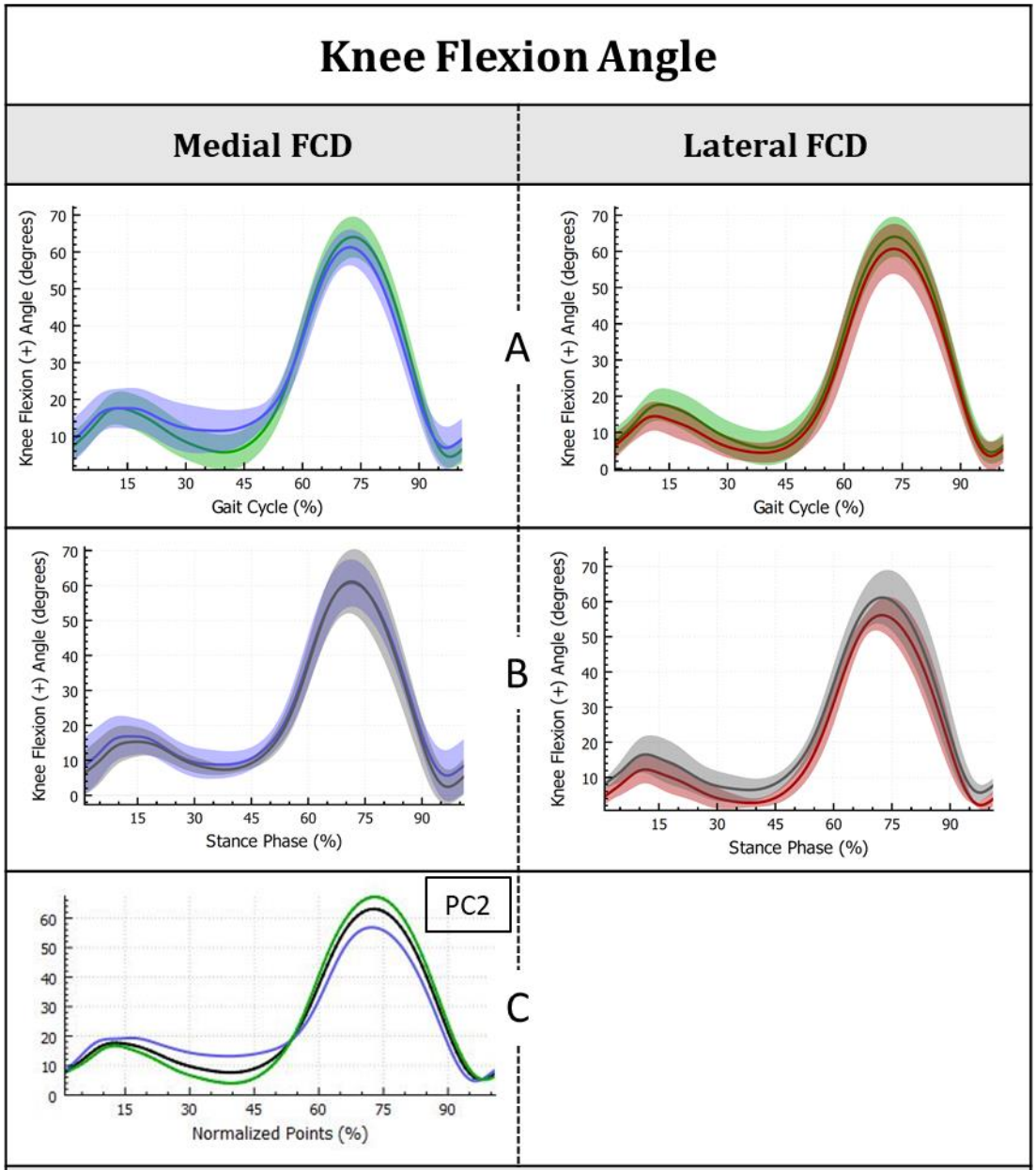

Group	PC	Var Exp. (%)	Feature of FCD patients	Sig. *p*	Δ	Sig. *p*
Medial	2	17.3	↓ Range of motion	**.019**	Healthy ←	.830

Figure 3.3-8 – Knee flexion (+) angle ensemble-averaged waveforms (lines) and standard deviations (shaded areas) for Medial FCD and Lateral FCD subjects relative to Control subjects **(A)** and relative to Post-surgery **(B)**. Extreme plots are presented representing the mean (black) and ±1 standard deviation PC reconstructions colour coded to represent group differences corresponding to mean PC scores **(C)**.

Table 3.3-8 – Principal component features of gait waveforms that significantly differed (p≤0.05) between groups and longitudinal change in PC variance six-months following surgery.

3.3.4.4 Quadriceps activation

Visual comparison of quadriceps waveforms revealed that medial FCD subjects are over-activating all three examined muscles during mid- to late-stance (20-50% gait cycle), but this was not reflected in lateral FCD subjects who showed no clear deficiencies in quadriceps function (Figure 3.3-9, Figure 3.3-10 & Figure 3.3-11). PCA found significant ($p \leq 0.05$) differences in the medial group quadriceps activation variances reflective of this feature, represented by PC 1 differences.

Following surgery, medial FCD subjects persisted to aberrantly activate all three quadricep muscles, evidenced by the lack of- or very subtle longitudinal changes in average waveform or PC variances. These subtle changes involved the rectus femoris and vastus medialis showing trends towards improved function, contrasting the vastus lateralis showing a stronger trend towards pathological function, evidenced by changes in mid- to late stance activation.

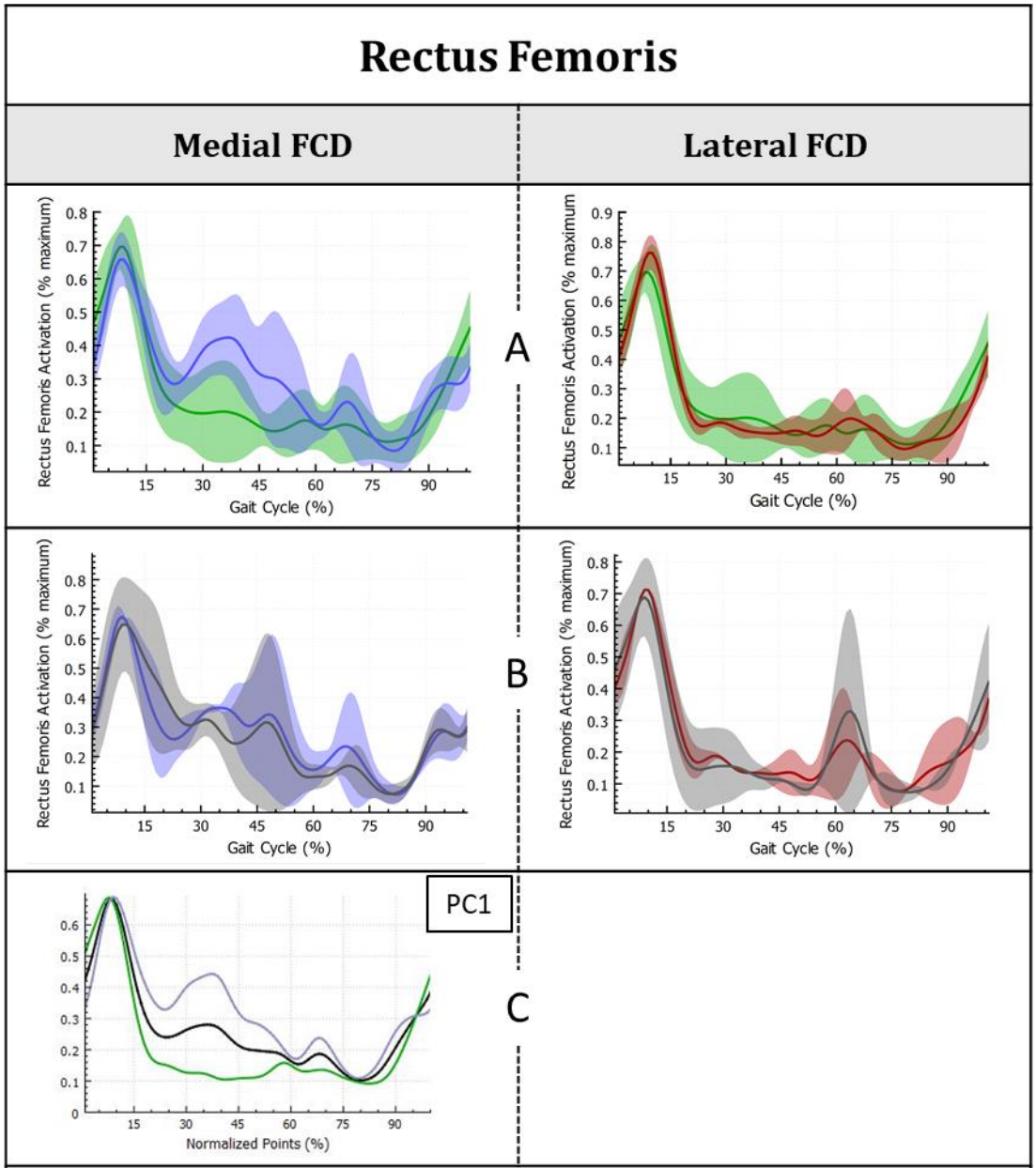

Group	PC	Var Exp. (%)	Feature of FCD patients	Sig. *p*	Δ	Sig. *p*
Medial	1	50.7	↑ activation (mid-stance to toe-off)	**.012**	Healthy ←	.849

Figure 3.3-9 – Rectus femoris activation ensemble-averaged waveforms (lines) and standard deviations (shaded areas) for Medial FCD and Lateral FCD subjects relative Control to subjects **(A)** and relative to Post-surgery **(B)**. Extreme plots are presented representing the mean (black) and ±1 standard deviation PC reconstructions colour coded to represent group differences corresponding to mean PC scores **(C)**.

Table 3.3-9 – Principal component features of gait waveforms that significantly differed (p≤0.05) between groups and longitudinal change in PC variance six-months following surgery.

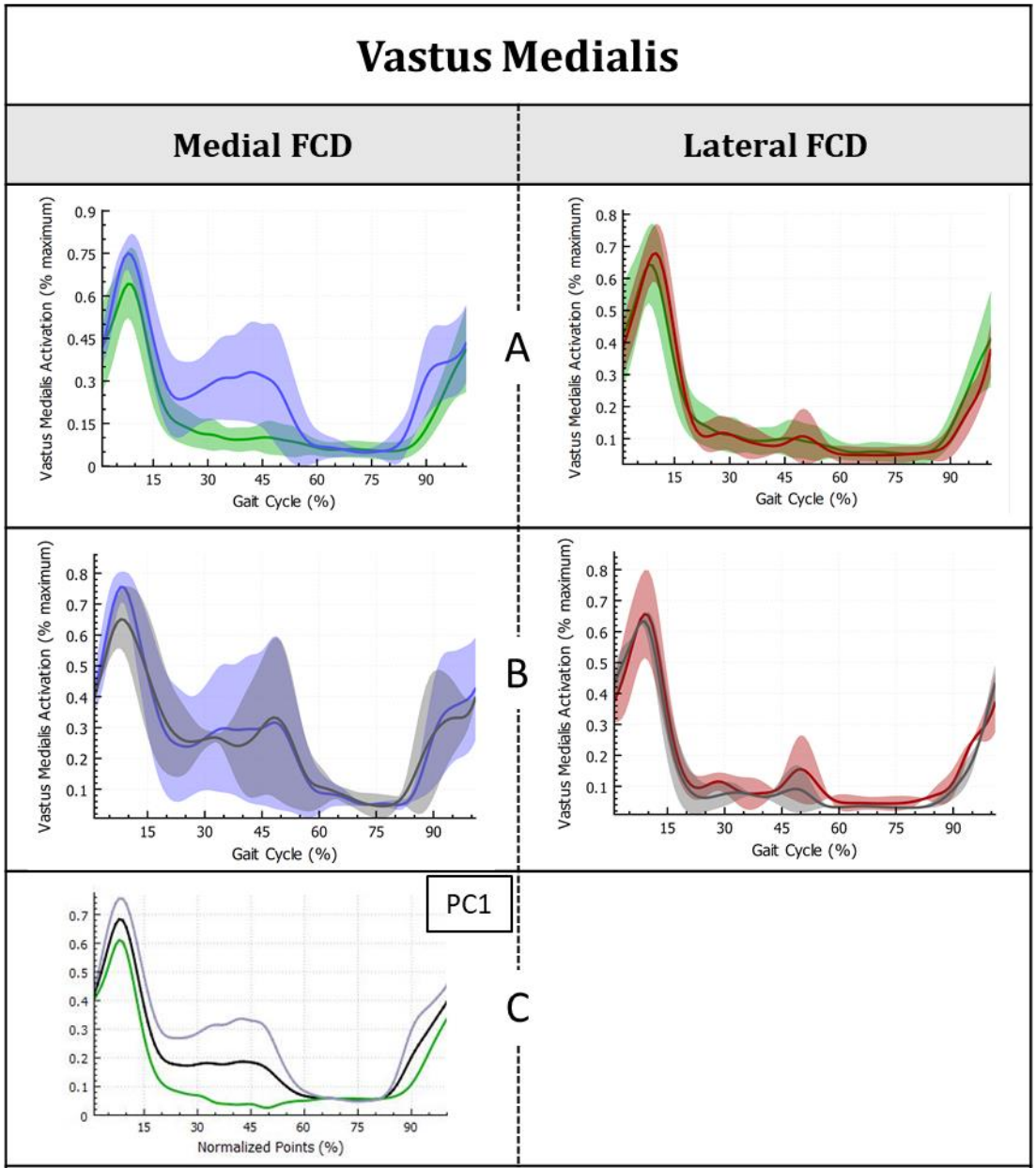

Group	PC	Var Exp. (%)	Feature of FCD patients	Sig. *p*	Δ	Sig. *p*
Medial	1	62.5	↑ activation (mid-stance to toe-off)	.006	Healthy ←	.871

Figure 3.3-10 – Vastus medialis activation ensemble-averaged waveforms (lines) and standard deviations (shaded areas) for Medial FCD and Lateral FCD subjects relative to Control subjects **(A)** and relative to Post-surgery **(B)**. Extreme plots are presented representing the mean (black) and ±1 standard deviation PC reconstructions colour coded to represent group differences corresponding to mean PC scores **(C)**.

Table 3.3-10 – Principal component features of gait waveforms that significantly differed ($p \leq 0.05$) between groups and longitudinal change in PC variance six-months following surgery.

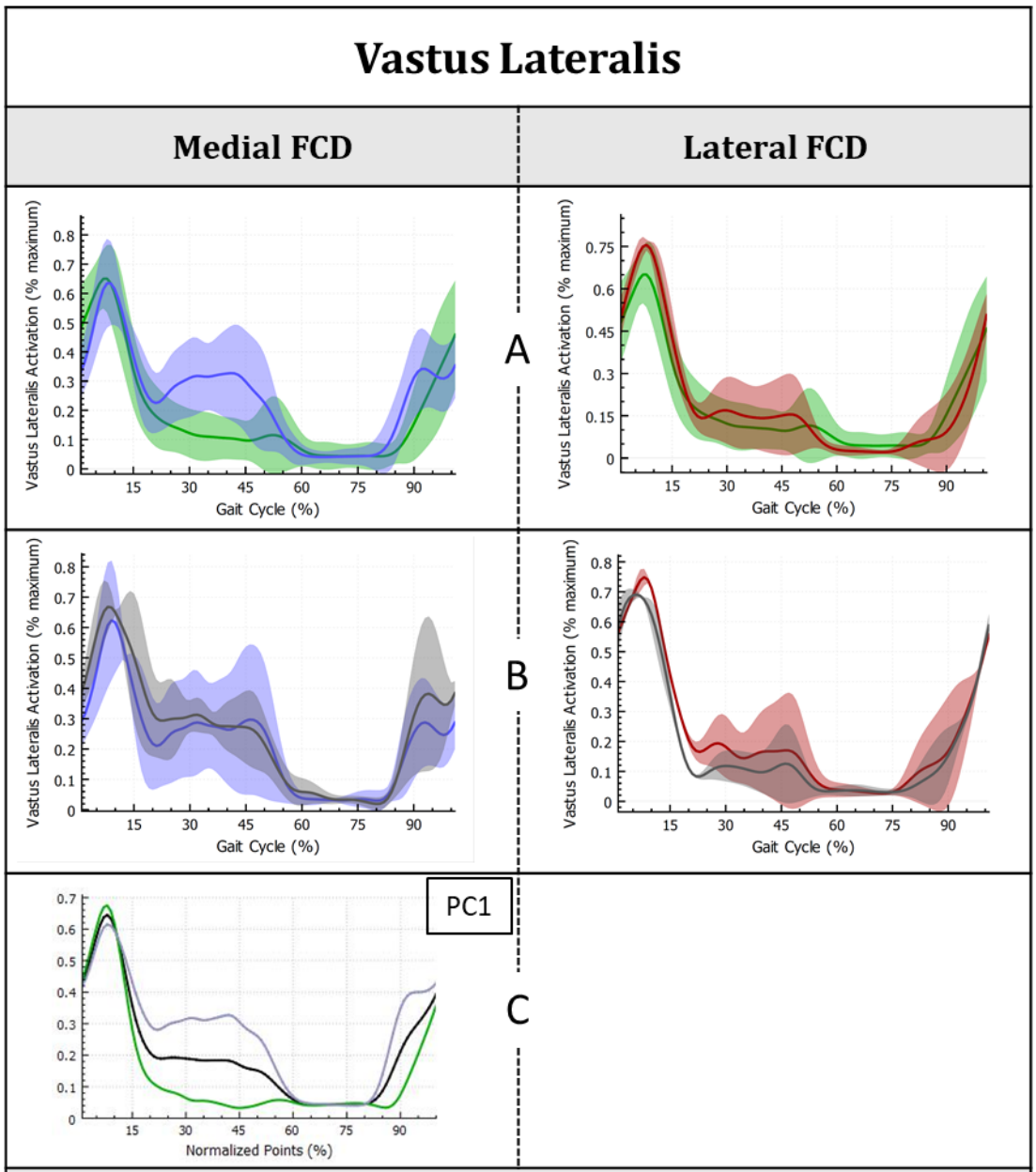

Group	PC	Var Exp. (%)	Feature of FCD patients	Sig. *p*	Δ	Sig. *p*
Medial	1	51.9	↑ activation (mid-stance to toe-off)	**.029**	→ Path	.557

Figure 3.3-11 – Vastus lateralis activation ensemble-averaged waveforms (lines) and standard deviations (shaded areas) for Medial FCD and Lateral FCD subjects relative to Control subjects **(A)** and relative to Post-surgery **(B)**. Extreme plots are presented representing the mean (black) and ±1 standard deviation PC reconstructions colour coded to represent group differences corresponding to mean PC scores **(C)**.

Table 3.3-11 – Principal component features of gait waveforms that significantly differed (p≤0.05) between groups and longitudinal change in PC variance six-months following surgery.

3.3.4.5 Hamstrings activation

Assessment of the hamstring ensemble-averaged activation waveforms revealed excessive hamstring activation in both FCD groups to some degree from heel-strike to late-stance, however this was only significantly reflected PC1 variance differences between medial FCD subjects and controls (Figure 3.3-12 & Figure 3.3-13). On the other hand, both medial and lateral FCD subjects exhibited reduced pre-heel-strike hamstring activation. With closer inspection of the average waveforms, it appears this pre-activation is delayed until immediately during or after heel-strike in both groups compared to controls.

Longitudinal changes in hamstrings activation waveforms showed a trend towards more pathological biceps femoris activation during late-stance in the medial FCD group, whereas the lateral group showed a significant ($p \leq 0.05$) improvement in biceps femoris heel-strike pre-activation patterns, reflective of improved function.

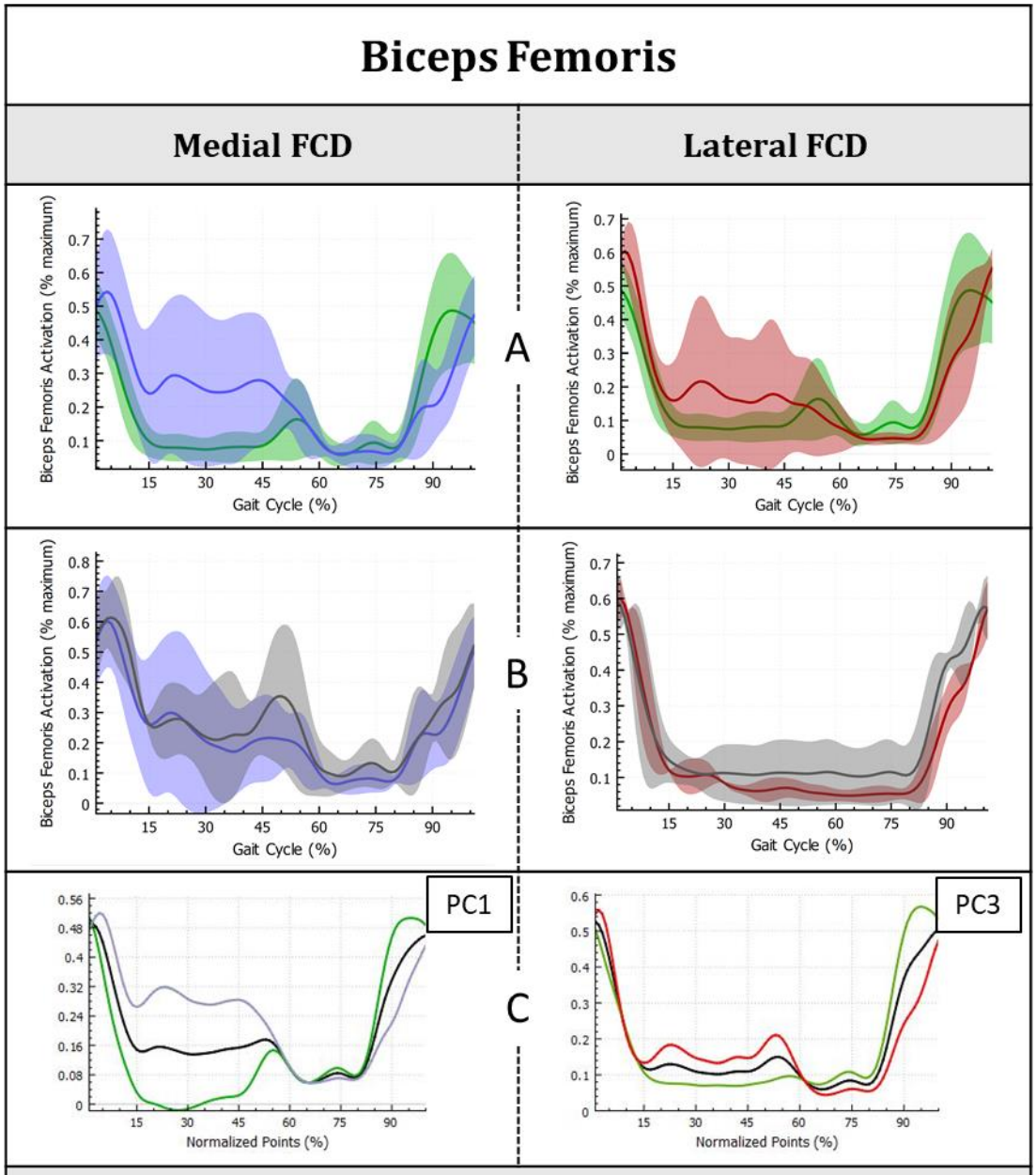

Group	PC	Var Exp (%)	Feature of FCD patients	Sig. *p*	Δ	Sig. *p*
Medial	1	56.6	↑ activation (heel-strike to toe-off), ↓ heel-strike pre-activation	**.007**	→ Path	.152
Lateral	3	13.2	↓ heel-strike pre-activation	**.05**	Healthy ←	**.04**

Figure 3.3-12 – Biceps femoris activation ensemble-averaged waveforms (lines) and standard deviations (shaded areas) for Medial FCD and Lateral FCD subjects relative to Control subjects **(A)** and relative to Post-surgery **(B)**. Extreme plots are presented representing the mean (black) and ±1 standard deviation PC reconstructions colour coded to represent group differences corresponding to mean PC scores **(C)**.

Table 3.3-12 – Principal component features of gait waveforms that significantly differed ($p \leq 0.05$) between groups and longitudinal change in PC variance six-months following surgery.

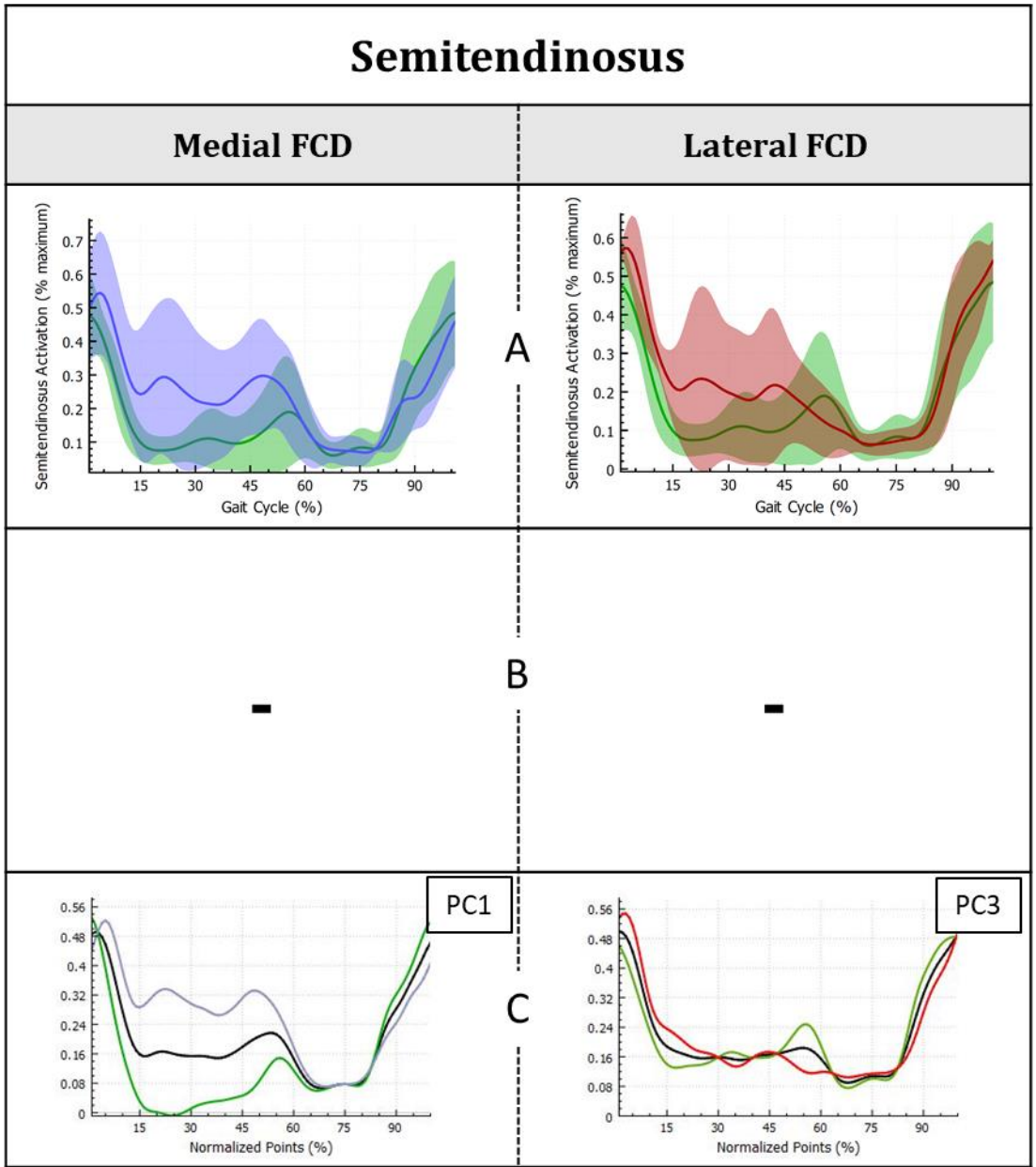

Group	PC	Var Exp. (%)	Feature of FCD patients	Sig. *p*	Δ	Sig. *p*
Medial	1	51.8	↑ activation (early-stance to toe-off)	**.03**	-	-
Lateral	3	10.8	↓ late pre-activation at heel-strike	**.042**	-	-

Figure 3.3-13 – Semitendinosus activation ensemble-averaged waveforms (lines) and standard deviations (shaded areas) for Medial FCD and Lateral FCD subjects relative to Control subjects **(A)** Extreme plots are presented representing the mean (black) and ±1 standard deviation PC reconstructions colour coded to represent group differences corresponding to mean PC scores **(C)**.

Table 3.3-13 – Principal component features of gait waveforms that significantly differed (p≤0.05) between groups and longitudinal change in PC variance six-months following surgery.

3.3.4.6 Summary of functional differences and trends

The findings revealed characteristic functional and patient-reported differences dependent on occurrence or the mediolateral location of tibiofemoral lesions **(Figure 3.3-14)**. The most distinctive and important trends included:

- Medial FCD subjects exhibited increased self-reported pain and reduced self-reported function relative to the lateral FCD group, which appears to be consistent with the more prominent objective functional deficits found in the medial FCD group, including significantly aberrant hip moments, sagittal plane parameters, as well as quadricep and hamstring activation

- Both disease groups showed reduction of the dynamic GRF double-peak magnitudes, which is representative of altering of the typical acceleration-deceleration cycle of the centre of mass during gait. This indicates compensatory gait mechanisms (including reduction of gait speed) in order to ultimately reduce joint reaction forces

- FCD disease groups exhibited altered frontal plane parameters (moments and angles) reflective of overloading the respective diseased knee condyle. E.g. Medial FCD subjects exhibit dynamic varus malalignment, resulting in increased knee adduction moments that could signify increased medial knee loading

- Functional deficits in disease groups are associated with gait cycle events depending on the mediolateral location of the lesion (i.e. medial FCD subjects exhibit functional deficits predominantly during late-stance, and lateral FCD subjects during early-stance)

		Medial	Lateral
KOOS scores	Pain	High	Medium
	Symptoms	High	High
	Function	Very low	Low
Vertical	GRF	↓ GRF double-peak magnitude	↓ GRF double-peak magnitude
Frontal plane	GRF	Normal	Normal
	Angle	Dynamic varus alignment	Dynamic valgus alignment
	Moment	High late-stance KAM	Low early-stance KAM
Sagittal plane	GRF	Normal	Normal
	Angle	High late-stance KFA	Low early-stance KFA
	Moment	High late-stance KEM	Reduced early-stance KFM
Quadriceps	RF	High stance-phase activation	Normal
	VM	High stance-phase activation	Normal
	VL	High stance-phase activation	Normal
Hamstrings	BF	High stance-phase activation	Late pre-heelstrike activation
	S	High stance-phase activation	Late pre-heelstrike activation

Figure 3.3-14 – Summary of most important differences between medial and lateral FCD subjects on self-reported KOOS scores, biomechanics and muscle activity

3.4 DISCUSSION

3.4.1 Key findings for Objective 1

The first objective of this chapter was to use 3D motion capture and EMG methods to identify lower limb functional features of knee focal cartilage defect subjects from non-pathological control subjects. It was hypothesised that FCD patients experience differing biomechanical and neuromuscular activity acting in the lower limbs compared to non-pathological controls.

Temporal Parameters

Despite significant patient-reported knee pain, OA symptoms and reduced function in the FCD subjects associated with this study relative to controls, a lack of significant differences were found in all spatio-temporal parameters, however there was a trend towards decreased walking speed, increased stance and double limb support time and decreased steps per minute in the medial FCD subjects. This pattern is reflective of worse functioning in the medial group, likely related to the worse mean clinical measures (i.e. increased pain, symptoms, reduced self-perceived function) experienced by medial FCD subjects relative to the lateral group, since acute knee pain has been shown to cause subjects to lower speed, likely in an attempt to reduce peak contact forces in the joint and ultimately reduce pain (Shrader et al., 2004, Boyer et al., 2012). Walking speed is well-recognised to influence dynamic biomechanical parameters such as the ground reaction force (GRF), and the magnitudes of the joint moments, leading to difficult interpretation of kinetic data in relation to disease (Landry et al., 2007, Andersson et al., 1981). Furthermore, walking speed has shown in several studies to influence neuromuscular mechanisms in both healthy and pathological populations (Neptune et al., 2008). The statistical similarity in gait speed between the disease subjects and controls allows for a more meaningful interpretation of kinematic and kinetic gait differences compared to severe OA studies, however this pattern in medial FCD subjects is an important consideration for interpretations.

Vertical ground reaction force and centre of mass

Assessment of waveform variances using PCA of the vertical GRF showed similar differences for both FCD groups compared to controls. PC1s for both comparisons represented a decrease in overall GRF magnitude in disease groups and lessening of the 'double-peak' characteristic. Closer inspection of the loading vectors showed that mid-

stance GRFs are more similar to controls but the first and second peaks were relatively reduced. This may be attributed to reduced movement (acceleration/deceleration), of the patients' vertical CoM during walking, which is related to the body's downward velocity being slowed (upwards body mass acceleration) during the first GRF peak in loading response, and the propulsion required during push-off to accelerate the CoM upwards during the second peak (Levange and Norkin, 2011). Another feature of both PC1s is the decreased overall gradient and amplitude seen in the initial (0 – 15%) load response phase seen in FCD subjects. Since this is during the double limb support phase, contrary to results seen in temporal parameters it could be inferred that they are shifting weight bearing onto the affected limb more slowly or require more support from the unaffected limb.

FCD subjects exhibit frontal plane overload of affected knee compartment due to dynamic knee malalignment

Assessment of KAM waveform PC variances revealed that both medial and lateral FCD subjects presented significantly different overall magnitudes of the waveform relative to controls (represented by PC1), whereby the medial group found increased frontal plane moments in contrast to the lateral subjects. This infers that FCD subjects are overloading their respective affected condyle, since the KAM is considered a surrogate measure of medial compartmental loading (Andriacchi and Favre, 2014) and is shown to significantly represent variances in medial knee contact forces measured by instrumented knee implants (Zhao et al., 2007, Kutzner et al., 2013). Further investigation of the PC reconstructions and mean waveforms revealed that the largest differences between lateral FCD subjects and controls are during the load response (first peak) up to mid-stance that lessens during late-stance, whereas the medial group seem to be showing an increased magnitude across the whole of stance which is elevated towards late-stance. It is reasonable to suggest that overloading of the affected condyle may be a critical and likely causal feature of FCD pathogenesis and progression in those experiencing increased moments.

To determine why the disease groups experienced differences in the external KAM, dynamic frontal plane knee alignment (KAAs), centre of pressure (CoP) relative to the knee position, and the medio-lateral GRF vector were considered, as the magnitude of the KAM is a product of the GRF vector times the moment lever arm (i.e. distance between GRF vector and centre of knee rotation). Assessment of GRF vectors showed no clear group differences, however, medial FCD subjects presented increased dynamic varus angles relative to controls, which were reciprocal to the increased valgus angles in

the lateral group. This suggests dynamic frontal plane malalignment of the knee is likely causative of the increased joint moments in most subjects, consistent with previous studies that have demonstrated the correlation between knee alignment and joint overloading in medial and lateral OA subjects (Hunt et al., 2006, Felson et al., 2013).

Knee co-morbidities may be partly responsible for frontal plane functional differences

Qualitative analysis of clinical measures revealed that nine out of the twelve FCD subjects presented meniscal tears or loss preceding or concurrently with their FCDs, of which a proportion had partial meniscectomies during the microfracture surgery. Of those nine, seven of them thought their condition related to a historical injury, which ranged between one to eight years prior to data collection. It is possible that these factors are contributing to the observed differences in frontal plane moments and knee angles, as previous authors have suggested that joint malalignment can develop as a result of meniscal extrusion or articular cartilage loss due to an injury that narrows one side of the joint (Felson et al., 2000, Sharma et al., 2001). Indeed, previous studies have found associations between KAM peak magnitudes and medial meniscus tears or extrusion (Vanwanseele et al., 2010, Davies-Tuck et al., 2008a), suggesting a combination of meniscal loss and possibly chondral damage from lesions may generate morphological changes that misalign the knee, ultimately leading to increased compartmental loads.

Medial FCD subjects do not adequately extend their knee during late stance to reduce peak extension forces and ultimately negate pain

Assessment of knee flexion (+) and extension (-) moment waveform found that medial FCD subjects presented reduced both early- and late-stance moment magnitudes. Notably the extension moment during late-stance was drastically dampened, which was accompanied with inadequate extension of the knee during late-stance. The reduced extension moment is therefore likely consequent of this prolonged knee flexion, since the extension moment is calculated as a product of the anteroposterior GRF multiplied by the moment lever arm. During push-off in late-stance, the anteroposterior GRF typically projects anteriorly to the knee, forcing the joint into extension. However, an increasingly flexed knee during this period of stance would bring the knee centre of rotation anterior towards the GRF vector, ultimately shortening the moment arm and thus avoiding high extension moments. PC variances of the KFA in medial FCD subjects also showed an overall reduced range of motion across the whole gait cycle, which indicates they may be walking with a ‘stiff’ knee style of gait. It is reasonable to postulate that that medial FCD subjects are keeping the knee flexed during late-stance to reduce

contact forces at the knee generated during late-stance extension moments, ultimately to reduce pain. This explanation is compatible with that medial knee subjects typically experience higher medial compartment loading during late-stance, which is found in normal knee force patterns during gait but also amplified by the increased KAMs generated (Van Rossom et al., 2017, Kutzner et al., 2013). These findings are consistent with the reduced knee extension moments exhibited in moderate to severe knee OA subjects that appear to be more prominent with progressing severity (Astephen et al., 2008, Deluzio and Astephen, 2007). It is likely lateral FCD subjects did not exhibit similar adaptations during late-stance as the lateral condyle is typically offloaded at this stage of the gait cycle, which is also evident by the normal KEMs and KFAs experienced.

Medial defect subjects also compensate for pain at the knee by altering hip biomechanics

The significantly reduced HAM 1^{st}:2^{nd} peak ratio in the medial FCD group relative to controls is reflective of the reduced first peak seen in the ensemble mean waveforms. It is likely that the reduced early-stance HAM corresponds to alterations at the knee in early-stance found in medial FCD subjects, since the lower limb joints act as kinematic chain whereby the hip is likely compensating for the altered alignment at the knee or the compensatory gait adaptations for pain as previously suggested (Astephen et al., 2008, Mundermann et al., 2004). Studies investigating hip moments in medial OA subjects have also reported a reduction in peak HAMs in medial OA subjects thought to be a mechanism to compensate for attempting to reduce KAMs, but their peak magnitude reductions were present in both peaks of the waveform (Brandon and Deluzio, 2011, Astephen et al., 2008, Mundermann et al., 2005a, Chang et al., 2005). Since only the first peak was reduced in the medial FCD group compared to controls, it could be suggested that decreased hip moments during late-stance may a feature of later-stage progression. The HAM is largely balanced by the hip abductor muscle moment, thus a compensatory decrease in the HAM over a long-period may consequently result in hip abductor muscle weakness and poor postural control (Chang et al., 2005).

Lateral defect subjects show subtle signs of compensatory mechanisms during early-stance

Although it was not captured by calculated PC variances, the collective trends of reduced knee flexion moments and angles during early-stance suggests that a proportion of lateral FCD subjects may be approaching weight-acceptance with a straighter knee, to avoid the high flexion moment typically experienced during this period. During weight-acceptance the anteroposterior GRF projects behind the knee, forcing it into flexion

which requires additional opposing from the knee extensors (i.e. the quadriceps) to keep the knee stable until mid-stance. By keeping the knee extended at and following heel-strike, this would ultimately reduce the increased net joint forces generated at the knee by this stabilising mechanism and reduce work required from the quadriceps (Duffell et al., 2014). This is thought to be one of the mechanisms by which OA subjects develop quadriceps weakening in the later-stages of pathology, therefore these findings could be an early indication of this process (Hubley-Kozey et al., 2008).

Medial FCD subjects abnormally co-contract thigh muscles during stance

The most distinguishing feature of quadriceps activation was the abnormally prolonged activity of the vastus medialis, lateralis and rectus femoris during stance, consistent across the three muscles in medial FCD subjects, that was not reflected in lateral FCD subjects. This reflected an increased activation during early-to-mid-stance (20%) to toe-off (60%), which is concurrent with when the anteroposterior GRF vector typically passes anteriorly from behind the knee. However, since medial FCD subjects did not adequately extend the knee in the concurrent period during stance to reduce knee extension moments, these findings imply that the anteroposterior GRF remained posterior to the knee centre, thus supporting the knee in a fixed flexion. The result of this is that increased quadriceps (knee extensor) activity is required to generate an internal extensor moment to compensate and retain knee stability. Interestingly, medial FCD subjects were also found to aberrantly increase activation of both hamstrings (i.e. biceps femoris and semitendinosus) during stance relative to controls, concurrently with altered quadriceps activation. This is in line with previous studies that have suggested that coupled quadriceps and hamstring co-contraction has a vital effect on the maintenance of knee stability during flexion-extension, by supporting the anterior cruciate ligament in negating excessive anterior translation and rotation of the tibia (Hirokawa et al., 1991, Hubley-Kozey et al., 2008). Ultimately, it is though that subject will use this adaptive strategy to make up for the instability caused by destabilisation of the joint following knee injury. Supportively of this hypothesis, this difference in variance in the medial group is dominated by two subjects (LP and TR) whom are the only subjects to present ACL damage and laxity reported in the pivot shift test prior to surgery, which is commonly associated with knee instability (Andriacchi and Muendermann, 2006, Efe et al., 2012, Hubley-Kozey et al., 2008).

Aberrant quadriceps contraction prior to weight acceptance in lateral FCD subjects

A distinct feature of lateral FCD gait was the reduced pre-activation of both hamstring muscles examined prior to heel-strike which was followed by excessive activation immediately following heel-strike. This distinct feature in the lateral group may relate to the prominent biomechanical differences found during weight acceptance of this group. It is possible this evidence is reflective of a gait adaptation to lower joint reaction forces during the load response of the gait cycle by loading the affected limb at a slower rate and negating acute deceleration of the centre of mass. The hamstrings are important for deceleration as during heel-strike at initial contact, the anteroposterior GRF vector projects anterior to the knee, and therefore an internal flexor moment is required to bring the knee into flexion for foot flat (Levange and Norkin, 2011). For this reason, pre-activation of the hamstrings is required and thus an increased pre-activation lends itself to a more acute deceleration. It is possible that lateral FCD subjects are not activating hamstrings pre-heel strike to the same degree as controls to keep a more consistent velocity through to mid-stance and avoid high joint reaction forces generated with acute deceleration at the load response.

3.4.2 Key findings for Objective 2

The second objective of this chapter was to assess longitudinal changes in lower limb functional indicators of FCD pathology six-months following treatment with microfracture surgery. It was hypothesised that microfracture surgery would not improve functional outcomes, since cartilage repair techniques have no intention to target knee biomechanics.

Medial FCD subjects exhibit reduced gait speed following surgery

Following surgery, medial FCD subjects walked significantly slower with no improvements in stance time or double limb support time, in contrast to the lateral group who showed a trend towards higher speeds. Reducing gait speed is thought to be an adaptive gait strategy to avoid increased loading of the knee and negate pain associated with higher speeds (Mundermann et al., 2004), however this is not concomitant with changes in patient-reported pain levels or self-perceived function, which were both found to improve following surgery. It is possible that this is resultant of longer recovery times for medial FCD subjects, since they presented lower function than lateral subjects prior to surgery.

Reciprocal effect of surgery on vertical GRF and CoM

In the medial FCD group, there was a very prominent decrease in acuteness of the 'double peak' characteristic of the vertical GRF post-surgery, characterised by an increase in the magnitude between 20-80% of stance phase, predominantly during midstance. This change in waveform shape has before been associated with reduction in gait speed, whereby it is suggested that the body CoM will displace less in the vertical axis in response to slower movement (Chen et al., 1997, Landry et al., 2007). As the affected limb is loaded at a slower rate, less upward acceleration of the CoM is required at the weight acceptance phase to counteract the downward velocity generated post-swing phase. This slower rate of change therefore subsequently results in the CoM fluctuating less during mid-stance, and the vertical GRF therefore stays consistent. Conversely, lateral FCD subjects exhibited increased acuteness of the double peak characteristic, as well as an increase in overall magnitude of the GRF. This is representative of the opposite effect, whereby a mean increase in gait speed is increasing the upward acceleration required to resist downward movement of the CoM. These findings suggest that lateral FCD subjects are generally loading the affected limb more similar to controls, likely as a result of improved recovery and thus increased gait speeds and confident loading of the affected limb.

Microfracture surgery is ineffective at correcting frontal plane knee alignment and thus pathological compartmental loading for most subjects

As expected, there were no significant longitudinal group changes found for knee adduction moments in either FCD disease group following microfracture surgery, which is suggestive that pathological compartmental loading overall has not been altered by microfracture surgery. Inspection of the average waveforms of medial FCD subjects revealed that second peak KAMs appear to be slightly reduced on average, however this is likely resultant of the decreased walking speed which is shown to lower mediolateral GRFs, and well as the consequently reduce inertial forces acting on the lower limbs. This is also substantiated by the lack of post-operative change in KAAs, which infers that all FCD subjects continued to exhibit dynamic knee malalignment following surgery.

Despite the lack of significant group changes detected by PCA, there appeared to be a trend towards increased first peaks of the knee adduction moment in lateral FCD subjects post-surgery, suggestive of a shift of loading distribution in early-stance towards equal compartmental distributions more closely resembling that of the control cohort. This indicates improved function particularly since early-stance appears to be affected in laterally-affected subjects, though this early stance functional improvement was not found with respect to knee adduction angles, suggesting this may possibly be a function of the increased inertial forces acting on lower segments induced by faster walking speeds.

Improved sagittal knee function in lateral, but not medial, FCD subjects

There was a significant reduction in the overall knee flexion-extension waveform in the medial FCD group, which is indicative of a decreased flexion moment and increased extension moment, however unexpectedly this was not accompanied by changes in knee flexion angles suggesting that medial subjects continued to over-flex their knee during late-stance. It is therefore likely that differences seen in the flexion-extension waveform are more related to the reduction in anteroposterior GRFs, possibly due to slowed gait speed. A lower flexion moment during early stance would imply less demand from knee extensor muscles, as thus an overall lessened net moment acting around the knee which is desirable for knee stability. These findings suggest that medial FCD patients are still compensating for pain by reducing gait speed to perhaps further reduce loading during weight acceptance, however the increased knee extension moment does not appear to demonstrate a reasonable explanation.

In contrast, assessment of lateral FCD subjects showed a trend of overall increased magnitude of the knee flexion-extension waveform towards patterns seen in control subjects, though this was not significant at the $p \leq 0.05$ level. This finding again demonstrates an improvement of knee function in the lateral group, which is consistent with their improving clinical pain and self-perceived knee function. It is noteworthy however that there were no original substantial differences between pre-operative lateral FCD subjects and controls with regards to flexion-extension moments, therefore this may be representative of a smaller improvement resultant of increased gait speed. This is further evidenced by the lack of differences found in knee flexion angles which implies moment changes are more-so related to anteroposterior GRFs and inertial forces as opposed to changes in kinematics of the knee.

Medial FCD subjects continue to abnormally co-contract thigh muscles following surgery

No pre-post significant changes were found in medial FCD group quadriceps or hamstrings activation waveforms, indicating that aberrant protective muscle activation patterns seen in medial FCD subjects were retained six-months after surgery. This is certainly interesting when taking into account the significant improvement seen in self-reported pain, which has been shown to have a direct effect on neuromuscular activation in severe OA subjects before and after analgesic intake (Felson et al., 2000). Furthermore, following surgery subjects are submitted to 3 months of physiotherapy, which involved thigh muscle strengthening and conditioning with increasing levels of weight bearing. It is likely that although some pain has diminished, the medial FCD subjects have been conditioned to activate their muscles in these altered patterns for some time to protect the affected compartment of the knee both prior to and post-surgery. Therefore a 'carry-over' effect may be present whereby subjects continue to abnormally contract the quadriceps. It is necessary to conduct a longer study with much later time-points post-surgery to determine the ultimate effect surgical outcomes have on neuromuscular functioning.

3.4.3 General discussion

This chapter provides first evidence of altered lower limb biomechanics and neuromuscular functioning in individuals with symptomatic tibiofemoral FCDs. The findings are reflective of increased pathological compartmental knee loading likely due to dynamic knee malalignment, as well as possible gait adaptative strategies for pain

avoidance in both disease groups relative to controls. Furthermore, preliminary evidence has shown that subjects suffering from chondral damage in the lateral compartment may be better functioning than those of medial damage following microfracture treatment. These findings are importantly suggestive of the requirement of additional treatment strategies for some individuals undergoing cartilage repair, since microfracture alone does not appear to be adequate to improve function. Moreover, the distinct differences between medial and laterally-affected individuals both prior to and following surgery suggests a requirement for targeted treatment groups that may benefit from tailored intervention (Knoop et al., 2011, Driban et al., 2010).

To date, only one research paper has explored joint loading patterns specific to knee FCD patients that characterised biomechanical differences between patellofemoral and tibiofemoral full thickness articular defect subjects. Using 3D gait analysis combined with inverse dynamic modelling, Thoma and colleagues reported the presence of tibiofemoral FCDs, but not patellofemoral FCDs, affected joint loading patterns. Explicitly, tibiofemoral FCD subjects showed lower overall tibiofemoral joint reaction forces in the early-stance of gait and increased midstance forces (Thoma et al., 2017). However, when controlling for gait speed, they found no difference between groups, suggesting that tibiofemoral FCD subjects walked slower to reduce total peak joint tibiofemoral forces. This is consistent with results from this study suggesting medial FCD subjects may be walking slower both at baseline and significantly slower 6 months post-microfracture surgery to reduce medial joint loading. However, their study does not account for medio-lateral locations of the lesions within their analysis, which could potentially lead to averaging out of differences in frontal plane joint dynamics, an important factor considering results from this chapter. Furthermore, they did not use controls and based their interpretations on differences between patellofemoral and tibiofemoral groups, which may lead to presumptuous interpretation of 'normal' functioning.

One of the most substantial findings within this chapter is that frontal plane knee adduction moments vary between disease groups in an opposing effect and both groups relatively to controls. These differences are indicative of pathological compartmental overload that ultimately alters the mechanical environment of joint tissues and independently explains the progression of tibiofemoral lesions for those subjects (Andriacchi and Favre, 2014). However, this is by no means conclusive evidence of the initial causes of FCDs in these subjects, as many reported previous joint injuries which likely initiated pathogenesis (Roos, 2005, Felson, 2013). The initial response of tissue to

joint impact involves a pro-inflammatory cytokine response (Bigoni et al., 2013, Lieberthal et al., 2015, Haller et al., 2015), changes in the structure and composition of bone and cartilage (Gilbert et al., 2018), upregulated bone cell remodelling activities (Liu et al., 2009) and increased catabolic chondrocyte signalling (Bader et al., 2011). However, most of these biological responses to injury tend to be perpetuated over the course of post-traumatic degenerative pathologies such as OA, particularly inflammation (Watt et al., 2016, Struglics et al., 2015), bone structural changes such as attrition or sclerosis (Neogi, 2012, Burr and Gallant, 2012), as well as cartilage degradation (Biswal et al., 2002). Therefore, the question is whether these biological processes are driven by the consequence of pathomechanics.

As discussed previously, a plethora of previous independent studies have demonstrated the magnitude of the external KAM correlates with directly measured medial-to-lateral knee compartmental forces in instrumented knee implant studies (Kutzner et al., 2013, Kutzner et al., 2010, Zhao et al., 2007, Walter et al., 2010, Schipplein and Andriacchi, 1991). Reflecting on the results in this study, it seems rational that patients are overloading the respective diseased condyle of the knee due to the location of the focal damage. Indeed, many studies have linked the external KAM and dynamic knee malalignment with medial osteoarthritic damage progression (Andrews et al., 1996, Miyazaki et al., 2002, Teichtahl et al., 2003, Foroughi et al., 2009, Baliunas et al., 2002, Walter et al., 2010) and lateral OA progression (Felson et al., 2013).

Interestingly, most previous studies investigating OA gait found that their subjects had radiographically varus aligned ('bow-legged') knees which could significantly explain variances in the KAM. In contrast, within this study, no static valgus or varus malalignment was reported for any FCD subject by clinical examination according to the surgical notes. However, it was clear that dynamic frontal plane knee angles were concomitant with increased KAMs, demonstrating that static knee alignment measurements may not be sensitive to predict dynamic alignment in this early stage of disease. It is noteworthy that suspected OA patients, but not early stage patients, are diagnosed using static long-leg X-rays to assess morphological factors, whereby hip-knee-ankle (HKA) angles are determined with up to ±1.25° accuracy, allowing more informed decisions and planning for joint realignment surgeries such as high tibial osteotomy (Coventry et al., 1993, McDaniel et al., 2010). Though, it is possible that malalignment at the knee only presents itself during dynamic activities, whereby forces acting at the knee during gait are amplified because of inertial and gravitational forces acting on the body centre of mass. Average peak compressive loads of up to three times

bodyweight are seen during level gait (Mow, 1991), therefore increased bending forces will be experienced at the knee resulting in further malalignment of the joint than is found in static assessments.

With further analysis into the clinical background of this cohort, it was evident that nine out of the eleven FCD subjects presented meniscal tears or loss concomitant with the site of the lesions, of which a proportion had partial meniscectomies during the microfracture surgery. Of those nine, seven of them thought their condition related to a historical injury, which ranged between one to eight years prior to the date of data collection. These structural changes in the joint are important to consider as possible drivers of FCD pathogenesis, since they are required for normal stability of the joint. Felson et al. (2000) have suggested that joint malalignment can develop as a result of meniscal extrusion or articular cartilage loss due to an injury that narrows one side of the joint. A previous study found a strong association between meniscal damage, malposition and cartilage loss in a cohort of 257 symptomatic OA patients (Hunter et al., 2006). Additionally, other studies have revealed a link between the external KAM peak amplitude and medial meniscus tears or extrusion (Vanwanseele et al., 2010, Davies-Tuck et al., 2008a). Based on this previous work, it is probable that the majority of FCD patients in this study developed these lesions due to morphologic change in the joint following an earlier injury that resulted in loss of articular cartilage or menisci, which may be altering dynamic frontal plane alignment of the knee.

During articulation and loading of the knee, compressive, tensile and shear forces are produced. The menisci exist to promote wider distribution of these forces transmitted through the articular surfaces, by deforming radially. The radial reaction force (F_{rad}) generated from the tensile hoop stress (F_{cir}) on the curved superior surface of the menisci balances femoral horizontal forces (Athanasiou and Sanchez-Adams, 2009). It is possible that loss of meniscal tissue is impairing the load distributing mechanism of the knee, leading to focal regions of stress on the articular cartilage. Both meniscal and ligament ruptures are recognised as potent risk factors for post-traumatic OA (PTOA) development, a well-documented 'accelerated OA' phenotype. This is thought to be due to the increased joint instability and laxity that accompanies these pathologies, which leads to increased loading of mal-adapted, previously non-weight bearing regions of cartilage in the joint and therefore catalyses joint degeneration (Felson et al., 2000, Buckwalter and Lane, 1997, Sharma et al., 2001, Logan et al., 2004). Indeed, multiple studies have shown that 19-43% of acute ACL rupture patients are diagnosed with accompanying FCDs (Tandogan et al., 2004, Flanigan et al., 2010, Maffulli et al., 2003). In

one of these studies it was also shown that 80% of those with chondral defects also had meniscal lesions (Tandogan et al., 2004). Furthermore, 2.7 times increased odds were found for having a grade III/IV chondral lesion at 2-5 years post ACL-rupture and 12.6 times at post-5 years rupture (Tandogan et al., 2004). Considering these figures, it is valid to attribute at least part of FCD development with the co-pathologies evident in this cohort.

The medial FCD group examined within this study presented several late-stance (push-off) deficits in hip, knee and ankle function similar to that seen in established OA, notably increased KAMs, as well as neuromuscular adaptations representative of abnormal muscle co-contractions similar to that found in ACL-injury/knee instability subjects (Roos, 2005, Andriacchi and Favre, 2014). Moreover, biomechanical differences found in the sagittal plane (i.e. inadequate knee extension and lower knee extension moments) are indicative of gait adaptations for pain avoidance, which also occurred in late-stance. In contrast, the lateral group only appeared to present differences in early-stance (weight acceptance), predominantly involving frontal plane biomechanics indicative of lateral compartmental loading, reduced knee flexion moments and angles, as well as muscular activation differences prior to weight acceptance that may be representative of pain anticipation. Collectively, these indicators support the hypothesis that lesion-related pathogenesis, progression, instability and pain may be dependent on mediolateral location of the lesion. Furthermore, the event period of the gait cycle in which functional deficits are presented also related to mediolateral location of joint damage. This finding can likely be explained by the significant asymmetry in the kinematics of the two knee compartments due to the differing anatomy. The medial compartment exhibits increased anteroposterior glide during gait as the convex tibial-to-concave femoral contact area is much greater than the convex-to-convex contact area of the lateral compartment during weight-bearing activity (Koo and Andriacchi, 2008). With an alteration in gait due to injury, loss of meniscus or ligament laxity, the increased loaded surface area that has potential to change could increase the sensitivity of the medial compartment to smaller kinematic changes (Quatman et al., 2012).

Our collaborative colleagues have importantly demonstrated using musculoskeletal models taking into account ligament geometry, muscle forces and elastic response of articular surfaces, that areas of pressure and force distributions during weight acceptance of the healthy knee are roughly relatively equal amongst the two compartments (Figure 3.4-1 – **Average knee cartilage thickness (mm) distribution**

of fifteen healthy subjects quantified by T1rho MRI imaging and segmentation techniques (A) and peak contact pressures during weight-acceptance (first peak) and push-off (second peak) during normal gait (B) – Adapted from (Van Rossom et al., 2017)), whereas during push-off, forces are higher in the medial compartment relative to the lateral side (Van Rossom et al., 2017). It is understood that during the final 20° of knee extension in late-stance, the anterior tibial glide on the medial condyle persists as its dimensions are longer than that of the lateral condyle. This prolonged medial anterior glide generates an external rotation of the tibia, known as the 'screw-home' mechanism, and is responsible for shifting load onto the medial condyle during push-off (Figure 3.4-1 – **Average knee cartilage thickness (mm) distribution of fifteen healthy subjects quantified by T1rho MRI imaging and segmentation techniques (A) and peak contact pressures during weight-acceptance (first peak) and push-off (second peak) during normal gait (B) – Adapted from** (Van Rossom et al., 2017)).

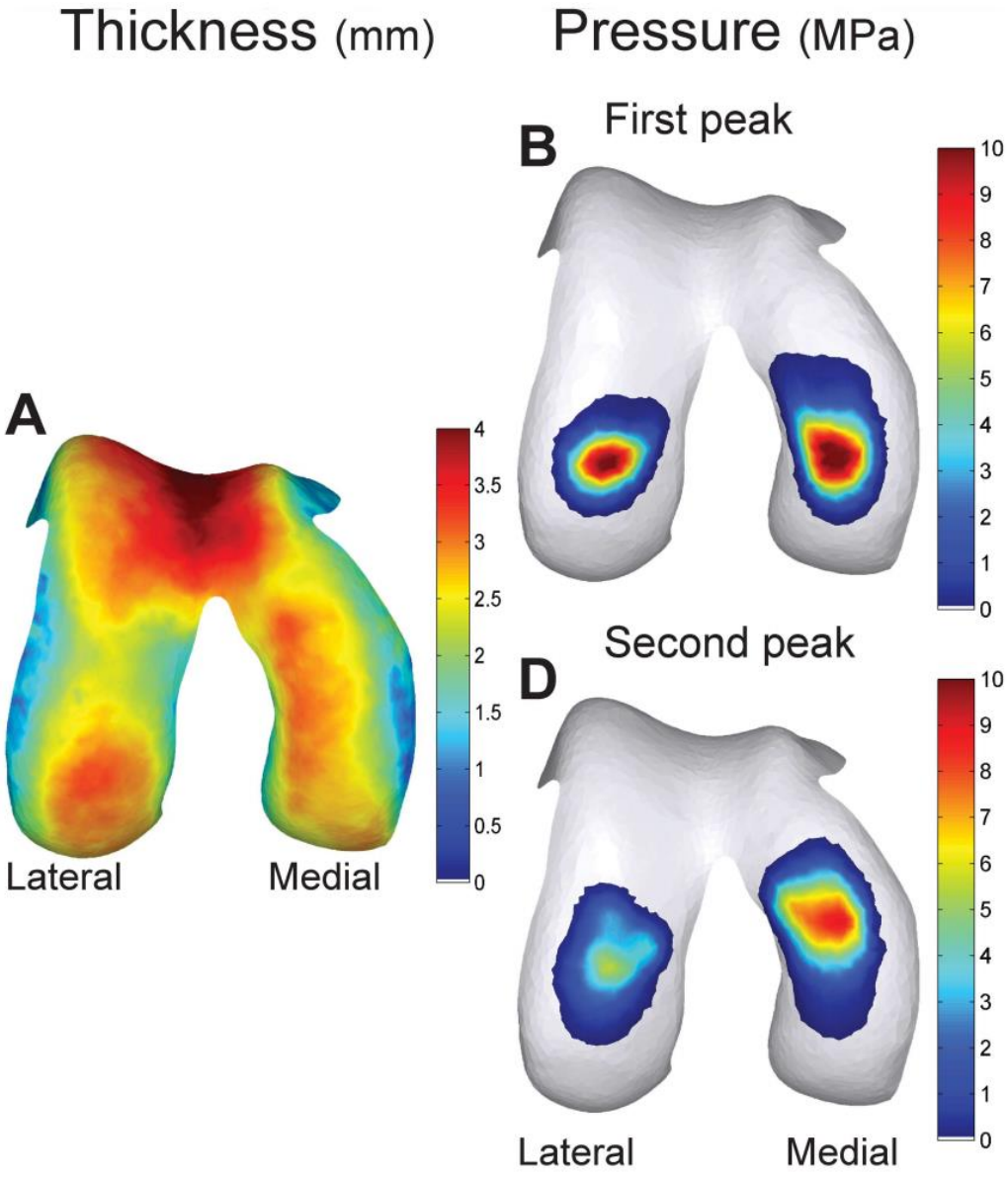

Figure 3.4-1 – Average knee cartilage thickness (mm) distribution of fifteen healthy subjects quantified by T1rho MRI imaging and segmentation techniques (A) and peak contact pressures during weight-acceptance (first peak) and push-off (second peak) during normal gait (B) – Adapted from **(Van Rossom et al., 2017)**

This mechanism may be explanatory of the disparity between biomechanical alterations for the medial versus the lateral FCD group relative to controls during specific events of the gait cycle. In the lateral group, valgus dynamic knee malalignment may lead to redistribution of the typically equal mediolateral knee loading during early-stance toward the lateral compartment, leading to excessive forces applied to lateral knee joint tissues, which evens out during late-stance. Whereas for the medial group, dynamic varus malalignment will favour increased loading of the medial condyle during both early-stance and late-stance. This increased burden in medial FCD subjects could be mechanistically related to why the medial FCD group were generally worse functioning and why medial knee pathology is more commonly reported (Favre and Jolles, 2016). However, the altered kinematics may have an abnormal loading effect on the cartilage conditioned in the joint to suit the mechanical environment during pre-FCD weight-bearing activity (Figure 3.4-1 – **Average knee cartilage thickness (mm) distribution of fifteen healthy subjects quantified by T1rho MRI imaging and segmentation techniques (A) and peak contact pressures during weight-acceptance (first peak) and push-off (second peak) during normal gait (B) – Adapted from** (Van Rossom et al., 2017)). Ultimately, enhanced maladaptive loading of the already pre-disposed and damaged cartilage in the joint may be an important driving factor of FCD progression towards an OA state.

Modifying muscular control strategies depends on coordination and strength, which importantly contribute to postural control, joint loading and stability. Medial FCD subjects were found to substantially increase activation of their quadriceps and hamstrings during early- to late-stance, suggesting they may be attempting to excessively support the knee during foot contact in compensation of the experienced instability, which is consistent with neuromuscular functional deficiencies of knee medial, but not lateral, OA subjects (Schmitt and Rudolph, 2008, Fallah-Yakhdani et al., 2012, Childs et al., 2004, Lewek et al., 2005). Cadaveric studies have shown that coupled co-contraction of quadriceps and hamstrings has a vital effect on the maintenance of knee stability during flexion-extension, by supporting the anterior cruciate ligament in negating excessive anterior translation and rotation of the tibia (Hubley-Kozey et al., 2008, Hirokawa et al., 1991). Lewek and colleagues noted that attempts to stabilise the knee with greater co-contraction presumably contributes to higher joint compression due to the higher internal moments generated on the knee, and thus consequently may exacerbate tissue destruction (Lewek et al., 2005). This may have important implications for long-term surgical outcomes of marrow stimulation in medial FCD subjects, since they continued to co-contrast thigh muscles following surgery despite undergoing

physiotherapy rehabilitation programmes. However, the importance of co-contraction for retaining knee stability in knee OA patients has been challenged by other authors in the field, who claim protecting the knee from excessive shear stress caused by instability is more important than reducing compressive loads for protecting the knee from tissue degeneration (Schmitt and Rudolph, 2008). Regardless of these arguments, increased co-contraction could be a risk factor for FCD progression, and further work should be carried out to determine the effect excessive co-contractions would have on lesion progression.

Conventional cartilage repair treatments for FCDs (e.g. microfracture and autologous chondrocyte implantation) may improve local tissue biomechanics by replacing the lost or damaged focal regions of cartilage with a plug of neo-fibrocartilage (Seo et al., 2011), however evidence for the impact of these techniques on restoration of whole joint biomechanics is limited. Findings from this chapter revealed that microfracture surgery led to worsening knee function in medial FCD subjects after six-months of recovery, surprisingly regardless of the improved reported pain, symptoms and self-perceived function. This was in contrast to lateral FCD subjects who appeared to exhibit some degree of improved function, evident by the faster walking speed which resulted in first peak knee adduction moments and flexion-extension moments more similar to that of controls. However, it should be considered that the lateral FCD group showed better functioning as well as patient-reported pain, symptoms and function at baseline relative to medial FCD subjects, which are likely to be at least partially explanatory factors of this disparity. Whilst cartilage repair alone may be appropriate for the lateral defect subjects, medial subjects may benefit from a combination of repair surgery and interventions aimed at re-aligning the dynamic mechanical axis of the knee, such as gait retraining (Zhao et al., 2007, Fregly, 2012) or lateral-wedge shoe implants (Radzimski et al., 2012, Morin et al., 2018) to attempt to reduce peak joint loads that may be driving progression.

Despite some improvements in the lateral FCD group, both disease group subjects demonstrated no change in dynamic frontal plane alignment angles, which is hypothesised to be the primary cause of FCD pathogenesis within this chapter and well-recognised to be a risk factor for OA development (Felson et al., 2013). If this biomechanical alteration continues into recovery, it is likely that newly formed fibro-cartilage will still be subjected to increased loads, which may result in reoccurring cartilage degeneration. This is particularly the case in cartilage repair subjects, since fibro-cartilage is shown to be mechanically-inferior relative to the surrounding hyaline cartilage (Falah et al., 2010, Seo et al., 2011), therefore subjecting it to altered stress

patterns. Large clinical interventional studies may benefit from monitoring dynamic knee malalignment and the knee adduction moment for prediction of long-term outcomes of cartilage repair.

Chapter 4

The characterisation and longitudinal assessment of synovial fluid and serum biomarkers of joint pathology in focal cartilage defect subjects undergoing microfracture surgery

4.1 Introduction

The previous chapter identified biomechanical mechanisms of pathogenesis associated with increased knee compartmental loading that may be partially explanatory of FCD presence. Since there is previous evidence to suggest altered mechanical loading would have consequences to joint biological homeostasis, there is likely to be biological mechanisms involved in FCD pathology and progression that have to date not been evidenced. Therefore, the first objective of this chapter was to investigating a range of candidate biomarkers relating to mechanical loading of bone (Glutamate, Sclerostin), turnover of bone (ALP, CTX-I, RANKL, OPG) and cartilage (CTX-II, COMP), as well as inflammatory signalling molecules (IL-1β, IL-2, IL-4, IL-6, IL-8, IL-10, IL-12p70, IL-13, TNF-α and IFN-γ) in synovial fluid from FCD patients relative to unicompartmental knee OA (uOA) patients, and in serum from FCD patients relative to non-pathological control subjects.

Synovial fluid analysis aimed to investigate mechanisms of FCD pathophysiology in the joint and determine biomarkers of FCD progression towards established 'moderate' OA that may be reflected in serum. This is particularly important since FCDs are shown to typically progress to clinical unicompartmental OA in their natural course (Davies-Tuck et al., 2008b). Whereas serum analysis was used to reveal biomarkers that may be representative of FCD pathology systemically that could be used for diagnostic, prognostic, and outcome measures in interventional studies.

The rheumatology field is becoming increasingly aware of OA heterogeneity, with mounting evidence of the need for personalised treatments for distinct phenotypic groups (Karsdal et al., 2014). Therefore, multivariate analysis (PCA) was utilized to investigate inter- and intra-disease group variances by combining linear combinations of biomarkers into principal components, combined with cluster analysis to identify possible phenotypes of disease.

The final aim of this chapter was to utilize serum biomarkers for the longitudinal characterisation of the biological response microfracture surgery, to establish typical responses of good and bad outcome that could reveal biochemical clinical predictors. This was achieved by investigating longitudinal changes in serum biomarker levels from time of microfracture surgery (baseline) to six-months post-surgery, which were interpreted individually and related to subject-reported clinical outcomes (such as OA-related pain, symptoms and function). Ultimately, the findings from this chapter could be used to identify progressing pathophysiological mechanisms of FCDs and associated

disease states as well as evaluate outcomes of existing and developing interventions for the treatment of FCDs, to aid clinical decision making.

Chapter Aim: Investigate biomarkers of OA-related pathology in symptomatic FCD patient synovial fluid and serum to further the understanding of pathophysiological mechanisms of disease, and develop diagnostic and prognostic biomarkers for assessing longitudinal outcomes of microfracture surgery

Objective 1: To measure candidate molecules of bone and cartilage turnover, mechanical loading of bone and inflammation in synovial fluid (FCD compared to uOA) and serum (FCD compared to healthy controls) to identify mechanisms and biomarkers of FCD pathogenesis.

Hypothesis: *Molecules representing turnover, mechanical loading and inflammation differ in tibiofemoral FCD subjects compared with uOA and healthy subjects*

Objective 2: Use multivariate analysis and clustering tools to identify possible inter- or intra-disease group variances or phenotypes from linear combinations of synovial fluid biomarkers

Hypothesis: *Multivariate combinations of synovial fluid biomarkers will reveal clusters that are representative of disease phenotypes*

Objective 3: To assess longitudinal changes in biomarkers of turnover, mechanical loading and inflammation to establish a pattern of typical repair and poor outcomes of microfracture surgery

Hypothesis: *Changes in biomarker concentrations representing turnover, mechanical loading and inflammation will reveal typical repair / poor outcomes 6 months following microfracture surgery*

4.2 Methodology

The methods for collection, processing and quantification of biomarker concentrations for analysis was previously described in section 2.6.

4.2.1 Correlation analysis

Spearman's Rho was used to measure the strength of bivariate associations. It was chosen to opt for a non-parametric test due to the small sample sizes which could lead to major influences of outlying samples in a parametric test such as the Pearson's correlation. In several tables within this chapter, correlation heatmaps were used to visually represent the strength of the coefficient (ρ) whereby denser colour gradients represented stronger associations. Furthermore, the density of orange represented strength of positive correlation, and the density of blue represented the strength of an inverse correlation.

4.2.2 Normality Testing

The Shapiro Wilk's test was used for testing of the normality of distribution of group biomarker concentrations (IBM SPSS, USA) to satisfy the assumptions of the parametric ANCOVA. Variables that were skewed were first rank-transformed prior to group testing.

4.2.3 Group comparisons

Group comparisons of synovial fluid or serum biomarker concentrations were tested for differences using ANCOVAs, with age and BMI as covariates (IBM SPSS, USA). *p*-values were adjusting for age and BMI.

4.2.4 Wilcoxon signed-rank test

Longitudinal changes of serum concentrations were tested for by using Wilcoxon signed-rank test (IBM SPSS, USA). A non-parametric paired test was used in all circumstances due to the low sample size (n=5) which may lead to unrepresentative distributions of data.

4.3 Results

4.3.1 Sample collection and cohort characteristics

Synovial fluid samples were collected from eleven knee FCD subjects (10 male, 1 female; mean(SD) age = 47 (13) years, BMI = 29.2 (4) kg/m^2) undergoing microfracture surgery and eleven unicompartmental knee OA (uOA) subjects (8 male, 3 female; mean(SD) age = 51.6 (5.5) years, BMI = 27.9 (3.6) kg/m^2) undergoing high tibial osteotomy surgery (Appendix A.1). uOA subjects were on average older relative to FCD subjects, but both groups presented similar BMIs. All FCD subjects had Outerbridge grade II tibiofemoral chondral lesions, nine of which had accompanying meniscal tears/damage in the affected compartment and one subject had an ACL year with a positive (+Glide) pivot shift (Appendix A.1). All uOA subjects had radiographic varus knee alignment (1.9° – 15.4°) and KL grade 2-4 OA.

Serum was collected and processed from thirteen knee FCD subjects (11 male, 2 female; mean (SD) age = 44.1 (17) years, BMI = 28.9 (5) kg/m^2) and eight healthy control subjects (6 male, 2 female; mean (SD) age = 31.8 (9), BMI = 25.45 (2) kg/m^2). There were no significant differences found in age and BMI between groups, however FCD subjects were on average older than controls. The same additional co-pathologies applied to the FCD group as previously mentioned. There were eight FCD subjects with linked synovial fluid and serum data assessed in this chapter.

4.3.2 Correlations of inter-fluid biomarker levels

To determine if biomarker concentrations in the joint were reflected systemically, Spearman's Rho (1-tailed) correlations were tested for biomarkers common to synovial fluid and serum in eight subjects (Table 4.3-00). Surprisingly, only synovial fluid levels of IL-13, sclerostin and CTX-I were significantly reflected in serum levels ($p \leq 0.05$). Additionally, glutamate and IL-10 showed moderate positive ($R > 0.40$) relationships that were not statistically validated at the $p \leq 0.05$ level. In contrast, pro-inflammatory chemokine IL-8 showed a significant inverse inter-fluid relationship ($p \leq 0.001$).

4.3.3 Correlations of biomarker levels with demographics

Age significantly ($p \leq 0.05$ to ≤ 0.001) associated with decreased glutamate and sclerostin levels in synovial fluid, decreased RANKL and RANKL:OPG ratio in serum, and increased

serum IL-6 (Table 4.3-0). Whereas BMI significantly ($p \leq 0.05$) correlated with higher synovial fluid CTX-I and serum ALP levels.

Spearman's Rho	Inter-fluid Correlation	Synovial Fluid		Serum	
		Affected by age?	Affected by BMI?	Affected by age?	Affected by BMI?
TNF-α	-0.117	0.177	0.010	-0.077	0.241
IFN-γ	0.033	-0.229	0.623	-0.093	0.132
IL-6	-0.143	0.455	-0.121	**0.540***	0.218
IL-8	**-0.85****	0.233	-0.242	-0.177	0.032
IL-10	0.452	0.004	0.382	-0.155	0.185
IL-12p70	0.267	0.578	-0.204	0.120	-0.015
IL-13	0.9*	0.252	0.140	-0.099	0.203
RANKL	0.2	0.354	-0.261	**-0.539***	0.015
OPG	0.267	0.050	0.161	0.056	-0.094
RANKL/ OPG	0.464	0.293	-0.252	**-0.518***	0.091
Glutamate	0.452	**-0.785****	0.363	-0.014	0.250
Sost	0.643*	**-0.536***	0.022	-0.061	0.112
ALP	0.394	-0.151	0.440	-0.055	**0.615***
CTX-I	0.765**	0.311	0.592*	0.437	0.362
COMP	-	-	-	-0.058	-0.426

Table 4.3-0- Spearman's Rho (1-tailed) testing for positive correlations of analyte inter-fluid levels and analyte relationships to demographic features. Grey cells with bold face values are statistically significant relationships.

* significant at $p<0.05$. ** significant at $p<0.01$.

4.3.3.1 Group comparisons of biomarker levels in synovial fluid and serum (Objective 1)

Analysis of covariance (ANCOVA) was used for testing group differences of biomarker levels whilst adjusting for age and BMI (Figure 4.3-1 to 4.3-7) to reveal discriminatory metabolites of FCD subjects relative to controls (in serum) and uOA subjects (in synovial fluid). Testing of synovial fluid biomarkers revealed that levels of three of the fifteen biomarker features were elevated ($p \leq 0.05$) in uOA synovial fluid relative to FCD subjects, including pro-inflammatory mediators IL-6 and IL-8, as well as bone resorption inhibitor OPG. In contrast, anti-inflammatory cytokines IL-10 and IL-13 were significantly ($p \leq 0.05$) decreased in uOA synovial fluids. With serum testing, FCD subjects presented higher ($p \leq 0.05$) levels of serum glutamate and CTX-I, as well as decreased ($p \leq 0.05$) anti-inflammatory activity (IL-10) and proinflammatory cytokine TNF-α relative to healthy controls.

4.3.3.2 Longitudinal changes in serum biomarker levels (Objective 3)

Paired comparisons of means testing (Wilcoxon signed-rank tests, 2-tailed) and visual assessment of individual changes were assessed to determine longitudinal changes in biomarkers that may be reflective of the response to microfracture surgery (Figure 4.3-1 to 4.3-7).

For inflammatory molecules, significant changes ($p \leq 0.05$) were found in IL-8 (1.5-fold) and IL-13 (1.35-fold), both significantly elevated following surgery. There were also considerable mean increases in TNF-α (1.13-fold) and IL-10 (1.08-fold) that did not reach significance at the $p \leq 0.05$ level. In contrast, levels of IL-6, IL-10 and IFN-γ appeared to vary in direction across the group. Notably, one subject (RP) appeared to show more prominent biomarker changes, some in the opposite effect relative to the group. The clearest being decreases in IFN-γ and IL-10, as well as a sharp increase in IL-8.

For bone signalling biomarkers, only glutamate levels significantly ($p \leq 0.05$) decreased (0.71-fold) across the group, however sclerostin (0.76-fold), RANKL (0.7-fold) and the RANKL/OPG (0.67-fold) ratio also revealed considerable mean decreases across the group. For biomarkers of tissue turnover, there was significantly ($p \leq 0.05$) declined CTX-I levels (0.76-fold) and contrasting significant ($p \leq 0.01$) increases in COMP levels (1.2-fold), however changes in ALP levels varied in direction across the group.

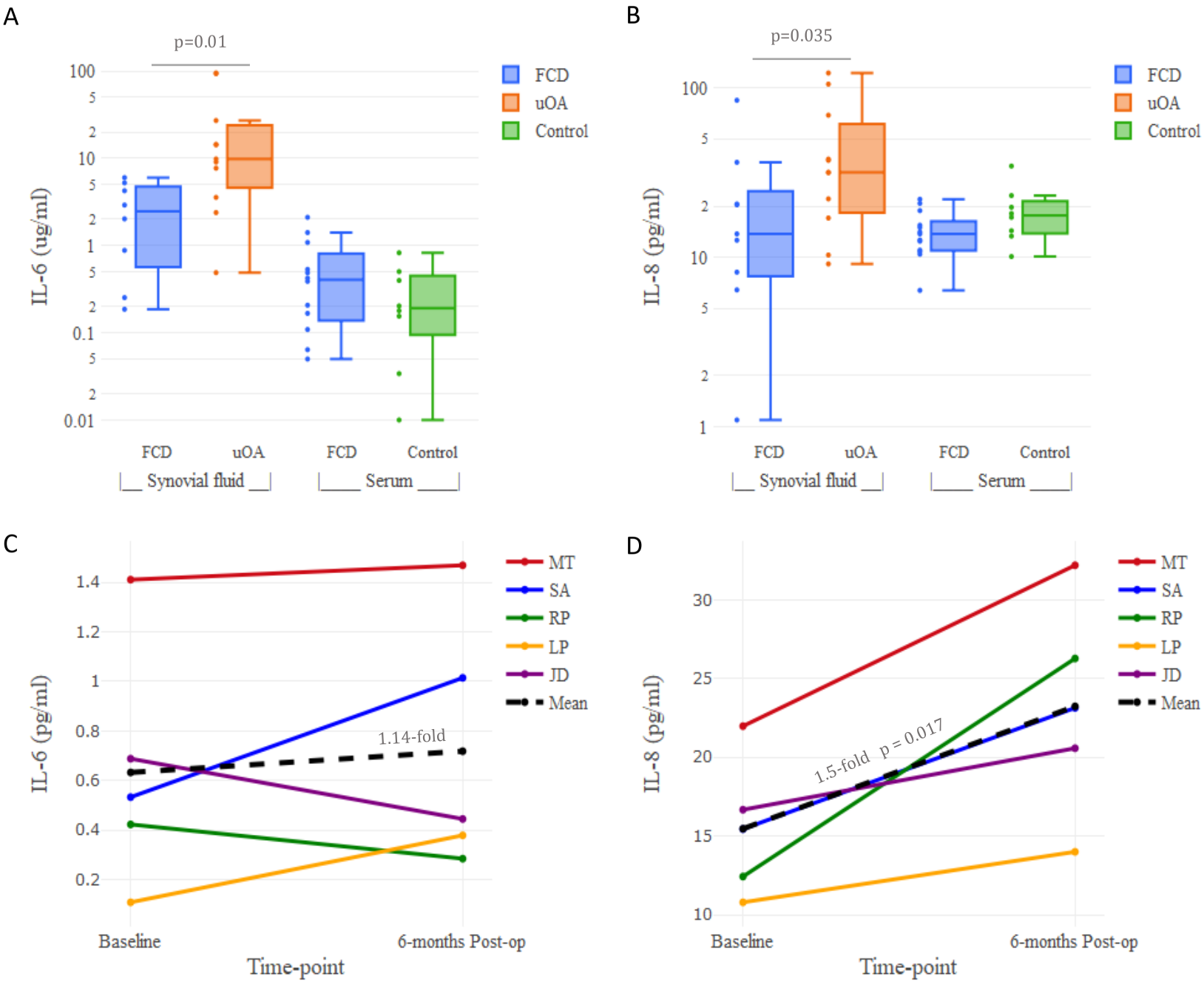

Figure 4.3-1 – Distribution of synovial fluid and serum IL-6 (A) and IL-8 (B) concentrations in FCD (n=8 IL-6; n=8 IL-8), OA (n=11 IL-6; n=11 IL-8) and control (n=8 IL-6; n=8 IL-8) groups, and longitudinal changes (n=5) in serum IL-6 (C) and IL-8 (D) concentrations for each patient (initials) from pre- to 6-months post microfracture surgery. Additional patient characteristics are in Appendix Table 1 & 2. Main findings: Both IL-6 and IL-8 levels were significantly increased in OA synovial fluids relative to the FCD group, however they were not found to differ in FCD serum relative to controls. Group IL-8 levels were found to significantly increase post-surgery by 1.5-fold, however this was not consistent with self-reported KOOS scores or clinical characteristics. Group biomarker concentration differences were tested for by ANCOVAs whilst adjusting for age and BMI. Longitudinal group changes were tested for using Wilcoxon-signed rank test. For both tests, $p<0.05$ was considered significant.

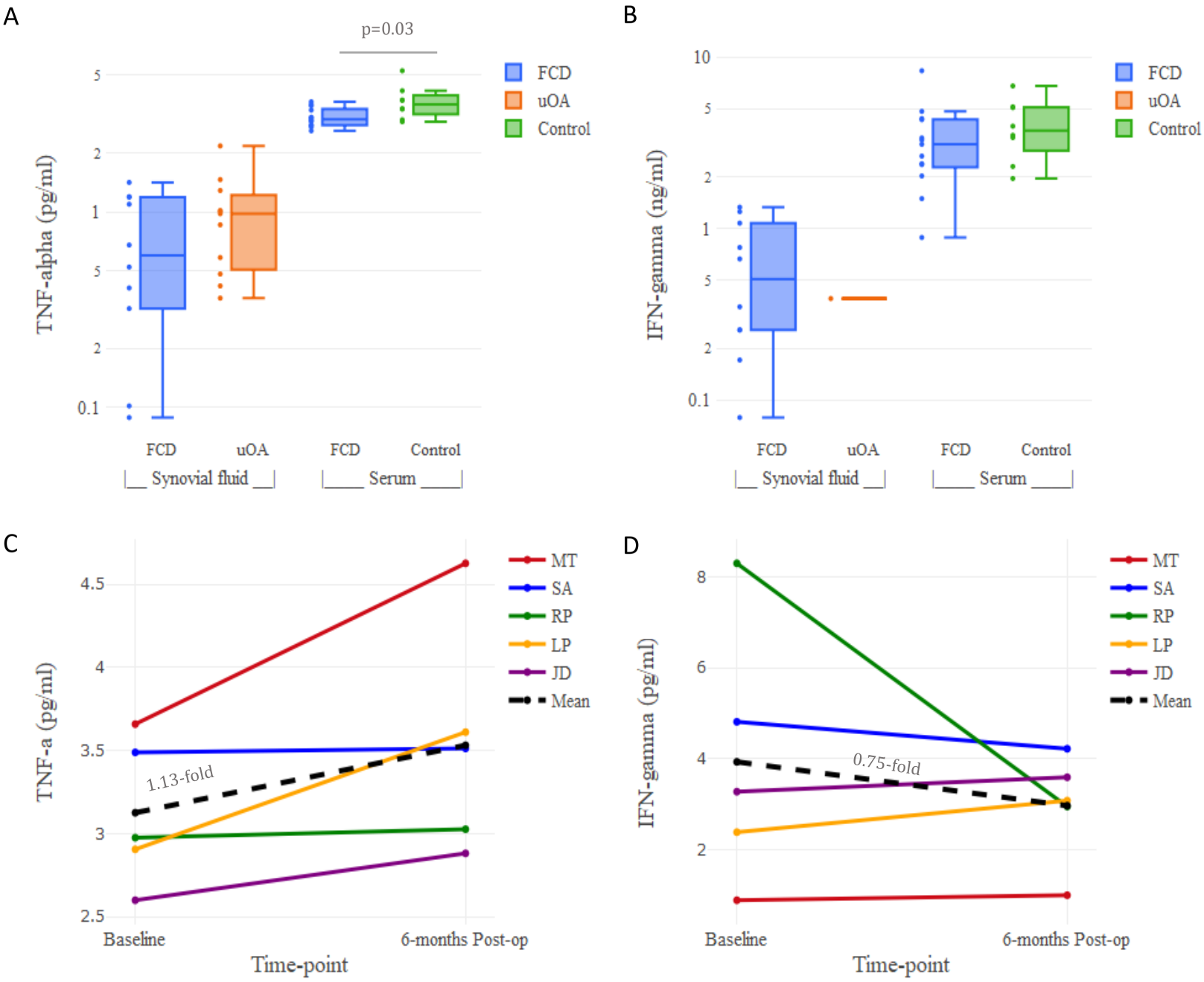

Figure 4.3-2 - Distribution of synovial fluid and serum TNF-α (A) and IFN-γ (B) concentrations in FCD (n=9 TNF-α; n=10 IFN-γ), OA (n=11 TNF-α; n=1 IFN-γ) and control (n=8 TNF-α; n=8 IFN-γ) groups, and longitudinal changes (n=5) in serum TNF-α (C) and IFN-γ (D) concentrations for each patient (initials) from pre- to 6-months post microfracture surgery. Additional patient characteristics are in Appendix Table 1 & 2. Main findings: Serum TNF-α levels were significantly ($p<0.05$) decreased in FCD serum relative to controls. Subject RP (green) distinctly exhibited decreased IFN-γ post-surgery, consistent with their distinctly increased pain exhibited (Appendix Table 2). Group biomarker concentration differences were tested for by ANCOVAs whilst adjusting for age and BMI. Longitudinal group changes were tested for using Wilcoxon-signed rank test. For both tests, $p<0.05$ was considered significant.

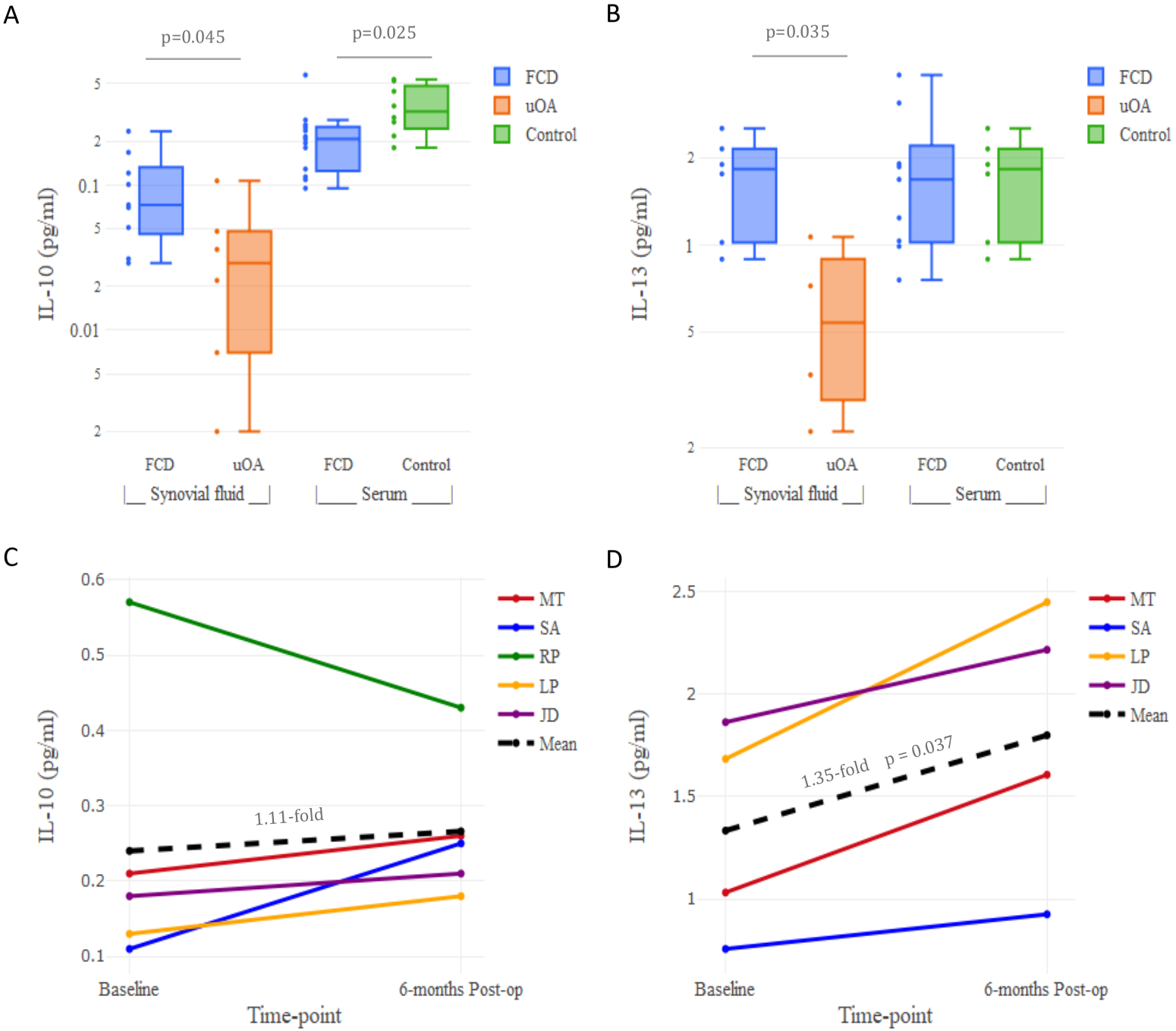

Figure 4.3-3- Distribution of synovial fluid and serum IL-10 (A) and IL-13 (B) concentrations FCD (n=8 IL-10; n=8 IL-13), OA (n=6 IL-10; n=4 IL-13) and control (n=8 IL-10; n=6 IL-13) groups, and longitudinal changes (n=5) in serum IL-10 (C) and IL-13 (D) concentrations for each patient (initials) from pre- to 6-months post microfracture surgery. Additional patient characteristics are in Appendix Table 1 & 2. Main findings: The uOA group exhibited significantly decreased synovial fluid IL-10 and IL-13 levels compared to the FCD group. FCD subjects also showed significantly reduced IL-10 relative to control subjects. Subject RP (green) distinctly exhibited decreased IL-10 in contrast to the group, in line with their worsening self-reported clinical scores exhibited (Appendix Table 2). Group biomarker concentration differences were tested for by ANCOVAs whilst adjusting for age and BMI. Longitudinal group changes were tested for using Wilcoxon-signed rank test. For both tests, $p<0.05$ was considered significant.

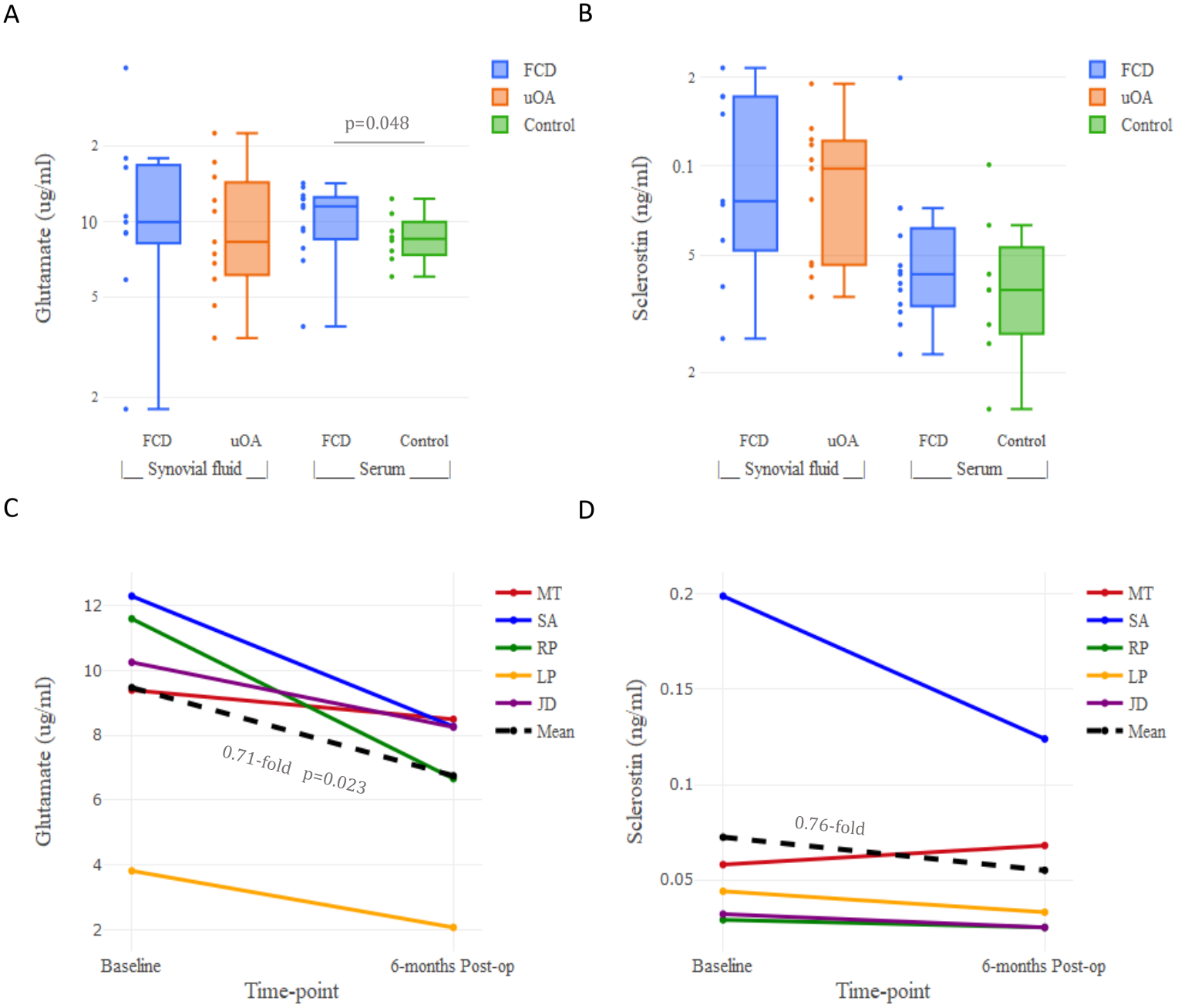

Figure 4.3-4 - Distribution of synovial fluid and serum Glutamate (A) and Sclerostin (B) concentrations FCD (n=9 glut; n=8 sost), OA (n=11 glut; n=11 sost) and control (n=8 glut; n=8 sost) groups, and longitudinal changes (n=5) in serum Glutamate (C) and Sclerostin (D) concentrations for each patient (initials) from pre- to 6-months post microfracture surgery. Additional patient characteristics are in Appendix Table 1 & 2. Main findings: The FCD group presented significantly increased serum glutamate relative to controls. Subject SA who before surgery had high sclerostin, distinctly presented a substantial decrease in sclerostin levels post-surgery which was consistent with their improvement in self-reported clinical scores (Appendix Table 2). Group biomarker concentration differences were tested for by ANCOVAs whilst adjusting for age and BMI. Longitudinal group changes were tested for using Wilcoxon-signed rank test. For both tests, $p<0.05$ was considered significant.

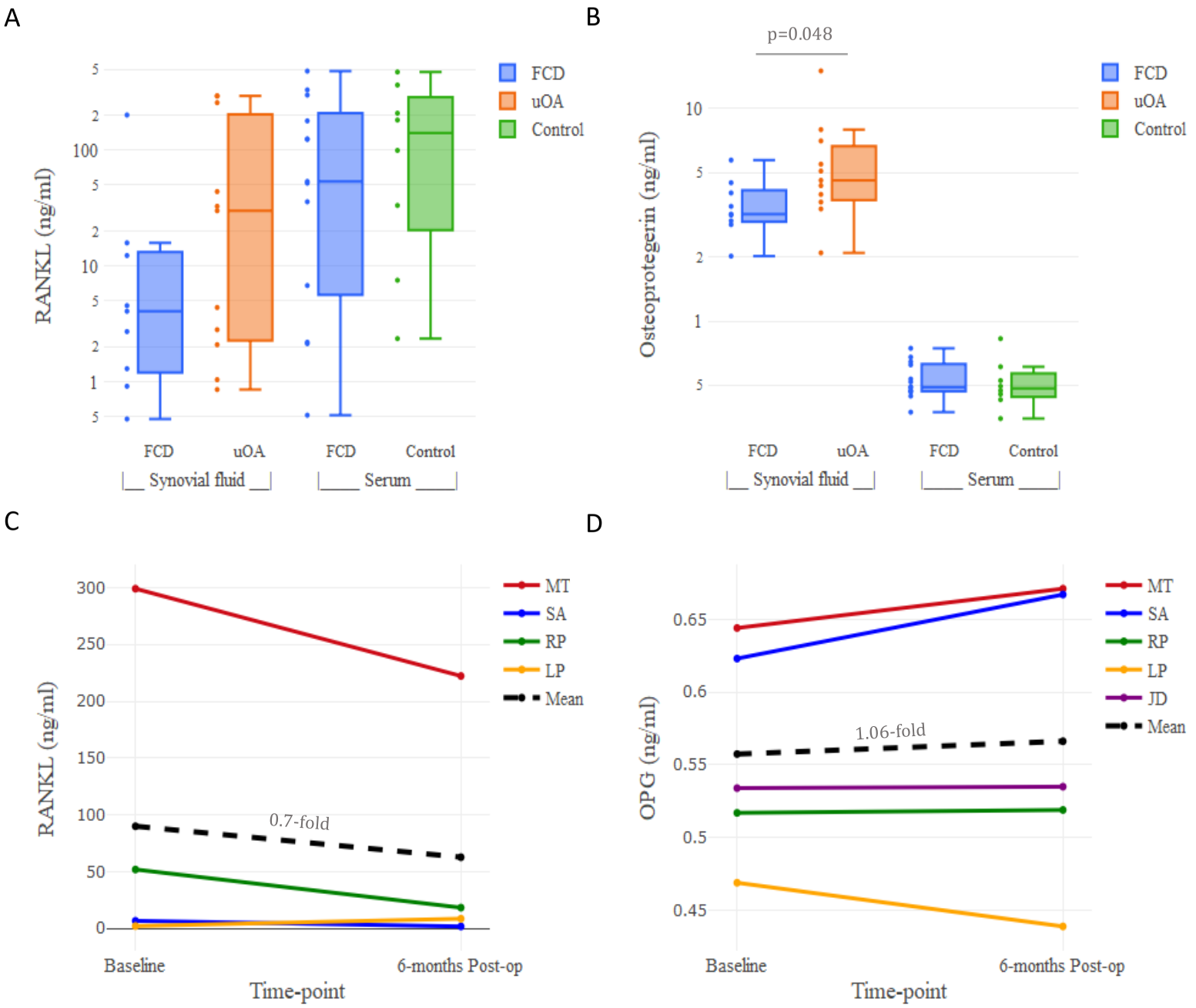

Figure 4.3-5 - Distribution of synovial fluid and serum RANKL (A) and OPG (B) concentrations FCD (n=8 RANKL; n=9 OPG), OA (n=10 RANKL; n=11 OPG) and control (n=8 RANKL; n=8 OPG) groups, and longitudinal changes (n=5) in serum Glutamate (C) and Sclerostin (D) concentrations for each patient (initials) from pre- to 6-months post microfracture surgery. Additional patient characteristics are in Appendix Table 1 & 2. Main findings: The OA group exhibited significantly increased synovial fluid OPG levels relative to FCD subjects. Group biomarker concentration differences were tested for by ANCOVAs whilst adjusting for age and BMI. Longitudinal group changes were tested for using Wilcoxon-signed rank test. For both tests, $p<0.05$ was considered significant.

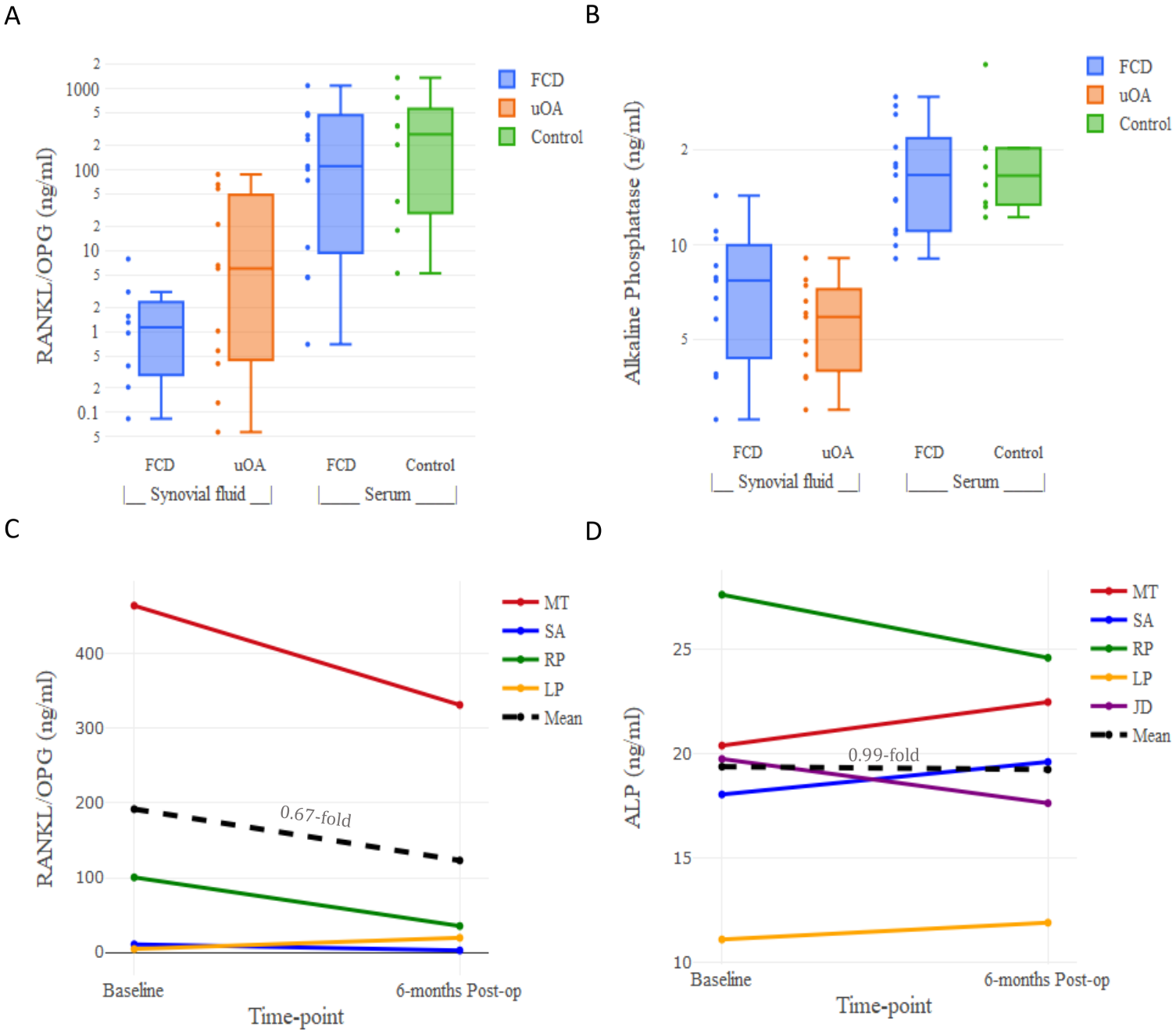

Figure 4.3-6 - Distribution of synovial fluid and serum RANKL/OPG ratio (A) and ALP (B) concentrations FCD (n=8 RANKL/OPG; n=11 ALP), OA (n=11 RANKL/OPG; n=11 ALP) and control (n=7 RANKL/OPG; n=8 ALP) groups, and longitudinal changes (n=5) in serum Glutamate (C) and Sclerostin (D) concentrations for each patient (initials) from pre- to 6-months post microfracture surgery. Additional patient characteristics are in Appendix Table 1 & 2. Group biomarker concentration differences were tested for by ANCOVAs whilst adjusting for age and BMI. Longitudinal group changes were tested for using Wilcoxon-signed rank test. For both tests, $p<0.05$ was considered significant.

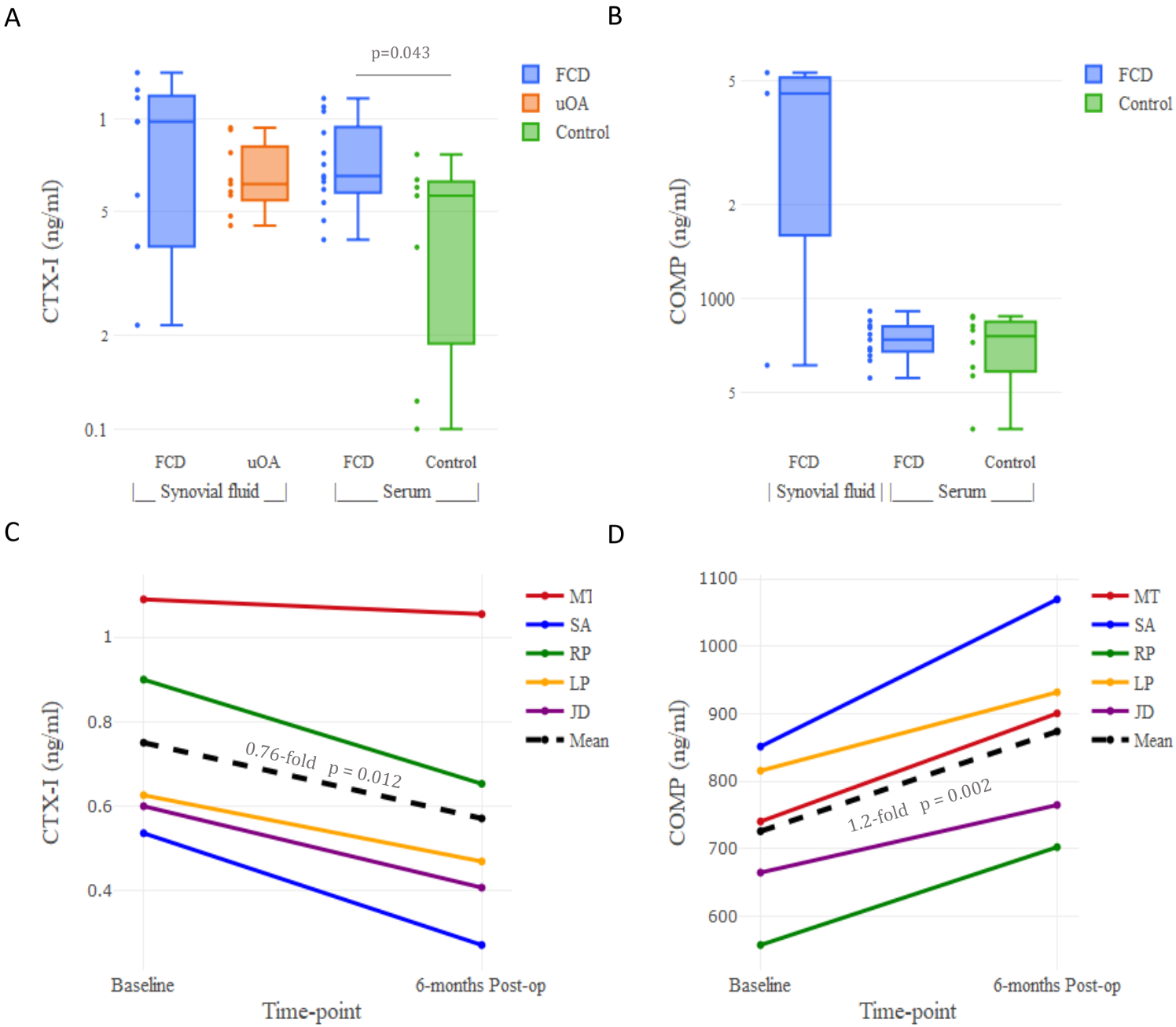

Figure 4.3-7 - Distribution of synovial fluid and serum CTX-I (A) and COMP (B) concentrations FCD (n=7 CTX-I; n=3 COMP), OA (n=11 CTX-I; n=0 COMP) and control (n=7 CTX-I; n=8 COMP) groups, and longitudinal changes (n=5) in serum Glutamate (C) and Sclerostin (D) concentrations for each patient (initials) from pre- to 6-months post microfracture surgery. Additional patient characteristics are in Appendix Table 1 & 2. Main findings: There were significantly higher levels of serum CTX-I in the FCD subjects relative to controls. Following surgery, serum CTX-I levels were significantly reduced, and serum COMP levels significantly increased. Group biomarker concentration differences were tested for by ANCOVAs whilst adjusting for age and BMI. Longitudinal group changes were tested for using Wilcoxon-signed rank test. For both tests, $p<0.05$ was considered significant.

4.3.3.3 Correlations of intra-fluid biomarker levels

Correlations amongst synovial fluid and serum biomarker levels within fluid types were analysed to identify pathobiological mechanisms relating to cartilage degradation, bone remodelling, mechanical loading of bone and inflammation that complement interpretations of group comparisons (Figure 4.3-8). The most notable patterns include:

- The positive trends/significant associations ($p \leq 0.05$) of pro-inflammatory mediators in synovial fluid, whereby IL-6 correlated with TNF-α and IL-8 levels, as well as IL-8 with TNF-α. However, only the association between IL-8 and TNF-α was retained in serum.

- The positive associations of osteoblast-dependent osteoclastogenic pathway activation (i.e. RANKL and the RANKL:OPG ratio) with pro-inflammatory mediators (i.e. IL-6 and IL-8), contrasting with the negative relationship of osteoclastogenic pathway activation with anti-inflammatory IL-10 levels.

- The significant ($p \leq 0.05$) negative correlations of sclerostin with anti-inflammatory cytokines (i.e. IL-10, IL-12p70 and IL-13) in synovial fluid

- The inverse relationships ($p \leq 0.05$) found between cartilage turnover/degradation (COMP) and bone turnover (CTX-I and ALP) in serum, as well as the positive relationship of COMP with sclerostin.

	SERUM													
ρ	**TNF-α**	0.127	0.066	**0.561**	**0.612**	0.296	0.089	0.190	0.152	0.164	-0.230	-0.142	0.406	0.135	-0.191
Sig. p		0.582	0.782	**0.008**	**0.003**	0.192	0.752	0.410	0.511	0.478	0.329	0.540	0.067	0.559	0.407
ρ	0.030	**IFN-γ**	-0.113	-0.017	**0.431**	0.157	-0.146	0.022	-0.286	0.069	-0.041	-0.135	-0.056	-0.212	-0.022
Sig. p	0.934		0.636	0.942	**0.050**	0.496	0.603	0.924	0.209	0.767	0.865	0.559	0.810	0.357	0.924
ρ	**0.491**	-0.151	**IL-6**	0.283	0.035	-0.215	-0.193	-0.221	0.331	-0.256	0.195	-0.081	0.262	0.266	0.012
Sig. p	**0.033**	0.699		0.227	0.885	0.363	0.491	0.349	0.154	0.277	0.424	0.734	0.265	0.257	0.960
ρ	**0.586**	-0.116	**0.809**	**IL-8**	0.238	0.056	0.079	0.365	0.377	0.325	-0.290	-0.036	**0.477**	0.081	0.018
Sig. p	**0.005**	0.751	**<0.001**		0.300	0.810	0.781	0.104	0.092	0.151	0.214	0.876	**0.029**	0.729	0.938
ρ	0.193	0.117	-0.379	-0.218	**IL-10**	0.321	0.057	0.236	-0.010	0.195	-0.083	**-0.583**	0.313	0.136	-0.403
Sig. p	0.491	0.764	0.201	0.435		0.156	0.840	0.302	0.964	0.397	0.729	**0.006**	0.167	0.556	0.070
ρ	0.209	0.042	0.083	-0.145	0.370	**IL-12p70**	**0.493**	**0.179**	-0.097	0.199	-0.265	-0.238	0.195	0.184	-0.031
Sig. p	0.537	0.915	0.831	0.670	0.293		**0.062**	**0.437**	0.674	0.388	0.259	0.300	0.397	0.424	0.893
ρ	0.016	**0.695**	-0.482	-0.231	0.357	**0.867**	**IL-13**	-0.132	0.204	-0.114	0.029	-0.196	-0.271	-0.282	0.011
Sig. p	0.957	**0.056**	0.133	0.448	0.255	**0.001**		0.639	0.467	0.685	0.923	0.483	0.328	0.308	0.970
ρ	0.182	-0.217	**0.474**	0.419	**-0.654**	0.067	-0.200	**RANKL**	-0.104	**0.988**	-0.011	-0.119	**0.453**	0.231	-0.169
Sig. p	0.455	0.576	**0.047**	0.074	**0.015**	0.865	0.555		0.654	**<0.001**	0.965	0.606	**0.039**	0.313	0.464
ρ	-0.254	0.400	0.199	0.155	-0.086	-0.479	-0.301	-0.351	**OPG**	-0.173	0.051	0.130	0.035	-0.082	0.400
Sig. p	0.280	0.286	0.428	0.514	0.771	0.162	0.342	0.141		0.454	0.830	0.575	0.880	0.724	0.072
ρ	0.207	-0.217	0.383	0.351	**-0.599**	0.167	-0.055	**0.977**	**-0.489**	**RANKL/ OPG**	-0.048	-0.070	0.408	0.230	-0.155
Sig. p	0.395	0.576	0.117	0.141	**0.031**	0.668	0.873	**<0.001**	**0.033**		0.840	0.763	0.067	0.316	0.504
ρ	-0.006	**-0.583**	-0.172	-0.056	-0.125	-0.236	-0.266	-0.175	-0.057	-0.172	**Glut**	0.183	-0.020	-0.057	0.059
Sig. p	0.980	**0.099**	0.494	0.816	0.670	0.511	0.404	0.473	0.811	0.482		0.439	0.935	0.811	0.806
ρ	-0.343	-0.083	0.055	0.077	**-0.538**	**-0.842**	**-0.650**	-0.119	0.146	-0.147	0.338	**Sost**	-0.179	-0.204	**0.490**
Sig. p	0.139	0.831	0.829	0.748	**0.047**	**0.002**	**0.022**	0.627	0.539	0.547	0.145		0.437	0.375	**0.024**
ρ	0.055	0.241	0.109	0.153	0.393	0.073	0.132	-0.056	-0.015	-0.019	0.236	0.048	**ALP**	0.410	**-0.479**
Sig. p	0.814	0.474	0.658	0.507	0.147	0.832	0.668	0.819	0.950	0.937	0.316	0.840		0.065	**0.028**
ρ	0.454	0.055	0.004	0.090	**0.531**	-0.008	0.036	-0.146	-0.169	-0.026	-0.249	-0.271	0.372	**CTX-I**	**-0.440**
Sig. p	0.067	0.880	0.987	0.733	0.075	0.983	0.915	0.590	0.531	0.922	0.353	0.310	0.129		**0.046**
	SYNOVIAL FLUID														**COMP**

Figure 4.3-8 - Correlation (Spearman's ρ) matrix heatmap of serum and synovial fluid analyte concentrations. (Red) Positive correlations and (Blue) inverse correlations. Bold face white values are of statistical significance ($p<0.05$).

4.3.4 Correlations of biomarker levels with patient-reported measures

Subject-reported pain at baseline significantly (p≤0.05) associated with synovial fluid IFN-γ and IL-13 levels, but inversely associated with serum IFN-γ and IL-10 at baseline as well as longitudinal changes following microfracture surgery (Figure 4.3-8). OA-related symptoms at baseline were also significantly related to synovial fluid IL-13, as

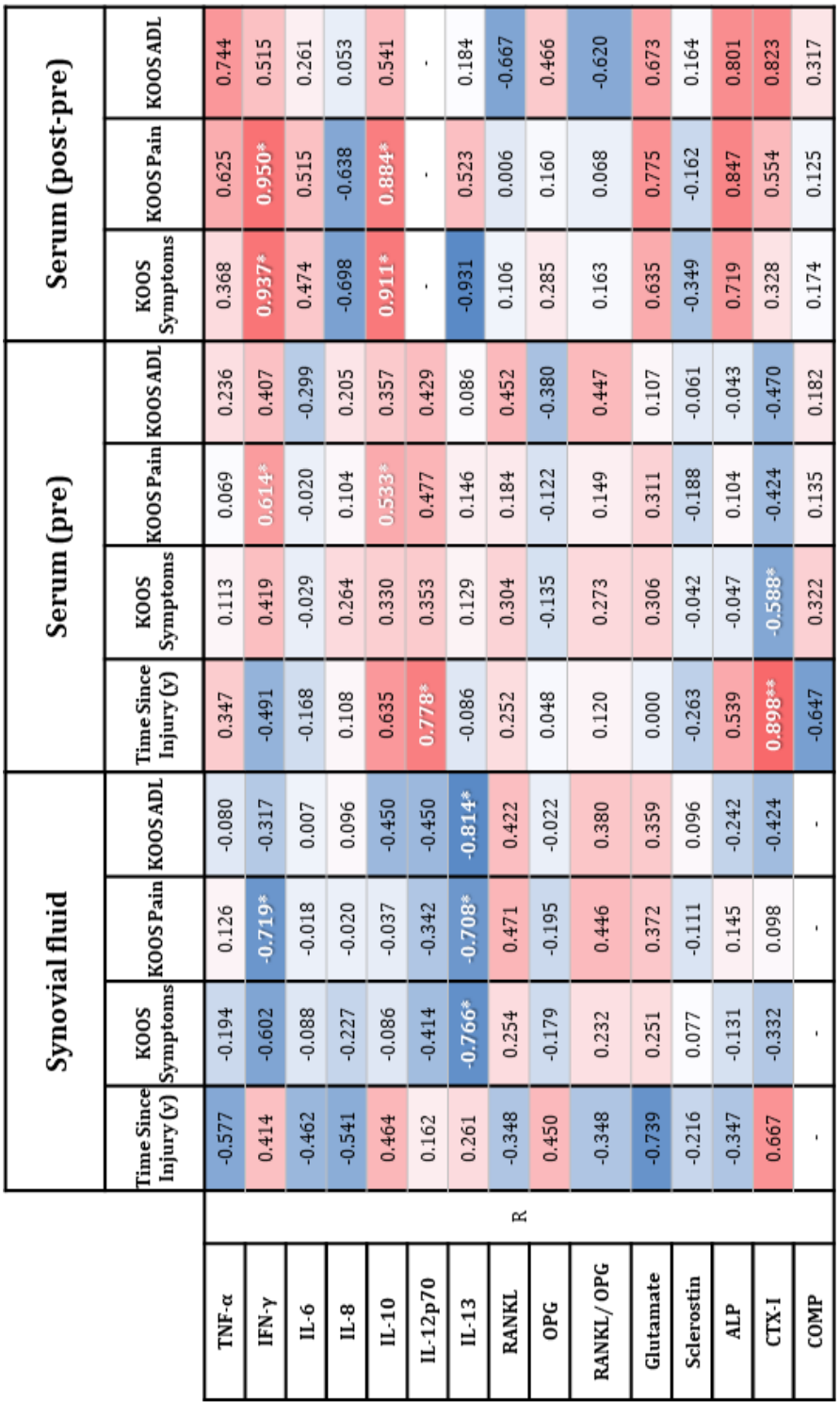

Figure 4.3-8 - Spearman's Rho correlations of candidate synovial fluid biomarkers, serum analytes and longitudinal change in analyte levels with subject-reported clinical scores measured by the Knee Osteoarthritis Outcome Survey (KOOS). * significant at the <0.05 level.

well as serum CTX-I levels. Finally, self-perceived knee function at baseline was only associated with IL-13 levels in synovial fluid.

4.3.5 Results for objective 2 (PCA)

Principal component analysis (PCA) was applied to identify inter- or intra-disease group variances or phenotypes from linear combinations of synovial fluid biomarkers (Figure 4.3-9). Two components were generated explaining 50.2% of the variance collectively (PC1; 28.2%, PC2; 22%). Visual assessment of the score space identified 3 major clusters within the data.

Cluster 1: Increased bone turnover (CTX-I and ALP), increased osteogenic signalling (reduced sclerostin), decreased osteoclastogenic signalling (RANKL/OPG) and increased anti-inflammatory (IL-10) activity compared to average weightings.

Cluster 2: Increased osteoclastogenic signalling (RANKL/OPG), decreased turnover (CTX-I and ALP) compared to average weightings

Cluster 3: Decreased osteogenic signalling (increased sclerostin), decreased bone resorption (CTX-I), increased glutaminergic signalling and decreased anti-inflammatory signalling

The PC1 variable weightings revealed a signature of mechanical loading (glutamate, sclerostin and OPG) and pro-inflammatory (IL-6 and IL-8) biomarkers associated with positive PC1 scores, and anti-inflammatory (IL-12p70, IL-13 and IL-13) and IFN-γ (pro- and anti-inflammatory) associated with negative PC1 scores. In contrast, PC2 weightings showed a pattern consistent with bone turnover (ALP and CTX-I) in favour of bone formation/osteo-protection (ALP and IL-10 for more extreme scores) associated with positive PC2 scores, and canonical bone resorption (RANKL and RANKL/OPG) associated with negative scores.

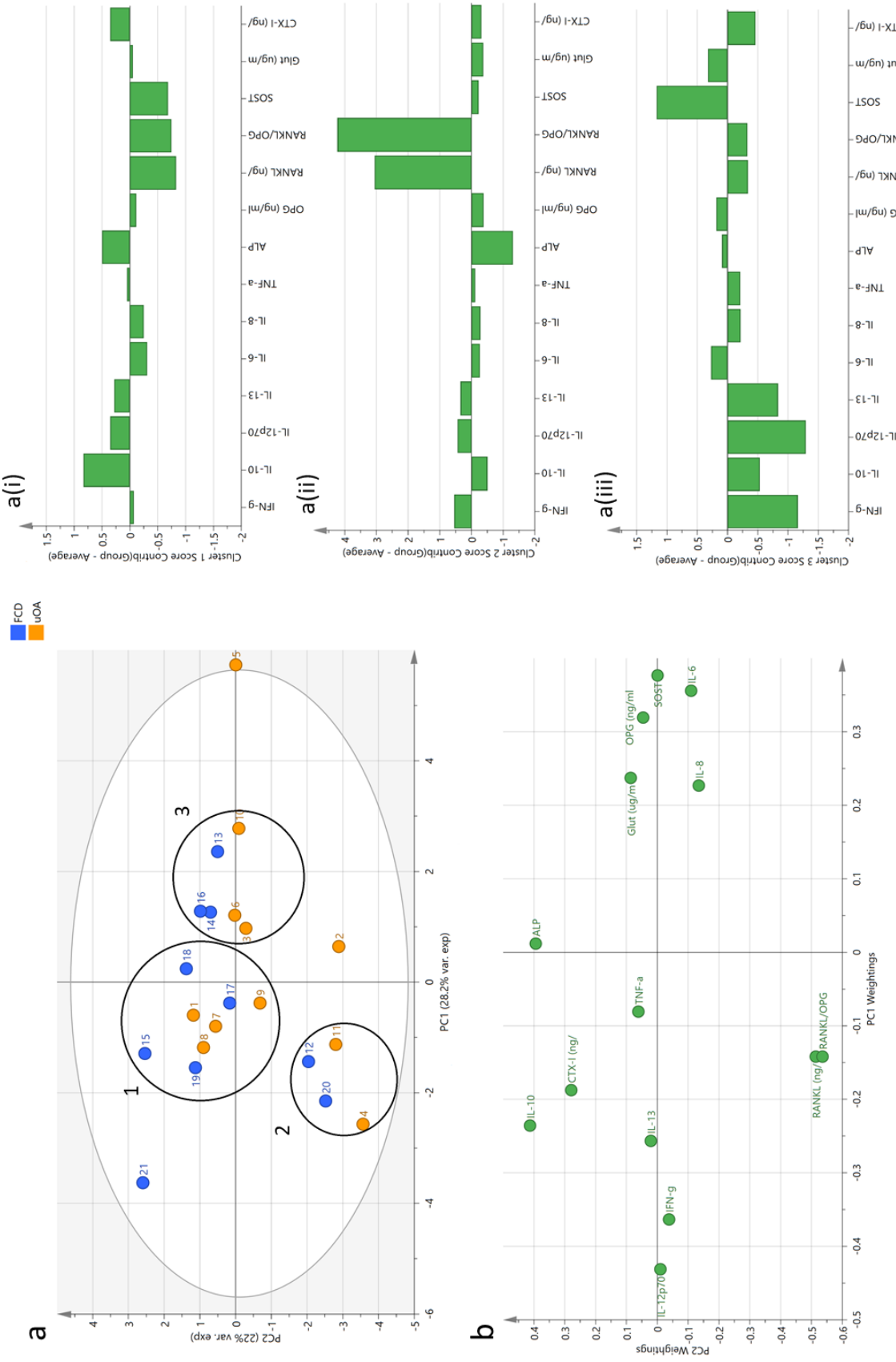

Figure 4.3-9 - Principle component analysis based on components explaining 50.2% of the variance collectively (PC1; 28.2%, PC2; 22%) with cluster analysis. (a) Variable score plot shows three main clusters in FCD (blue) and uOA (orange) subjects. (i) Cluster 1 subjects show increased anti-inflammatory signalling and reduced bone remodelling signalling compared to average group weightings. (ii) Cluster 2 subjects show increased bone remodelling signalling and reduced bone mineralisation compared to average weightings. (iii) Cluster 3 subjects show increased sclerostin levels coupled with reduced anti-inflammatory signalling and IFN-γ. (b) Analyte weightings for PC1 and PC2.

4.3.6 Additional results for Objective 3 (longitudinal analysis)

4.3.6.1 Subject-reported clinical measures

Six months after microfracture surgery, OA-related pain, symptoms and function improved for four of the five FCD subjects tested. However, in contrast, one subject (RP) exhibited worsening of all factors (Figure 4.3-710).

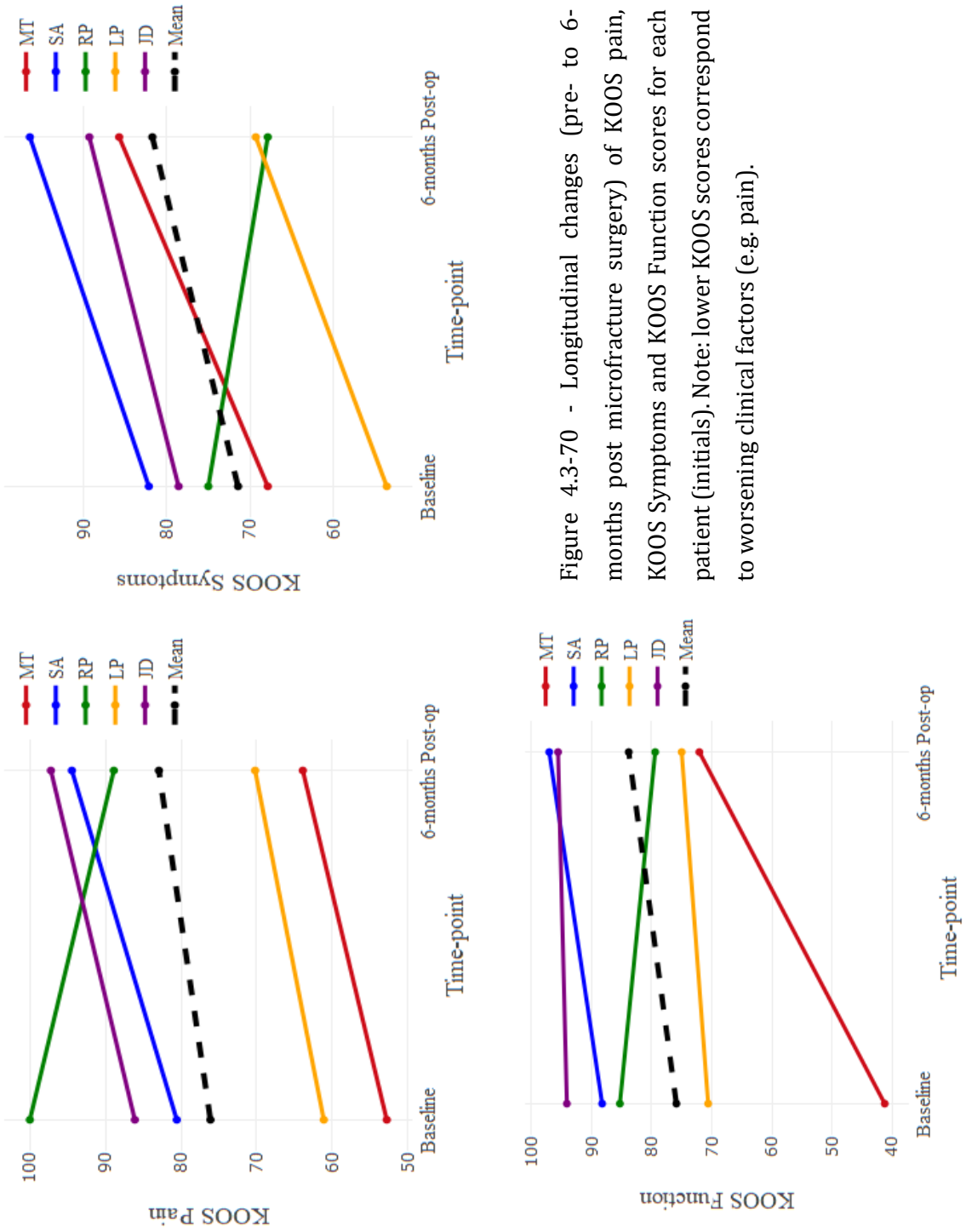

Figure 4.3-70 - Longitudinal changes (pre- to 6-months post microfracture surgery) of KOOS pain, KOOS Symptoms and KOOS Function scores for each patient (initials). Note: lower KOOS scores correspond to worsening clinical factors (e.g. pain).

4.3.6.2 Correlations of longitudinal changes of biomarker levels

Correlation analysis of longitudinal changes in serum biomarkers (Figure 4.3-1) revealed three notable patterns which include:

- Longitudinal changes of pro-inflammatory mediator TNF-α which positively ($p \leq 0.05$) correlated with decreases in glutamate and CTX-I levels. Changes in CTX-I also associated ($p \leq 0.05$) with glutamate levels, showing concomitant decreases of all three biomarkers following surgery.

- Changes in IL-12p70 positively ($p \leq 0.05$) associated with IL-6 levels and negatively with sclerostin.

- COMP changes showed strong positive trends with OPG and IL-6, as well as a negative association with changes in sclerostin contradictory to previous findings.

	TNF-α	IFN-γ	IL-6	IL-8	IL-10	IL-12p70	IL-13	RANKL	OPG	RANKL/ OPG	Glutamate	Sclerostin	ALP	CTX-I	COMP
r															
Sig. p															
r	0.567														
Sig. p	0.319														
r	0.018	0.333													
Sig. p	0.977	0.584													
r	-0.223	-0.826	-0.196												
Sig. p	0.719	0.085	0.752												
r	0.245	0.780	0.788	-0.522											
Sig. p	0.691	0.120	0.113	0.367											
r	-0.227	0.376	**0.932**	-0.361	0.811										
Sig. p	0.714	0.533	**0.021**	0.550	0.096										
r	0.846	0.856	-0.117	-0.251	-0.421	-0.398									
Sig. p	0.154	0.144	0.883	0.749	0.579	0.602									
r	-0.456	0.126	0.599	-0.633	0.240	0.678	-0.080								
Sig. p	0.544	0.874	0.401	0.367	0.760	0.322	0.949								
r	-0.244	-0.042	0.310	0.415	0.414	0.333	-0.764	-0.385							
Sig. p	0.692	0.946	0.611	0.487	0.489	0.584	0.236	0.615							
r	-0.406	0.189	0.633	-0.681	0.290	0.701	-0.060	**0.998**	-0.388						
Sig. p	0.594	0.811	0.367	0.319	0.710	0.299	0.962	**0.002**	0.612						
r	**0.894**	0.814	-0.064	-0.539	0.390	-0.161	0.772	-0.345	-0.216	-0.287					
Sig. p	**0.041**	0.093	0.918	0.349	0.517	0.796	0.228	0.655	0.727	0.713					
r	0.603	-0.081	-0.734	0.142	-0.598	**-0.896**	0.717	-0.599	-0.521	-0.596	0.488				
Sig. p	0.282	0.897	0.158	0.820	0.287	**0.040**	0.283	0.401	0.368	0.404	0.405				
r	0.565	0.643	0.769	-0.219	0.863	0.604	0.167	-0.087	0.382	-0.028	0.500	-0.296			
Sig. p	0.321	0.242	0.129	0.724	0.060	0.280	0.833	0.913	0.526	0.972	0.391	0.628			
r	**0.961**	0.482	-0.131	-0.062	0.168	-0.366	0.660	-0.674	-0.067	-0.630	**0.889**	0.658	0.501		
Sig. p	**0.009**	0.411	0.834	0.921	0.788	0.545	0.340	0.326	0.915	0.370	**0.046**	0.227	0.390		
r	-0.295	-0.135	0.701	0.415	0.497	0.650	-0.574	-0.020	0.836	-0.024	-0.415	-0.732	0.524	-0.245	
Sig. p	0.630	0.828	0.187	0.488	0.394	0.236	0.426	0.980	0.078	0.976	0.488	0.159	0.365	0.692	

Figure 4.3-11 - Correlation (Spearman's ρ) matrix heatmap of pre-post microfracture surgery changes of analyte levels. Bold face and white values are statistically significant ($p<0.05$) relationships between analyte levels.

4.4 Discussion

4.4.1 Overview

Major findings for objective 1, 2 and 3 will first be discussed, followed by the relation of this study's findings to literature for each category of marker (bone and cartilage turnover, bone mechanical signalling markers and inflammatory markers) in the general discussion.

4.4.2 Major findings for Objective 1

The first objective of this chapter was to measure candidate molecules of bone and cartilage turnover, mechanical loading of bone and inflammation in synovial fluid (FCD compared to uOA) and serum (FCD compared to healthy controls) to identify suitable biomarkers and mechanisms of FCD pathogenesis.

Synovial fluid biomarkers are poorly reproduced in serum

Notably, out of the 14 biomarkers measured, only CTX-I, sclerostin and IL-13 significantly ($p \leq 0.05$) positively correlated across fluid types, indicating that several mechanisms of activity in the joint are poorly reflected systemically. Most non-significant biomarkers were either moderately (RANKL/OPG, glutamate and IL-10) or weakly (RANKL, OPG, ALP, IL-12p70) correlated, however in contrast pro-inflammatory cytokines (TNF-α, IL-6, IL-8) and IFN-γ had no positive association. This is likely due to the short half-lives of most cytokines and chemokines, which are required to act only on cells in close proximity to their release (Zhou et al., 2010). Furthermore, RANKL and OPG only have purpose in bone signalling, thus may exhibit similar properties for this reason. The lack of commonality for many candidates is a considerable factor when identifying appropriate biomarkers of discriminatory potential between FCD subjects and controls and must be taken into account to reduced false interpretation.

Loading and inflammation pathways in osteoblast-mediated osteoclastogenic activity

Synovial fluid OPG levels were significantly elevated in uOA group to FCD subjects, however this was concurrent with a trend of increased RANKL expression, leading to an overall higher RANKL:OPG ratio in uOA subjects. However, the overall group differences were not significant at the $p \leq 0.05$ level due to the considerable number of overlapping

values. The RANK:OPG ratio is a surrogate indicator of net osteoclast activation through the canonical osteoblast-mediated pathway, indicating that a larger proportion of uOA subjects may be exhibiting higher subchondral bone activated osteoclast numbers and increased bone resorption activity (Tat et al., 2008b). The increased RANKL:OPG ratio is likely resultant of the increased osteoblastic RANKL expression induced by higher levels of pro-inflammatory activity (Kim et al., 2017, Lam et al., 2000), which is evidenced by the significant positive association of IL-6 (and moderate trends of IL-8) with soluble RANKL found in the correlation analysis. On the other hand, OPG is regulated by mechanical loading of subchondral bone (Kim et al., 2006a, Kusumi et al., 2005), evidenced by the significantly elevated levels in uOA subjects who exhibit higher knee loading relative to FCD subjects (evidenced in chapter 4). Together, the findings suggest that mechanical loading and inflammation of subchondral bone have contradictory effects on canonical NF-κB-induced osteoclastogenesis, however subjects with increased knee loads accompanied by up-regulated pro-inflammatory activity in the joint may be exposed to higher RANKL/OPG ratios, and thus, increased recruitment of mature osteoclasts in subchondral bone.

Increased bone resorption is indicative of FCD presence, but not of disease state

The trend of increased RANKL:OPG signalling in the uOA group was not reflected in osteoclastic bone resorption activity represented by CTX-I levels (Garnero et al., 2003), which showed no clear trends in disease group analysis, but larger individual differences in the FCD group. Furthermore, CTX-I showed no clear trend with canonical osteoclastogenic signalling markers (RANKL, OPG and RANKL/OPG) in synovial fluid, and only weak trends in serum. In contrast, the moderate relationships between CTX-I and inflammatory mediators TNF-α and IL-10 in synovial fluid imply a larger influence of bone resorption activity through non-canonical pathways (Knowles and Athanasou, 2009, Sabokbar et al., 2016). Notably, synovial fluid CTX-I significantly (≤ 0.05) correlated with BMI, which is evident of a positive involvement of mechanical signalling pathways on osteoclast activity, despite the lack of associations to glutamate or sclerostin levels. Although bone resorption activity did not favour a disease group, there was a trend of declining bone formation marker ALP in uOA synovial fluids relative to FCD, which may signify a net shift towards a bone resorption-formation imbalance of resorption consistent with disease advancement. In contrast of the disease group analysis, there was increased bone resorption activity in FCD subjects relative to controls evidenced the significantly ($p \leq 0.05$) increased serum CTX-I levels, which justifies serum CTX-I as a suitable biomarker of FCD presence. However, in similar respects to the

disease group analysis, there were no clear favoured mechanisms of this increase when considering associations to other serum biomarkers.

Involvement of glutamatergic signalling in FCD pathogenesis

Group comparisons found significantly ($p \leq 0.05$) higher levels of glutamate in FCD serum relative to controls, implying an involvement of glutamatergic signalling in FCD pathogenesis. Glutamatergic signalling has been largely implicated in OA as it is functional in bone, cartilage, meniscus and synovium tissues (Wen et al., 2015) and is involved in mechanically regulated bone remodelling (Brakspear and Mason, 2012). Higher FCD serum levels may be resultant of aberrant exocytotic release and transporter activity that regulate extracellular glutamate in response to altered loading of subchondral bone in the FCD joint. The positive correlation of synovial fluid glutamate and ALP may be indicative of osteoblast ionotropic glutamate receptor (iGluR) activation responsible for increased Runx2 activity, a positive regulator of osteogenic gene expression (Hinoi et al., 2002, Ho et al., 2005). Activation of iGluRs on the surface of progenitor/mature osteoclasts up-regulates NF-κB-induced osteoclastogenesis (Merle et al., 2003) and activity (Mentaverri et al., 2003), though these mechanisms were not evident in correlations of synovial fluid glutamate and CTX-I levels or the RANKL:OPG ratio. Furthermore, experimental models of inflammatory arthritis have also revealed glutamatergic modulation of inflammatory and nociceptive pathways (Bonnet et al., 2015, Flood et al., 2007), however this was not evident in correlations with pro-inflammatory cytokines or KOOS scores. These incongruities may be related to the distinctive regulation of extracellular glutamate levels in the joint by exocytotic release mechanisms and elimination by glutamate transporters (Wen et al., 2015).

Elevated pro-/anti-inflammatory imbalance concurrent with disease progression

A substantial finding is the clear pattern of pro-inflammatory cytokine (IL-6, IL-8, TNF-α) activity in uOA joints compared to FCD joints, with significant increases in IL-6 and IL-8 levels, coupled with the decline in anti-inflammatory mediator IL-10 and IL-13 activity. Collectively, these findings represent an increasingly pathogenic inflammatory regulation of the anabolic/catabolic imbalance in subjects representing increased disease severity and joint loading (uOA relative to FCD). This is a likely a critical mechanism for disease progression, since pro-inflammatory cytokines including TNF-α, IL-1β, IL-6 and IL-8 are of the most consistent and notable soluble biomarkers mediators associated with alterations in bone and cartilage degeneration in animal models of OA

(Legrand et al., 2017, Pelletier et al., 2001) and human OA studies (Findlay and Kuliwaba, 2016). This is linked their self-propagation, promotion of tissue turnover (osteoclastogenic/osteoblast-inhibiting) pathways, upregulation of proteolytic matrix degrading enzymes (MMPs, ADAMTS), and production of destructive and nociception-inducing molecules such as prostaglandins E2 (PGE_2) and nitric oxide (Fernandes et al., 2002, Lotz et al., 2013). Correlation analysis corroborated the self-stimulatory mechanism in which occurs, evidenced by the significant relationships of IL-8 with IL-6 and TNF-α, as well as IL-6 with TNF-α. However, only the association between IL-8 and TNF-α was retained in serum which is reflective of the low associations between joint inflammation and systemic levels.

Conversely, anti-inflammatory mediators such as IL-10 and IL-13 on the other hand play an antagonistic role to disease progression, through the potent inhibition of pro-inflammatory cytokine expression and osteo-/chondro-protective down-regulation of tissue turnover pathways (e.g. inhibition of canonical osteoclastogenesis pathway), and suppression of PGE_2 production through the suppression of cyclooxygenase-2 (COX-2) expression (Wojdasiewicz et al., 2014, Onoe et al., 1996, Scanzello, 2017). Additionally, IL-10 levels were significantly lower in FCD relative to control serum and found a moderate inter-fluid correlation, therefore may be a promising serum biomarker representing inflammatory dysregulation with its declining levels with tibiofemoral FCD progression towards an established OA state.

Nociceptive pathways in FCD pathogenesis

Notably, synovial fluid IL-13 and IFN-γ inversely correlated with KOOS pain, symptoms and function scores, implying they may be responsible for worsening clinical factors. Conversely, serum IFN-γ and IL-10 which positively associated with KOOS scores may be protective of the burden. The paradoxical opposing findings for anti-inflammatory cytokines IL-10 and IL-13, as well as for IFN-γ in serum compared to synovial fluid, indicates that they may act on differing pathways in the joint relative to systemically. This may be related to selective activation of peripheral or central sensitization pathways, however to date, these paradoxical effects are undocumented. As previously discussed, declining serum IL-10 levels are consistent with FCD presence (and progression in synovial fluid), therefore may also be useful as an indicator of increased pain induction pathway activation alongside patient-reported outcome measures, which are prone to response shift (lack of an internal perceptual reference of pain).

4.4.3 Major findings for Objective 2

The second objective of this chapter was to use multivariate analysis tools to identify inter- and intra-group variances that are indicative of disease subgroups, or 'phenotypes' of disease. PCA revealed three main clusters and three individuals that are representative of varying disease processes, which will be discussed with regards to their individual distinctive features.

Cluster 1: Bone formation phenotype

Subjects associated with cluster 1 of the PCA, which locate closest to the PC1 and PC2 origins, presented increased bone turnover relative to average, evident by the coupled increases in synovial fluid ALP (formation) and CTX-I (resorption). Sclerostin is a Wnt/β-catenin pathway inhibitor (Li et al., 2005), therefore relatively reduced levels would be consistent with an up-regulation of transcription factor Runx2 activity in osteoblasts, and consequent expression of osteogenic genes including those of ALP, osteocalcin and collagen type-I (Krishnan et al., 2006). On the other hand, anti-inflammatory cytokine IL-10 is osteo- and chondro-protective, due to its inhibition of NF-κB activity in osteoclasts, down-regulation of pro-inflammatory cytokine expression (Moore et al., 2001), and stimulation of Runx2 activity (Jung et al., 2013). Finally, the reduced RANKL:OPG ratio which appears to be due to down-regulated RANKL expression is reflective of decreased osteoblast-mediated osteoclastogenic activity. Collectively, these findings are indicative of osteoblast activation towards an osteogenic state, therefore implying this group is biased towards the formation of subchondral bone. It is reasonable to postulate that higher turnover of bone favouring osteogenesis could represent subjects with subchondral bone thickening and stiffening, a common radiographic feature thought to be related to the progression of focal cartilage damage (Muratovic et al., 2016, Radin and Rose, 1986) and later-stages of OA development (Burr and Gallant, 2012, Karsdal et al., 2014).

Cluster 2: Bone resorption phenotype

The second cluster identified present high canonical osteoclastogenic pathway activation, evidenced by the substantially elevated RANKL levels and consequently elevated RANKL:OPG ratio, coupled with lower relative bone formation represented by depleted ALP relative to CTX-I levels. Both mechanisms mentioned are related to osteoblast activity, whereby the pattern points toward a switch from bone formation to bone resorptive behaviour via increased RANKL expression. In addition, the relatively moderate levels of sclerostin activity and reduced IL-10 activity relative to cluster 1,

suggest a down-regulation of Runx2 activity (via differential pathways) and consequently reduced bone matrix formation (Jung et al., 2013, Krishnan et al., 2006).

Cluster 3: Cartilage degradation phenotype

The final cluster of subjects presented high sclerostin expression coupled with reduced anti-inflammatory (IL-10, IL-12p70 and IL-13) activity and IFN-γ. This pattern appears to be consistent with an inflammatory and/or catabolic phenotype although this is not substantiated by markers of bone remodelling (ALP, RANKL/OPG ratio). This pattern therefore may be more-so related to the activity of affected cartilage, as sclerostin is found to be overexpressed by articular chondrocytes in focal areas of damaged cartilage in ovine and murine models of post-traumatic OA (Chan et al., 2011, Lewiecki, 2014). Indeed, investigation of serum biomarker correlations revealed a significant positive association of sclerostin on COMP levels, as well as a moderate inverse correlation of IL-10 with COMP. Assuming these mechanisms in serum are reflective of joint activity, these findings indicate that cluster 3 may have increased focal articular cartilage degradation, which in turn may result from increased mechanical loading on the joint surface. The observed increased glutamate concentrations previously reported to be associated with inflammatory and osteoarthritis (Flood et al., 2007, Bonnet et al., 2015) and implicated with increased joint loading is consistent with this cluster (Brakspear and Mason, 2012). Further studies investigating a larger range of cartilage signalling and degradation biomarkers in a larger cohort should be conducted to validate this hypothesis.

Collective interpretation of PCA clusters

PCA variances revealed three main clusters that appear to be predominantly distinctive by variations in Wnt/β-catenin pathway activation by the key regulator sclerostin, anti-inflammatory activity as well as RANKL expression. In bone, the secretion of sclerostin by resting osteocytes disrupts the Wnt/β-catenin by binding to low density lipoprotein receptor-related protein-5/6 (LRP5/6), and downstream inhibition of osteoblast proliferation, differentiation and matrix deposition (e.g. ALP) genes orchestrated by the transcription factor Runx2 (Sebastian and Loots, 2017, Raggatt and Partridge, 2010). However, the loss of sclerostin expression by osteocytes occurs through activation of mechanotransduction pathways, in other words when subchondral bone osteocytes are loaded in compression. In cartilage, sclerostin is expressed by chondrocytes exposed to pro-inflammatory cytokines in regions of focal damage, and inhibition of Wnt/β-catenin in chondrocytes leads to down-regulation of catabolic pathway (MMP and ADAMTS) expression, inhibition of anabolic pathway (aggrecan, collagen type-II and TIMPs) expression, increased hypertrophic differentiation and increased apoptotic signalling

(Chan et al., 2011, Zhu et al., 2008). Furthermore, the production of osteo- and chondro-protective anti-inflammatory cytokine IL-10 depends on Wnt/β-catenin activation in osteocytes, macrophages and synovial tissues (Li et al., 2008, Suryawanshi et al., 2016). This link is substantiated by the significant ($p \leq 0.05$ to $p \leq 0.01$) negative correlations of sclerostin with IL-10, IL-12p70 and IL-13 identified in synovial fluid, which is a clear illustration of this pathway.

Considering these mechanisms, the PCA variances may relate to that of three phenotypes of which present either:

- A bone formation (anabolic osteoblast), anti-inflammatory phenotype caused by increased loading of subchondral bone and high β-catenin activation, who may develop subchondral plate thickening and stiffening due to increased bone deposition and osteo-protective mechanisms
- A catabolic osteoblast phenotype that down-regulate bone matrix formation (low β-catenin activation) and upregulate osteoclastogenic signalling (high RANKL expression) resulting in net subchondral bone loss, possibly in the form of BMLs
- A low catabolic/anabolic/apoptotic chondrocyte phenotype that may present increased focal articular cartilage damage and breakdown

Cluster 1: Tissue repair phenotype

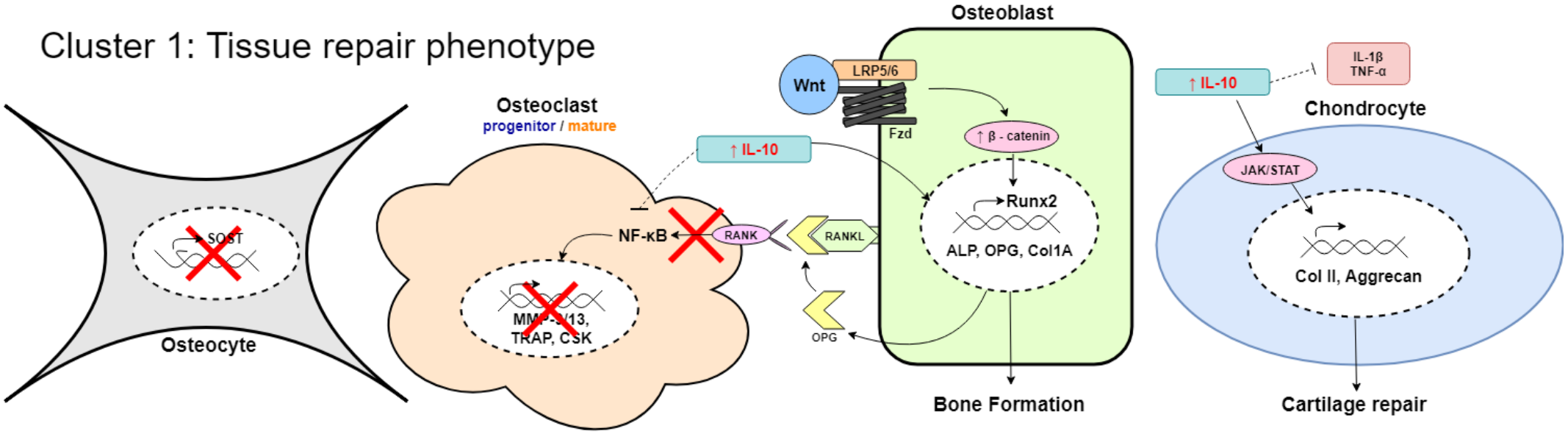

Cluster 2: Tissue degradation phenotype

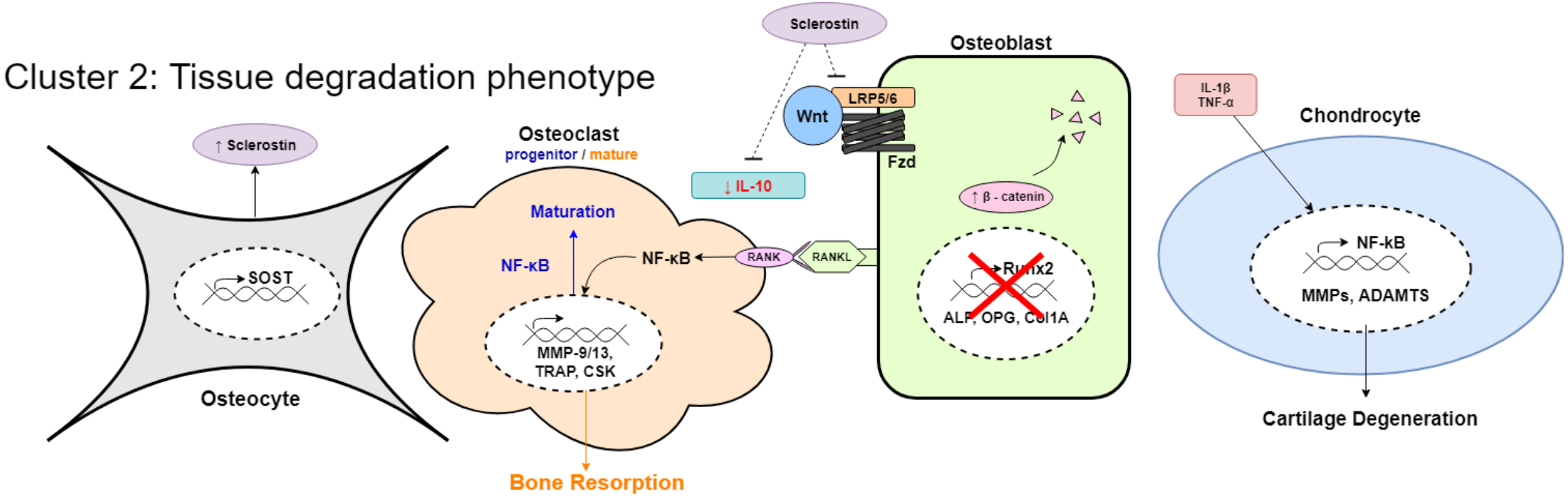

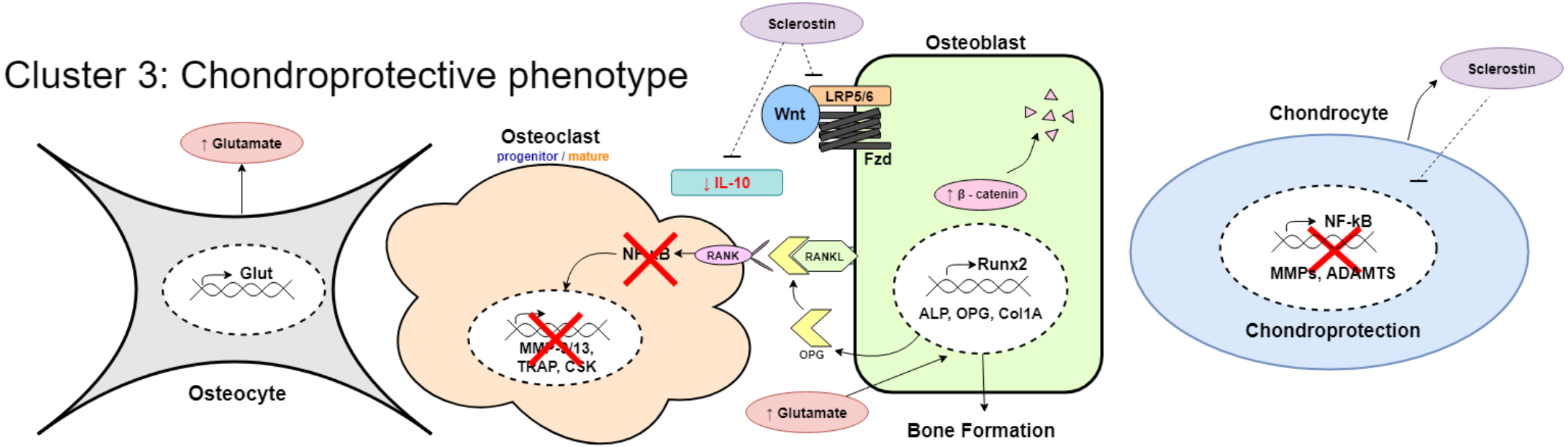

Figure 4.3-12 – Schematic representing hypothetical mechanisms associated with subject clusters in the multivariate analysis, based on known mechanisms:

Cluster 1 is representative of a bone formation / cartilage repair phenotype – in this group there was a pattern of reduced sclerostin activity coupled with increased anti-inflammatory cytokine (e.g. IL-10) levels. Low sclerostin levels permits for canonical Wnt (β-catenin pathway) signalling to ensue. Since β-catenin signalling is an upstream positive regulator of Runx2, osteoblastogenesis and expression of bone formation (osteoblastic) genes, including ALP, OPG and Col I, are upregulated (Li et al., 2008). The higher IL-10 levels would also lead to increased anabolic bone activity through activation of the SMAD kinase pathway and ERK1/2 MAP (Wojdasiewicz et al., 2014). This is substantiated by the increased ALP detected within this cluster. IL-10 is also chondroprotective in the course of OA, since it is involved in stimulating collagen type II and aggrecan synthesis through its interaction with intracellular JAK1/STAT3 pathway as well as downregulation of pro-inflammatory cytokine production (Wojdasiewicz et al., 2014, Iannone et al., 2001). The osteoblastic production of OPG blocks NF-κB-dependent osteoclastogenesis and upregulation of osteoclast bone resorption activity through the activation of RANK (Boyce et al., 2015). Altogether, these mechanisms point toward a group that exhibit increased bone formation, cartilage repair and reduced bone loss.

Cluster 2 is representative of a bone degradation phenotype – Moderate levels of sclerostin are present which contribute to down-regulation of IL-10 synthesis, and potent inhibition of the Wnt (β-catenin) pathway in osteoblasts. When sclerostin binds to the LRP5/6 and Frizzled co-receptors on the osteoblast surface, canonical Wnt (β-catenin) signalling is inhibited since endogenous β-catenin is degraded (Li et al., 2005). Runx2 is downregulated in osteoblasts, negating production of new bone and reducing OPG release (Li et al., 2012). Decreased IL-10 also results in higher levels of pro-inflammatory cytokine activity, thus promoting catabolic chondrocyte signalling and production of proteases (MMPs) and aggrecanases (ADAMTS) which break down cartilage (Wojdasiewicz et al., 2014). On the other hand, increased RANKL expression on the surface of osteoblasts leads to enhanced activation of the RANK-dependent NF-kB pathway in progenitor and differentiated osteoclasts, promoting osteoclastogenesis and increased production of bone resorption enzymes (MMP-9 and -13, TRAP, CSK) (Tat et al., 2008b). Overall, these mechanisms point towards a group who exhibit reduced bone formation and increased bone resorption.

Cluster 3 is representative of a chondroprotective phenotype – High levels of sclerostin is present, possibly produced by chondrocytes as a chondroprotective response to tissue damage, since it is a potent inhibitor of NF-κB-dependent expression of MMP and aggrecan synthesis in injured chondrocytes (Chang et al., 2018). Since sclerostin inhibits osteoblast activity, Runx2 expression through the Wnt pathway is inhibited. However, increased glutamate presence likely due to loaded subchondral bone activates Runx2 through the activation of iGluRs on the surface of osteoblasts, increasing osteogenic gene expression (substantiated by the increased ALP) and inhibition of osteoclast activity.

4.4.4 Major findings for objective 3

The final objective of the chapter was to assess longitudinal changes in serum biomarkers to determine possible mechanisms of repair/progression that relate to positive or poor clinical outcomes 6 months post-microfracture surgery.

Reduced bone resorption activity following microfracture surgery

The significantly reduced serum CTX-I levels post-surgery is indicative of reduced bone resorption, a mutual feature across all subjects and may represent a switch toward subchondral bone formation as a possible repair mechanism following bone marrow stimulation. Interestingly, subject MT who showed the smallest decrease in CTX-I levels was the eldest (76 years) relative to the others (between 20-46 years), which could therefore be reflective of the inhibitory effect of age on osteogenic repair capabilities (Gibon et al., 2016). Decreases in CTX-I levels significantly correlated with decreases in glutamate and TNF-α levels, implying they may be important regulators of bone resorption. The relation of CTX-I to TNF-α levels is also reflective of the positive correlation found in the cross-sectional analysis, substantiating involvement of pro-inflammatory activity with bone resorption. It is also noteworthy that glutamate levels were also significantly reduced following surgery across the group, further supporting its association with an arthritic degenerative state.

In contrast, changes in bone resorption activity did not appear to be regulated by canonical osteoclast signalling, evident by the negative correlation between CTX-I levels and the RANKL/OPG ratio. Therefore, in the context of biomarkers examined, these findings propose a mechanism by which reduced focal loading of subchondral bone halts glutamate release by Ca^{2+}-mediated exocytosis mechanisms and production of TNF-α by mechano-sensitive cells, negating non-canonical osteoclast-activation pathway activation that occurs through the activation of ionotropic glutamate (Merle et al., 2003, Mentaverri et al., 2003) and TNF receptors (Osta et al., 2014) on the surface of progenitor and mature osteoclasts. Findings from chapter 2 demonstrated that compartmental knee loading was not significantly altered post-surgery, therefore it is possible that marrow stimulation from the surgery would have resulted in a new fibrous layer of cartilage formed over the defect site that could promote focal load distribution and protect underlying subchondral bone.

Increased cartilage matrix deposition or degradation following microfracture surgery

A contrasting result reflected across all subjects was the significantly increased levels of COMP in serum following surgery, which signifies increased chondrocytic matrix deposition (Recklies et al., 1998) or cartilage matrix destruction (Attur et al., 2013). Six-months post-surgery may be an early time-point for delineating the effects of repair from that of poor biological outcomes, since cartilage compositional changes assessed by MRI are still taking place up to two years following marrow-stimulation techniques (Theologis et al., 2012, Lansdown et al., 2018). Increases in COMP correlated strongly with decreases in sclerostin levels, suggesting that upregulation of Wnt/β-catenin signalling in chondrocytes may be involved in this process. However further study involving later-time points may be required to understand the long-term effect microfracture has on maintaining cartilage health.

Dysregulation of inflammatory signalling following microfracture surgery may correlate with poor patient-reported outcomes

Following microfracture surgery, IL-10 and IL-13 were considerably elevated for 4/5 subjects, but one subject (RP) showed the opposite for IL-10 levels (but was not included in IL-13 testing). A similar pattern was observed for IFN-γ changes, whereby RP presented a sharp decline in concentrations relative to the group. These clear patterns are associated with the bad clinical outcomes (worsening pain, symptoms and function) presented by RP relative to the improvements seen in other subjects. It is therefore reasonable to hypothesise that anti-inflammatory dysregulation is responsible for these poor outcomes. Indeed, it was revealed both in the cross-sectional analysis as well as the present that both serum IL-10 and IFN-γ significantly ($p \leq 0.05$) correlated with baseline KOOS clinical scores as well as longitudinal changes in scores, which is substantial evidence for this effect. IL-10 is protective of neuropathic pain induced by peripheral and central nerve injury in mice (Shao et al., 2015). However in contrast IFN-γ appears to stimulate in nociceptive pathways by potentiating NMDA receptors (Sonekatsu et al., 2016). The incongruencies with IFN-γ findings in relation to literature may be related to the inconsistent concentrations of synovial fluid and serum levels, which is substantiated by the opposing relationship of synovial fluid IFN-γ with pain in the cross-sectional analysis.

The next sections discuss the clinical significant and relation of key findings from this study to the field within each category of biomarker (tissue turnover, mechanical and inflammatory).

4.4.5 Biomarkers of bone and cartilage turnover

4.4.5.1 Osteoclastogenic pathways in FCD pathogenesis

The increased levels of CTX-I in FCD serum relative to controls is indicative of a net increase of bone resorption activity, however a notable observation was that the RANKL/OPG ratio did not exhibit a relationship with CTX-I levels in synovial fluid or serum. As previously suggested, this is evident of non-canonical osteoclastogenic pathway activity that shares regulation of pathogenic bone remodelling signalling in disease states such as FCD and uOA. Further understanding of the influence of canonical and non-canonical pathways in FCD pathogenesis is critical to developing anti-resorptive therapies such as those used in trials for preserving bone in rheumatoid arthritis (Gamez-Nava et al., 2013).

A key finding within this study was that RANKL expression appears to be predominantly dependent on pro-inflammatory regulators, whereas OPG may be influenced by subchondral bone loading due to its discriminatory ability of FCD and uOA synovial fluid. The canonical bone remodelling pathway is dependent on the activation of receptor activator of NF-κB (RANK) found on the surface of pre and mature osteoclasts, which when activated by RANKL located on activated osteoblasts, osteocytes and some immune cell types, stimulates osteoclast differentiation and bone resorption through intracellular stimulation of the NF-κB pathway (Tat et al., 2008b, Wijenayaka et al., 2011). However, OPG secreted by osteoblasts can inhibit the activity of RANK by binding and deactivating RANKL, thus the relative quantities of RANKL and OPG can provide an index of bone resorption pathway activation (Tat et al., 2009). The dependence of osteoclast activity on the RANK/RANKL system is evident with investigations into RANKL-knockout mice, which suffer from unopposed bone growth due to the lack of osteoclast maturation and activity (Odgren et al., 2003). In normal functioning, the level of RANKL and OPG expression is dependent on a wide variety of signalling promotors and inhibitors, with multiple levels of ligand and receptor activity.

In earlier years it was recognised that key regulators such as parathyroid hormone (Horwood et al., 1998) and pro-inflammatory cytokines including TNF-α, IL-1β and IL-6 locally produced are involved in canonical bone regulation (Hofbauer et al., 1999). Consistent with the positive correlation found of synovial fluid IL-6 and RANKL within this study, it has been established that IL-6 receptor activation on the osteoblast surface stimulates the janus kinase (JAK) and signal transducer and activators of transcription

(STAT) pathway, leading to an upregulation of RANKL expression (Osta et al., 2014). There has also been previous evidence of negative regulation of the RANKL/OPG system by anti-inflammatory cytokines. One study investigating IL-10-deficient bone-marrow macrophages observed enhanced osteoclastogenesis and bone resorption relative to controls (Liu et al., 2006). In this model, subsequent introduction of IL-10 reversed this effect evident by down-regulated RANKL mRNA expression coupled with enhanced OPG expression. This mechanism may explain the negative correlation between RANKL and IL-10 found within the correlation analysis.

Sclerostin is primarily known for inhibition of osteogenic gene expression through disruption of the Wnt/β-catenin pathway. However, there is evidence to suggest another role in supporting osteocyte-driven osteoclastogenesis (Wijenayaka et al., 2011). Recombinant human sclerostin was found to dose-dependently down-regulate the expression of OPG mRNA and up-regulate RANKL expression in human primary pre-osteocyte culture and in mouse osteocyte-like MLO-Y4 cells. Furthermore, co-culture of MLO-Y4 cells on a 'bone-like' substrate with peripheral blood mononuclear cells in the presence of sclerostin resulted in a 7-fold increase in bone resorption activity, which was eliminated by introduction of OPG (Wijenayaka et al., 2011). This is relevant when considering the PCA results within this study that revealed variances representative of sclerostin and RANKL expression, as it further substantiates sclerostin as a key regulator and discriminatory factor of the identified phenotypes. In a review of the RANKL/OPG system, Tat and colleagues have proposed based on previous literature that OA subchondral bone osteoblasts can be divided into two subpopulations defined as 'low-OA' or 'high-OA' types (Tat et al., 2009). It was suggested that the 'low-OA' phenotype presenting high RANKL/OPG ratios and low endogenous PGE_2 production promote subchondral bone loss, whereas the 'high-OA' phenotype that present low RANKL/OPG ratios and high PGE_2 promote subchondral bone thickening and sclerosis that is often attributed to later-stage OA (Tat et al., 2009). This theory could accommodate sclerostin as a possible mechanistic 'switch' involved in the transition of osteoblast states.

In vitro studies have shown a number of cytokines and growth factors capable of substituting the effect of RANK to increase osteoclastogenesis of progenitors. These include TNF-α (Mabilleau et al., 2012), IL-6 and IL-8 (Knowles and Athanasou, 2009), which activate NF-κB intracellular signalling through their own surface receptors. This is could explain the relationship between TNF-α and CTX-I levels found within this study, which was not reflected in TNF-α and RANKL associations, inferring that TNF-α activity is independently promoting bone matrix breakdown. The stronger relationship implies

TNF-α may have a stronger influence on bone resorption in this disease process. This hypothesis is consistent with the correlation between longitudinal changes in TNF-α and CTX-I and implies that the regulation of TNF-α activity may a key mechanism is the switch toward subchondral bone repair.

Glutamatergic signalling may be in part influencing the incongruities between RANKL/OPG ratio values and bone resorption. Reviews of reported transcript and protein expression of bone cell glutamatergic signalling components found that osteoclasts express iGluRs activated by NMDA, AMPA and kainate, mGluRs and EAATs, implying osteoclasts respond to, as well as regulate extracellular glutamate levels (Brakspear and Mason, 2012, Wen et al., 2015). Early in vitro cultures of osteoclasts exposed to the NMDA glutamate receptor antagonist MK-801 revealed downregulation of osteoclast differentiation and resorption activity, evident by the reduced resorption pits in dentine (Peet et al., 1999). A later study substantiated these findings in two individual *in vitro* models, one using the murine myelomonocytic RAW 264.2 cell line and the other mouse bone marrow cells, by demonstrating that two antagonists of NMDA receptor (NMDAR), MK-801 and AP-5, dose-dependently inhibited osteoclastogenesis, suggesting that osteoclast progenitors require NMDAR activation for differentiation (Merle et al., 2003). These findings are supportive of the correlation between longitudinal changes in serum glutamate and CTX-I levels, equivalent to that found with TNF-α, implying both mechanical and inflammatory components influence of pathological bone resorption.

4.4.5.2 CTX-I as a biomarker of bone resorption

CTX-I is an indicator of the osteoclastic metabolism of collagen type-I, the predominant collagen in bone and meniscal tissues, it is often utilized as a selective marker for bone turnover for the characterisation of human bone pathologies such as osteopenia, osteoporosis and arthritis (Cremers et al., 2008). Consistent with the findings from this study, CTX-I is elevated in animal models of OA development and progression. In a murine post-traumatic OA (PTOA) model simulated by tibial compression overload and ACL rupture, significantly increased serum levels of CTX-I were observed for up to 56 days post-injury relative to unloaded controls (Khorasani et al., 2015). Although correlations were not explored, the same cohort of mice experienced significant trabecular bone loss explanatory of the increased CTX-I levels, as well as subchondral bone thickening, determined by quantitative structural μCT. Another study investigating changes in a canine partial-medial meniscectomy model which developed tibial

osteochondral lesions similarly showed CTX-I increases which corresponded to worsening histological scoring of subchondral bone and cartilage OA-related changes (Connor et al., 2009). In human OA studies, it has been shown that CTX-I levels appear to be a risk factor for disease progression and increases in serum precede increases biomarkers of cartilage metabolism, reflecting the earlier pathological changes in bone in the disease (Garnero et al., 2005, Attur et al., 2013). However, interestingly the increased bone resorption only appears to be relevant in the presence of progressing OA states, since individuals with 'non-progressing OA' characterised by a lack of change in K/L grade do not exhibit abnormal CTX-I levels (Bettica et al., 2002).

Changes in bone have also been recognised in previous studies investigating joint FCDs. One investigation demonstrated that urinary CTX-I levels were in the 'upper range of normal' for patients with tibiofemoral FCDs accompanying ACL insufficiency. Furthermore, CTX-I correlated with reduced tibiofemoral subchondral bone area and cartilage volume determined by MRI methods (Streich et al., 2011), reiterating the sensitivity of CTX-I for detecting relevant bone changes. It is thought that loss of bone and dysregulated remodelling often accompanies FCDs in the form of bone marrow lesions (BMLs), focal areas of bone attrition/sclerosis underlying FCDs, which may be a crucial contributor to the aetiology of FCDs due to their association with rapid articular cartilage loss (Xu et al., 2012). BMLs detected and scored by MRI methods have proven to be strong predictors of defect progression, defined by worsening of chondral lesion MRI scores (Dore et al., 2010). Since bone is a highly mechano-responsive tissue, the presence of BMLs in relation to FCD pathogenesis is likely related to abnormal joint loading. In fact, remodelling is influenced by both mechanical and inflammatory pathways in which it is apparent are both involved in FCD pathogenesis (Burr and Gallant, 2012, Cremers et al., 2008).

The findings from this study corroborate with others regarding the utility of CTX-I as a marker of altered bone resorption activity, therefore may be useful in longitudinal studies where FCDs have been diagnosed. However, it is noteworthy that CTX-I as an individual marker lacks selectivity. Due to the substantial number of regulatory and homeostatic processes involved with bone resorption, non-joint specific bone resorption could potentially affect the diagnostic and prognostic utility. Increased acidity of blood due to diet, osteoporosis as a result of menopause as well as levels of physical activity are just some examples of factors that may affect individual differences (Burr and Gallant, 2012, Cremers et al., 2008). The latter example was demonstrated in a study aiming to distinguish between altered CTX-I levels with the effect of increased exercise

compared to development of OA in horses, who found similar increases in both groups, stressing the importance of considering such factors in interpretations (Frisbie et al., 2008). Notably from this study, synovial fluid CTX-I significantly associated with BMI, suggesting altered body mass alone may reduce the sensitivity of CTX-I in cross-sectional studies. Perhaps CTX-I may not be a reliable individual marker of pathology, but may be better selective in a combinatory panel with other discriminatory markers or in longitudinal studies whereby many mentioned factors remain consistent.

4.4.5.3 COMP as a biomarker of cartilage remodelling

Several independent studies have demonstrated the potential utility of COMP as a diagnostic and prognostic serum biomarker of cartilage structural degradation in knee OA, due to its sensitivity to joint space narrowing and its known abundance in cartilage tissue where its function involves providing stability to the matrix (Attur et al., 2013, Kraus et al., 2017, Sowers et al., 2009, Halasz et al., 2007). In the cross-sectional analysis, it was evident that serum COMP levels did not vary between FCD subjects and controls. Since FCDs are characterised by progressive focal articular cartilage loss, this finding was unexpected and suggests serum COMP may not be selective of cartilage degradation at this stage of pathology. Consistent with these findings, Streich and colleagues (2012) investigating serum COMP concentrations in individuals with ACL-rupture with accompanying FCDs reported levels within the 'normal' clinical ranges, with only weak correlations to medial femoral cartilage area detected by MRI (Streich et al., 2011). However, they found a more reliable link between FCD presence and CTX-II levels, as well as a moderate relationship between CTX-II and cartilage volume and subchondral bone area, suggesting CTX-II may be a stronger indicator of cartilage loss in the earlier stages of pathology.

A likely explanation for the lack of differing COMP levels may be related to its sensitivity to joint activity. Andersson and colleagues (2006) showed that serum COMP levels are significantly elevated after 60 minutes of strenuous exercise, which proceed to significantly return to resting levels 60 minutes following rest (Andersson et al., 2006b). Whereas another group independently demonstrated that even a moderate walking activity of 30 minutes could significantly influence serum COMP up to 9.4% above resting levels (Mundermann et al., 2005b). Due to the difficulties in controlling for activity levels within the tested cohort in this study, it is likely that differences in recent activity may have increased individual variances, ultimately obscuring group differences resultant of chondral defect presence. It could be that the elevated COMP levels following activity are

either related to the anabolic biosynthetic response of chondrocytes following joint activity, or simply the release from cartilage matrix following structural matrix deformation (Attur et al., 2013).

It is noteworthy that COMP levels were significantly increased following microfracture surgery concomitant with decreased sclerostin levels, implying that COMP synthesis may be important to cartilage repair processes. Indeed, previous authors have demonstrated that COMP is involved in fibril formation of collagen type-I and II by catalysing fibrillogenesis with unique organisation, as well as a possible involvement in supporting mediation of aggrecan interaction (Halasz et al., 2007, Chen et al., 2007). Furthermore, it has been recognised that Wnt signalling is actively regulated during repair, whereby it is involved in chondrogenic or osteogenic lineage commitment of mesenchymal stem cells (MSCs), maintenance of a chondrogenic phenotype and matrix synthesis (Yuan et al., 2016). This suggests the upregulation of COMP synthesis by chondrocytes may be regulated by Wnt following the down-regulation of sclerostin. Considering these findings, serum COMP may be a good indicator of cartilage repair activity in the early stages following marrow stimulation techniques.

On the other hand, overstimulation of Wnt signalling in disease states can promote chondrogenic hypertrophic differentiation and apoptosis, leading to accelerated destruction of cartilage (Yuan et al., 2016, Lewiecki, 2014). Furthermore, from a macroscopic perspective, it is well established that bone marrow stimulation techniques generate a mechanically inferior and disorganised 'fibrocartilage' in place of the lost hyaline cartilage, therefore increased COMP levels could be representative of the accelerated destruction of neocartilage in response to continued aberrant loading of the joint. Considering these contrasting mechanisms, longer term studies investigating the persistence of serum COMP are required to understand cartilage repair/degenerative mechanisms in the course of recovery to function following surgery.

4.4.6 Biomarkers of bone mechanical loading

4.4.6.1 Glutamatergic signalling in knee pathogenesis

Glutamate is a key signalling molecule in bone within the OA disease process thought to have disease modifying characteristics, due to its substantially elevated concentrations in the joint following acute injury (Bonnet et al., 2015) and in arthritis (McNearney et al., 2000). The pathophysiological influence of glutamate has been demonstrated previously

within our research group in a murine *in vivo* model of antigen-induced inflammatory arthritis (AIA), whereby induction led to upregulation of glutamate production and tissue deterioration, whereas inhibition of glutamate signalling by NBQX, an AMPA/KA glutamate receptor (GluR) antagonist during the acute response dramatically reduced joint inflammation, nociception and histological cartilage, bone and synovium OA-related changes (Bonnet et al., 2015). Considering these findings, the increased levels of glutamate in FCD relative to control serum within this study importantly suggests that FCD pathogenesis may be enhanced by pathological glutamatergic signalling. Furthermore, since previous work has demonstrated that glutamate levels may be regulated by mechanical loading of bone, this is an important finding in the context of FCD and uOA pathogenesis, which as previous discussions suggest are mechanically-driven. It is reasonable to hypothesise that increased glutamate in FCD serum may be attributed to increased loading of the affected knee compartment, as revealed by varying KAMs relative to controls found in chapter 2.

The mechanistic consequences of pathophysiological glutamatergic signalling in the OA joint are still yet to be fully established, however some studies have revealed potential mechanisms. The involvement of glutamatergic signalling in inflammatory pathways has been evidenced by several studies. Flood and colleagues (2007) showed that inhibition of N-methyl-D-aspartate (NMDA) glutamate receptors (NMDARs) in fibroblast-like synoviocytes of the rheumatoid arthritic joint significantly reduced IL-6 expression and regulated MMP-2 release of these cells. Whereas Piepoli and colleagues (2009) studying the effects of glutamate in chondrocyte cultures found that while IL-1β in chondrocytes enhanced the production of pro-inflammatory cytokines and proteolytic enzymes, inhibiting the NMDARs suppressed this response, suggesting a potentially unique role in glutamate receptors on chondrocytes in modulating the inflammatory process in OA. In another study, blocking AMPA/KA receptors in a murine AIA model with NBQX reduced the expression of IL-6 mRNA in meniscal tissues, and reduces cartilage fibrillation and proteoglycan loss induced by inflammatory processes (Bonnet et al., 2015). MRI methods have revealed that early compositional changes of cartilage relating to FCD development involved the loss of proteoglycan followed by collagen structures (Theologis et al., 2012), therefore joint inflammation following injury concurrent with enhanced glutamatergic signalling could be a major contributing factor to cartilage loss in FCD development.

High joint glutamate levels is also implicated in altered bone function. An *in vitro* study demonstrated high levels of extracellular glutamate reduced the proliferation of MC3T3-E1 osteoblasts towards self-renewal through the upregulation of nuclear factor E2 p45-

related factor 2, stunting bone formation (Uno et al., 2007). It was suggested that substantially elevated concentrations of glutamate may inhibit cysteine/glutamate antiporters (GLASTs) on the surface of osteoblasts, suppressing proliferation and down-regulating Runx2 activation as a consequence of glutathione depletion (Uno et al., 2007, Brakspear and Mason, 2012). The proposed mechanisms suggest pathophysiological loading of bone may enhance bone resorption by promoting increased osteoclastogenesis through continued stimulation of the NF-κB pathway, coupled with reduced osteoblastic activity through GLAST deactivation, yielding a net loss of bone. This hypothesis is consistent with the correlation found between longitudinal decreases in serum glutamate and CTX-I levels following marrow stimulation

Taken together, it is likely and supports the development of glutamatergic signalling inhibitors as others have suggested (Bonnet et al., 2015, Wen et al., 2015), to reduce physiological changes in bone that contribute to FCD development following injury or progression.

4.4.6.2 Sclerostin as a switch of pathological phenotype

Sclerostin importantly functions in the adaptation of bone to mechanical signals from the environment, however the role of sclerostin signalling in the pathogenesis of OA is complex and less defined, with contradictory reports in the field (Lewiecki, 2014). The variances captured by PC clustering analysis within this study revealed that both FCD and uOA cohorts presented low and high sclerostin subpopulations which respectively corresponded to high or low bone turnover. As previously suggested, this is likely resultant of altered subchondral bone and cartilage loading, which appears to regulate the expression of sclerostin and therefore may modulate disease pathogenesis (Robling et al., 2008, Zhu et al., 2009).

As a potent Wnt/β-catenin pathway inhibitor, sclerostin has control over important osteogenic pathways in bone, including inhibition of downstream expression of osteoblast proliferation, differentiation and matrix deposition genes orchestrated by the transcription factor Runx2 (Sebastian and Loots, 2017, Raggatt and Partridge, 2010). Sclerostin also carries an important role in maintaining cartilage, since the Wnt/β-catenin pathway in chondrocytes activates catabolic pathways, leading to the expression of proteases (MMPs) and aggrecanases (ADAMTS), but paradoxically promotes anabolic pathways through up-regulation of aggrecan and collagen type-II synthesis (Chan et al., 2011, Zhu et al., 2009).

Mice lacking the sclerostin gene present high anatomical bone mass that is detectable as early as 1 month and peaks around 18 months of age, with increased levels of bone formation on trabecular surfaces relative to controls (Lin et al., 2009). In another mouse sclerostin-knockout study, it was shown that cartilage is preserved despite the increased bone volume, however destabilization of the joint by surgically removing the medial meniscus lead to higher cartilage damage than wild-type mice, accompanied by increased aggrecanase and type X collagen expression (Bouaziz et al., 2015). Furthermore, this effect was reversed by introducing sclerostin, which inhibited the Wnt canonical pathway as well as the non-canonical Wnt-phosphorylated JNK pathway in cartilage. Consistent with this, adult transgenic mice where the β-catenin pathway was stabilized displayed an osteoarthritis-like hypertrophic phenotype of articular chondrocytes that differentiated prematurely (Zhu et al., 2009). In contrast, over-expression of *SOST* in mice correlates with lower bone mass and high bone fracture rates, even with the administration of parathyroid hormone (a potent bone anabolic stimulant), highlighting the potentially dominant role of sclerostin in catalysing bone loss disease states (Kramer et al., 2010). Whereas inhibition of Wnt/β-catenin signalling in transgenic mice associates with increased apoptotic articular chondrocytes, and subsequent destruction of articular cartilage (Zhu et al., 2008). Despite these contrasting findings, the general consensus among researchers is that increased sclerostin expression in damaged cartilage may predominantly be a chondro-protective mechanism, since it interrupts catabolic pathway activation (Chan et al., 2011, Lewiecki, 2014).

Together, these studies collectively suggest that either high or low pathophysiological levels of sclerostin may attribute to OA pathogenesis through dysregulated β-catenin signalling, particularly after the induction of disease. Furthermore, sclerostin signalling in the OA joint may differ in various tissues, resulting in contrasting pathological effects. Chan and colleagues interestingly reported increased sclerostin expressed in regions of focal cartilage damage in both sheep and mice models of surgically-induced knee OA, whilst reduced sclerostin expression was detected in sclerotic regions of subchondral bone (Chan et al., 2011). Considering this literature, it is likely that the multiple subgroups revealed in the PCA cluster analysis of high and low sclerostin levels may be representative of individuals who exhibit varying levels of cartilage damage and bone sclerosis, as previously suggested.

These findings are important in that the rheumatology field is becoming increasingly aware of OA heterogeneity, with mounting evidence of the need for personalised

treatments for distinct phenotypic groups (Kraus et al., 2011, Lotz et al., 2013). The identification those at more risk of progression due to bone loss in the form of bone marrow lesions in the earlier stage following injury that may benefit from anti-resorptives (Karsdal et al., 2014), from others that are prone to cartilage loss due to the altered tissue properties resultant of subchondral bone sclerosis in later stages of disease (Tat et al., 2008b), is critical to improving the efficacy and longevity of future therapies.

4.4.7 Biomarkers of inflammation

4.4.7.1 Pro-inflammatory mediators in knee disease

Pro-inflammatory mediators have been widely acknowledged for their diagnostic and prognostic potential for clinical knee OA (Fernandes et al., 2002, Kapoor et al., 2011, Liu-Bryan and Terkeltaub, 2015), as well as knee FCDs (Cuellar et al., 2016, Tsuchida et al., 2012, Streich et al., 2011). These molecules arise from specific inflammatory tissues such as the synovium, infiltrating leukocytes, or traumatised bone and cartilage cells, and facilitate autocrine and paracrine signalling to stimulate the production of themselves in a positive feedback loop (Wojdasiewicz et al., 2014). This was evident within associations of TNF-α, IL-6 and IL-8 within this study. Aside from self-propagation, pro-inflammatory cytokines stimulate chondrocytes and osteoclasts to upregulate production of matrix degrading proteolytic matrix metalloproteinases (MMPs), aggrecanases (ADAMTS), prostaglandins and nitric oxide (NO), associated with cartilage and bone degradation (Houard et al., 2013). Furthermore, as previously discussed cytokines are involved in bone remodelling pathways including the canonical and non-canonical osteoclastogenesis pathways (Osta et al., 2014).

The increase in IL-6 in line with advancing disease states found within this study is in line with a recent study by Cuellar and colleagues (2016) who investigated inflammatory cytokines, chemokines and proteases in joint fluid of 70 arthroscopy patients, and demonstrated that IL-6 was the strongest predictor of severe chondral lesions (Cuellar et al., 2016). IL-6 production and signalling has been documented in all joint tissues, but is primarily regulated by osteoblasts, chondrocytes, macrophages and adipocytes (Guerne et al., 1990, Akeson and Malemud, 2017). Although mostly considered a pro-inflammatory cytokine, IL-6 multidirectional interactions in cartilage and bone homeostatic processes, confers conflicting roles in OA pathophysiology. In more recent

years, there has been mounting evidence and interest in the substantially elevated levels of IL-6 found with the acute tissue response to joint injury (Watt et al., 2016) and more specifically isolated ACL tears (Struglics et al., 2015), ACL tears with meniscal injuries (Bigoni et al., 2013) and acute tibial plateau fracture (Haller et al., 2015).

Increased IL-6 concentrations following injury may be associated with its increased expression in response to mechanical stimulation. Earlier work subjecting normal and OA chondrocytes to high fluid-induced shear stress (>10 dyn/cm^2) showed significant upregulation of IL-6 by normal chondrocytes, which induced levels released by OA chondrocytes (Mohtai et al., 1996). More recently, it was discovered that IL-6 synthesis following shear stress is dependent on activation of the P13-L/Akt-dependent NF-kB pathway (Wang et al., 2010). Sanchez and colleagues (2009) also demonstrated a significant upregulation IL-6 in cultured osteoblasts following physiological compression loading. These findings are significant considering FCD and uOA phenotypes exhibit increased overloading of the affected condyle as a result of dynamic joint malalignment during gait, which is recognised to be a critical risk factor for OA development and progression (Felson et al., 2000, Sharma et al., 2001). The increased static knee malalignment exhibited in uOA relative to FCD knees (determined by clinical x-ray) may partially explain differences found in IL-6 levels.

IL-8 is largely characterised in inflammatory knee pathology as a leukocyte chemoattractant and stimulant of cytokine production by synovial tissues (Feldmann and Maini, 2001, Yuan et al., 2001, Scanzello, 2017), but is also directly involved in joint tissue pathogenesis. Merz and colleagues (2003) demonstrated that primary articular chondrocytes express IL-8 receptors (CXCLR1, CXCLR2), which following activation by IL-8 enhance expression of tissue inhibitor of metalloproteinase-3 (TIMP-3), hypertrophic markers (type-X collagen, MMP-13 and ALP), and induce matrix calcification. Hypertrophic chondrocytes yield dysregulated 'fibrocartilage' matrix, a feature of cartilage repair surgery that is thought to be a key factor in long-term failure rates, due to its mechanical inferiority to hyaline cartilage (Layton et al., 2015, Falah et al., 2010). The increased calcification of cartilage in regions associated with high IL-8 expression would result in focal concentrations of interfibrillar mineral deposition, leading to further inconsistencies in matrix mechanical properties, disrupting normal dissipation of load through the affected cartilage. Furthermore, the stimulation of MMP-13 release suggests a role for IL-8 in cartilage matrix degradation, though this mechanism is not evident in serum biomarker correlations with COMP within this study.

Collectively, the findings suggest that pro-inflammatory mediators both indicate and facilitate joint tissue damage with increased levels in the joint being consistent with advancing disease state. However, it is notable that preliminary evidence from this study suggests at the FCD stage, serum pro-inflammatory cytokine levels are not representative of joint activity. This is consistent with several large cohort studies including from the Knee Injury Cohort at the Kennedy (KICK) cohort of 150 subjects who found poor ($r < 0.25$) longitudinal correlations for IL-6 over 3-months (Watt et al., 2016), and the Knee Anterior Cruciate Ligament, Non-surgical versus Surgical Treatment (KANON) cohort who showed very weak-to-no ($r < 0.1$) commonality for IL-6, IL-8, TNF-α or IFN-γ in 121 subjects over 5 years (Struglics et al., 2015). Together, these findings suggest serum analysis therefore may be inappropriate for longitudinal interventional trials with intention of using the least invasive methods of analysis.

4.4.7.2 Anti-inflammatory mediators in knee disease and repair

IL-10 and IL-13 are predominantly considered anti-inflammatory mediators due to their common role in the suppression and regulation of pro-inflammatory cytokine activity, however their direct involvement in osteo- and chondro-protective, as well as pathogenic mechanisms have also been documented (Wojdasiewicz et al., 2014, Liu et al., 2006, Feldmann and Maini, 2001). This makes IL-10 and IL-13 crucial immuno-compensatory and tissue conserving players in the course of inflammatory-driven joint pathologies such as OA. Previous studies have reported the potential utility of IL-10 as a biomarker of OA pathogenesis (Wojdasiewicz et al., 2014), progression (Mabey and Honsawek, 2015) and joint sensitization (Imamura et al., 2015). However, this is the first report of IL-10 as an indicator of FCD pathogenesis in serum evident by the significant decreased levels relative to controls, and further decrease with disease advancement toward uOA. Due to the commonality of joint and systemic levels, IL-10 is a promising clinically useful representative biomarker of the increasing inflammatory dysregulation accompanying FCD progression, or to assess the biological outcomes of longitudinal intervention trials.

The function of IL-10 relies on activation of IL-10R on the surface of bone cells, chondrocytes, synoviocytes and infiltrating leukocytes, which promotes the intracellular recruitment of JAK/STAT3, required to self-propagate and down-regulate of NF-kB activity (Mosser and Zhang, 2008). IL-10R activation has been linked to the disruption of the intracellular p38 mitogen-activated protein kinase (p38-MAPK) pathway, thus inferring its specific dysregulation of IL-1β and TNF-α expression (Ji and Suter, 2007). In

other studies, IL-10 has been shown to downregulate intracellular signalling by TNF-α by upregulating TNF decoy receptors, and for IL-1β by enhancing production of IL-1R antagonist (Moore et al., 2001). IL-10- and IL-13-dependent inhibition of chemokines (IL-8, MIP-1 and GM-CSF) in human monocyte cultures has also been revealed, demonstrating their importance in dampening the exponential propagation of pro-inflammatory signalling by circulating immune cells in the acute phase of inflammation (de Waal Malefyt et al., 1991, Malefyt et al., 1993).

The negative association between RANKL and IL-10 within this study is in line with previous studies, showing that IL-10 antagonised IL-1β and IL-6-dependent upregulation of RANKL expression in human periodontal ligament cells (Wu et al., 2013), and showing a direct concentration-dependent downregulation of RANKL expression coupled with an upregulation of OPG expression in ligament fibroblasts (Zhang et al., 2016). Both studies exemplify the bone anti-resorptive activities of IL-10 in joint tissues. Consistent with this, IL-10(-/-) knockout mice showed significant loss of alveolar bone relative to wild-type mice during development, indicating the crucial osteo-protective properties of IL-10 in development as well as disease (Garcia-Hernandez et al., 2012). IL-10 also appears to be involved in the regulation of cartilage growth. When studying protein expression in foetal, adult, and OA chondrocytes, the highest levels of IL-10 and its receptors were detected in foetal, followed by normal adult cells, implying its importance in developmental stages and normal chondrocyte functioning (Iannone et al., 2001). In another study IL-10(-/-) knockout mice exhibited shortening of the tibial growth plate proliferative zone during development, which was reversed by administration of IL-10 (Jung et al., 2013). Furthermore, within *in vitro* adult and OA chondrocyte cultures, Jansen and colleagues (2008) demonstrated IL-10-dependent upregulation of proteoglycan and type II collagen expression, two major components of cartilage. Together, these studies are indicative of the important protective function of IL-10 in the developing and mature joint, therefore dysregulation is likely a potent contributor to pathogenesis.

A consistent finding in the biological outcomes of microfracture surgery includes the elevated IL-10 and IL-13 activity in the majority of subjects, apart from RP who correspondingly suffered from poor outcomes. Interestingly, the anti-inflammatory effects of MSCs have previously been recognised (Pers et al., 2015). A previous *in vitro* study who showed introduction of mouse BM-MSCs were able to increase the number of functional induced $CD4^+$ regulatory T lymphocytes and enhanced IL-10 secretion in cultured T regulatory cells that were induced to differentiate into Th1 or Th17 cells (Luz-

Crawford et al., 2013). This may suggest an important role of marrow stimulation in suppressing the catabolic effect increased pro-inflammatory activity has in the progressing degenerative joint.

4.4.7.3 IL-10 as an indicator of patient-reported pain and poor outcome

The severity of OA is only weakly correlated with clinical factors such as acute and resting joint pain and symptoms such as joint stiffness and swelling (Dieppe and Lohmander, 2005, Felson et al., 2000). For this reason, pain pathogenesis and symptoms are in as much need of study as joint damage.

IL-10 is protective of neuropathic pain induced by peripheral and central nerve injury in mice (Shao et al., 2015). As discussed previously, the benefit of IL-10 in the joint involves its intracellular downregulation of NF-kB and disruption of IL-1β and TNF-α-related intracellular signalling. Knowledge of these mechanisms alone implies the involvement of IL-10 in inhibiting sensitization induced by TNF-α and IL-1β through activation of hyper-nociceptive pathways, as well as reducing the production of PGE_2 and NO. The effects of IL-10 on pain inhibition have been validated in animal models, such as one murine study employing intraspinal quisqalic acid, which produces excitotoxic nerve injury as a result of increased IL-1β, COX-2 and iNOS expression. Following quisqalic acid injection, subsequent injection with IL-10 delayed aforementioned pathway expression and demonstrated inhibitory effects of IL-1β and iNOS mRNA, as well as delayed onset of pain-inducing behaviour such as increased 'grooming' (Plunkett et al., 2001). Interestingly, a separate study showed that intrathecal injections of IL-10 in rats down-regulated both mRNA and protein levels of voltage-gated sodium channels (VGSCs) on dorsal root ganglion neurons following induced peripheral nerve injury. This suggests also an independent and direct role of IL-10 in dampening neuropathic pain generated by ectopic discharges of damaged neurons (Shen et al., 2013).

The evidence of IL-10 sensitization pathway inhibition and correlation with patient reported outcomes in this preliminary study adds to the utility of IL-10 as clinical measure of disease burden and supports the targeting of inflammatory pathways in the treatment of earlier disease states such as FCD pathogenesis for better longitudinal outcomes.

4.4.8 Chapter summary and conclusion

Although there has been extensive exploratory work in development of OA biomarkers, evidence of reliable markers of early knee pathology phenotypes that could be used in the clinic or as outcome measures for interventional trials are lacking (Kraus et al., 2011, Lotz et al., 2013). Previous studies have investigated tissue degradation (Streich et al., 2011, Kraus et al., 2017), turnover and inflammatory (Cuellar et al., 2016) markers in individuals with knee chondral and osteochondral lesions, however there are no single studies that have compared the same breadth of markers in both synovial fluid and blood, with relevance to non-pathological controls and an established OA phenotype. Moreover, there is a deficit of studies characterising pathological bone remodelling signalling and turnover pathways in human OA, which are likely involved in the presence of bone marrow lesions (BMLs) often accompanying FCDs, thought to contribute to their development and progression (Dore et al., 2010).

It was hypothesised that molecules representing bone and cartilage turnover, bone mechanical loading and inflammation would be discriminatory of tibiofemoral FCD and uOA synovial fluids, allowing a further understanding of biological changes in the knee that may reflect disease advancement. The most prominent finding was the increased imbalance of pro-inflammatory/anti-inflammatory activity in the joint with advancing disease state, which is at least partially responsible of the accelerated bone and cartilage loss through the stimulation of protease and aggrecanase production (Berenbaum, 2013), and influence on tissue turnover pathways (Wojdasiewicz et al., 2014) such as osteoclastogenic RANKL-RANK signalling as supported in this study. Furthermore, this is the first identified clustering of knee pathology subjects based RANKL/OPG levels and sclerostin, a surrogate measure of the tissue response to load, which could point toward disease phenotypes relating to joint loading patterns of subchondral bone and cartilage. This is a particularly important finding since FCD and uOA pathogenesis reveals altered stress patterns on the joint surface caused by biomechanical alterations, as demonstrated in FCD subjects within the previous chapter. Consistent with this, the link between longitudinal changes in CTX-I and glutamate levels following marrow stimulation suggests a potentially important function for mechanically-regulated glutamatergic signalling in disease as well as repair of bone.

Single discriminatory, or combinatory panels of biomarkers of disease states will improve diagnosis, prognosis and classification of patients with early to late-stage OA phenotypes for targeted treatment (Kraus et al., 2011, Lotz et al., 2013). Assessment of molecular differences between FCD and control serum led to the identification of

promising novel candidate clinical biomarkers of FCD pathogenesis. Firstly, CTX-I that is representative of the net increased bone resorption/turnover activity, glutamate that may be indicative of the mechanically-regulated glutamatergic signalling activity in response to aberrant loading patterns of subchondral bone, and finally IL-10 that is reflective of the inflammatory dysregulation that accompanies pathogenesis and progression mechanisms as well as neuropathic pathway activation. Moreover, although pro-inflammatory cytokines have been identified as emerging markers in the field for disease severity and progression, preliminary evidence from this study suggests at the FCD stage, serum pro-inflammatory cytokine levels are not representative of joint activity and therefore are inappropriate for longitudinal interventional trials.

To date, there are no known reports of longitudinal changes of synovial fluid or serum biomarkers of tissue turnover, loading or inflammation following treatment of human knee FCDs. Characterising the response to repair can improve the objective comparison of current or new interventions, since common clinical endpoints such as MRI scoring or patient-reported outcomes may provide evidence for point-of-failure, but not reasons for failure. The preliminary results from this study have identified that a typical six-month outcome of marrow stimulation includes down-regulated bone resorption and glutamatergic signalling activity, up-regulated chondrocyte matrix deposition (or possible deterioration) and a shift toward homeostatic levels of inflammatory regulation. These changes are likely related to the anti-inflammatory and reparative effect introducing BM-MSCs will have in the joint. Moreover, poor six-month patient-reported outcomes (based on only one patient) appears to be related to inadequate relief of inflammatory dysregulation. It is likely however that 6-months following surgery for the assessment of treatments such as marrow stimulation is too short considering the course of repair, and longer-term studies with much larger sample sizes are required to determine the leading cause of high failure rates of microfracture surgery.

Chapter 5

Relationship amongst indicators of dynamic knee loading and synovial fluid biomarkers in FCD and unicompartmental OA subjects

5.1 Chapter introduction

As introduced in chapter 1, there is currently a deficit of translational research correlating indicators of knee biology to those of knee function in humans with degenerative knee pathology. This is essential for elucidating mechanisms of pathogenesis at various stages and characterising distinct phenotypes (Karsdal et al., 2014, Lotz et al., 2013). A stronger understanding of these links in individuals would improve the development of comprehensive therapeutic strategies to enhance the efficacy and longevity of intervention (Kraus et al., 2011). Moreover, patient-based research studies can be advantageous in the understanding of human risk factors and distinct mechanisms of pathogenesis that cannot be simulated in animal studies, due to the differing physiology (Felson et al., 2000, Legrand et al., 2017). Individuals with knee FCDs and uOA are valid human *in vivo* models for studying the link between joint loading and biology, since tissue damage in the joint is unicompartmental and focal in nature, thus a substantial mechanical perturbation, affecting one side of the joint is implicated. In this chapter, FCD and uOA subjects will be further assessed to investigate the relationship between indicators of knee loading and biomarkers of tissue turnover, biomechanical loading of bone and inflammation, to further progress our knowledge of this crucial link.

The most common type of knee OA is unicompartmental in nature, therefore alterations in frontal plane (medial-lateral) knee biomechanical parameters such as the knee adduction moment (KAM) are most frequently used to describe OA-related knee function in gait analysis studies (Andriacchi and Muendermann, 2006, Duffell et al., 2014). Strong correlations between frontal plane moments and knee OA disease severity (Astephen et al., 2008), progression (Foroughi et al., 2009), cartilage degeneration (Hunt et al., 2013) and inflammation (Pietrosimone et al., 2017) have previously been reported. Although conflicting evidence exists, numerous studies have demonstrated the high correlation between KAM waveforms and directly measured medial knee compartmental forces (Kutzner et al., 2010, Zhao et al., 2007) and medial force ratios (Kutzner et al., 2013) in instrumented knee studies, validating it as a crude surrogate measure of medial-to-lateral compartmental loading in gait studies.

In chapter 3, it was revealed that the KAM was a discriminatory biomechanical parameter of both medial and lateral FCD groups relative to controls, which appears to be predominantly resultant of altered dynamic knee varus or valgus angles, respectively. This implies that altered frontal plane loading may be a driving factor for the focal

compartmental damage observed in the FCD joint, which is consistent with OA studies that have demonstrated the association of frontal plane knee moments and static knee alignments with unicompartmental knee disease severity detected by MRI (Sharma et al., 1998, Andriacchi and Muendermann, 2006, Andriacchi and Favre, 2014). For this reason, frontal plane knee parameters including peak KAM values, KAM impulse (KAAI) and peak knee adduction angles (KAAs) were utilized as functional variables to explore the association between knee loading patterns and joint biology.

Multivariate analysis of biomarker variances in the previous chapter revealed subpopulations of FCD and uOA subjects reflective of high and low bone remodelling groups proposed to reflect high/low joint loading groups or possibly etiological phenotypes. This chapter aims to use multivariate analysis to consider functional and biological variables together, to further examine the influence of biomechanical parameters on intra- and inter-disease group variances. Furthermore, the association of OA-related symptoms (e.g. joint pain and stiffness) with disease severity and joint function has been controversial (Hurwitz et al., 2000, Dieppe and Lohmander, 2005), therefore the inclusion of clinical scores in the multivariate model allowed further understanding of potential biological and mechanical influencing factors.

Chapter Aim: To use interdisciplinary and statistical tools to explore bivariate and integrated relationships of biomechanical, biological and clinical characteristics of individuals with knee tibiofemoral FCDs and uOA.

> **Objective 1:** To examine the association of pathological knee function during walking with synovial fluid biomarker levels of mechanical bone signalling, bone turnover and inflammation.
>
> **Hypothesis 1:** *Frontal plane knee loading will influence biomarker concentrations reflecting bone remodelling, mechanically-driven bone signalling and inflammation*
>
> **Objective 2:** Use PCA combined with HCA to assess inter- and intra-group variances and identify FCD and uOA subject phenotypes based on similarities of biomechanical, biological and clinical characteristics
>
> **Hypothesis:** *Multivariate analysis will reveal inter- and intra-group variances reflecting differing disease states and phenotypes associated with sub-groups*

5.2 Methods

5.2.1 Subject selection

FCD subjects common to chapter 2 and 3, as well as uOA subjects from chapter 3 with linked biomechanics and biomarker data were selected for this chapter's analysis. All previous study criteria were applied.

5.2.2 Data collection

Clinical data

Clinical data was collected as previously described (section 2.3).

Gait analysis

3D motion analysis was captured for all subjects as previously described (section 2.4).

Sample collection and processing

Synovial fluid was collected as previously described (section 2.6.1).

5.2.3 Biomechanical variable generation

Knee adduction moment (KAMs) and angle (KAAs) waveforms were calculated from Visual 3D musculoskeletal models (section 2.4) for each subject and moments waveforms were normalised to %bodyweight*height. Next, parameterisation was used to break the waveform into relevant discrete representations of dynamic peak and cumulative frontal plane knee loading and dynamic knee alignment (Table 5.1). The following discrete parameters were used for this analysis:

Table 5.2-1 - Discrete biomechanical parameters utilised for regression and multivariate analysis.

Parameter	Abbreviation	Representation
Knee Adduction Angular (KAM) Impulse	KAAI	Cumulative (medial) knee load over stance-phase of gait
1st Peak Knee Adduction Moment	1st peak KAM	Peak (medial) knee load during weight acceptance
2nd Peak Knee Adduction Moment	2nd peak KAM	Peak (medial) knee load during push-off
Knee Adduction Angle during 1st Peak KAM	1st peak KAA	Knee (frontal) alignment angle during peak load (weight acceptance)
Knee Adduction Angle during 2nd Peak KAM	2nd peak KAA	Knee (frontal) alignment angle during peak load (push-off)

The following calculations were applied to dynamic waveforms using Visual 3D pipeline tools (C-motion, USA) to generate discrete parameters:

- KAAI – Positive integral (area under curve) of the KAM waveform
- 1st peak KAM – maximum KAM waveform value between 0-50% stance-phase
- 2nd peak KAM – maximum KAM waveform value between 50-100% stance-phase
- 1st peak KAA – knee angle during instance (frame) of 1st peak KAM
- 2nd peak KAA – knee angle during instance (frame) of 2nd peak KAM

Parameters were calculated for at least six waveforms for the affected limb per subject and then averaged to a single value per subject prior to use in the statistical analysis. Outliers defined as values above or below 2.5 standard deviations from the mean value were removed from the analysis.

5.2.4 Biomarker measurements

Absolute concentrations were calculated for synovial fluid biomarkers as previously described (section 2.6.3). A total of eleven biomarkers were used within this chapter analysis (Table 5.2-2) based on the availability of linked data. Biomarkers with ≥5 measurements matched with biomechanical parameter data were included in the analysis.

Table 5.2-2 - Synovial fluid biomarkers utilised for regression and multivariate analysis.

Biomarker	Abbreviation	Representation in the joint
C-terminal telopeptide for collagen type I	CTX-I	Bone resorption (osteoclastic) activity
Alkaline Phosphatase	ALP	Bone formation (osteoblastic) activity
Receptor activator of nuclear factor κ-B ligand	RANKL	Canonical osteoclast pathway activation
Osteoprotegerin	OPG	Canonical osteoclast pathway inhibitor
RANKL:OPG ratio	RANKL/OPG	Surrogate measure of net canonical osteoclast activation
Glutamate	-	Glutaminergic signalling agonist, Mechanical regulator of bone physiology, inflammatory regulator
Sclerostin	-	Wnt signalling inhibitor, Mechanical regulator of bone physiology
Tumor necrosis factor alpha	TNF-α	Acute phase pro-inflammatory cytokine
Interleukin-6	IL-6	Acute phase pro-inflammatory cytokine, osteoclast signalling
Interleukin-8	IL-8	Inflammatory chemokine (neutrophil chemotaxis)
Interleukin-10	IL-10	Anti-inflammatory cytokine, bone formation

Biomarker absolute concentrations calculated from absorbance values that situated outside of the recommended readable zone of the assay standard curve were excluded from the analysis, due to the unknown effect on the regression analysis coefficients.

5.2.5 Regression analysis (Objective 1)

Biomechanical parameters and biomarker data were tested for normal distribution using the Shapiro-Wilk test (IBM SPSS, USA) to satisfy the normality assumption of regression. Non-normal data were log-transformed (Log_{10}[biomarker]) to make highly skewed distributions less skewed. Next, there were two regression analyses carried out with separate cohort sets:

1. Medial knee FCD and uOA subjects (as medial compartment affected group)
2. Medial and lateral FCD subjects together, without uOA subjects

This was required since the KAM and KAA are surrogate measures of medial knee loading. Therefore, a positive influence of any joint loading parameter on biomarker levels would be represented by a positive linear correlation for medial knee disease subjects, whereas for lateral knee disease subjects an inverse linear correlation is expected. Therefore, to involve both medial and lateral FCD subjects in this analysis as a second cohort, quadratic regression analysis was applied. This is further explained in the examples below.

In the first analysis involving the medial-affected subjects, original or log-transformed biomarker variables were used as dependent variables in multiple linear regression models with biomechanical parameters as independent variables, whilst controlling for age and BMI. There was no requirement to adjust for sex, since the cohort was all male. The regression equation was:

$$y = A + Bx + Age + BMI$$

An example of an expected positive relationship of knee loading with biomarker levels is demonstrated below:

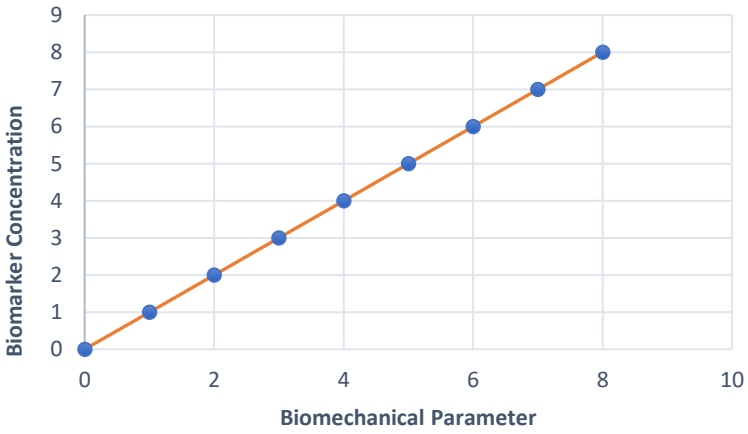

The second analysis involving all FCD-subjects only, original or log-transformed biomarker variances were used as dependent variables in a multiple quadratic regression with biomechanical parameters used as independent variables, whilst controlling for age and BMI. The regression equation was:

$$y = A + Bx + Cx^2 + Age + BMI$$

An example of an expected positive relationship of knee loading with biomarker concentration is represented below:

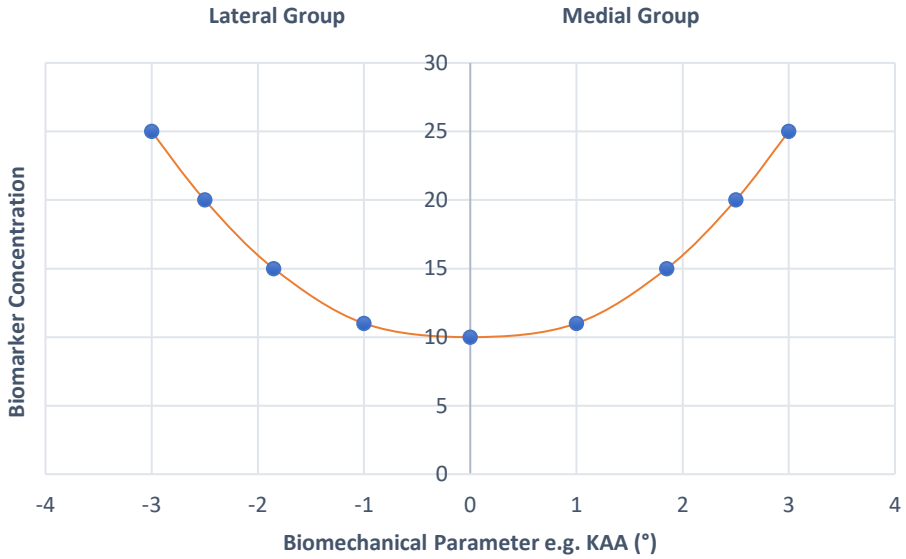

β-coefficients, R^2 values and *p* values adjusted for partial-correlations of age and BMI with biomarker levels were calculated for both linear and quadratic regression analyses (IBM SPSS, USA) and reported as individual tests. β-coefficients were also presented as a correlation heatmap to qualitatively assess relationships.

5.2.6 Principal component analysis (Objective 2)

Next, principal component analysis (PCA) was carried out to assess inter- and intra-group variances using linear combinations of biomechanical, biological and clinical (KOOS scores) variables of all subjects (section 2.7).

Since PCA interpretation relies on the positive correlations of variables to identify clustering of variables that were found to be similar across the observations, it was necessary to transform several parameters to allow simplicity of interpretation. The following transformations were applied to PCA input variables:

- All biomechanical variables presentative of joint loading or alignment were expressed as the number of standard deviations away from the control mean

values (extracted from chapter 2 results) for each variable. This made it so that higher positive values always correspond to increased medial (varus) or lateral (valgus) knee loading or angles relative to the control group.

- Clinical KOOS scores were expressed as (1-score value) for each variable to make it so that higher KOOS scores correspond to worsening clinical factors (i.e. with the new scores, if KOOS pain clustered with IL-6 then it would mean IL-6 was associated with pain).

Ultimately, both transformations together permit simpler interpretation, since clustering of any two variables in the PCA variable loadings plot would now be indicative of a positive relationship/similarity between those variables. Furthermore, matching observation (subject) clusters on the score plot with spatial distribution of variable loadings on the loadings plot will allow easy association of clusters with a set of relating variables.

Finally, hierarchical cluster analysis (HCA) was applied to the variable loadings plot using the Ward's method criterion to generate distinct variable clusters, which could be used to objectively describe relationships between groups of variables based on multivariate variances (SIMCA 14.1, Umetrics, Sweden). A cut-off was applied when under 5 clearly identifiable clusters were generated from all 18 variables as this was deemed a suitable summarization of variable clusters for interpretation.

5.3 Results

5.3.1 Cohort characteristics

Seven knee FCD subjects (all male; mean (SD) age = 42.7 (17.3) years, BMI = 28.5 (5.2) kg/m^2) and seven knee uOA subjects (all male; mean (SD) age = 50.3 (6.2) years, BMI = 28.7 (3.9) kg/m^2 with linked biomechanics and biomarker data were assessed in this chapter. There was no group difference in BMI, however there was a non-significant trend of increased age in the uOA group (Table 5.3-1). FCD subjects experienced on average higher levels of reported pain and reduced self-reported function of the affected knee, however this was not significant at the $p \leq 0.05$ level.

All FCD subjects had Outerbridge grade II tibiofemoral chondral lesions (3 medial, 4 lateral compartment) accompanied by meniscal tears/damage in the affected compartment, whereas no static knee malalignment was reported for any subject (Appendix A.1). One FCD subject (LP) had an ACL tear with a positive (+Glide) pivot shift. All uOA subjects had radiographic varus knee alignment (1.9° – 15.4°), ACL laxity (+Glide) and meniscal loss on the affected side. Two uOA subjects had mild OA (KL grade 2), three subjects had moderate OA (KL 3) and one subject had severe OA (KL 4).

From all involved subjects, only one subject (KM) from the FCD group reported using an analgesic (150mg Tramadol) approximately 1 hour prior to motion capture data collection, however no subjects reported analgesic use on the day of synovial fluid collection.

Table 5.3-1 - Group demographics and patient-reported clinical KOOS scores.

	Focal Cartilage Defect		Unilateral Osteoarthritis		
	Mean	±St Dev	Mean	±St Dev	Sig. *p* (2-tailed)
N	7		7		
Age (y)	42.7	±17.3	50.3	±6.2	.298
BMI (kg/m^2)	28.5	±5.2	28.7	±3.9	.930
Symptoms	70.1	±17.9	77.4	±17.0	.472
Pain	69.1	±21.6	83.3	±10.1	.168
Function	72.9	±23.4	89.4	±9.7	.137

5.3.2 Variable transformations

Shapiro-Wilk testing determined that IL-6, IL-8, OPG, RANK, RANKL/OPG and sclerostin were significantly not normally distributed ($p<0.05$). Following logarithmic transformation of skewed variables, IL-6, OPG and RANKL/OPG were no longer skewed. Normality of IL-8 and RANKL were substantially improved but not resolved. The skewness of both variables appears to be related to two outlying subjects of which the values remained included in the analysis due to the small sample size.

5.3.3 Influence of joint function on synovial fluid analyte levels in FCD and uOA subjects

Multiple linear regression models were firstly calculated to explore the effect of knee biomechanical function on synovial fluid biomarker levels in medial knee pathology (FCD and uOA) subjects, whilst controlling for age and BMI. Then, quadratic regression models next explored the effect of knee function on synovial fluid biomarkers in medial and lateral knee FCD subjects combined, whilst controlling for age and BMI. The results for these analyses are converged in the sections below:

5.3.3.1 Effect of knee loading on bone turnover

Across medial knee pathology subjects (Table 5.3-2), variances in OPG levels were significantly ($p\leq0.05$ to ≤0.01) predicted by all knee function parameters except for 2nd peak KAAs. However, when taking into account the minimal predictability of RANKL levels from loading parameters, the RANKL/OPG ratio was overall not influenced by knee function. The variance of CTX-I levels was significantly ($p\leq0.05$ to ≤0.01) predicted by 2nd peak KAMs and 1st and 2nd peak KAAs, however ALP was weakly inversely correlated, indicating a shift of bone remodelling towards decreased bone formation (i.e. increased net bone resorption) with increasing joint loads. In contrast, assessment of the FCD group alone (Table 5.3-5) revealed that increased varus/valgus 1st peak KAAs significantly ($p\leq0.05$) explained variance in ALP, whereas 2nd peak KAAs significantly ($p\leq0.05$) predicted CTX-I levels. A considerable association was also found for CTX-I and 1st peak KAAs, however this did not reach significance at the $p\leq0.05$ level. Together this is indicative of increased overall bone turnover in FCD subject's concomitant with the degree of dynamic knee malalignment.

		KAAI	*1st Peak KAM*	*2nd Peak KAM*	*1st peak KAA*	*2nd peak KAA*
RANKL †	β coefficient	0.055	0.159	0.339	0.142	0.285
	R^2	0.003	0.025	0.115	0.020	0.081
	p	.889	.682	.372	.716	.457
	N	9	9	9	9	9
OPG †	β coefficient	**0.833**	**0.747**	**0.642**	**0.773**	0.486
	R^2	**0.694**	**0.558**	**0.412**	**0.598**	0.236
	p	**.003**	**.013**	**.045**	**.009**	.154
	N	**10**	**10**	**10**	**10**	10
RANKL/OPG †	β coefficient	-0.256	-0.166	0.049	-0.189	0.048
	R^2	0.066	0.028	0.002	0.036	0.002
	p	.507	.67	.901	.626	.902
	N	9	9	9	9	9
CTX-I	β coefficient	0.377	0.396	**0.464**	**0.536**	**0.636**
	R^2	0.142	0.157	**0.215**	**0.287**	**0.404**
	p	.131	.118	**.035**	**.045**	**.002**
	N	8	8	**8**	**8**	**8**
ALP	β coefficient	-0.242	-0.2	-0.261	-0.15	-0.165
	R^2	0.059	0.040	0.068	0.023	0.027
	p	.725	.497	.366	.611	.585
	N	10	10	10	10	10

Table 5.3-2 - Multiple linear regression for the prediction of bone turnover biomarker variations from functional parameters. Standardised β coefficients, R^2 values and *p* values are representative of predicted variation following adjustment for age and BMI. † log-transformed variables. Bold face values represent significant adjusted coefficients at the $p \leq 0.05$ level (2-tailed).

5.3.3.2 Effect of knee loading on biomarkers of bone mechanical loading

Exploring the effect of knee function on mechanically-regulated bone markers unexpectedly found that regardless of controlling for demographics, neither biomarker was significantly associated to knee loading or angle parameters (Table 5.3-3). However, sclerostin variances were moderately (β = 0.4 – 0.49) predicted by 1st and 2nd peak KAAs, though this trend was not strongly reflected for loading parameters.

5.3.3.3 Effect of knee loading on inflammatory molecules

Across medial knee pathology subjects (Table 5.3-4), 2nd peak KAMs significantly ($p \leq 0.05$) explained TNF-α, IL-6 and IL-8 variances, whereas the KAAI significantly ($p \leq 0.05$ to ≤ 0.01) predicted IL-6 and IL-8. Furthermore, IL-6 levels were also significantly ($p \leq 0.05$) predicted by 1st peak KAAs. Considering non-significant relationships, there appeared to be an emerging pattern of a positive influence of knee loading on pro-inflammatory molecule levels with a contrasting negative effect on anti-inflammatory cytokine IL-10. Assessment of FCD subjects alone (Table 5.3-5) revealed a considerable moderate prediction of IL-6 levels by 1st peak varus or valgus angles, however this was also not significant at the $p \leq 0.05$ level.

		KAAI	*1st Peak KAM*	*2nd Peak KAM*	*1st peak KAA*	*2nd peak KAA*
Glutamate	β coefficient	-0.056	-0.128	-0.107	0.046	-0.006
	R^2	0.003	0.016	0.011	0.002	0.000
	p	.877	.725	.768	.899	.987
	N	10	10	10	10	10
Sclerostin	β coefficient	0.272	0.254	0.152	0.49	0.401
	R^2	0.074	0.065	0.023	0.240	0.161
	p	.447	.478	.675	.151	.251
	N	10	10	10	10	10

Table 5.3-3 - Multiple linear regression for the prediction of biomarkers of bone mechanical loading variations from functional parameters. Standardised β coefficients, R^2 values and *p* values are representative of predicted variation following adjustment for age and BMI. Bold face values represent significant adjusted coefficients at the $p \leq 0.05$ level (2-tailed).

		KAAI	*1st Peak KAM*	*2nd Peak KAM*	*1st peak KAA*	*2nd peak KAA*
TNF-α	β	0.536	0.37	**0.648**	0.158	0.296
	R^2	0.287	0.137	**0.420**	0.025	0.088
	p	.111	.293	**.043**	.662	.406
	N	10	10	**10**	10	10
IL-6 †	β	**0.848**	0.542	**0.732**	**0.698**	0.563
	R^2	**0.719**	0.294	**0.536**	**0.487**	0.317
	p	**.004**	.131	**.025**	**.037**	.115
	N	**9**	9	**9**	**9**	9
IL-8 †	β	**0.682**	0.509	**0.731**	0.587	0.467
	R^2	**0.465**	0.259	**0.534**	0.345	0.218
	p	**.03**	.133	**.016**	.074	.174
	N	**10**	10	**10**	10	10
IL-10	β	-0.465	-0.546	-0.442	-0.638	-0.577
	R^2	0.216	0.298	0.195	0.407	0.333
	p	.353	.262	.38	.173	.231
	N	6	6	6	6	6

Table 5.3-4 - Multiple linear regression for the prediction of inflammatory biomarker variations from functional parameters. Standardised β coefficients, R^2 values and *p* values are representative of predicted variation following adjustment for age and BMI. † log-transformed variables. Bold face values represent significant adjusted coefficients at the $p \leq 0.05$ level (2-tailed).

		1st Peak KAA	*2nd Peak KAA*
CTX-I	β coefficient	0.811	**0.854**
	R^2	0.658	**0.730**
	p	.116	**.049**
	N	7	**7**
ALP	β coefficient	**0.899**	
	R^2	**0.809**	
	p	**.036**	
	N	**7**	
IL-6 †	β coefficient	0.82	
	R^2	0.673	
	p	.107	
	N	7	
IL-8 †	β coefficient	0.661	
	R^2	0.437	
	p	.316	
	N	7	

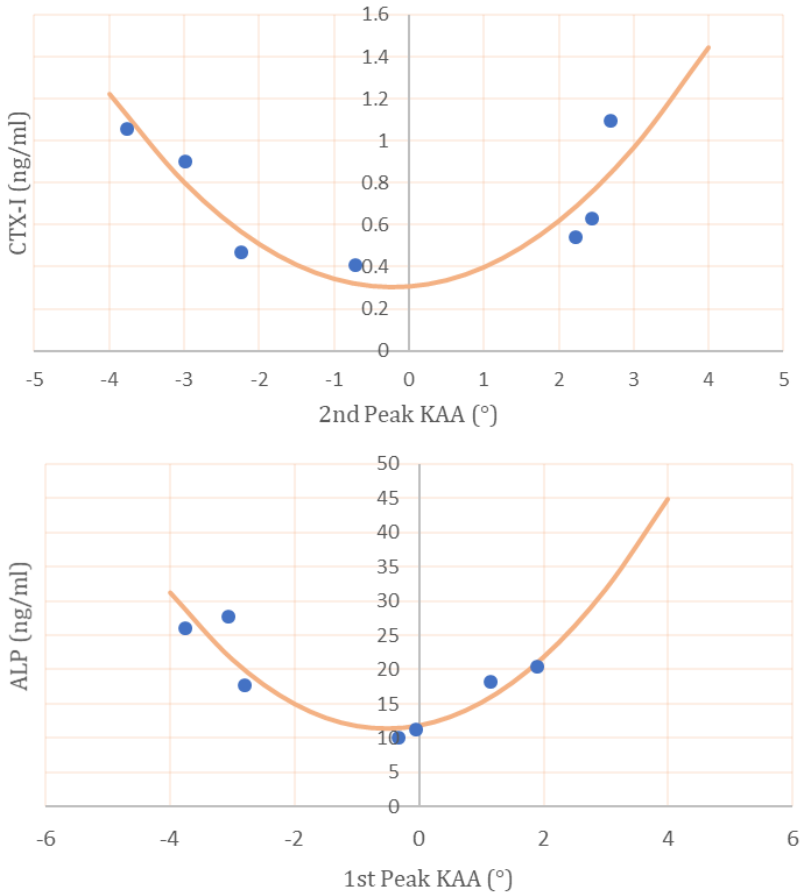

Table 5.3-5 & Figure 5.3-1 – Quadratic regression for the prediction of all biomarker variations from all functional parameters ($R^2 \geq 0.4$ only). (A) Regression model with original data points for prediction of CTX-I levels from 2nd peak KAAs ($p \leq 0.05$). (B) Regression model for prediction of ALP levels from 1st peak KAAs ($p \leq 0.05$). † log-transformed variables. Bold face values represent significant adjusted coefficients at $p \leq 0.05$.

5.3.4 Principal component analysis

Next, principal component analysis (PCA) was carried out to assess inter- and intra-group variances using linear combinations of biomechanical, biological and clinical variables (Figure 5.3-6; A & B). Two subjects (FCD subject JD and uOA subject 700) were excluded from PCA due to >50% missing data leading to substantial influences on the model. Two components were generated explaining 55.6% of the variance collectively (PC1; 33.3%, PC2; 22.3%). Visual analysis of the PCA score space revealed a clear separation of the groups based on PC 1 scores for all subjects except FCD subject LP and uOA subject 1271 who closely associated with the opposite respective group.

The most discriminating features of the uOA relative to FCD group (contribution score of >0.75) were increased cumulative (KAAI) and peak knee loading (1st and 2nd peak KAM), increased peak knee angles (1st and 2nd peak KAA), elevated pro-inflammatory activity (TNF-α, IL-6 and IL-8) and canonical bone resorption signalling (RANKL, RANKL/OPG), as well as decreased sclerostin. For biomechanical variables, the KAAI was most discriminatory of the uOA group from controls, whereas the 2nd peak KAM and 2nd peak KAAs were least discriminatory. For biomarkers, TNF-α closely followed by IL-6 were the most discriminatory variables, whereas CTX-I showed no discriminatory power.

HCA identified three primary clusters in the PCA variable loadings (Figure 5.3-6; C & D). Group 1 loaded negatively on PC1 and represented bone formation (ALP & IL-10) and mechanical loading (glutamate & sclerostin) biomarkers. Group 2 loaded positively on PC2 and represented KOOS pain, symptoms and function scores and OPG (CTX-I appears to be relatively independent). Finally, group 3 loaded positively on PC1 and included knee loading (KAAI, KAMp1 and KAMp2) and angle (KAAp1 and KAAp2) parameters, pro-inflammatory markers (IL-6, IL-8 and TNF-α) and bone resorption signalling markers (RANKL, RANKL/OPG).

The score space also identified outlying individuals (possible phenotypes) from each group (Figure 5.3-7). From the FCD group, subject LP was notably more closely clustered with the uOA group and presented increased cumulative and peak knee loading accompanied by increased pro-inflammatory activity (TNF-α), reduced bone formation (ALP) and possibly increased subchondral bone loading (reduced sclerostin) relative to the FCD group average. Whereas uOA intra-group variances revealed 3 possible subpopulations: (1) The largest cluster of three subjects who were featured at the PC origin and showed similar characteristics to the FCD group. (2) Subjects 505 and 16, who presented relatively high knee loading and varus alignment, increased pro-inflammatory

activity, high RANKL/OPG ratios, as well as reduced anti-inflammatory activity. (3) Subject 975, who presented relatively high cumulative knee loading, peak varus angles, lower glutamate levels, but most prominently worse reported clinical factors relative to average.

Figure 5.3-6 - Principle component analysis (PCA) of FCD and uOA biomechanical, biological and clinical features; PC1 - 33.3% variance explained; PC 2 - 22.3% variance explained. (A) Score space of FCD (green) and uOA (blue) subject PC scores. (B) Disease group discriminatory analysis. Coefficients represent variable differences from FCD to uOA group (i.e. variables of positive coefficients were relatively higher in uOA group). (C) Hierarchical cluster analysis of PCA variable loadings. (D) PCA variable loadings plot – spatial distribution of variables corresponds to the subject scores in the score space.

Figure 5.3-7 - Principle component analysis (PCA) of FCD and uOA biomechanical, biological and clinical features; PC1 - 33.3% variance explained; PC 2 - 22.3% variance explained. (A) Score space of FCD (green) and uOA (blue) subject PC scores. (B) PC 1+2 coefficients that represent the difference of subject LP relative to FCD group average (i.e. variables of positive coefficients were relatively higher in LP). (C) PC 1+2 coefficients that represent the difference of subjects 16 and 505 relative to group average. (D) PC 1+2 coefficients that represent the difference between subject 975 relative to group average. To note: Biomechanical variables are expressed as the number of standard deviations away from the control mean values (extracted from chapter 2 results) for each variable KOOS scores are expressed as 1-score (higher score = worsening clinical factors).

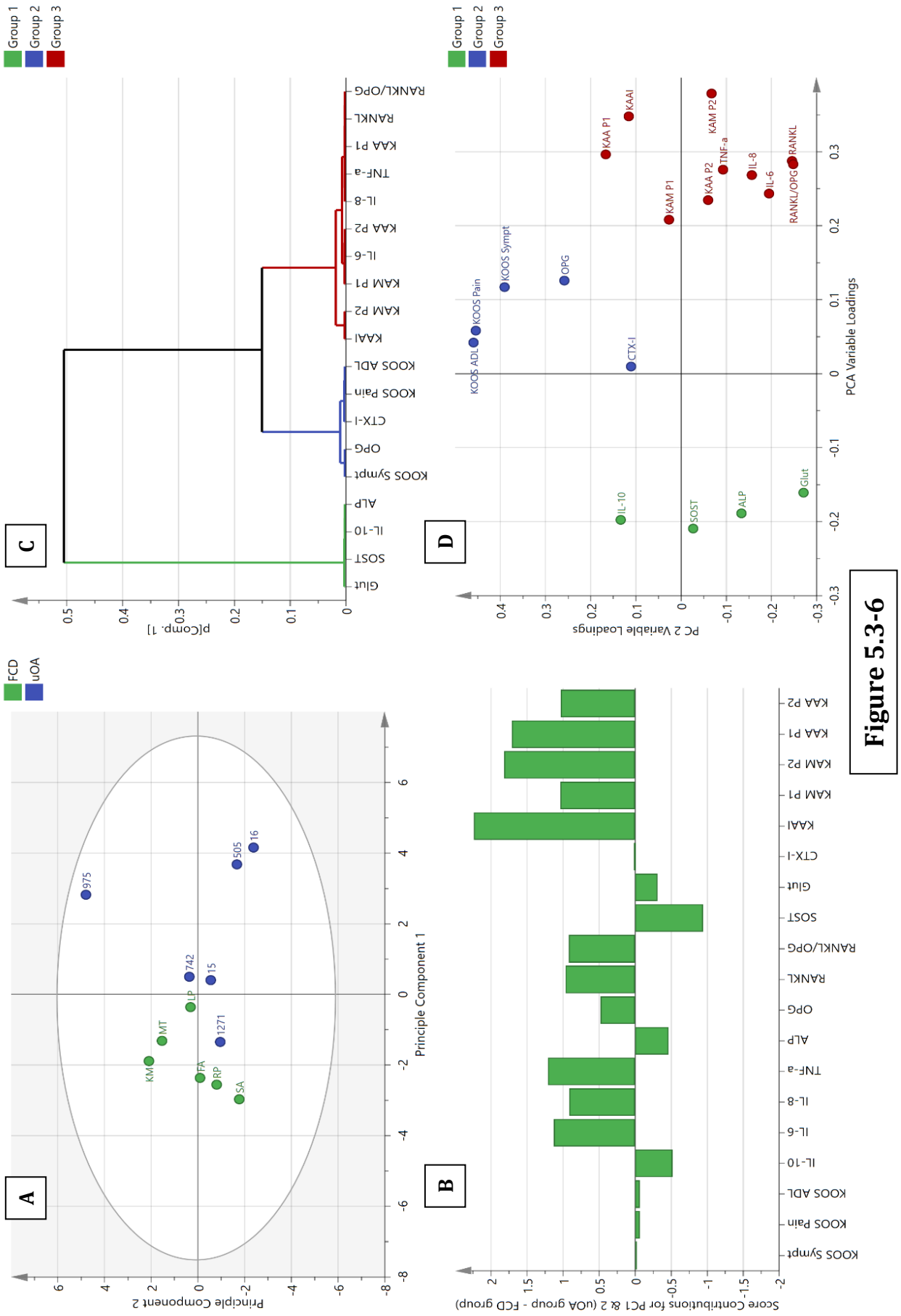
A
FCD
uOA
Principle Component 2
Principle Component 1
975
505
16
742
15
LP
MT
1271
KM
FA
RP
SA
B
Score Contributions for PC1 & 2 (uOA group - FCD group)
KOOS Sympt
KOOS Pain
KOOS ADL
IL-10
IL-6
IL-8
TNF-a
ALP
OPG
RANKL
RANKL/OPG
SOST
Glut
CTX-I
KAAI
KAM P1
KAM P2
KAA P1
KAA P2
C
Group 1
Group 2
Group 3
pl(Comp. 1)
Glut
SOST
IL-10
ALP
KOOS Sympt
OPG
CTX-I
KOOS Pain
KOOS ADL
KAAI
KAM P2
KAM P1
IL-6
KAA P2
IL-8
TNF-a
KAA P1
RANKL
RANKL/OPG
D
Group 1
Group 2
Group 3
PC 2 Variable Loadings
PCA Variable Loadings
KOOS ADL
KOOS Pain
KOOS Sympt
OPG
CTX-I
KAAI
KAA P1
KAM P1
KAM P2
KAA P2
TNF-a
IL-8
IL-6
RANKL/OPG
RANKL
IL-10
SOST
ALP
Glut

Figure 5.3-6

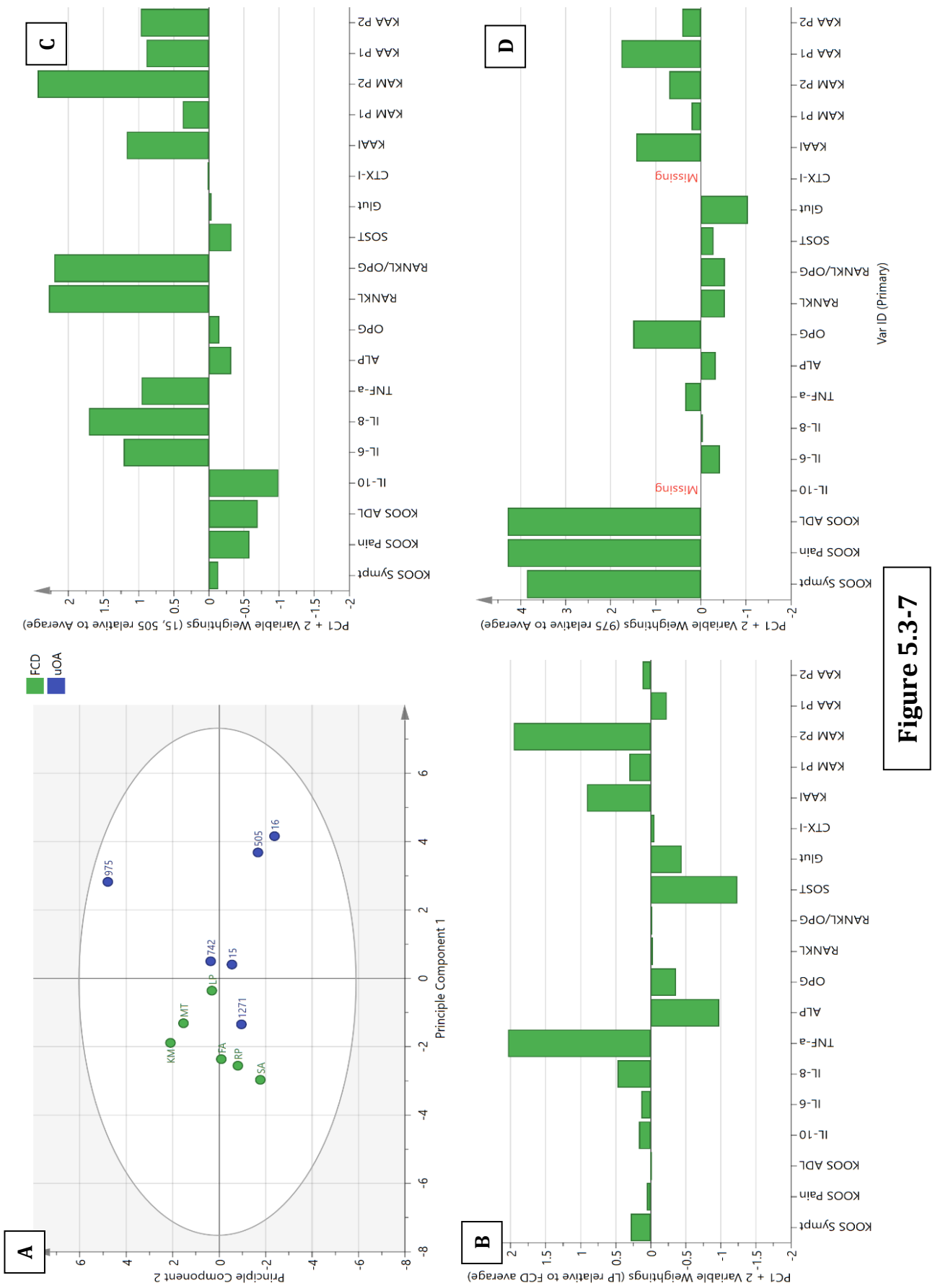
A
FCD
uOA
Principle Component 2
Principle Component 1
975
505
16
742
15
LP
MT
1271
KM
FA
RP
SA
B
PC1 + 2 Variable Weightings (LP relative to FCD average)
KOOS Sympt
KOOS Pain
KOOS ADL
IL-10
IL-6
IL-8
TNF-a
ALP
OPG
RANKL
RANKL/OPG
SOST
Glut
CTX-I
KAAI
KAM P1
KAM P2
KAA P1
KAA P2
C
PC1 + 2 Variable Weightings (15, 505 relative to Average)
D
PC1 + 2 Variable Weightings (975 relative to Average)
Missing
Var ID (Primary)

Figure 5.3-7

5.4 Discussion

5.4.1 Overview

Key findings from objective 1 and 2 of the analysis will firstly be discussed individually, followed by general discussion with association of the combined findings to current literature for each biomarker group (turnover, mechanical loading, inflammation).

5.4.2 Key findings for objective 1

The first objective of this chapter was to investigate the effect of knee biomechanical parameters of frontal plane knee loading and alignment angles during walking on synovial fluid biomarkers of bone turnover, mechanical loading of bone, and inflammation.

This present study provides new evidence detailing the relationship between levels of biomarkers in the joint and measures of dynamic knee loads relevant to FCD and OA pathogenesis. After log-transformations and controlling for age and BMI, a total of five examined biomarkers were significantly influenced by joint function, reflecting changes in bone remodelling, notably osteoclastogenic signalling and activity, as well as pro-inflammatory activity – all previously implicated in knee OA pathogenesis, but not shown to be significantly associated with function (Kraus et al., 2017, Chen et al., 2017, Legrand et al., 2017). By contrast, assessment of FCD subjects alone revealed a less prominent influence of joint loading on analyte patterns in this preliminary study, however early findings show an association between dynamic knee alignment and bone turnover (i.e. bone resorption and formation), as well as a considerable relation to pro-inflammatory IL-6 and IL-8 activity. This is suggestive that there may be an 'inflamed' phenotype associated with increased bone turnover and a catabolic joint that may do worse after microfracture surgery.

Utility of functional measures as predictors of tissue response

All functional loading parameters significantly explained variances of at least one biomarker, implying that the pathological tissue response may be sensitive to both cumulative and peak knee loading. However, the 2nd peak KAM appeared to be the best predictor, significantly explaining variances of all five mechano-sensitive molecules. Interestingly, this contrasted with the 1st peak KAM that only significantly predicted the variances of OPG. These findings are consistent with the most recent study to correlate

KAMs with direct knee forces measured using instrumented knee implants that showed the 2nd peak KAM better predicted actual peak medial knee forces relative to the 1st peak, though they were both significant predictors (Kutzner et al., 2013). The 2nd peak may therefore be a better predictor of tissue loading and furthermore, loading of the knee during the 2nd half of stance may be a more important functional deficiency in causing this consequential tissue response.

Peak moments are less sensitive measures at lower speeds, since this is an effective method of lowering peak joint loads and consequently pain (Simic et al., 2011), whereas the impulse is more sensitive to changes with varying gait speed since it reflects both the duration and degree of knee loading (Robbins and Maly, 2009, Landry et al., 2007). Therefore, it was unexpected that both types of dynamic loading measure demonstrated similar associations despite the high variance in gait speed in the combined cohort (range: 0.64 - 1.27 m/s, mean (SD): 1.1 (0.2) m/s). It is noteworthy though that the KAAI did not significantly predict TNF-α and CTX-I variations, suggesting peak joint loads ultimately have a stronger overall influence. This importantly indicates that there may be a benefit to slowing walking speed or altering gait patterns to reduce peak loads that appear to have a more potent influence on the catabolic response of joint tissues.

The disparity between the five significantly predicted variances by 2nd peak KAM and the single predicted variance by 2nd peak KAAs suggests peak moments are more sensitive than peak angles as representative measures of tissue loading. Interestingly, when assessing FCD subjects alone, dynamic knee alignment appears to be a better predictor of biomarker levels, since quadratic relationships similar to those of the linear regression (CTX-I and IL-6) were only found in relation to peak KAAs. Though, it is a possibility this is a limitation of the sample size of this study, since single outliers appeared to strongly influence coefficients of the quadratic regressions.

Altered knee loading promotes inflammatory dysregulation

This is the first study to demonstrate that the magnitude of knee compartmental peak load, cumulative load or degree of knee alignment over the human gait cycle are significantly associated with pro-inflammatory activity in unilateral knee pathology. The pattern of increased IL-6, IL-8 and TNF-α with a negative effect on IL-10 concomitant with increased loading is consistent with a catabolic environment (Kapoor et al., 2011). This is in keeping with findings of chapter 3 that revealed increased IL-6 and IL-8 levels coupled with decreased IL-10 and IL-13 as the largest discriminating features of the uOA group relative to the FCD group, which warrants further investigation into the individual contributions of pathological knee loading and disease severity/knee damage to

inflammatory dysregulation. Delineating the effect of biomechanical loading and severity can be complex, since factors such as joint space narrowing and cartilage loss which define joint severity also contribute to knee malalignment, and thus altered knee loading. The potential relationship of increased knee malalignment with IL-6 in FCD subjects alone is also an important finding, since it was not previously possible to confirm pro-inflammatory cytokine involvement in FCD relative to control serum, due to the poor inter-fluid correlations. These findings are consistent with the hypothesis that inflammation contributes to the experienced joint damage in knee OA as consequence of pathomechanics (Felson, 2013).

Subchondral bone loading promotes increased bone remodelling that shifts towards bone resorption with disease advancement

A distinctive feature of FCD group findings was the significant effect knee loading had on bone turnover, evidenced by the quadratic relationships to bone formation (ALP) and resorption (CTX-I) markers. The up-regulation of ALP reflects the adaptive anabolic response of bone to a mechanical stimulus (Burr and Gallant, 2012), however these results suggest a possible maladaptive response in regards to pathophysiological levels of loading, since ALP levels were up to 2.5 to 3-fold higher in those experiencing the highest degrees of malalignment. When involving uOA subjects however, the loading effect on bone resorption levels was consistent, but in contrast bone formation was no longer associated with higher levels of loading. Together, these findings suggest a mechanism by which the effect on bone remodelling shifts towards bone resorption at higher levels of knee loading and disease severity, a previously unreported feature of disease progression in humans which may be critical to the development of established OA.

Interestingly, the progressive feature of increased resorption activity concomitant with loading is not consistent with the loading effect on the canonical osteoclastogenesis pathway activation through the RANK/RANKL/OPG system, since the pathway inhibitor OPG appears to be significantly up-regulated with response to load. The OPG response to load is reflective of the mechano-regulatory processes that occur in adaptation mechanisms of bone, indicating a molecular switch towards bone formation by inhibition of osteoclast activation (Burr and Gallant, 2012). However, normal functioning of this response appears to be disrupted by the altered regulation of RANKL expression, since RANKL:OPG ratio values were not ultimately influenced by functional parameters. Considering the evident correlations of synovial fluid IL-6 and IL-8 with RANKL levels found in chapter 3, it is reasonable to suggest the effect joint loading has on pro-

inflammatory cytokine production may be indirectly counteracting the effect compensatory mechano-regulation of OPG levels has on canonical osteoclastogenesis pathway activation.

Mechanically-regulated bone markers may be dysregulated in disease states

Unexpectedly, there were no clear influences of peak or cumulative knee loads on sclerostin or glutamate levels in the joint, which is further evidence for the altered bone regulatory pathways in the pathological knee. Previous studies have identified the association of pro-inflammatory signalling on expression of sclerostin by osteocytes (Baek et al., 2014, Kim et al., 2017). Sclerostin expression and production is typically down-regulated by mechanical stimulus of osteocytes (Robling et al., 2008) yet pro-inflammatory signalling is positively influenced, thus these mechanisms would be opposing in the regulation of sclerostin levels in the joint - a paradoxical effect of increased loads. Since the modulation of sclerostin is a mechanism in which osteocytes co-ordinate local and regional osteogenesis, disruption of normal regulation may be a contributing factor for the shift towards bone resorption in enhanced loading conditions. As Chan et al. reported, sclerostin is also expressed by chondrocytes in focal regions of chondral damage (Chan et al., 2011). This is consistent with the significant inverse trend of serum sclerostin with COMP levels revealed in the previous chapter, since COMP is an indicator of cartilage structural degradation. Release of sclerostin could be involved in an autocrine or paracrine chondro-protective response to stress, since the Wnt signalling pathway stimulates production of catabolic enzymes in chondrocytes (Chan et al., 2011).

The incongruencies of glutamate with biomechanical parameters are inconsistent with previous findings that have demonstrated the expression of functional components of glutamate including receptor subunits (Szczesniak et al., 2005), transporters (Mason et al., 1997) and possibly release mechanisms (Mason, 2004) are mechanically-regulated, therefore it is likely other influencing regulators may be involved. Glutamate concentrations in the joint are altered by functional components of exocytotic (accumulated) release and transporters that remove it from the extracellular space found on the surface of most joint tissue cell types (Wen et al., 2015, Brakspear and Mason, 2012). The joint space may therefore be subjected to relatively rapid fluctuations in glutamate signalling windows in response to mechanical activity causing synovial fluid concentrations to be prone to incongruencies with mechanical loading measures. It is relevant to consider that subjects waited typically 2 hours with minimal activity prior to synovial fluid aspiration. Further investigation controlling for recent activity is required to clarify the potential involvement of glutamatergic signalling in the excessively loaded

joint, since glutamate was one of few molecules shown to be significantly elevated in FCD serum relative to controls in the previous chapter which is suggestive of its involvement.

5.4.3 Key findings for Objective 2

The second objective of this chapter was to use PCA to assess inter- and intra-group variances and identify patient subtypes based on similarities of clinical, biomechanical and biological characteristics

Combined functional and biomarker variances, but not clinical factors, discriminate disease group

The unsupervised separation of FCD and uOA subject scores in the PCA score space is contrasting to that of chapter 3, which suggests that biomechanical variables heavily influenced variances of the PCA model compared to biomarkers alone. On assessment of the variable loadings plot, it was evident that increased uOA subjects were more associated with a pattern of high knee loading and catabolic signalling, whereas FCD subjects with better knee function were associated with osteogenic activity and bone formation. These data are consistent with the understanding that uOA subjects are reported to have static joint varus malalignment, which is explanatory of the consequent higher dynamic knee loading and dynamic angles (Sharma et al., 2001). Moreover, many biomarker group differences can be explained when considering the effect increased joint loading has on biomarker variances as found in the regression analyses. Notably, the 1st peak KAM and 2nd peak KAA were less discriminatory of disease group, which suggests they may be less associated with knee malalignment. Interestingly, both variables also explained lower percentages of biomarker variances than their counterparts. Together it is reasonable to suggest 2nd peak KAM, 1st peak KAA and KAAI may be overall stronger predictors of the tissue response to joint loading.

HCA revealed that strikingly, patient-reported pain, symptoms and knee function scores were not discriminatory of disease groups, nor were they associated with functional and biological features as revealed by the HCA. When assessing PC 1 variances alone, it appears clinical KOOS scores (particularly symptoms) favours the uOA group, however variance introduced by PC 2 demonstrates the disassociation of clinical OA factors and physiological factors, which is supportive of the often reported weak correlation of OA severity with clinical scores (Dieppe and Lohmander, 2005).

Biomarkers of bone mechanical loading best describe FCD subjects in multivariate analysis

Bone mechanical loading markers, glutamate and sclerostin, were strongly representative of the FCD group in multivariate analysis, heavily negatively loading on PC1 in contrast to biomechanical variables. These findings with regards to sclerostin are expected, as sclerostin expression in bone is typically down-regulated in the osteocytic response to load (Robling et al., 2008), therefore subjects of higher subchondral bone loading would logically present decreased extracellular concentrations. However, the weak positive association of sclerostin with functional parameters may suggest other regulators are involved as previously suggested.

The association of glutamate with the FCD group when considering other variables is likely related its osteogenic influences, based on the correlation of synovial fluid glutamate with ALP levels found in the previous chapter. It has been suggested that glutamatergic signalling is involved in osteogenic pathway stimulation through the activation of ionotropic glutamate receptors on the surface of osteoblasts, which lead to the up-regulation of Runx2/cbfa1 activity and expression of osteogenic genes including that of ALP (Ho et al., 2005, Wen et al., 2015). The stronger relationship of glutamate to ALP relative to CTX-I levels in synovial fluid of the FCD joint suggests glutamate regulation and signalling is more evident in the anabolic response to load rather than resorption activity, however this requires further clarification possibly using co-culture studies involving multiple bone cell types (Vazquez 2014).

Identifying FCD and OA phenotypes

PCA identified intra-group outliers, namely FCD subject LP and uOA subjects 16 and 505 of a higher peak knee loading (2nd peak KAM) and pro-inflammatory type relative to their respective groups. These features could represent a type that might be at higher risk of disease progression due to the increased catabolic environment evidenced by biomarker patterns in response to load. Further investigation of clinical factors for LP relative to the FCD group revealed that this subject uniquely suffered from ACL injury, which is supportive of the hypothesis that ACL-damage as a co-morbidity may be a larger influence on FCD progression than the presence of isolated FCDs or FCDs with meniscal loss alone, which has been suggested by others (Tandogan et al., 2004).

Further exploration of the variable features of uOA subjects 16 and 505 highlighted that the 2nd peak of the KAM distinguished them from the group far more than other biomechanical factors. This could suggest that the catabolic response is a result of high

peak contact stresses on the joint surface rather than cumulative medial loading. The reduced pain and symptoms reported in these subjects relative to average may be partially explanatory of this finding, since subjects with joint pain tend to adopt adaptive gait strategies such as reducing gait speed to lower peak contact forces (Boyer et al., 2012). Indeed, assessment of gait speeds indicated that both subjects walked faster (~1.2m/s) compared to the group average (1.05m/s). Moreover, there were no other clinical or demographic distinctive factors that could distinguish both subjects from the group (Appendix A.1). Together, these findings suggest higher walking speeds as a consequence of reduced pain may be an important risk factor for uOA subjects, since it appears to induce higher pro-inflammatory activity coupled with osteoclastogenesis signalling.

uOA subject 975 who presented worsening clinical factors relative to average was surprisingly of the lowest disease severity grade from the uOA group (KL 2) and presented reduced pro-inflammatory activity and canonical osteoclastogenic signalling relative to the uOA group. The biomechanical characteristics of this subject of low peak loads but higher cumulative loading may be indicatory of compensatory gait mechanisms to reduce pain induced by high joint loads, in contrast to subjects 16 and 505. Indeed, this is further substantiated by the lower walking speed (0.86 m/s) of this subject relative to the group average (1.05m/s). This gait strategy is likely a consequence of the increased joint pain exhibited by this subject during gait.

5.4.4 General discussion

The aetiology of OA is a complex and multiscale problem, involving mechanical, biological and structural pathways. Despite important advances in understanding functional and biological characteristics of the OA process individually, there currently lacks an integrated view of the disease in humans (Cattano et al., 2017). Further elucidating these mechanisms by establishing links between indicators of knee function and biology in humans is critical for developing effective treatment strategies, since the population of OA patients is heterogeneous and treatments may be more effective if they could be individually tailored to the patient (Driban et al., 2010). Individuals with FCDs and uOA are useful disease models for understanding the involvement of aberrant joint loading in knee pathology, since their pathology is unicompartmental in nature, meaning that an underlying mechanical component is involved in disease progression. With the understanding that FCD and uOA subjects overload their knees, the hypothesis of this chapter was that biomarkers representative of tissue turnover, degradation,

inflammation and the mechanical response of bone measured in the affected joint fluids would correlate with biomechanical indicators of pathological joint loading. To date, this is one of few studies to combine interdisciplinary tools to explore and evidence this link.

The earliest reported study, far ahead of its time, aimed to relate indicators of knee loading with disease severity and cartilage degradation in 23 severe OA subjects, by correlating peak knee adduction moments with KL grades, joint space width values and the release of HA, a component of cartilage matrix, into serum (Sharma et al., 1998). Although they found promising relationships of joint loading with OA severity and joint space narrowing (JSN), there were no clear links to HA levels, despite controlling for age and sex. However, they concluded the possibility that the magnitude of the adduction moment influences structural changes in cartilage, and that matrix breakdown is undoubtedly related (Sharma et al., 2001).

In more recent years, the link between knee pathomechanics and biology has been somewhat invigorated. One study examining the relationship between KAAIs and peak KAMs with markers of cartilage matrix degeneration, including serum COMP, serum HA, urinary CTX-II and type II collagen cleavage neoepitope (uC2C) in 17 medial tibiofemoral OA subjects found that cumulative knee loading represented by the KAAI significantly predicted variation in urinary CTX-II levels, though adjusting for disease severity and walking speed eliminated these relationships (Hunt et al., 2013). It could be argued however that disease severity in medial OA is at least in part contributing to the fundamental finding, since it has been established in larger studies such as the Multicentre Osteoarthritis Study and the Osteoarthritis Initiative that architectural tissue changes that accompany disease severity influence knee malalignment and ultimately knee loading (Felson et al., 2013). Interestingly, data from the CHECK cohort of 1002 subjects found that unlike other cartilage markers examined, urinary CTX-II closely associated with serum and urinary biomarkers of bone turnover (CTX-I, sPINP, uNTX-I and osteocalcin), raising questions of its origin (van Spil et al., 2013). If indeed CTX-II is more representative of changes in bone, the findings from Hunt and colleagues would be consistent with those found within this study of higher CTX-I levels in association with increased knee loads.

Another smaller study by Pietrosimone et al. (2017) investigated the influence of KAM and ground reaction force (GRF) parameters on serum CTX-II, serum matrix metalloproteinase-3 (MMP-3) and serum IL-6 in ACL transection patients at baseline and 6 months following ACL reconstruction in 18 ACL-tear subjects. Unexpectedly, they found that 6-months following surgery, subjects with lesser biomechanical loading of the

affected limb at the 6-month follow-up exhibited increased plasma MMP-3 and IL-6, as well as elevated serum CTX-II. They hypothesised that this was owed to biological changes reflecting consistent offloading of the joint over the 6-months, evidenced by the decreased KAM and GRFs of the affected limb relative to the contralateral limb, since it is well established that catabolic cartilage and bone changes by stimulated by both underloading and overloading (Pietrosimone et al., 2017, Heijink et al., 2012).

Although these recent studies found some interesting potential relationships between pathological gait mechanics and the tissue response to joint load, there are some limitations of this work. Notably, only urinary or serum biomarkers have been explored which do not accurately reflect the activities of the affected joint for some molecules, as demonstrated in the previous chapter whereby several molecules, notably pro-inflammatory molecules and others poorly correlated across fluid types. Also, mostly only cartilage structural degradation markers have been investigated, which are strongly influenced by recent activity levels and exercise (Kraus et al., 2017, Lotz et al., 2013). Furthermore, cartilage structural markers are only partially representative of the true nature of OA as a whole joint disease (Findlay and Kuliwaba, 2016). In particular, there is a deficit of research exploring the biological response of subchondral bone to *in vivo* loads of the human knee, which has been consistently encouraged by previous authors due to the evident early molecular and structural changes which may precede changes in cartilage (Day et al., 2004, Burr, 2004, Chen et al., 2017).

This study has provided preliminary evidence that in the tibiofemoral FCD joint, increased dynamic loading of the affected compartment in the knee stimulates bone turnover activity and possibly increased pro-inflammatory cytokine production. However, when accounting for established knee OA joints it is evident that higher compartmental loads elicit a pro-inflammatory cytokine response and shift of the bone remodelling balance towards increased resorption activity, as well as a possible disruption of homeostatic osteoclastogenic pathway inhibition mechanisms and down-regulation of osteogenic bone formation. Moreover, investigation of individual variances using multivariate modelling identified an individual FCD subject who presented increased joint loads and stronger catabolic biomarker patterns relative to the rest of the group that may be attributed to their ACL tear. Assessment of variances in the OA group identified that levels of joint pain may influence self-perceived function, causing those of lower pain to walk faster, consequently increase peak knee loads and ultimately stimulate the shift towards pro-inflammatory and catabolic signalling in the joint.

5.4.5 Mechanical loading and inflammation in pathology

As Felson noted, the question with regards to inflammation and OA is not whether it is present, but rather whether inflammation contributes to the experienced joint damage as consequence of pathomechanics (Felson, 2013). Considerable evidence has been shown by several clinical studies of the secondary inflammatory response to injury of the knee joint, though the delineation of biomechanical influences from the tissue response to damage in human studies has not been possible. The current findings are clearly supportive of the mechano-sensitivity of pro-inflammatory signalling in the pathological joint. However, this study is not conclusive evidence that loading is directly responsible for the pro-inflammatory response, since it was not possible to correct for factors such as degree of tissue damage or disease severity due to the lack of MRI data or reported clinical severity scores common to both FCD and uOA subjects. Is it considerable that larger clinical studies describing the joint response to injury discussed in the previous chapter, including that of the KICK cohort (Watt et al., 2016) and KANON (Struglics et al., 2015) report an initial peak, followed by down-regulation and continued lower level involvement of pro-inflammatory cytokines such as IL-6 and TNF-α at 6 months to 5 years following initial joint injury. Another clinical study has shown using MRI in the examination of 1368 knees that the co-occurrence of synovitis with isolated meniscal tears in individuals of non-radiographic OA is very common (Roemer et al., 2009). It is likely that the change in knee biomechanics and altered surface stress patterns that accompanies structural tissue damage and loss of ACL and meniscal function following injury may therefore be responsible for altered pro-inflammatory cytokine release (Andriacchi and Favre, 2014).

In vitro studies have generated supportive evidence of the cellular and tissue inflammatory response to load through investigation of mechanotransduction pathways. A study by Koyama et al. demonstrated that compression of alveolar bone osteoblasts cultures revealed a force- (0.5-3.0g/cm^2) and time- (1-24h) dependent upregulation of mRNA and cytokine expression of IL-1β, IL-6 and TNF-α, which continued to increase for up to 24 hours post-loading (Koyama et al., 2008). In another study 3D matrix-embedded primary murine calvaria osteoblasts subjected to 1.7MPa compression at 1Hz upregulated IL-6 mRNA expression after just 1 hour of loading, followed by up to a 32-fold increase on IL-6 protein levels (Sanchez et al., 2009). Furthermore, specific inhibitors revealed that α-5-β1 integrin, NF-κB, ERK 1/2 as well as intracellular Ca^{2+} are involved in this mechanotransduction pathway. It has been well established that integrins and stretch-activated Ca^{2+} channels have a role to play in force transduction

from the ECM into the nucleus (Liedert et al., 2006), as is the involvement of NF-κB in pro-inflammatory signalling transduction and enhancement (Wojdasiewicz et al., 2014).

Chondrocytes in articular cartilage are also thought to play an important role in the inflammatory response to pathophysiological loads through aberrant stimulation of integrin mechanotransduction pathways (Bader et al., 2011). *In vitro* studies using 3D culture models have shown that activation of α5β1 integrins signalling by excessive compressive and shear stress disrupts the actin cytoskeletal network, conversely stimulating NF-κB components ERK1/2, JNK1/2 and p38α and in turn, catalysing a range of catabolic processes including the synthesis of pro-inflammatory cytokines (primarily IL-1β and TNF-α), proteolytic enzymes (MMPs) and ADAMTSs (Stanton et al., 2002, Guo et al., 2009, Honda et al., 2000). Additionally, cartilage matrix components including fibronectin fragments (FN-f), C-/N-terminal collagen peptides (such as CTX-II), fibromodulin, decorin and COMP, which occur in excess in the presence of cleavage enzymes further pathologically activate integrins leading to a catabolic feedback loop through aberrant NF-κB pathway activation (Chowdhury et al., 2010, Bader et al., 2011). This ultimately implies that once an excessive mechanical stimulus activates chondrocytes to breakdown the surrounding matrix, the pro-inflammatory response will be self-perpetuating, a possible mechanism for cartilage fibrillation and degradation in FCD pathogenesis.

Together, previous and current understandings implicate increased joint loading in pro-inflammatory-driven tissue deterioration during the course of OA pathogenesis. Further understanding of these links is critical for identifying individuals at higher risk of progressive tibiofemoral defects that may go on to develop OA. However, continued study with larger sample sizes controlling for disease severity are critical to further substantiate this link.

5.4.6 Mechanical loading and bone remodelling in pathology

As previously detailed, past studies have identified promising associations between indicators of altered joint loading patterns and cartilage degradation (Andriacchi and Favre, 2014). However, the *in vivo* response of bone to loading of the human joint remains unexplored. This is surprising considering in recent years, molecular and compositional changes in subchondral bone have emerged as being of the earliest indicators of OA onset, and though to largely contribute to cartilage degeneration through modifying its viscoelastic properties (Burr, 2004, Burr and Gallant, 2012).

Remodelling of subchondral bone is dependent on the mechanical nature of its environment (Burr and Gallant, 2012). In the OA knee, pathophysiological signals result in structural abnormalities that hypothesised to contribute to disease (Favero et al., 2015). Alterations in subchondral bone includes overgrowth and thickening, bone marrow lesions and attrition, most frequently occurring in the overloaded knee compartment (Neogi, 2012). These features are clearly suggestive of a link between aberrant joint loading and dysregulated bone remodelling, though the primary pathways responsible have to date not been elucidated.

The association of elevated bone turnover with dynamic knee malalignment in medial and lateral FCD subjects is consistent with the hypothesis that high focal knee loads may be responsible for the presence of BMLs, since MRI studies show BMLs are very prevalent with tibiofemoral FCDs and composed of focal areas of bone attrition and sclerosis underlying the defect (Xu et al., 2012). Since BMLs detected and scored by MRI methods have proven to be strong predictors of defect progression, defined by worsening of chondral lesion MRI scores, they may play an important role in FCD pathogenesis (Dore et al., 2010). In a recent study, Zhu and colleagues exploring longitudinal relationships between BMLs and inflammation in 192 OA patients found a significant association of serum IL-6 levels with BML MRI scores both at baseline and at the 12-month follow up assessment (Zhu et al., 2017). The moderate quadratic relationship between peak KAAs and synovial fluid IL-6 levels found within this study is supportive of this hypothesis, and may explain the increased CTX-I in response to altered joint loads concomitant with malalignment in the FCD joint (Felson et al., 2013). The increased presence of ALP however was expected as the activity of transcription factor Runx2 which orchestrates ALP gene expression (and other osteogenic genes) is positively mechanically-regulated through several pathways, including the Wnt/β-catenin (Robling et al., 2008) pathway, ERK/MAPK-dependent phosphorylation (Li et al., 2012), as well as the recruitment of SMAD proteins to transcriptionally or directly activate Runx2 through synergistic interactions with BMP-2 signalling (Kopf et al., 2012). The activation of these pathways is typically involved in the anabolic repair process, however combined stimulation of catabolic pathways in response to pathophysiological loads are likely resulting in the highly disorganised tissue found in the composition of lesion-affected bone.

Strikingly, when involving uOA subjects experiencing higher joint loads, the relationship of pathophysiological loading to ALP is abolished. Previous *in vitro* work suggests this dysregulation may be related to the influence of inflammatory signalling pathways.

Firstly, it has been found that osteoblastic IL-6 signalling inhibits the MAPK pathways by activated signal transducers and activators of transcription (STAT) (Osta et al., 2014). Whereas TNF-α activates SMAD ubiquitination regulatory factor-1 (SMURF1) and SMURF2 leading to dysregulated SMAD protein function which ultimately represses BMP signalling, also an important regulator of Runx2 activity (Yamazaki et al., 2009). Furthermore, IL-10 stimulates Runx2 activity through the activation of STAT-3 and the Smad1/5/8 and ERK-1/2 MAP kinase pathways, as well as through upregulation of BMP expression, thus reduced IL-10 activity will ultimately repress ALP synthesis (Jung et al., 2013). The consequence of increased pro-inflammatory cytokine production in the overloaded joint may therefore be explanatory of these findings.

Whilst bone formation appears to be repressed by pathophysiological joint loading, bone resorption is enhanced, evident by the significant association of CTX-I levels with indicators of both cumulative and peak joint loading even with controlling for age and BMI. However, the canonical osteoclast activation pathway does not seem to be involved in this trend, since RANKL/OPG values are dissociated from indicators of loading and did not correlate with CTX-I levels in the previous chapter either. It is possible that the bone resorption imbalance is more-so related to the increasing inflammatory dysregulation associated with loads, since IL-6, TNF-α and IL-10 are potent regulators of bone remodelling through independent non-canonical pathways (Osta et al., 2014, Yamazaki et al., 2009). Furthermore, the lack of association of glutamate and sclerostin levels with increasing joint loads is further evidence of the disruption of normal bone remodelling processes that occurs in pathophysiological states. These findings suggest further investigation of the involvement of non-canonical pathways involved in subchondral bone remodelling during the course of OA are critical to developing effective molecular targets to reverse bone abnormalities that may contribute to lesion and OA progression.

Interestingly, the conflicting RANKL/OPG association with mechanical load is reflected in previous literature, which is recognised by authors in the field (Robling and Turner, 2009). A study using oscillatory fluid flow-induced shear stress on a co-culture of murine bone marrow stromal (osteoblast-like) cells and RAW 265.7 (osteoclast progenitor) monocytes showed that peak shear stresses of 1Pa induced a significant increase in OPG and decrease in RANKL gene expression over 2 hours, with a lower number of mature osteoclasts quantified at the end of the experiment in contrast to unloaded controls (Kim et al., 2006a). This experiment was also replicated by independent authors using just MC3T3-E1 pre-osteoblastic cells, who also found a significant decrease in the RANKL/OPG ratio expression (Yoo et al., 2014). In contrast, a study investigating

compression of murine primary calvaria osteoblasts in a 3D membrane culture at 1.7MPa found a decreasing trend of OPG mRNA expression after 4 hours of loading, with no change in in RANKL expression (Sanchez et al., 2009). Similarly, it was shown that mesenchymal stem cells (MSCs) exposed to varying (10-36 kPa) pressure at 0.25Hz frequency during osteodifferentiation promoted osteoclastogenic signalling (increased RANKL/OPG mRNA) at all pressures tested relative to controls over 8 hours (Liu et al., 2009). It is possible that the contrasting results depend on experimental factors such as cell line, mechanical stress induction (e.g. shear vs compression) and physio-/pathophysiological ranges of stress, therefore in vivo models may be more reliable for understanding these pathways.

The findings from this study suggest that OPG may be more heavily involved in the response to mechanical load given its strong correlation to loading parameters, whereas RANKL expression may be more sensitive to the balance of local pro-inflammatory signalling. Indeed, it has been established that under inflammatory conditions, IL-6 reception via IL-6R activates JAK/STAT-dependent upregulation of RANKL expression in osteoblasts, whereas TNF-α inhibits SMAD-dependent downregulation of RANKL expression (Osta et al., 2014). On the other hand, Runx-2-dependent OPG expression in osteoblasts is upregulated by the p38 mitogen-activated protein kinase (MAPK) pathway, SMAD proteins, as well as the canonical Wnt (β-catenin) pathway, all of which are perpetually inhibited by sclerostin during the resting state (Galea et al., 2017, Kusumi et al., 2005). However, mechanical stimulation of osteocytes downregulates sclerostin expression and inhibits its release, therefore increasing mechanical loading of bone will ultimately enhance OPG expression and synthesis. In the case of subjects 16 and 505 in the multivariate analysis of this study, the excessive joint loads are likely both stimulating OPG expression in osteoblasts, as well as the production of pro-inflammatory cytokines that influence RANKL expression, however due to their relatively high RANKL/OPG levels it is clear that inflammatory signalling is the more potent influencing factor.

Since the compensatory osteoblastic response to increased bone loading represented by OPG appears to be maintained even at pathophysiological levels of loading in the FCD and uOA knee, pro-inflammatory pathway inhibitors may be useful in restoring normal regulation of bone resorption activity by the canonical signalling pathway. Interestingly, clinical studies investigating the use of TNF inhibitors in rheumatoid arthritis have reported anti-resorptive effects on bone, which supports a possible route for controlling early bone loss and BML pathogenesis in the OA process (Kawai et al., 2012).

5.4.7 Biomechanical bone markers

As described in the introductory chapter, bone depends on a physiological loading stimulus for adaptive remodelling in which sclerostin and glutamate are importantly involved, acting as mechano-tropic agents linking cell mechanotransduction pathways and bone cell maturity and activity (Galea et al., 2017, Brakspear and Mason, 2012, Mason et al., 1997, Robling et al., 2008). Within this cohort however, neither analyte demonstrated clear trends with indicators of biomechanical loading in either analysis, even when accounting for age and BMI. Interestingly, the multivariate analysis found that both molecules were strongly representative of members from the FCD cohort who experienced the lowest cumulative and peak loads relative to whole cohort and clustered with bone formation favouring markers ALP and IL-10 in the HCA. The multivariate analysis findings for sclerostin are in line with the established typical response to loading of subchondral bone, whereby the expression and release of sclerostin by mechanically stressed osteocytes in the joint is down-regulated, promoting osteogenic activity to repair stressed areas of bone (Galea et al., 2017, Robling et al., 2008). Sclerostin negatively weighted on the PC 1 hyperplane opposing weightings of the loading parameters, which is suggestive of its negative involvement. However, contradictory to this, the weak positive relationship found when predicting sclerostin variances from loading parameters was unexpected and implies that other regulators may be involved.

Pro-inflammatory activity has recently been suggested to influence osteocytic expression of sclerostin (Baek et al., 2014, Kim et al., 2017). Baek and colleagues demonstrated that treatment of MLO-T4 osteocytes with TNF-α led to significantly increased sclerostin expression, and TNF-α-dependent sclerostin expression was inhibited by blocking of NF-κB activation with small interfering RNAs (Baek et al., 2014). Furthermore, they showed using chromatin immunoprecipitation and a luciferase reporter assay that NF-κB binds directly to binding elements on the murine *sost* promoter and consequently up-regulates expression of sclerostin. In a more recent study supportive of these findings, TNF-α inhibitor (infliximab) significantly reduced the number of sclerostin-positive osteocytes and *SOST* expression in alveolar osteoblasts from mice with periodontitis or type 1 diabetes (Kim et al., 2017). Furthermore, intravenous TNF-α antagonist administration increased mandible osteoid area, reversing the bone loss associated with periodontitis and diabetes. These findings importantly describe another mechanism in which the bone formation response is inhibited in the inflamed joint, by which TNF-α ultimately disrupts Wnt signalling in bone through the regulation of sclerostin. Besides TNF-α, IL-6 (Wang et al., 2003) and IL-1β

(Rigoglou and Papavassiliou, 2013) are also shown to stimulate the NF-κB pathway in osteocytes, implicating their involvement in this mechanism.

As mentioned in the previous chapter, it has been recognised that chondrocytes from sheep and mouse joint destabilization PTOA models showed enhanced expression of sclerostin in regions of focal cartilage damage, whilst reduced sclerostin expression was detected in regions of sclerotic subchondral bone (Chan et al., 2011, Lewiecki, 2014). This is consistent with the significant correlation of serum sclerostin with COMP levels found in the previous chapter, suggesting that the degree of cartilage degradation in the FCD joint may be associated with sclerostin expression by affected chondrocytes. Furthermore, sclerostin is biologically active in chondrocytes, inhibiting Wnt/β-catenin activation responsible for catabolic MMP and ADAMTS expression, but also decreasing expression of collagen type-II and aggrecan. Due to these contrasting effects which have been verified more recently (Chang et al., 2018), this response has sparked controversy over whether or not it is a chondro-protective mechanism. Extracellular release into the joint could be an auto- and paracrine response to the high mechanical stress and/or pro-inflammatory conditions to protect local regions of cartilage from excess degradation.

Considering aforementioned findings, synovial fluid sclerostin levels may increase in the inflamed bone and damaged cartilage in response to continued mechanical insult, thus obscuring the typical inverse relationship expected from bone signalling. Whilst heightened sclerostin in synovial fluid produced by cartilage may have a more targeted localised effect in the healthy joint, there is evidence to suggest that aberrant loading in the arthritic joint promotes cartilage and bone crosstalk, since structural damage causes microfractures in bone and cartilage that expose deeper layers of subchondral bone to articular activity (Findlay and Kuliwaba, 2016). If this is the case, increased sclerostin production by chondrocytes may have important consequences on bone remodelling in the FCD and OA joint. The enhanced disruption of Wnt-β-catenin signalling in osteoblasts would inhibit differentiation and osteogenic activity (Sebastian and Loots, 2017), whilst promoting bone resorption through activation of osteocytic-mediated RANKL-RANK activation of osteoclast progenitors (Wijenayaka et al., 2011). This mechanism could therefore be a major contributing factor to the formation of BMLs following injury which is commonly reported and a risk factor for FCD development (Muratovic et al., 2016).

The amount of glutamate available for release by osteoblasts may be also partially regulated by altered sclerostin activity as others have suggested (Cowan et al., 2012), since canonical Wnt pathway activation in osteoblasts has been shown to negatively regulate the conversion of intracellular stores of glutamate to glutamine by glutamine

synthase (GS)– thought to be a strategic mechanism to control osteogenic glutamate activity in bone (Olkku and Mahonen, 2008, Cowan et al., 2012). However, this theory is not fitting with the clustering of glutamate with sclerostin in the multivariate analysis, nor the moderate positive association of synovial fluid glutamate with sclerostin levels found in the previous chapter, in which the reasons are unclear and warrants further investigation.

Glutamate signalling mechanisms appear to be mechanically-regulated at multiple levels, since the expression of transporters (EAATs) that remove it from the extracellular space as well as receptor (iGluR) subunits are sensitive to loading of bone (Szczesniak et al., 2005, Ho et al., 2005, Mason et al., 1997). However, knee functional parameters poorly predicted glutamate variations, suggesting there are other influential regulators. It is considerable though that functional components including vesicular glutamate transporters (VGLUTs) necessary for Ca^{2+}-mediated exocytosis are thought to accumulate glutamate for release, and are expressed by rat primary osteoblasts (Hinoi et al., 2002) and osteoclasts (Morimoto et al., 2006). Furthermore, in cartilage, endogenous release of glutamate by chondrocytes and uptake appears to also be dependent on vesicle recycling activity, and uptake is enhanced by extracellular sodium and calcium in a dose-dependent manner, similar to that of bone cells, glial cells and neurons (Piepoli et al., 2009). The joint space is therefore potentially subjected to relatively rapid changes in glutamate signalling windows in response to mechanical activity patterns regulated by uptake and release mechanisms (Brakspear and Mason, 2012). Furthermore, glutamatergic transduction and cellular responses are regulated locally by transporter activity and ionotropic and metabotropic receptor abundance. It is considerable that activity levels were not controlled for within this study, however subjects typically had a two-hour period prior to surgery in which activity levels were minimal, that may have impacted congruencies between indicators of joint loading and glutamate signalling activity.

The clustering of glutamate with ALP in the multivariate analysis may be reflective of results from the previous chapter whereby they positively correlated in synovial fluid. The relationship of glutamate with ALP is consistent with the involvement of glutamatergic signalling in the regulation of osteoblastic differentiation and activity in bone (Wen et al., 2015). A number of studies have shown antagonising AMPA and NMDA osteoblast receptors leads to inhibition of Runx2/Cbfa-1 activity and consequently the expression of osteogenic genes including ALP, osteocalcin, osteopontin and collagen type I in cultured osteoblasts (Hinoi et al., 2003, Ho et al., 2005, Lin et al., 2008). Conversely,

activating them with agonists AMPA and NMDA in glutamate-free media leads to the upregulation of osteocalcin mRNA and matrix mineralisation (Lin et al., 2008). Thus, glutamate signalling plays a physiological role in mediating osteogenesis and bone formation. Within this study, ALP variances were significantly predicted by dynamic knee malalignment of the FCD joint suggesting a mechano-regulatory response, however sclerostin levels did not relate to ALP, therefore it is likely glutamate is at least partially mediating this osteoblastic response. Further investigation is required to validate these mechanisms in the human joint where controlling for activity levels is possible.

5.4.8 Phenotyping FCD and OA subjects

Identified phenotypes may represent different pathophysiologic etiologic subtypes of individuals with knee FCDs or OA and may be highly relevant to disease treatment (Driban et al., 2010, Kraus et al., 2017). Multiple approaches to phenotype identification have been advocated including those selective of drug target groups (Kraus et al., 2011), functional groups that could be targeted by physical therapy (Thoma et al., 2017) and clinical groups that could influence disease management strategies (Lotz et al., 2013, Hunt et al., 2013, Knoop et al., 2011). It was discussed in the previous chapter exploring biomarker variances that FCD and uOA subjects clustered based on relative synovial fluid levels of sclerostin, RANKL/OPG and anti-inflammatory signalling. Although these findings point out potential signalling subtypes, they may not be clinically meaningful alone. Since the subjects examined were clinically relevant groups with a clear functional component to their pathology, this chapter set out to combine functional, biological and clinical features that may identify variances with a more integrated view of the problem.

Dell'lsola et al. carried out a systematic review on 24 studies that aimed to identify distinct phenotypes of knee OA, and through qualitative synthesis of evidence from 79 reported phenotypes, proposed the existence of six dominant phenotypes: 1) chronic pain with prominent central sensitisation mechanisms active; 2) inflammatory, classified by elevated cytokine levels; 3) metabolic syndrome, classified by metabolic disturbances such as obesity and diabetes; 4) Bone and cartilage metabolism, classified by alterations in local turnover activities; 5) mechanical overload, classified by altered knee malalignment and unicompartmental disease; and finally 6) minimal joint disease, classified as minor clinical symptoms and low progression (Dell'Isola et al., 2016). This was a thorough review and surprisingly, a lack of studies featuring multiple variable types were present, as each was classified as either of a 'biomarker', 'imaging', 'genetic', 'functional' or 'epidemiological' type.

Preliminary evidence from this study suggests it is possible that there may be overlapping features which could not be identified without investigation of linked functional, biological, imaging and clinical data in a 'systems' approach. For example, it was evident from both regression and multivariate analysis that mechanical overload (unicompartmental disease) subtypes experience high levels of pro-inflammatory activity dependent on the level of loading, which could be a possible relationship of these apparent distinct phenotypes. Furthermore, introducing clinical features in the multivariate analysis revealed distinctive individual mechanisms. For example, uOA subjects 16 and 505 with increased clinical symptoms to the rest exhibited overloading of their knees which was associated with higher levels of inflammation and osteoclastogenic signalling coupled with lower bone synthesis. Whereas subject 975 exhibited improved clinical symptoms, lower peak knee loads by slowing their gait speed, associated with reduced inflammatory and osteoclastogenic signalling. These patterns are in line with gait analysis studies that show subjects experiencing acute knee pain develop adaptive gait strategies such as slowing gait speed to avoid pain by lowering peak loading of the affected compartment (Boyer et al., 2012). Interestingly, it has been shown that patients who successfully reduce medial loading parameters (including KAM and KAAI) using adaptive gait strategies to pain have a slower rate of knee OA disease progression (Felson et al., 2013, Sharma et al., 2001).

Other notable observations resulting from this analysis included FCD subject LP who may have experienced enhanced overloading and/or injury-induced inflammation, due to an ACL-comorbidity, which consequently led to a biomarker pattern of an increased inflammatory and catabolic state relative to the FCD group. This is consistent with the observation that FCD subjects with accompanying ACL-tears present faster progressing and more severe lesions than those with isolated damage (Davies-Tuck et al., 2008b, Tandogan et al., 2004). In contrast to progressive groups, PCA identified uOA subject 1271 who associated closely with the FCD group and demonstrated evidence of lower knee loading and inflammation relative to the uOA group. Peculiarly, this subject is in line for a relatively invasive surgery (HTO) to correct varus joint alignment, therefore these factors alone may suggest that decision-making based off static joint alignment measured by X-ray alone may not always be representative of dynamic knee loading. Furthermore, biological characteristics of this subject are representative of an earlier disease state, which implies they may not be susceptible to the same rate of progression.

These findings collectively demonstrate an integrated approach combining multiple variable types may reveal patients that suffer from distinct etiological mechanisms that

may respond differently to treatment (Driban et al., 2010). Although some interesting results were found here, larger-scale studies are required to gain full benefit from such analyses. This approach could further identify influences of other factors such as response to treatment, disease severity, use of pain medication and activity levels on OA disease mechanisms that affect the joint as a system, rather than individual factors. Furthermore, to aid exploratory analyses such as this, avenues for future research should focus on identifying the link between phenotypes of biomechanical, biological, structural and clinical similarities and hard clinical endpoints such as requirement for revision surgeries, or total knee replacement (Lotz et al., 2013). This would ultimately improve retrospective decision-making dependent on objective assessment to further optimise treatments.

5.4.9 Chapter limitations

5.4.9.1 No control group

Collection of biomechanical and serum biomarker data from control subjects occurred during various stages of the study and involved different subjects, leading to an unmatched biomechanics-biomarker dataset. Previous chapters have identified biomechanical and biomarker features that differ in FCD subjects from controls, which suggests there may be important functional and biological links to validate for the purpose of further elucidating mechanisms of FCD pathogenesis. It is noteworthy that many important analytes including pro-inflammatory cytokines, IL-10, RANKL, OPG and ALP were poorly reflected in serum likely due to their localised mechanisms of action, meaning that control groups reflecting serum biomarkers alone would not contribute to the interpretation of relationships between biological and biomechanical variables. Therefore, future studies should aim to involve controls with the inclusion of synovial fluid biomarker concentrations.

5.4.9.2 Covariates and confounding factors

Disease severity

An objective of this chapter was to determine discriminating patterns relating to disease state (i.e. FCD and uOA) defined by clinical status, however a common clinical score defining individual disease severity was not testable since FCD subjects are clinically scored based on the Outerbridge grading system during arthroscopy (Lasmar et al.,

2011), whereas uOA are radiographically graded based on the Kellgren-Lawrence system (Kellgren and Lawrence, 1957). Since radiographs were not taken for FCD subjects due it being an 'unnecessary' exposure to X-rays, it was not possible to assess joint space narrowing, presence of osteophytes or bone sclerosis, all crucial factors in KL grading definitions. Furthermore, the joint surfaces are not exposed during HTO surgery (for realigning the uOA joint) to allow for Outerbridge scoring. This affected the ability to control for- or investigate the effect of disease severity across the cohort. An assessible measure of disease severity is particularly relevant since the level of tissue damage is likely a confounding variable of the association of loading with biomarkers; loss of cartilage and meniscal tissue correlates with knee malalignment and tissue damage with common biomarkers of OA (Attur et al., 2013, Andriacchi and Favre, 2014). It is noteworthy that variations in KL grade correlate with CTX-II levels, but this was not found for CTX-I (Karsdal et al., 2010).

In the last decade, structural MRI scoring and modelling methods have emerged as a useful research tools for qualitatively or quantitatively assessing structure and biochemical composition of joint tissues to better characterise stages of early to late stage OA-related tissue changes (Favero et al., 2015, Frobell, 2011, Matzat et al., 2013, Theologis et al., 2012, Van Rossom et al., 2017). Incorporating such parameters into multivariate analyses such as this presented may be a better substitute for differing clinical stratification scoring systems based on narrow disease stage sensitivities (such as Outerbridge), to provide a more objective understanding of the link between functional and biological mechanisms and disease related tissue structural or compositional changes. This is already being investigated in some groups in more recent years in both animal models and humans (Gilbert et al., 2018, Van Rossom et al., 2017).

Diurnal variation

The daily variation of molecular concentrations in relevant biological fluids is becoming increasingly recognised in the search for valid diagnostic and prognostic OA biomarkers. Several studies have described significant daily variation in serum and synovial fluid levels of OA-related cartilage and bone activity and metabolism markers in knee OA patients (Kong et al., 2006). This can relate to the activity of clock proteins that regulate circadian processes (Akagi et al., 2017, Bjarnason et al., 2002), diet patterns (Bjarnason et al., 2002) and levels of activity (Andersson et al., 2006a, Cattano et al., 2017). Degradative components of bone (e.g. CTX-I) and cartilage (e.g. COMP) as well as the activity of matrix degrading enzymes (MMPs) have notably been shown to significantly vary (Cattano et al., 2017, Kong et al., 2006, Yang and Meng, 2016). It is noteworthy

however that diurnal synovial fluid levels have not been examined. Within this preliminary study it was not possible to control for these factors, particularly since synovial fluids were extracted at time of surgery that was allocated to a slot between 7am to 5pm. Particularly for the context of this chapter, activity levels were not controlled for which could have had an impact on congruencies between indicators of knee loading and mechanically-sensitive molecules such as glutamate and sclerostin, which introduced difficulty in delineating the effect of high mechanical loads from molecular elimination processes (such as the activity of glutamate transporters). In this study subjects typically fasted overnight before surgery and had a 2 hour wait prior to anaesthesia in which activity levels were minimal, which may have normalised some of these effects. However, since the clearance rate of molecules from the joint space vary substantially (Kong et al., 2006), further investigation is necessary to determine the effects of this.

5.5 Conclusions

This study is one of few attempting to bridge the gap between our understanding of biomechanical, biological and clinical characteristics of degenerative knee pathology in human subjects. Preliminary evidence has shown that the degree of joint mechanical overload is correlated to inflammatory molecules in the synovial fluid and changes in bone remodelling mechanisms. It is therefore critical to identify early pathology subjects in which can benefit from physical therapy methods such as gait retraining, or surgery aimed at correcting functional deficiencies of the knee such as meniscal replacements or high tibial osteotomy (HTO). These findings may, at least in part, be explanatory of the poor outcomes of cartilage repair methods (such as microfracture surgery) alone in some individuals with tibiofemoral FCDs that continue to abnormally load the joint following surgery and therefore drive catabolic processes (Layton et al., 2015).

The rheumatology field is becoming increasingly aware of OA heterogeneity, with amounting evidence of the need for personalised treatments for distinct phenotypic groups (Karsdal et al., 2014). Within this study, several potential intra-group FCD and uOA phenotypes were identified using multivariate tools. Identification of individuals at an early stage that can benefit from correction of lower limb mechanical function is critical to their long-term joint health. Conversely, patients with normal levels of joint function with chronic inflammation may benefit more from anti-inflammatory therapy, whilst others with enhanced bone turnover imbalance towards net loss may be more

appropriately treated with antiresorptive treatments. Clinical decision making aided by research tools such as that presented here will surely optimise treatment for efficacy and longevity that current practice is lacking.

Chapter 6
Conclusions and Future Work

6.1 Summary and recommendations for future work

The overarching aim of this thesis was to advance our understanding of the characteristic features and etiologic factors of progressive knee FCDs, as well as the shortfalls of current surgical practice, to aid clinical decision making in the choice of effective treatments. The chapters presented here set out to achieve four objectives to satisfy this aim. For this final chapter, the key findings for each thesis objective will be summarised with suggestions for future work.

Objective 1: *To identify biomechanical and neuromuscular pathways of tibiofemoral FCD pathogenesis in patients and assess longitudinal functional outcomes of microfracture surgery*

In chapter 3, it was hypothesised that individuals with tibiofemoral FCDs would experience altered lower limb biomechanical and neuromuscular function, since progressive damage in the FCD joint is focal and in weight-bearing regions of the knee. Furthermore, that monitoring longitudinal biomechanical and neuromuscular alterations could be useful in assessing the efficacy of microfracture surgery for restoring lower limb function.

It was found that both medial and lateral FCD subjects may be overloading the respective affected compartment of the knee, evident by the altered dynamic KAMs accompanied by knee malalignment. This is an important finding in relation to the pathogenesis and progression of tibiofemoral FCDs, since it is reasonable to suggest based on results from chapter 6 that overloading of the remaining damaged tissue in the joint will be contributing to catabolic signalling and consequently the progression of focal tissue damage. Although there was some evidence for improvement in lateral FCD subjects evident by trends towards faster walking speeds, more 'normal' KAM and KFM waveforms and improved hamstrings activation, it appears that microfracture surgery was generally ineffective at restoring biomechanical function to medial FCD subjects. An

important factor to consider here is that patient-reported outcomes (even for medial FCD subjects) were indicative of positive improvements, however, clearly neither FCD group showed changes in dynamic knee frontal plane alignment (KAAs), which were though to be causative of the increased compartmental loading (KAMs), consistent with others findings in OA subjects (Bennell et al., 2011, Felson et al., 2013). This suggests that microfracture surgery alone may not be adequate for eliminating the long-term risk of FCD progression. Furthermore, other conventional techniques such as ACI and MACI that have shown promising success over microfracture surgery may also have little overall effect on the knee alignment axis, which is influenced by a combination of factors including cartilage and meniscal tissue loss, alterations in bone structure, as well as ligament laxity that all introduce joint destabilization (Felson et al., 2000, Hunter et al., 2006). Knee malalignment has long been thought as a primary risk factor for OA pathogenesis, therefore identifying this in earlier stage could help preventative strategies.

Medial and lateral groups also showed distinct gait adaptations, reflective of the location of the lesion in relation to loading patterns in the joint during gait. Medial knee FCD subjects demonstrated prominent compensatory mechanisms during late-stance whereby they inadequately extended the knee, likely to reduce peak knee contact forces generated by the extension moment during push-off. This was accompanied by aberrant co-contraction of the quadriceps and hamstrings during stance, reflective of attempted protection of the knee from instability. Lateral FCD subjects on the other hand showed a delayed hamstrings contraction prior to heel-strike, possibly to reduce knee loading during weight-acceptance when increased lateral compartmental forces occur. Finally, a proportion of both medial and lateral FCD subjects may be shifting their centre of mass contralateral to the affected knee compartment to reduce compartmental forces. Together, these findings suggest pain caused by tibiofemoral FCDs may be influencing the loss of normal dynamic postural control, thought to attribute to abnormal muscle adaptations and weakness, another important risk factor for knee OA development (Takacs et al., 2013, Duffell et al., 2014). Furthermore, co-contraction of antagonistic muscles may be influencing further compression of the joint structures, further influencing pathobiological mechanisms as introduced in chapter 5 (Heiden et al., 2009). Future work should aim to identify the benefit of neuromuscular conditioning programs in the earlier stage of FCD development or following surgery, to ensure restoration of long-term healthy joint function and longevity of treatments.

Objective 2: *To identify biological pathways and biomarkers of tibiofemoral FCD pathogenesis by investigating molecules relating to tissue turnover, mechanobiology of bone and inflammation in synovial fluid and serum of tibiofemoral FCD subjects undergoing microfracture surgery*

The rationale behind chapter 4 was that biomarkers representing tissue turnover, biomechanical loading and inflammation that discriminated FCD fluid from controls and OA fluids would be useful in elucidating biological pathogenic pathways in the FCD-affected knee, as well as for generating biomarkers that could be used for the longitudinal assessment of microfracture surgery.

It was demonstrated that a pattern of increased dysregulation of inflammatory signalling was concomitant with increasing disease state (i.e. control > FCD > uOA), however this was only validated by consistent decreases of IL-10 levels, since pro-inflammatory cytokine activity in the joint was poorly represented in serum. Despite this, the consistent contrasting relationship between IL-10 and pro-inflammatory cytokines in all aspects of this thesis implies this molecule may be a valid representative biomarker of this critical dysregulation in serum. The implications of dysregulated inflammatory signalling in the joint is relevant to disease progression. Pro-inflammatory cytokines IL-6 and IL-8 were shown to be strongly associated with osteoblastic RANKL signalling, a potent activator of osteoclastogenesis that will ultimately stimulate bone resorption (Boyce et al., 2015, Kim et al., 2017), whereas TNF-α appeared to stimulate bone resorption through non-canonical pathways, evident by its independent association with CTX-I (Steeve et al., 2004). Furthermore, anti-inflammatory cytokines IL-10 and IL-13 showed important compensatory pathways through demonstrating strong negative associations with RANKL and positive trends with bone formation marker ALP. It could be that drugs intended for the treatment of inflammatory disease such as rheumatoid arthritis that have shown promise, such as TNF-α blockers (Feldmann and Maini, 2001), may be useful at this early stage in subjects exhibiting high inflammatory activity, to discourage perpetuating inflammatory dysregulation that may be influencing pathogenesis and ultimately irreversible changes in joint tissues.

Aside from cytokine activity, the role of biomarkers of subchondral bone loading (i.e. sclerostin and glutamate) showed involvement with pathology groups that is under-characterised in current literature. These findings are important in highlighting the involvement of bone in degenerative knee pathologies, which has long thought be important in the process (Findlay and Kuliwaba, 2016, Chen et al., 2017). The elevated levels of glutamate levels in FCD serum relative to controls is suggestive of enhanced

glutamatergic signalling, which has previously been demonstrated in our research group and others to be an important mediator of inflammatory, bone resorptive, cartilage degenerative and nociceptive pathways (Flood et al., 2007, Bonnet et al., 2015, Wen et al., 2015). However, it is likely the distinct regulatory mechanisms of extracellular glutamate obscured relationships to other pathways in the joint, hindering interpretation relative to FCD pathogenesis. Further study is recommended looking into this response whilst controlling for recent activity, since components of glutamate exocytosis and uptake appear to be mechanically-regulated (Mason et al., 1997, Szczesniak et al., 2005).

A prominent finding in the multivariate analysis was that of the distinction of inflammatory and bone remodelling subgroups which appears to be related to sclerostin activity in the joint, which supports its role as a key regulator of disease (Lewiecki, 2014). Since sclerostin is highly regulated by mechanical loading of bone and produced by injured cartilage, it may be a useful biological measure in the stratification of clinical cases into treatment groups for targeted therapy of bone or cartilage related pathology. Further investigation into relationship between sclerostin activity and bone/cartilage compositional and structural changes using technology such as MRI may further clarify the utility of sclerostin for such methods. Aside from the molecules examined within this thesis, many other important biological pathways were not taken into consideration due to time and funding constraints. The most important being signalling mechanisms in cartilage such as the TGF-β pathways, critical in cartilage homeostasis and OA development (Finnson et al., 2012), mechanically-induced integrin-mediated catabolic pathway activation in chondrocytes (Bader et al., 2011), the production of matrix-degrading enzymes such as MMPs and aggrecanases, as well as many others (Chen et al., 2017, Jorgensen et al., 2017).

Finally, it was shown that biological outcomes microfracture reflected a positive repair response in most FCD subjects, which was evident six-months post-surgery. Indeed, previous authors have recognised the therapeutic effect of introducing MSCs for treating OA, since they possess trophic and immunomodulatory properties that could enhance repair pathway activation in the affected joint (Pers et al., 2015). This finding importantly demonstrates that bone marrow stimulation combined with an appropriate method of correcting the dynamic mechanical joint axis for high joint loaders may provide positive long-term outcomes without the requirement of drugs or implants. Although the results are preliminary, it appears that poor outcomes of microfracture surgery may be related to a lack of improved inflammatory dysregulation in the joint

following surgery. However, it was not clear whether this outcome was a consequence of loading at the knee, since this subject (RP) belonged to the lateral knee FCD group who were better functioning both at prior to- and following surgery.

Objective 3: *To characterise the effect of altered knee mechanical loading on joint biology in tibiofemoral FCD and OA pathogenesis*

The relationship between mechanics and biology in the pathogenesis of degenerative knee pathology is undeniable, however these mechanisms are poorly characterised in humans. Chapter 5 set out to further elucidate if the aberrant joint biology that is associated with FCD and OA pathogenesis as validated in chapter 4 is a consequence of the pathomechanics relating to altered knee loading patterns.

It was clearly evident that indicators of dynamic knee compartmental loading and alignment significantly associated with inflammatory activity and bone remodelling activity reflective of increased net bone resorption. Furthermore, it was suggested that the healthy positive feedback response of bone loading with the osteoblastic production of OPG, an important osteoclast inhibitor and promoter of bone formation, was disrupted by the effect pathophysiological loads had on inflammatory mechanisms. Osteoblastic RANKL expression is upregulated by pro-inflammatory cytokine signalling, as substantiated in chapter 4, thus counteracting the negative effect OPG has on bone resorption pathways by blocking the action of RANKL, a paradoxical effect. Although these mechanisms are consistent with *in vitro* and animal model work studying the mechano-response to loading, it has not been clarified whether the effect joint loading has on this biological condition is at least partially consequent of tissue damage severity in the joint, since it was not possible to control for this factor. Further study incorporating larger cohorts, with a range of severity scores such as KL grades or MRI tissue structural or composition scores is recommended to further elucidate clarify whether these striking associations are conclusive evidence of joint mechanics as a key driver of FCD and OA pathogenesis.

Interestingly, it appears that at the FCD stage inflammatory dysregulation and enhancement of bone resorption concomitant with increasing compartmental loads is less prominent, however there is preliminary results to show that the degree of dynamic joint malalignment influencing loading patterns at this early stage could be an important risk factor for progression, due to its significant association with increased bone remodelling activity and possibly pro-inflammatory (IL-6) cytokine synthesis. Collectively, the results from this chapter encourage interventional studies investigating if cartilage repair techniques at this early stage are more effective for high knee loaders

when accompanied by interventions aimed at offloading the affected knee compartment by correcting the mechanical axis of the knee, such as gait retraining (Khalaj et al., 2014), lateral wedge insoles (Radzimski et al., 2012) or high tibial osteotomy surgery (Morin et al., 2018).

6.2 Thesis limitations

Several limitations have been discussed throughout each individual chapter, however there were general limitations that are relevant to consider for this study:

6.2.1 Study cohorts

For involvement of control subjects, collection of gait data was at the start of the recruitment period, whereas it was only possible to collect serum later in the study due to lack of accessibility to a phlebotomist. This led to a mismatch of biomechanics-biology linked data for the control cohorts. The lack of a consistent control subject group throughout the study restricted the ability to distinguish between relationships of joint biomechanics and biology representative of a normal homeostatic environment relative to pathological conditions. Exploring this disparity could improve the understanding of whether the effect of joint loading patterns on the observed biological response is a consequence of pathomechanics alone, or pathomechanics with the initiation of joint damage. This could improve our understanding of the etiologic factors of tibiofemoral FCDs in those that have not suffered joint injuries. Andriacchi noted that cyclic normal joint loading may be important for homeostatic regulation in health, but a critical risk factor to disease initiation following a traumatic event (Andriacchi and Muendermann, 2006). Further investigation of the relationships of mechanics and biology whilst taking healthy subjects into account would further substantiate this hypothesis.

For involvement of OA subjects, synovial fluid samples were used from the ARUK BBC bio-bank. This resulted in the requirement for two cohorts examined across the thesis (i.e. unilateral OA in chapter 4 and 5 and severe OA in chapter 6), which was due to not having access to unilateral OA synovial fluid samples until later in the project, as this was under the decision of the ARUK centre for progression of this body of work. Ideally, unilateral OA subjects rather than severe OA subjects would have been the consistent comparator over chapter 4, 5 and 6, since FCDs have been more commonly reported to predispose to unilateral OA on their natural course, rather than total joint OA which may occur in much later stages (Davies-Tuck et al., 2008b, Carnes et al., 2012, Spahn and

Hofmann, 2014). Furthermore, unilateral OA joint tissue damage similarly to tibiofemoral FCD damage is focal in nature, typically isolated to a single compartment of the knee. Therefore, it is likely they experience more similar pathophysiological and etiological characteristics. Finally, unilateral OA subjects were younger with lower BMIs relative to severe OA subjects, which meant they were more demographically matched to FCD subjects. Together, it is evident that involvement of unilateral OA subjects rather than severe OA would allow for more clinically meaningful comparison when representing an advanced disease state, a consideration for future study.

6.2.2 Sample size and heterogeneity

A recurring factor within the outcomes of each chapter was the clear heterogeneity in the cohorts examined, evident by the intra-group variations detected by multivariate analysis methods. It is likely that several factors were likely responsible for these variations such as that of demographics and co-morbidities including meniscal and ligament pathologies which were clearly influential of mechanical and biological factors. Although it was possible to adjust for age and BMI in some statistical aspects of the study, the small sample size did not allow for the controlling of variation in co-morbidities, disease severity (for findings involving uOA cohorts), use of pain medication, diurnal changes in biological markers, or levels of joint activity, which have been suggested at some degree to be confounding of the results of this thesis. Further investigations using larger sample sizes will permit better interpretation of these factors in relation to FCD and OA pathogenic and etiologic mechanisms of disease.

6.3 Final conclusion

Collectively, these findings propose a mechanism by which daily cyclic pathophysiological loads acting on joint tissues in the affected knee compartment is driving lesion progression through the activation of deleterious pathways in the surrounding cells. Increased synthesis of pro-inflammatory cytokines in response to increased tissue loading generates a catabolic environment by stimulating the production of matrix degrading enzymes and causing a cellular switch from matrix production to matrix breakdown (Scanzello, 2017). The prolonged catabolic conditions and loss of consistent underlying subchondral bone composition leads to eventual structural degradation of cartilage, which exposes the remaining cartilage to increased forces due to the smaller surface area. Loss of cartilage structure influences further

malalignment of the joint, leading to higher compartmental loading (Felson et al., 2013). Ultimately, this mechanism describes a potential destructive feedback loop.

This contribution of knowledge has identified new potential disease pathways and a plethora of candidate functional and biomolecular markers that could be useful for improving current strategies or informing clinical decision making for the treatment for tibiofemoral FCDs. Furthermore, the preliminary findings from this study clearly demonstrate the shortfalls of microfracture surgery may be related to our ignorance of the true complexity of knee degenerative pathology, which should be treated accordingly. Future areas of research and clinical studies encompassing mechanical, biological and structural pathways are essential for optimising treatments of FCDs for reproducible longevity and efficacy, in which current practice is lacking.

Chapter 7

References

AKAGI, R., AKATSU, Y., FISCH, K. M., ALVAREZ-GARCIA, O., TERAMURA, T., MURAMATSU, Y., SAITO, M., SASHO, T., SU, A. I. & LOTZ, M. K. 2017. Dysregulated circadian rhythm pathway in human osteoarthritis: NR1D1 and BMAL1 suppression alters TGF-beta signaling in chondrocytes. *Osteoarthritis Cartilage,* 25**,** 943-951.

AKESON, G. & MALEMUD, C. 2017. A Role for Soluble IL-6 Receptor in Osteoarthritis. *Journal of Functional Morphology and Kinesiology,* 2**,** 27.

ANDERSSON, G. B. J., ANDRIACCHI, T. P. & GALANTE, J. O. 1981. Correlations between Changes in Gait and in Clinical Status after Knee Arthroplasty. *Acta Orthopaedica Scandinavica,* 52**,** 569-573.

ANDERSSON, M. L., PETERSSON, I. F., KARLSSON, K. E., JONSSON, E. N., MANSSON, B., HEINEGARD, D. & SAXNE, T. 2006a. Diurnal variation in serum levels of cartilage oligomeric matrix protein in patients with knee osteoarthritis or rheumatoid arthritis. *Ann Rheum Dis,* 65**,** 1490-4.

ANDERSSON, M. L., THORSTENSSON, C. A., ROOS, E. M., PETERSSON, I. F., HEINEGARD, D. & SAXNE, T. 2006b. Serum levels of cartilage oligomeric matrix protein (COMP) increase temporarily after physical exercise in patients with knee osteoarthritis. *BMC Musculoskelet Disord,* 7**,** 98.

ANDREWS, M., NOYES, F. R., HEWETT, T. E. & ANDRIACCHI, T. P. 1996. Lower limb alignment and foot angle are related to stance phase knee adduction in normal subjects: A critical analysis of the reliability of gait analysis data. *Journal of Orthopaedic Research,* 14**,** 289-295.

ANDRIACCHI, T. P. & FAVRE, J. 2014. The nature of in vivo mechanical signals that influence cartilage health and progression to knee osteoarthritis. *Curr Rheumatol Rep,* 16**,** 463.

ANDRIACCHI, T. P., KOO, S. & SCANLAN, S. F. 2009. Gait mechanics influence healthy cartilage morphology and osteoarthritis of the knee. *J Bone Joint Surg Am,* 91 Suppl 1**,** 95-101.

ANDRIACCHI, T. P. & MUENDERMANN, A. 2006. The role of ambulatory mechanics in the initiation and progression of knee osteoarthritis. *Current Opinion in Rheumatology,* 18**,** 514-518.

AROKOSKI, J. P. A., JURVELIN, J. S., VAATAINEN, U. & HELMINEN, H. J. 2000. Normal and pathological adaptations of articular cartilage to joint loading. *Scandinavian Journal of Medicine & Science in Sports,* 10**,** 186-198.

ARTHRITIS RESEARCH UK 2017. Arthritis Data and Statistics Calculator.

ASTEPHEN, J. L., DELUZIO, K. J., CALDWELL, G. E. & DUNBAR, M. J. 2008. Biomechanical changes at the hip, knee, and ankle joints during gait are associated with knee osteoarthritis severity. *Journal of Orthopaedic Research,* 26**,** 332-341.

ATHANASIOU, K. A. & SANCHEZ-ADAMS, J. 2009. *Engineering the Knee Meniscus*.

ATTUR, M., KRASNOKUTSKY-SAMUELS, S., SAMUELS, J. & ABRAMSON, S. B. 2013. Prognostic biomarkers in osteoarthritis. *Current Opinion in Rheumatology,* 25**,** 136-144.

ATTUR, M. G., PATEL, I. R., PATEL, R. N., ABRAMSON, S. B. & AMIN, A. R. 1998. Autocrine production of IL-1 beta by human osteoarthritis-affected cartilage and differential regulation of endogenous nitric oxide, IL-6, prostaglandin E-2, and IL-8. *Proceedings of the Association of American Physicians,* 110**,** 65-72.

BADER, D. L., SALTER, D. M. & CHOWDHURY, T. T. 2011. Biomechanical Influence of Cartilage Homeostasis in Health and Disease. *Arthritis,* 2011.

BAEK, K., HWANG, H. R., PARK, H. J., KWON, A., QADIR, A. S., KO, S. H., WOO, K. M., RYOO, H. M., KIM, G. S. & BAEK, J. H. 2014. TNF-alpha upregulates sclerostin expression in obese mice fed a high-fat diet. *J Cell Physiol,* 229**,** 640-50.

BALIUNAS, A. J., HURWITZ, D. E., RYALS, A. B., KARRAR, A., CASE, J. P., BLOCK, J. A. & ANDRIACCHI, T. P. 2002. Increased knee joint loads during walking are present in subjects with knee osteoarthritis. *Osteoarthritis and Cartilage,* 10**,** 573-579.

BELL, A. L., PEDERSEN, D. R. & BRAND, R. A. 1990. A comparison of the accuracy of several hip center location prediction methods. *J Biomech,* 23**,** 617-21.

BENNELL, K. L., BOWLES, K. A., WANG, Y. Y., CICUTTINI, F. M., DAVIES-TUCK, M. & HINMAN, R. S. 2011. Higher dynamic medial knee load predicts greater cartilage loss over 12 months in medial knee osteoarthritis. *Annals of the Rheumatic Diseases,* 70**,** 1770-1774.

BENOIT, D. L., RAMSEY, D. K., LAMONTAGNE, M., XU, L., WRETENBERG, P. & RENSTROM, P. 2006. Effect of skin movement artifact on knee kinematics during gait and cutting motions measured in vivo. *Gait Posture,* 24**,** 152-64.

BERENBAUM, F. 2013. Osteoarthritis as an inflammatory disease (osteoarthritis is not osteoarthrosis!). *Osteoarthritis Cartilage,* 21**,** 16-21.

BETTICA, P., CLINE, G., HART, D. J., MEYER, J. & SPECTOR, T. D. 2002. Evidence for increased bone resorption in patients with progressive knee osteoarthritis - Longitudinal results from the Chingford study. *Arthritis and Rheumatism,* 46**,** 3178-3184.

BHOSALE, A. M. & RICHARDSON, J. B. 2008. Articular cartilage: structure, injuries and review of management. *British Medical Bulletin,* 87**,** 77-95.

BIGONI, M., SACERDOTE, P., TURATI, M., FRANCHI, S., GANDOLLA, M., GADDI, D., MORETTI, S., MUNEGATO, D., AUGUSTI, C. A., BRESCIANI, E., OMELJANIUK, R. J., LOCATELLI, V. & TORSELLO, A. 2013. Acute and Late Changes in Intraarticular Cytokine Levels Following Anterior Cruciate Ligament Injury. *Journal of Orthopaedic Research,* 31**,** 315-321.

BISWAL, S., HASTIE, T., ANDRIACCHI, T. P., BERGMAN, G. A., DILLINGHAM, M. F. & LANG, P. 2002. Risk factors for progressive cartilage loss in the knee: a longitudinal magnetic resonance imaging study in forty-three patients. *Arthritis Rheum,* 46**,** 2884-92.

BJARNASON, N. H., HENRIKSEN, E. E., ALEXANDERSEN, P., CHRISTGAU, S., HENRIKSEN, D. B. & CHRISTIANSEN, C. 2002. Mechanism of circadian variation in bone resorption. *Bone,* 30**,** 307-13.

BLAIN, E. J., GILBERT, S. J., WARDALE, R. J., CAPPER, S. J., MASON, D. J. & DUANCE, V. C. 2001. Up-regulation of matrix metalloproteinase expression and activation following cyclical compressive loading of articular cartilage in vitro. *Archives of Biochemistry and Biophysics,* 396**,** 49-55.

BLAKER, C. L., CLARKE, E. C. & LITTLE, C. B. 2017. Using mouse models to investigate the pathophysiology, treatment, and prevention of post-traumatic osteoarthritis. *Journal of Orthopaedic Research,* 35**,** 424-439.

BONNET, C. S., WILLIAMS, A. S., GILBERT, S. J., HARVEY, A. K., EVANS, B. A. & MASON, D. J. 2015. AMPA/kainate glutamate receptors contribute to inflammation, degeneration and pain related behaviour in inflammatory stages of arthritis. *Annals of the Rheumatic Diseases,* 74**,** 242-251.

BOUAZIZ, W., FUNCK-BRENTANO, T., LIN, H., MARTY, C., EA, H. K., HAY, E. & COHEN-SOLAL, M. 2015. Loss of sclerostin promotes osteoarthritis in mice via beta-catenin-dependent and -independent Wnt pathways. *Arthritis Res Ther,* 17**,** 24.

BOYCE, B. F., XIU, Y., LI, J. B., XING, L. P. & YAO, Z. Q. 2015. NF-kappa B-Mediated Regulation of Osteoclastogenesis. *Endocrinology and Metabolism-Enm,* 30**,** 35-44.

BOYER, K. A., ANGST, M. S., ASAY, J., GIORI, N. J. & ANDRIACCHI, T. P. 2012. Sensitivity of gait parameters to the effects of anti-inflammatory and opioid treatments in knee osteoarthritis patients. *Journal of Orthopaedic Research,* 30**,** 1118-1124.

BRAKSPEAR, K. S. & MASON, D. J. 2012. Glutamate signaling in bone. *Frontiers in Endocrinology,* 3**,** 97.

BRANDON, S. C. E. & DELUZIO, K. J. 2011. Robust features of knee osteoarthritis in joint moments are independent of reference frame selection. *Clinical Biomechanics,* 26**,** 65-70.

BRANDT, K. D., FIFE, R. S., BRAUNSTEIN, E. M. & KATZ, B. 1991. RADIOGRAPHIC GRADING OF THE SEVERITY OF KNEE OSTEOARTHRITIS - RELATION OF THE KELLGREN AND LAWRENCE GRAD TO A GRADE BASED ON JOINT SPACE NARROWING, AND CORRELATION WITH ARTHROSCOPIC EVIDENCE OF ARTICULAR-CARTILAGE DEGENERATION. *Arthritis and Rheumatism,* 34**,** 1381-1386.

BRIGGS, M. D., HOFFMAN, S. M. G., KING, L. M., OLSEN, A. S., MOHRENWEISER, H., LEROY, J. G., MORTIER, G. R., RIMOIN, D. L., LACHMAN, R. S., GAINES, E. S., CEKLENIAK, J. A., KNOWLTON, R. G. & COHN, D. H. 1995. Pseudoachondroplasia and Multiple Epiphyseal Dysplasia Due to Mutations in the Cartilage Oligomeric Matrix Protein Gene. *Nature Genetics,* 10**,** 330-336.

BRITTBERG, M., LINDAHL, A., NILSSON, A., OHLSSON, C., ISAKSSON, O. & PETERSON, L. 1994. TREATMENT OF DEEP CARTILAGE DEFECTS IN THE KNEE WITH AUTOLOGOUS CHONDROCYTE TRANSPLANTATION. *New England Journal of Medicine,* 331**,** 889-895.

BUCKWALTER, J. A. & LANE, N. E. 1997. Athletics and osteoarthritis. *American Journal of Sports Medicine,* 25**,** 873-881.

BUCKWALTER, J. A. & MANKIN, H. J. 1998. Articular cartilage: Tissue design and chondrocyte-matrix interactions. *Instructional Course Lectures, Vol 47 - 1998,* 47**,** 477-486.

BUCZEK, F. L., RAINBOW, M. J., COONEY, K. M., WALKER, M. R. & SANDERS, J. O. 2010. Implications of using hierarchical and six degree-of-freedom models for normal gait analyses. *Gait Posture,* 31**,** 57-63.

BURR, D. B. 2004. The importance of subchondral bone in the progression of osteoarthritis. *Journal of Rheumatology,* 31**,** 77-80.

BURR, D. B. & GALLANT, M. A. 2012. Bone remodelling in osteoarthritis. *Nature Reviews Rheumatology,* 8**,** 665-673.

CARNES, J., STANNUS, O., CICUTTINI, F. M., DING, C. & JONES, G. 2012. Knee cartilage defects in a sample of older adults: natural history, clinical significance and factors influencing change over 2.9 years. *Osteoarthritis and Cartilage,* 20**,** 1541-1547.

CATTANO, N. M., DRIBAN, J. B., CAMERON, K. L. & SITLER, M. R. 2017. Impact of physical activity and mechanical loading on biomarkers typically used in osteoarthritis assessment: current concepts and knowledge gaps. *Therapeutic Advances in Musculoskeletal Disease,* 9**,** 11-21.

CEREATTI, A., DELLA CROCE, U. & CAPPOZZO, A. 2006. Reconstruction of skeletal movement using skin markers: comparative assessment of bone pose estimators. *Journal of Neuroengineering and Rehabilitation,* 3.

CHAN, B. Y., FULLER, E. S., RUSSELL, A. K., SMITH, S. M., SMITH, M. M., JACKSON, M. T., CAKE, M. A., READ, R. A., BATEMAN, J. F., SAMBROOK, P. N. & LITTLE, C. B. 2011. Increased chondrocyte sclerostin may protect against cartilage degradation in osteoarthritis. *Osteoarthritis Cartilage,* 19**,** 874-85.

CHANG, A., HAYES, K., DUNLOP, D., SONG, J., HURWITZ, D., CAHUE, S. & SHARMA, L. 2005. Hip abduction moment and protection against medial tibiofemoral osteoarthritis progression. *Arthritis and Rheumatism,* 52**,** 3515-3519.

CHANG, J. C., CHRISTIANSEN, B. A., MURUGESH, D. K., SEBASTIAN, A., HUM, N. R., COLLETTE, N. M., HATSELL, S., ECONOMIDES, A. N., BLANCHETTE, C. D. & LOOTS, G. G. 2018. SOST/Sclerostin Improves Posttraumatic Osteoarthritis and Inhibits MMP2/3 Expression After Injury. *Journal of Bone and Mineral Research,* 33**,** 1105-1113.

CHAU, T. 2001. A review of analytical techniques for gait data. Part 1: fuzzy, statistical and fractal methods. *Gait & Posture,* 13**,** 49-66.

CHEN, D., SHEN, J., ZHAO, W. W., WANG, T. Y., HAN, L., HAMILTON, J. L. & IM, H. J. 2017. Osteoarthritis: toward a comprehensive understanding of pathological mechanism. *Bone Research,* 5.

CHEN, F. H., HERNDON, M. E., PATEL, N., HECHT, J. T., TUAN, R. S. & LAWLER, J. 2007. Interaction of cartilage oligomeric matrix protein/thrombospondin 5 with aggrecan. *J Biol Chem,* 282**,** 24591-8.

CHEN, I. H., KUO, K. N. & ANDRIACCHI, T. P. 1997. The influence of walking speed on mechanical joint power during gait. *Gait & Posture,* 6**,** 171-176.

CHILDS, J. D., SPARTO, P. J., FITZGERALD, G. K., BIZZINI, M. & IRRGANG, J. J. 2004. Alterations in lower extremity movement and muscle activation patterns in individuals with knee osteoarthritis. *Clinical Biomechanics,* 19**,** 44-49.

CHOWDHURY, R. H., REAZ, M. B., ALI, M. A., BAKAR, A. A., CHELLAPPAN, K. & CHANG, T. G. 2013. Surface electromyography signal processing and classification techniques. *Sensors (Basel),* 13**,** 12431-66.

CHOWDHURY, T. T., SCHULZ, R. M., RAI, S. S., THUEMMLER, C. B., WUESTNECK, N., BADER, A. & HOMANDBERG, G. A. 2010. Biomechanical modulation of collagen fragment-induced anabolic and catabolic activities in chondrocyte/agarose constructs. *Arthritis Res Ther,* 12**,** R82.

CHUNG, H. Y., CESARI, M., ANTON, S., MARZETTI, E., GIOVANNINI, S., SEO, A. Y., CARTER, C., YU, B. P. & LEEUWENBURGH, C. 2009. Molecular inflammation: Underpinnings of aging and age-related diseases. *Ageing Research Reviews,* 8**,** 18-30.

CIVININI, R., CARULLI, C., MATASSI, F., LEPRI, A. C., SIRLEO, L. & INNOCENTI, M. 2017. The Survival of Total Knee Arthroplasty: Current Data from Registries on Tribology: Review Article. *Hss j,* 13**,** 28-31.

CLARK, A. G., JORDAN, J. M., VILIM, V., RENNER, J. B., DRAGOMIR, A. D., LUTA, G. & KRAUS, V. B. 1999. Serum cartilage oligomeric matrix protein reflects osteoarthritis presence and severity - The Johnston county osteoarthritis project. *Arthritis and Rheumatism,* 42**,** 2356-2364.

COLLINS, T. D., GHOUSSAYNI, S. N., EWINS, D. J. & KENT, J. A. 2009. A six degrees-of-freedom marker set for gait analysis: Repeatability and comparison with a modified Helen Hayes set. *Gait & Posture,* 30**,** 173-180.

CONNOR, J. R., LEPAGE, C., SWIFT, B. A., YAMASHITA, D., BENDELE, A. M., MAUL, D. & KUMAR, S. 2009. Protective effects of a cathepsin K inhibitor, SB-553484, in the canine partial medial meniscectomy model of osteoarthritis. *Osteoarthritis and Cartilage,* 17**,** 1236-1243.

COVENTRY, M. B., ILSTRUP, D. M. & WALLRICHS, S. L. 1993. Proximal Tibial Osteotomy - a Critical Long-Term Study of 87 Cases. *Journal of Bone and Joint Surgery-American Volume,* 75A**,** 196-201.

COWAN, R. W., SEIDLITZ, E. P. & SINGH, G. 2012. Glutamate signaling in healthy and diseased bone. *Front Endocrinol (Lausanne),* 3**,** 89.

CREMERS, S., GARNERO, P. & SEIBEL, M. J. 2008. *Principles of Bone Biology*, Academic Press.

CUELLAR, V. G., CUELLAR, J. M., KIRSCH, T. & STRAUSS, E. J. 2016. Correlation of Synovial Fluid Biomarkers With Cartilage Pathology and Associated Outcomes in Knee Arthroscopy. *Arthroscopy-the Journal of Arthroscopic and Related Surgery,* 32**,** 475-485.

DAVIES-TUCK, M. L., WLUKA, A. E., TEICHTAHL, A. J., MARTEL-PELLETIER, J., PELLETIER, J. P., JONES, G., DING, C., DAVIS, S. R. & CICUTTINI, F. M. 2008a. Association between meniscal tears and the peak external knee adduction moment and foot rotation during level walking in postmenopausal women without knee osteoarthritis: a cross-sectional study. *Arthritis Research & Therapy,* 10.

DAVIES-TUCK, M. L., WLUKA, A. E., WANG, Y., TEICHTAHL, A. J., DING, C. & CICUTTINI, F. M. 2008b. The natural history of cartilage defects in people with knee osteloarthritis. *Osteoarthritis and Cartilage,* 16**,** 337-342.

DAY, J. S., VAN DER LINDEN, J. C., RANK, R. A., DING, M., HVID, I., SUMNER, D. R. & WEINANS, H. 2004. Adaptation of subchondral bone in osteoarthritis. *Biorheology,* 41**,** 359-368.

DE CAMPOS, G. C., NERY, W., JR., TEIXEIRA, P. E., ARAUJO, P. H. & ALVES, W. M., JR. 2016. Association Between Meniscal and Chondral Lesions and Timing of Anterior Cruciate Ligament Reconstruction. *Orthop J Sports Med,* 4**,** 2325967116669309.

DE RHAM, C., FERRARI-LACRAZ, S., JENDLY, S., SCHNEITER, G., DAYER, J. M. & VILLARD, J. 2007. The proinflammatory cytokines IL-2, IL-15 and IL-21 modulate the repertoire of mature human natural killer cell receptors. *Arthritis Res Ther,* 9**,** R125.

DE WAAL MALEFYT, R., ABRAMS, J., BENNETT, B., FIGDOR, C. G. & DE VRIES, J. E. 1991. Interleukin 10(IL-10) inhibits cytokine synthesis by human monocytes: an autoregulatory role of IL-10 produced by monocytes. *J Exp Med,* 174**,** 1209-20.

DELL'ISOLA, A., ALLAN, R., SMITH, S. L., MARREIROS, S. S. P. & STEULTJENS, M. 2016. Identification of clinical phenotypes in knee osteoarthritis: a systematic review of the literature. *Bmc Musculoskeletal Disorders,* 17.

DELUZIO, K. J. & ASTEPHEN, J. L. 2007. Biomechanical features of gait waveform data associated with knee osteoarthritis - An application of principal component analysis. *Gait & Posture,* 25**,** 86-93.

DIEPPE, P. A. & LOHMANDER, L. S. 2005. Pathogenesis and management of pain in osteoarthritis. *Lancet,* 365**,** 965-973.

DORE, D., MARTENS, A., QUINN, S., DING, C. H., WINZENBERG, T., ZHAI, G. J., PELLETIER, J. P., MARTEL-PELLETIER, J., ABRAM, F., CICUTTINI, F. M. & JONES, G. 2010. Bone marrow lesions predict site-specific cartilage defect development and volume loss: a prospective study in older adults. *Arthritis Research & Therapy,* 12.

DRIBAN, J. B., SITLER, M. R., BARBE, M. F. & BALASUBRAMANIAN, E. 2010. Is osteoarthritis a heterogeneous disease that can be stratified into subsets? *Clin Rheumatol,* 29**,** 123-31.

DUFFELL, L. D., SOUTHGATE, D. F. L., GULATI, V. & MCGREGOR, A. H. 2014. Balance and gait adaptations in patients with early knee osteoarthritis. *Gait & Posture,* 39**,** 1057-1061.

EFE, T., FUGLEIN, A., GETGOOD, A., HEYSE, T. J., FUCHS-WINKELMANN, S., PATZER, T., EL-ZAYAT, B. F., LAKEMEIER, S. & SCHOFER, M. D. 2012. Anterior Cruciate Ligament deficiency leads to early instability of scaffold for cartilage regeneration: a controlled laboratory ex-vivo study. *International Orthopaedics,* 36**,** 1315-1320.

FALAH, M., NIERENBERG, G., SOUDRY, M., HAYDEN, M. & VOLPIN, G. 2010. Treatment of articular cartilage lesions of the knee. *International Orthopaedics,* 34**,** 621-630.

FALLAH-YAKHDANI, H. R., ABBASI-BAFGHI, H., MEIJER, O. G., BRUIJN, S. M., VAN DEN DIKKENBERG, N., BENEDETTI, M. G. & VAN DIEEN, J. H. 2012. Determinants of co-contraction during walking before and after arthroplasty for knee osteoarthritis. *Clinical Biomechanics,* 27**,** 485-494.

FAVERO, M., RAMONDA, R., GOLDRING, M. B., GOLDRING, S. R. & PUNZI, L. 2015. Early knee osteoarthritis. *RMD open,* 1**,** e000062.

FAVRE, J. & JOLLES, B. M. 2016. Gait analysis of patients with knee osteoarthritis highlights a pathological mechanical pathway and provides a basis for therapeutic interventions. *EFORT Open Rev,* 1**,** 368-374.

FELDMANN, M. & MAINI, R. N. 2001. Anti-TNF alpha therapy of rheumatoid arthritis: what have we learned? *Annual Review of Immunology,* 19**,** 163-196.

FELSON, D. T. 2013. Osteoarthritis as a disease of mechanics. *Osteoarthritis and Cartilage,* 21**,** 10-15.

FELSON, D. T., LAWRENCE, R. C., DIEPPE, P. A., HIRSCH, R., HELMICK, C. G., JORDAN, J. M., KINGTON, R. S., LANE, N. E., NEVITT, M. C., ZHANG, Y. Q., SOWERS, M., MCALINDON, T., SPECTOR, T. D., POOLE, A. R., YANOVSKI, S. Z., ATESHIAN, G., SHARMA, L., BUCKWALTER, J. A., BRANDT, K. D. & FRIES, J. F. 2000. Osteoarthritis: New Insights. Part 1: The Disease and Its Risk Factors. *Annals of Internal Medicine,* 133**,** 635-646.

FELSON, D. T., NIU, J. B., GROSS, K. D., ENGLUND, M., SHARMA, L., COOKE, T. D. V., GUERMAZI, A., ROEMER, F. W., SEGAL, N., GOGGINS, J. M., LEWIS, C. E., EATON, C. & NEVITT, M. C. 2013. Valgus Malalignment Is a Risk Factor for Lateral Knee Osteoarthritis Incidence and Progression Findings From the Multicenter Osteoarthritis Study and the Osteoarthritis Initiative. *Arthritis and Rheumatism,* 65**,** 355-362.

FERNANDES, J. C., MARTEL-PELLETIER, J. & PELLETIER, J. P. 2002. The role of cytokines in osteoarthritis pathophysiology. *Biorheology,* 39**,** 237-246.

FINDLAY, D. M. & KULIWABA, J. S. 2016. Bone-cartilage crosstalk: a conversation for understanding osteoarthritis. *Bone Res,* 4**,** 16028.

FINNSON, K. W., CHI, Y., BOU-GHARIOS, G., LEASK, A. & PHILIP, A. 2012. TGF-b signaling in cartilage homeostasis and osteoarthritis. *Front Biosci (Schol Ed),* 4**,** 251-68.

FITZGERALD, J. B., JIN, M. & GRODZINSKY, A. J. 2006. Shear and compression differentially regulate clusters of functionally related temporal transcription patterns in cartilage tissue. *Journal of Biological Chemistry,* 281**,** 24095-24103.

FLANDRY, F. & HOMMEL, G. 2011. Normal Anatomy and Biomechanics of the Knee. *Sports Medicine and Arthroscopy Review,* 19**,** 82-92.

FLANIGAN, D. C., HARRIS, J. D., TRINH, T. Q., SISTON, R. A. & BROPHY, R. H. 2010. Prevalence of Chondral Defects in Athletes' Knees: A Systematic Review. *Medicine and Science in Sports and Exercise,* 42**,** 1795-1801.

FLOOD, S., PARRI, R., WILLIAMS, A., DUANCE, V. & MASON, D. 2007. Modulation of interleukin-6 and matrix metalloproteinase 2 expression in human fibroblast-like synoviocytes by functional ionotropic glutamate receptors. *Arthritis Rheum,* 56**,** 2523-34.

FOROUGHI, N., SMITH, R. & VANWANSEELE, B. 2009. The association of external knee adduction moment with biomechanical variables in osteoarthritis: A systematic review. *Knee,* 16**,** 303-309.

FRANK, C. B. 2004. Ligament structure, physiology and function. *J Musculoskelet Neuronal Interact,* 4**,** 199-201.

FREGLY, B. J. 2012. Gait modification to treat knee osteoarthritis. *Hss j,* 8**,** 45-8.

FRISBIE, D. D., AL-SOBAYIL, F., BILLINGHURST, R. C., KAWCAK, C. E. & MCLLWRAITH, C. W. 2008. Changes in synovial fluid and serum biomarkers with exercise and early osteoarthritis in horses. *Osteoarthritis and Cartilage,* 16**,** 1196-1204.

FROBELL, R. B. 2011. Change in Cartilage Thickness, Posttraumatic Bone Marrow Lesions, and Joint Fluid Volumes After Acute ACL Disruption A Two-Year Prospective MRI Study of Sixty-one Subjects. *Journal of Bone and Joint Surgery-American Volume,* 93A**,** 1096-1103.

GALEA, G. L., LANYON, L. E. & PRICE, J. S. 2017. Sclerostin's role in bone's adaptive response to mechanical loading. *Bone,* 96**,** 38-44.

GAMEZ-NAVA, J. I., ZAVALETA-MUNIZ, S. A., VAZQUEZ-VILLEGAS, M. L., VEGA-LOPEZ, A., RODRIGUEZ-JIMENEZ, N. A., OLIVAS-FLORES, E. M., GONZALEZ-MONTOYA, N. G., CORONA-SANCHEZ, E. G., ROCHA-MUNOZ, A. D., MARTINEZ-CORRAL, M. E., MARTIN-MARQUEZ, B. T., VAZQUEZ-DEL MERCADO, M., MUNOZ-VALLE, J. F., CARDONA-MUNOZ, E. G., CELIS-DE LA ROSA, A., CABRERA-PIVARAL, C. & GONZALEZ-LOPEZ, L. 2013. Prescription for antiresorptive therapy in Mexican patients with rheumatoid arthritis: is it time to reevaluate the strategies for osteoporosis prevention? *Rheumatol Int,* 33**,** 145-50.

GARCIA-HERNANDEZ, A., ARZATE, H., GIL-CHAVARRIA, I., ROJO, R. & MORENO-FIERROS, L. 2012. High glucose concentrations alter the biomineralization process in human osteoblastic cells. *Bone,* 50**,** 276-88.

GARNERO, P., FERRERAS, M., KARSDAL, M. A., NICAMHLAOIBH, R., RISTELI, J., BOREL, O., QVIST, P., DELMAS, P. D., FOGED, N. T. & DELAISSE, J. M. 2003. The type I collagen fragments ICTP and CTX reveal distinct enzymatic pathways of bone collagen degradation. *Journal of Bone and Mineral Research,* 18**,** 859-867.

GARNERO, P., MAZIERES, B., GUEGUEN, A., ABBAL, M., BERDAH, L., LEQUESNE, M., NGUYEN, M., SALLES, J. P., VIGNON, E. & DOUGADOS, M. 2005. Cross-sectional association of 10 molecular markers of bone, cartilage, and synovium with disease activity and radiological joint damage in patients with hip osteoarthritis: The ECHODIAH cohort. *Journal of Rheumatology,* 32**,** 697-703.

GARNERO, P., PIPERNO, M., GINEYTS, E., CHRISTGAU, S., DELMAS, P. D. & VIGNON, E. 2001. Cross sectional evaluation of biochemical markers of bone, cartilage, and synovial tissue metabolism in patients with knee osteoarthritis: relations with disease activity and joint damage. *Annals of the Rheumatic Diseases,* 60**,** 619-626.

GIBON, E., LU, L. & GOODMAN, S. B. 2016. Aging, inflammation, stem cells, and bone healing. *Stem Cell Res Ther,* 7**,** 44.

GILBERT, L., HE, X. F., FARMER, P., BODEN, S., KOZLOWSKI, M., RUBIN, J. & NANES, M. S. 2000. Inhibition of osteoblast differentiation by tumor necrosis factor-alpha. *Endocrinology,* 141**,** 3956-3964.

GILBERT, S. J., BONNET, C. S., STADNIK, P. S., DUANCE, V. C., MASON, D. J. & BLAIN, E. J. 2018. Inflammatory and Degenerative Phases Resulting From Anterior Cruciate Rupture in a Non-Invasive Murine Model of Post-Traumatic Osteoarthritis. *Journal of Orthopaedic Research,* 0.

GOLDRING, M. B. & GOLDRING, S. R. 2007. Osteoarthritis. *Journal of Cellular Physiology,* 213**,** 626-634.

GOLDRING, M. B. & OTERO, M. 2011. Inflammation in osteoarthritis. *Current Opinion in Rheumatology,* 23**,** 471-478.

GOULERMAS, J. Y., HOWARD, D., NESTER, C. J., JONES, R. K. & REN, L. 2005. Regression techniques for the prediction of lower limb kinematics. *J Biomech Eng,* 127**,** 1020-4.

GUAN, Y. J., YANG, X., YANG, W. T., CHARBONNEAU, C. & CHEN, Q. 2014. Mechanical activation of mammalian target of rapamycin pathway is required for cartilage development. *Faseb Journal,* 28**,** 4470-4481.

GUERMAZI, A., HAYASHI, D., ROEMER, F. W., NIU, J., QUINN, E. K., CREMA, M. D., NEVITT, M. C., TORNER, J., LEWIS, C. E. & FELSON, D. T. 2017. Brief Report: Partial- and Full-Thickness Focal Cartilage Defects Contribute Equally to Development of New Cartilage Damage in Knee Osteoarthritis: The Multicenter Osteoarthritis Study. *Arthritis Rheumatol,* 69**,** 560-564.

GUERNE, P. A., CARSON, D. A. & LOTZ, M. 1990. Il-6 Production by Human Articular Chondrocytes - Modulation of Its Synthesis by Cytokines, Growth-Factors, and Hormones Invitro. *Journal of Immunology,* 144**,** 499-505.

GUO, D., DING, L. & HOMANDBERG, G. A. 2009. Telopeptides of type II collagen upregulate proteinases and damage cartilage but are less effective than highly active fibronectin fragments. *Inflamm Res,* 58**,** 161-9.

HALASZ, K., KASSNER, A., MORGELIN, M. & HEINEGARD, D. 2007. COMP acts as a catalyst in collagen fibrillogenesis. *J Biol Chem,* 282**,** 31166-73.

HALLER, J. M., MCFADDEN, M., KUBIAK, E. N. & HIGGINS, T. F. 2015. Inflammatory Cytokine Response Following Acute Tibial Plateau Fracture. *Journal of Bone and Joint Surgery-American Volume,* 97A**,** 478-483.

HAYAMI, T., PICKARSKI, M., WESOLOWSKI, G. A., MCLANE, J., BONE, A., DESTEFANO, J., RODAN, G. A. & DUONG, L. T. 2004. The role of subchondral bone remodeling in osteoarthritis - Reduction of cartilage degeneration and prevention of osteophyte formation by alendronate in the rat anterior cruciate ligament transection model. *Arthritis and Rheumatism,* 50**,** 1193-1206.

HEIDEN, T. L., LLOYD, D. G. & ACKLAND, T. R. 2009. Knee joint kinematics, kinetics and muscle co-contraction in knee osteoarthritis patient gait. *Clinical Biomechanics,* 24**,** 833-841.

HEIJINK, A., GOMOLL, A. H., MADRY, H., DROBNIC, M., FILARDO, G., ESPREGUEIRA-MENDES, J. & VAN DIJK, C. N. 2012. Biomechanical considerations in the pathogenesis of osteoarthritis of the knee. *Knee Surgery Sports Traumatology Arthroscopy,* 20**,** 423-435.

HEIR, S., NERHUS, T. K., ROTTERUD, J. H., LOKEN, S., EKELAND, A., ENGEBRETSEN, L. & AROEN, A. 2010. Focal Cartilage Defects in the Knee Impair Quality of Life as Much as Severe Osteoarthritis A Comparison of Knee Injury and Osteoarthritis Outcome Score in 4 Patient Categories Scheduled for Knee Surgery. *American Journal of Sports Medicine,* 38**,** 231-237.

HERMANS, H. J. & FRERIKS, B. 1997. *The State of the Art on Sensors and Sensor Placement Procedures for Surface ElectroMyoGraphy: A proposal for sensor placement procedures*.

HERMENS, H. J., FRERIKS, B., DISSELHORST-KLUG, C. & RAU, G. 2000. Development of recommendations for SEMG sensors and sensor placement procedures. *J Electromyogr Kinesiol,* 10**,** 361-74.

HINOI, E., FUJIMORI, S., TAKARADA, T., TANIURA, H. & YONEDA, Y. 2002. Facilitation of glutamate release by ionotropic glutamate receptors in osteoblasts. *Biochem Biophys Res Commun,* 297**,** 452-8.

HINOI, E., FUJIMORI, S. & YONEDA, Y. 2003. Modulation of cellular differentiation by N-methyl-D-aspartate receptors in osteoblasts. *Faseb Journal,* 17**,** 1532-+.

HIROKAWA, S., SOLOMONOW, M., LUO, Z., LU, Y. & DAMBROSIA, R. 1991. Muscular Cocontraction and Control of Knee Stability. *Journal of Electromyography and Kinesiology,* 1**,** 199-208.

HIRSCH, M. S., LUNSFORD, L. E., TRINKAUSRANDALL, V. & SVOBODA, K. K. H. 1997. Chondrocyte survival and differentiation in situ are integrin mediated. *Developmental Dynamics,* 210**,** 249-263.

HO, M. L., TSAI, T. N., CHANG, J. K., SHAO, T. S., JENG, Y. R. & HSU, C. 2005. Down-regulation of N-methyl D-aspartate receptor in rat-modeled disuse osteopenia. *Osteoporos Int,* 16**,** 1780-8.

HOEY, D. A., TORMEY, S., RAMCHARAN, S., O'BRIEN, F. J. & JACOBS, C. R. 2012. Primary Cilia-Mediated Mechanotransduction in Human Mesenchymal Stem Cells. *Stem Cells,* 30**,** 2561-2570.

HOFBAUER, L. C., LACEY, D. L., DUNSTAN, C. R., SPELSBERG, T. C., RIGGS, B. L. & KHOSLA, S. 1999. Interleukin-1beta and tumor necrosis factor-alpha, but not interleukin-6, stimulate osteoprotegerin ligand gene expression in human osteoblastic cells. *Bone,* 25**,** 255-9.

HONDA, K., OHNO, S., TANIMOTO, K., IJUIN, C., TANAKA, N., DOI, T., KATO, Y. & TANNE, K. 2000. The effects of high magnitude cyclic tensile load on cartilage matrix metabolism in cultured chondrocytes. *Eur J Cell Biol,* 79**,** 601-9.

HORTOBAGYI, T., WESTERKAMP, L., BEAM, S., MOODY, J., GARRY, J., HOLBERT, D. & DEVITA, P. 2005. Altered hamstring-quadriceps muscle balance in patients with knee osteoarthritis. *Clinical Biomechanics,* 20**,** 97-104.

HORWOOD, N. J., ELLIOTT, J., MARTIN, T. J. & GILLESPIE, M. T. 1998. Osteotropic agents regulate the expression of osteoclast differentiation factor and osteoprotegerin in osteoblastic stromal cells. *Endocrinology,* 139**,** 4743-6.

HOUARD, X., GOLDRING, M. B. & BERENBAUM, F. 2013. Homeostatic mechanisms in articular cartilage and role of inflammation in osteoarthritis. *Curr Rheumatol Rep,* 15**,** 375.

HUBLEY-KOZEY, C., DELUZIO, K. & DUNBAR, M. 2008. Muscle co-activation patterns during walking in those with severe knee osteoarthritis. *Clinical Biomechanics,* 23**,** 71-80.

HUBLEY-KOZEY, C. L., ROBBINS, S. M., RUTHERFORD, D. J. & STANISH, W. D. 2013. Reliability of surface electromyographic recordings during walking in individuals with knee osteoarthritis. *Journal of Electromyography and Kinesiology,* 23**,** 334-341.

HUNT, M. A., BIRMINGHAM, T. B., GIFFIN, J. R. & JENKYN, T. R. 2006. Associations among knee adduction moment, frontal plane ground reaction force, and lever arm during walking in patients with knee osteoarthritis. *Journal of Biomechanics,* 39**,** 2213-2220.

HUNT, M. A., POLLOCK, C. L., KRAUS, V. B., SAXNE, T., PETERS, S., HUEBNER, J. L., SAYRE, E. C. & CIBERE, J. 2013. Relationships amongst osteoarthritis biomarkers, dynamic knee joint load, and exercise: results from a randomized controlled pilot study. *Bmc Musculoskeletal Disorders,* 14.

HUNTER, D. J., NEVITT, M., LOSINA, E. & KRAUS, V. 2014. Biomarkers for osteoarthritis: Current position and steps towards further validation. *Best Practice & Research in Clinical Rheumatology,* 28**,** 61-71.

HUNTER, D. J., ZHANG, Y. Q., NIU, J. B., TU, X., AMIN, S., CLANCY, M., GUERMAZI, A., GRIGORIAN, M., GALE, D. & FELSON, D. T. 2006. The association of meniscal

pathologic changes with cartilage loss in symptomatic knee ostoearthritis. *Arthritis and Rheumatism,* 54**,** 795-801.

HURWITZ, D. E., RYALS, A. R., BLOCK, J. A., SHARMA, L., SCHNITZER, T. J. & ANDRIACCHI, T. P. 2000. Knee pain and joint loading in subjects with osteoarthritis of the knee. *Journal of Orthopaedic Research,* 18**,** 572-579.

HWANG, H. S., PARK, S. J., CHEON, E. J., LEE, M. H. & KIM, H. A. 2015. Fibronectin fragment-induced expression of matrix metalloproteinases is mediated by MyD88-dependent TLR-2 signaling pathway in human chondrocytes. *Arthritis Research & Therapy,* 17.

IANNONE, F., DE BARI, C., DELL'ACCIO, F., COVELLI, M., CANTATORE, F. P., PATELLA, V., LO BIANCO, G. & LAPADULA, G. 2001. Interleukin-10 and interleukin-10 receptor in human osteoarthritic and healthy chondrocytes. *Clinical and Experimental Rheumatology,* 19**,** 139-146.

IMAMURA, M., EZQUERRO, F., ALFIERI, F., BOAS, L. V., TOZETTO-MENDOZA, T. R., CHEN, J., OZCAKAR, L., ARENDT-NIELSEN, L. & BATTISTELLA, L. R. 2015. Serum Levels of Proinflammatory Cytokines in Painful Knee Osteoarthritis and Sensitizationd. *International Journal of Inflammation***,** 8.

JACKSON, D. A. 1993. STOPPING RULES IN PRINCIPAL COMPONENTS-ANALYSIS - A COMPARISON OF HEURISTIC AND STATISTICAL APPROACHES. *Ecology,* 74**,** 2204-2214.

JI, R. R. & SUTER, M. R. 2007. p38 MAPK, microglial signaling, and neuropathic pain. *Mol Pain,* 3**,** 33.

JOLLIFFE, I. T. & CADIMA, J. 2016. Principal component analysis: a review and recent developments. *Philos Trans A Math Phys Eng Sci,* 374**,** 20150202.

JONES, L., BEYNON, M. J., HOLT, C. A. & ROY, S. 2006. An application of the Dempster-Shafer theory of evidence to the classification of knee function and detection of improvement due to total knee replacement surgery. *Journal of Biomechanics,* 39**,** 2512-2520.

JORGENSEN, A. E., KJAER, M. & HEINEMEIER, K. M. 2017. The Effect of Aging and Mechanical Loading on the Metabolism of Articular Cartilage. *Journal of Rheumatology,* 44**,** 410-417.

JUNG, Y. K., KIM, G. W., PARK, H. R., LEE, E. J., CHOI, J. Y., BEIER, F. & HAN, S. W. 2013. Role of interleukin-10 in endochondral bone formation in mice: anabolic effect via the bone morphogenetic protein/Smad pathway. *Arthritis Rheum,* 65**,** 3153-64.

KADABA, M. P., RAMAKRISHNAN, H. K. & WOOTTEN, M. E. 1990. MEASUREMENT OF LOWER-EXTREMITY KINEMATICS DURING LEVEL WALKING. *Journal of Orthopaedic Research,* 8**,** 383-392.

KAISER, H. F. 1960. THE APPLICATION OF ELECTRONIC-COMPUTERS TO FACTOR-ANALYSIS. *Educational and Psychological Measurement,* 20**,** 141-151.

KAPOOR, M., MARTEL-PELLETIER, J., LAJEUNESSE, D., PELLETIER, J. P. & FAHMI, H. 2011. Role of proinflammatory cytokines in the pathophysiology of osteoarthritis. *Nature Reviews Rheumatology,* 7**,** 33-42.

KARSDAL, M. A., BAY-JENSEN, A. C., LORIES, R. J., ABRAMSON, S., SPECTOR, T., PASTOUREAU, P., CHRISTIANSEN, C., ATTUR, M., HENRIKSEN, K., GOLDRING, S. R. & KRAUS, V. 2014. The coupling of bone and cartilage turnover in osteoarthritis: opportunities for bone antiresorptives and anabolics as potential treatments? *Annals of the Rheumatic Diseases,* 73**,** 336-348.

KARSDAL, M. A., BAY-JENSEN, B. A. C., HENRIKSEN, K., RIIS, B. J. & CHRISTIANSEN, C. 2010. Biochemical markers identify influences on bone and cartilage degradation in osteoarthritis - the effect of sex, Kellgren-Lawrence (KL) score, Body Mass Index (BMI), oral salmon calcitonin (sCT) treatment and diurnal variation. *Bmc Musculoskeletal Disorders,* 11.

KAWAI, V. K., STEIN, C. M., PERRIEN, D. S. & GRIFFIN, M. R. 2012. Effects of anti-tumor necrosis factor alpha agents on bone. *Curr Opin Rheumatol,* 24**,** 576-85.

KELLGREN, J. H. & LAWRENCE, J. S. 1957. RADIOLOGICAL ASSESSMENT OF OSTEO-ARTHROSIS. *Annals of the Rheumatic Diseases,* 16**,** 494-502.

KHALAJ, N., ABU OSMAN, N. A., MOKHTAR, A. H., MEHDIKHANI, M. & WAN ABAS, W. A. 2014. Effect of exercise and gait retraining on knee adduction moment in people with knee osteoarthritis. *Proc Inst Mech Eng H,* 228**,** 190-9.

KHORASANI, M. S., DIKO, S., HSIA, A. W., ANDERSON, M. J., GENETOS, D. C., HAUDENSCHILD, D. R. & CHRISTIANSEN, B. A. 2015. Effect of alendronate on post-traumatic osteoarthritis induced by anterior cruciate ligament rupture in mice. *Arthritis Research & Therapy,* 17.

KIM, C. H., YOU, L., YELLOWLEY, C. E. & JACOBS, C. R. 2006a. Oscillatory fluid flow-induced shear stress decreases osteoclastogenesis through RANKL and OPG signaling. *Bone,* 39**,** 1043-1047.

KIM, H. A., CHO, M. L., CHOI, H. Y., YOON, C. S., JHUN, J. Y., OH, H. J. & KIM, H. Y. 2006b. The catabolic pathway mediated by Toll-like receptors in human osteoarthritic chondrocytes. *Arthritis and Rheumatism,* 54**,** 2152-2163.

KIM, J. H., KIM, A. R., CHOI, Y. H., JANG, S., WOO, G. H., CHA, J. H., BAK, E. J. & YOO, Y. J. 2017. Tumor necrosis factor-alpha antagonist diminishes osteocytic RANKL and sclerostin expression in diabetes rats with periodontitis. *PLoS One,* 12**,** e0189702.

KLUCZYNSKI, M. A., MARZO, J. M. & BISSON, L. J. 2013. Factors associated with meniscal tears and chondral lesions in patients undergoing anterior cruciate ligament reconstruction: a prospective study. *Am J Sports Med,* 41**,** 2759-65.

KNOOP, J., VAN DER LEEDEN, M., THORSTENSSON, C. A., ROORDA, L. D., LEMS, W. F., KNOL, D. L., STEULTJENS, M. P. M. & DEKKER, J. 2011. Identification of Phenotypes With Different Clinical Outcomes in Knee Osteoarthritis: Data From the Osteoarthritis Initiative. *Arthritis Care & Research,* 63**,** 1535-1542.

KNOWLES, H. J. & ATHANASOU, N. A. 2009. Canonical and non-canonical pathways of osteoclast formation. *Histol Histopathol,* 24**,** 337-46.

KNUTSEN, G., DROGSET, J. O., ENGEBRETSEN, L., GRONTVEDT, T., LUDVIGSEN, T. C., LOKEN, S., SOLHEIM, E., STRAND, T. & JOHANSEN, O. 2016. A Randomized Multicenter Trial Comparing Autologous Chondrocyte Implantation with Microfracture Long-Term Follow-up at 14 to 15 Years. *Journal of Bone and Joint Surgery-American Volume,* 98**,** 1332-1339.

KONG, S. Y., STABLER, T. V., CRISCIONE, L. G., ELLIOTT, A. L., JORDAN, J. M. & KRAUS, V. B. 2006. Diurnal variation of serum and urine biomarkers in patients with radiographic knee osteoarthritis. *Arthritis and Rheumatism,* 54**,** 2496-2504.

KOO, S. & ANDRIACCHI, T. P. 2008. The knee joint center of rotation is predominantly on the lateral side during normal walking. *J Biomech,* 41**,** 1269-73.

KOPF, J., PETERSEN, A., DUDA, G. N. & KNAUS, P. 2012. BMP2 and mechanical loading cooperatively regulate immediate early signalling events in the BMP pathway. *BMC Biol,* 10**,** 37.

KOYAMA, Y., MITSUI, N., SUZUKI, N., YANAGISAWA, M., SANUKI, R., ISOKAWA, K., SHIMIZU, N. & MAENO, M. 2008. Effect of compressive force on the expression of inflammatory cytokines and their receptors in osteoblastic Saos-2 cells. *Archives of Oral Biology,* 53**,** 488-496.

KRAMER, I., LOOTS, G. G., STUDER, A., KELLER, H. & KNEISSEL, M. 2010. Parathyroid hormone (PTH)-induced bone gain is blunted in SOST overexpressing and deficient mice. *J Bone Miner Res,* 25**,** 178-89.

KRAUS, V. B., BURNETT, B., COINDREAU, J., COTTRELL, S., EYRE, D., GENDREAU, M., GARDINER, J., GARNERO, P., HARDIN, J., HENROTIN, Y., HEINEGARD, D., KO, A., LOHMANDER, L. S., MATTHEWS, G., MENETSKI, J., MOSKOWITZ, R., PERSIANI, S., POOLE, A. R., ROUSSEAU, J. C. & TODMAN, M. 2011. Application of biomarkers in the development of drugs intended for the treatment of osteoarthritis. *Osteoarthritis and Cartilage,* 19**,** 515-542.

KRAUS, V. B., COLLINS, J. E., HARGROVE, D., LOSINA, E., NEVITT, M., KATZ, J. N., WANG, S. X., SANDELL, L. J., HOFFMANN, S. C. & HUNTER, D. J. 2017. Predictive validity of biochemical biomarkers in knee osteoarthritis: data from the FNIH OA Biomarkers Consortium. *Annals of the Rheumatic Diseases,* 76**,** 186-195.

KRISHNAN, V., BRYANT, H. U. & MACDOUGALD, O. A. 2006. Regulation of bone mass by Wnt signaling. *Journal of Clinical Investigation,* 116**,** 1202-1209.

KURTZ, S., ONG, K., LAU, E., MOWAT, F. & HALPERN, M. 2007. Projections of primary and revision hip and knee arthroplasty in the United States from 2005 to 2030. *Journal of Bone and Joint Surgery-American Volume,* 89A**,** 780-785.

KUSUMI, A., SAKAKI, H., KUSUMI, T., ODA, M., NARITA, K., NAKAGAWA, H., KUBOTA, K., SATOH, H. & KIMURA, H. 2005. Regulation of synthesis of osteoprotegerin and soluble receptor activator of nuclear factor-kappaB ligand in normal human osteoblasts via the p38 mitogen-activated protein kinase pathway by the application of cyclic tensile strain. *J Bone Miner Metab,* 23**,** 373-81.

KUTZNER, I., HEINLEIN, B., GRAICHEN, F., BENDER, A., ROHLMANN, A., HALDER, A., BEIER, A. & BERGMANN, G. 2010. Loading of the knee joint during activities of daily living measured in vivo in five subjects. *Journal of Biomechanics,* 43**,** 2164-2173.

KUTZNER, I., TREPCZYNSKI, A., HELLER, M. O. & BERGMANN, G. 2013. Knee Adduction Moment and Medial Contact Force - Facts about Their Correlation during Gait. *Plos One,* 8.

LAM, J., TAKESHITA, S., BARKER, J. E., KANAGAWA, O., ROSS, F. P. & TEITELBAUM, S. L. 2000. TNF-alpha induces osteoclastogenesis by direct stimulation of macrophages exposed to permissive levels of RANK ligand. *Journal of Clinical Investigation,* 106**,** 1481-1488.

LANDRY, S. C., MCKEAN, K. A., HUBLEY-KOZEY, C. L., STANISH, W. D. & DELUZIO, K. J. 2007. Knee biomechanics of moderate OA patients measured during gait at a self-selected and fast walking speed. *Journal of Biomechanics,* 40**,** 1754-1761.

LANSDOWN, D. A., WANG, K., COTTER, E., DAVEY, A. & COLE, B. J. 2018. Relationship Between Quantitative MRI Biomarkers and Patient-Reported Outcome Measures After Cartilage Repair Surgery: A Systematic Review. *Orthopaedic Journal of Sports Medicine,* 6.

LASMAR, N. P., LASMAR, R. C., VIEIRA, R. B., DE OLIVEIRA, J. R. & SCARPA, A. C. 2011. ASSESSMENT OF THE REPRODUCIBILITY OF THE OUTERBRIDGE AND FSA CLASSIFICATIONS FOR CHONDRAL LESIONS OF THE KNEE. *Rev Bras Ortop,* 46**,** 266-9.

LAYTON, A., ARNOLD, R. J., GRAHAM, J., FRASCO, M. A., COTE, E. & LYNCH, N. M. 2015. LONG-TERM FAILURE RATES ASSOCIATED WITH KNEE MICROFRACTURE SURGERY. *Value in Health,* 18**,** A156-A156.

LEE, H.-S. & SALTER, D. 2015. *Biomechanics of Cartilage and Osteoarthritis, Osteoarthritis - Progress in Basic Research and Treatment,* Qian Chen, IntechOpen.

LEE, S. H., LEE, O. S., TEO, S. H. & LEE, Y. S. 2017. (Change) in gait after high tibial osteotomy: A systematic review and meta-analysis. *Gait & Posture,* 57**,** 57-68.

LEGRAND, C. B., LAMBERT, C. J., COMBLAIN, F. V., SANCHEZ, C. & HENROTIN, Y. E. 2017. Review of Soluble Biomarkers of Osteoarthritis: Lessons From Animal Models. *Cartilage,* 8**,** 211-233.

LEONG, D. J., GU, X. I., LI, Y. H., LEE, J. Y., LAUDIER, D. M., MAJESKA, R. J., SCHAFFLER, M. B., CARDOSO, L. & SUN, H. B. 2010. Matrix metalloproteinase-3 in articular cartilage is upregulated by joint immobilization and suppressed by passive joint motion. *Matrix Biology,* 29**,** 420-426.

LEQUIN, R. M. 2005. Enzyme immunoassay (EIA)/enzyme-linked immunosorbent assay (ELISA). *Clin Chem,* 51**,** 2415-8.

LEVANGE, P. K. & NORKIN, C. C. 2011. *Joint Structure and Function; A Comprehensive Analysis*, DavisPlus.

LEWEK, M. D., RAMSEY, D. K., SNYDER-MACKLER, L. & RUDOLPH, K. S. 2005. Knee stabilization in patients with medial compartment knee osteoarthritis. *Arthritis Rheum,* 52**,** 2845-53.

LEWIECKI, E. M. 2014. Role of sclerostin in bone and cartilage and its potential as a therapeutic target in bone diseases. *Ther Adv Musculoskelet Dis,* 6**,** 48-57.

LEWINSON, R. T. & STEFANYSHYN, D. J. 2016. Wedged Insoles and Gait in Patients with Knee Osteoarthritis: A Biomechanical Review. *Ann Biomed Eng,* 44**,** 3173-3185.

LI, C., YANG, Y., WU, D., LI, T., YIN, Y. & LI, G. 2016. Improvement of enzyme-linked immunosorbent assay for the multicolor detection of biomarkers. *Chem Sci,* 7**,** 3011-3016.

LI, X. D., OMINSKY, M. S., NIU, Q. T., SUN, N., DAUGHERTY, B., D'AGOSTIN, D., KURAHARA, C., GAO, Y. M., CAO, J., GONG, J. H., ASUNCION, F., BARRERO, M., WARMINGTON, K., DWYER, D., STOLINA, M., MORONY, S., SAROSI, I., KOSTENUIK, P. J., LACEY, D. L., SIMONET, W. S., KE, H. Z. & PASZTY, C. 2008. Targeted deletion of the sclerostin gene in mice results in increased bone formation and bone strength. *Journal of Bone and Mineral Research,* 23**,** 860-869.

LI, X. F., ZHANG, Y. Z., KANG, H. S., LIU, W. Z., LIU, P., ZHANG, J. G., HARRIS, S. E. & WU, D. Q. 2005. Sclerostin binds to LRP5/6 and antagonizes canonical Wnt signaling. *Journal of Biological Chemistry,* 280**,** 19883-19887.

LI, Y., GE, C., LONG, J. P., BEGUN, D. L., RODRIGUEZ, J. A., GOLDSTEIN, S. A. & FRANCESCHI, R. T. 2012. Biomechanical stimulation of osteoblast gene expression requires phosphorylation of the RUNX2 transcription factor. *J Bone Miner Res,* 27**,** 1263-74.

LIEBERTHAL, J., SAMBAMURTHY, N. & SCANZELLO, C. R. 2015. Inflammation in joint injury and post-traumatic osteoarthritis. *Osteoarthritis and Cartilage,* 23**,** 1825-1834.

LIEDERT, A., KASPAR, D., BLAKYTNY, R., CLAES, L. & IGNATIUS, A. 2006. Signal transduction pathways involved in mechanotransduction in bone cells. *Biochemical and Biophysical Research Communications,* 349**,** 1-5.

LIN, C., JIANG, X., DAI, Z., GUO, X., WENG, T., WANG, J., LI, Y., FENG, G., GAO, X. & HE, L. 2009. Sclerostin mediates bone response to mechanical unloading through antagonizing Wnt/beta-catenin signaling. *J Bone Miner Res,* 24**,** 1651-61.

LIN, T. H., YANG, R. S., TANG, C. H., WU, M. Y. & FU, W. M. 2008. Regulation of the maturation of osteoblasts and osteoclastogenesis by glutamate. *European Journal of Pharmacology,* 589**,** 37-44.

LIU, D. W., YAO, S. M. & WISE, G. E. 2006. Effect of interleukin-10 on gene expression of osteoclastogenic regulatory molecules in the rat dental follicle. *European Journal of Oral Sciences,* 114**,** 42-49.

LIU, J., ZHAO, Z., ZOU, L., LI, J., WANG, F., LI, X., ZHANG, J., LIU, Y., CHEN, S., ZHI, M. & WANG, J. 2009. Pressure-loaded MSCs during early osteodifferentiation promote osteoclastogenesis by increase of RANKL/OPG ratio. *Ann Biomed Eng,* 37**,** 794-802.

LIU-BRYAN, R. & TERKELTAUB, R. 2015. Emerging regulators of the inflammatory process in osteoarthritis. *Nature Reviews Rheumatology,* 11**,** 35-44.

LO, G. H., HUNTER, D. J., ZHANG, Y. Q., MCLENNAN, C. E., LAVALLEY, M. P., KIEL, D. P., MCLEAN, R. R., GENANT, H. K., GUERMAZI, A. & FELSON, D. T. 2005. Bone marrow lesions in the knee are associated with increased local bone density. *Arthritis and Rheumatism,* 52**,** 2814-2821.

LOESER, R. F. 2014. Integrins and chondrocyte-matrix interactions in articular cartilage. *Matrix Biology,* 39**,** 11-16.

LOESER, R. F., COLLINS, J. A. & DIEKMAN, B. O. 2016. Ageing and the pathogenesis of osteoarthritis. *Nature Reviews Rheumatology,* 12**,** 412-420.

LOESER, R. F., GOLDRING, S. R., SCANZELLO, C. R. & GOLDRING, M. B. 2012. Osteoarthritis: A disease of the joint as an organ. *Arthritis and Rheumatism,* 64**,** 1697-1707.

LOGAN, M., DUNSTAN, E., ROBINSON, J., WILLIAMS, A., GEDROYC, W. & FREEMAN, M. 2004. Tibiofemoral kinematics of the anterior cruciate ligament (ACL)-deficient weightbearing, living knee employing vertical access open "interventional" multiple resonance imaging. *American Journal of Sports Medicine,* 32**,** 720-726.

LOTZ, M., MARTEL-PELLETIER, J., CHRISTIANSEN, C., BRANDI, M. L., BRUYERE, O., CHAPURLAT, R., COLLETTE, J., COOPER, C., GIACOVELLI, G., KANIS, J. A., KARSDAL, M. A., KRAUS, V., LEMS, W. F., MEULENBELT, I., PELLETIER, J. P., RAYNAULD, J. P., REITER-NIESERT, S., RIZZOLI, R., SANDELL, L. J., VAN SPIL, W. E. & REGINSTER, J. Y. 2013. Value of biomarkers in osteoarthritis: current status and perspectives. *Annals of the Rheumatic Diseases,* 72**,** 1756-1763.

LUZ-CRAWFORD, P., KURTE, M., BRAVO-ALEGRIA, J., CONTRERAS, R., NOVA-LAMPERTI, E., TEJEDOR, G., NOEL, D., JORGENSEN, C., FIGUEROA, F., DJOUAD, F. & CARRION, F. 2013. Mesenchymal stem cells generate a CD4+CD25+Foxp3+ regulatory T cell population during the differentiation process of Th1 and Th17 cells. *Stem Cell Res Ther,* 4**,** 65.

MABEY, T. & HONSAWEK, S. 2015. Cytokines as biochemical markers for knee osteoarthritis. *World J Orthop,* 6**,** 95-105.

MABILLEAU, G., PASCARETTI-GRIZON, F., BASLE, M. F. & CHAPPARD, D. 2012. Depth and volume of resorption induced by osteoclasts generated in the presence of RANKL, TNF-alpha/IL-1 or LIGHT. *Cytokine,* 57**,** 294-9.

MACKINNON, P. C. B. 2005. Oxford textbook of functional anatomy. Vol. 1 Musculoskeletal system. *Oxford University Press,* 1.

MAFFULLI, N., BINFIELD, P. M. & KING, J. B. 2003. Articular cartilage lesions in the symptomatic anterior cruciate ligament-deficient knee. *Arthroscopy-the Journal of Arthroscopic and Related Surgery,* 19**,** 685-690.

MAGNUSSEN, R. A., DUNN, W. R., CAREY, J. L. & SPINDLER, K. P. 2008. Treatment of focal articular cartilage defects in the knee. *Clinical Orthopaedics and Related Research,* 466**,** 952-962.

MAKRIS, E. A., HADIDI, P. & ATHANASIOU, K. A. 2011. The knee meniscus: structure-function, pathophysiology, current repair techniques, and prospects for regeneration. *Biomaterials,* 32**,** 7411-31.

MALEFYT, R. D., FIGDOR, C. G., HUIJBENS, R., MOHANPETERSON, S., BENNETT, B., CULPEPPER, J., DANG, W., ZURAWSKI, G. & DEVRIES, J. E. 1993. Effects of Il-13 on Phenotype, Cytokine Production, and Cytotoxic Function of Human Monocytes - Comparison with Il-4 and Modulation by Ifn-Gamma or Il-10. *Journal of Immunology,* 151**,** 6370-6381.

MARTEL-PELLETIER, J. 1999. Pathophysiology of osteoarthritis. *Osteoarthritis and Cartilage,* 7**,** 371-373.

MARUOTTI, N., CORRADO, A. & CANTATORE, F. P. 2017. Osteoblast role in osteoarthritis pathogenesis. *J Cell Physiol,* 232**,** 2957-2963.

MASON, D. J. 2004. The role of glutamate transporters in bone cell signalling. *Journal of Musculoskeletal and Neuronal Interactions,* 4**,** 128-31.

MASON, D. J., SUVA, L. J., GENEVER, P. G., PATTON, A. J., STEUCKLE, S., HILLAM, R. A. & SKERRY, T. M. 1997. Mechanically regulated expression of a neural glutamate transporter in bone: A role for excitatory amino acids as osteotropic agents? *Bone,* 20**,** 199-205.

MATHIEU, M. C., LORD-DUFOUR, S., BERNIER, V., BOIE, Y., BURCH, J. D., CLARK, P., DENIS, D., HAN, Y., MORTIMER, J. R. & THERIEN, A. G. 2008. Mutual antagonistic relationship between prostaglandin E-2 and IFN-gamma: Implications for rheumatoid arthritis. *European Journal of Immunology,* 38**,** 1900-1912.

MATZAT, S. J., VAN TIEL, J., GOLD, G. E. & OEI, E. H. G. 2013. Quantitative MRI techniques of cartilage composition. *Quantitative Imaging in Medicine and Surgery,* 3**,** 162-174.

MCDANIEL, G., MITCHELL, K. L., CHARLES, C. & KRAUS, V. B. 2010. A comparison of five approaches to measurement of anatomic knee alignment from radiographs. *Osteoarthritis and Cartilage,* 18**,** 273-277.

MCNEARNEY, T., SPEEGLE, D., LAWAND, N., LISSE, J. & WESTLUND, K. N. 2000. Excitatory amino acid profiles of synovial fluid from patients with arthritis. *Journal of Rheumatology,* 27**,** 739-745.

MENTAVERRI, R., KAMEL, S., WATTEL, A., PROUILLET, C., SEVENET, N., PETIT, J. P., TORDJMANN, T. & BRAZIER, M. 2003. Regulation of bone resorption and osteoclast survival by nitric oxide: Possible involvement of NMDA-receptor. *Journal of Cellular Biochemistry,* 88**,** 1145-1156.

MERLE, B., ITZSTEIN, C., DELMAS, P. D. & CHENU, C. 2003. NMDA glutamate receptors are expressed by osteoclast precursors and involved in the regulation of osteoclastogenesis. *Journal of Cellular Biochemistry,* 90**,** 424-436.

MERZ, D., LIU, R., JOHNSON, K. & TERKELTAUB, R. 2003. IL-8/CXCL8 and growth-related oncogene alpha/CXCL1 induce chondrocyte hypertrophic differentiation. *Journal of Immunology,* 171**,** 4406-4415.

MILLWARD-SADLER, S. J. & SALTER, D. M. 2004. Integrin-dependent signal cascades in chondrocyte mechanotransduction. *Annals of Biomedical Engineering,* 32**,** 435-446.

MITHOEFER, K. 2013. Complex Articular Cartilage Restoration. *Sports Medicine and Arthroscopy Review,* 21**,** 31-37.

MITHOEFER, K., WILLIAMS, R. J., WARREN, R. F., WICKIEWICZ, T. L. & MARX, R. G. 2006. High-impact athletics after knee articular cartilage repair - A prospective evaluation of the microfracture technique. *American Journal of Sports Medicine,* 34**,** 1413-1418.

MIYAZAKI, T., WADA, M., KAWAHARA, H., SATO, M., BABA, H. & SHIMADA, S. 2002. Dynamic load at baseline can predict radiographic disease progression in medial compartment knee osteoarthritis. *Annals of the Rheumatic Diseases,* 61**,** 617-622.

MOBASHERI, A. 2013. The future of osteoarthritis therapeutics: emerging biological therapy. *Curr Rheumatol Rep,* 15**,** 385.

MOBASHERI, A., RAYMAN, M. P., GUALILLO, O., SELLAM, J., VAN DER KRAAN, P. & FEARON, U. 2017. The role of metabolism in the pathogenesis of osteoarthritis. *Nature Reviews Rheumatology,* 13**,** 302-311.

MOLINA-HOLGADO, E., ORTIZ, S., MOLINA-HOLGADO, F. & GUAZA, C. 2000. Induction of COX-2 and PGE(2) biosynthesis by IL-1beta is mediated by PKC and mitogen-activated protein kinases in murine astrocytes. *Br J Pharmacol,* 131**,** 152-9.

MOORE, K. W., DE WAAL MALEFYT, R., COFFMAN, R. L. & O'GARRA, A. 2001. Interleukin-10 and the interleukin-10 receptor. *Annu Rev Immunol,* 19**,** 683-765.

MORIMOTO, R., UEHARA, S., YATSUSHIRO, S., JUGE, N., HUA, Z., SENOH, S., ECHIGO, N., HAYASHI, M., MIZOGUCHI, T., NINOMIYA, T., UDAGAWA, N., OMOTE, H., YAMAMOTO, A., EDWARDS, R. H. & MORIYAMA, Y. 2006. Secretion of L-glutamate from osteoclasts through transcytosis. *Embo j,* 25**,** 4175-86.

MORIN, V., PAILHE, R., DUVAL, B. R., MADER, R., COGNAULT, J., ROUCHY, R. C. & SARAGAGLIA, D. 2018. Gait analysis following medial opening-wedge high tibial osteotomy. *Knee Surgery Sports Traumatology Arthroscopy,* 26**,** 1838-1844.

MOSSER, D. M. & ZHANG, X. 2008. Interleukin-10: new perspectives on an old cytokine. *Immunol Rev,* 226**,** 205-18.

MOW, V. C. H., W.C. 1991. *Basic Orthopaedic Biomechanics*.

MUNDERMANN, A., DYRBY, C. O. & ANDRIACCHI, T. P. 2005a. Secondary gait changes in patients with medial compartment knee osteoarthritis - Increased load at the ankle, knee, and hip during walking. *Arthritis and Rheumatism,* 52**,** 2835-2844.

MUNDERMANN, A., DYRBY, C. O., ANDRIACCHI, T. P. & KING, K. B. 2005b. Serum concentration of cartilage oligomeric matrix protein (COMP) is sensitive to physiological cyclic loading in healthy adults. *Osteoarthritis and Cartilage,* 13**,** 34-38.

MUNDERMANN, A., DYRBY, C. O., HURWITZ, D. E., SHARMA, L. & ANDRIACCHI, T. P. 2004. Potential strategies to reduce medial compartment loading in patients with knee

osteoarthritis of varying severity - Reduced walking speed. *Arthritis and Rheumatism,* 50**,** 1172-1178.

MURATOVIC, D., CICUTTINI, F. M., WLUKA, A., FINDLAY, D., WANG, Y. Y., OTTO, S., TAYLOR, D., HUMPHRIES, J., LEE, Y., LABRINIDIS, A., WILLIAMS, R. & KULIWABA, J. 2016. Bone marrow lesions detected by specific combination of MRI sequences are associated with severity of osteochondral degeneration. *Arthritis Research & Therapy,* 18.

MURRAY, D. W., CARR, A. J. & BULSTRODE, C. 1993. SURVIVAL ANALYSIS OF JOINT REPLACEMENTS. *Journal of Bone and Joint Surgery-British Volume,* 75**,** 697-704.

NEOGI, T. 2012. Clinical significance of bone changes in osteoarthritis. *Ther Adv Musculoskelet Dis,* 4**,** 259-67.

NEPTUNE, R. R., SASAKI, K. & KAUTZ, S. A. 2008. The effect of walking speed on muscle function and mechanical energetics. *Gait & Posture,* 28**,** 135-143.

NIKAHVAL, B., NAZIFI, S., HEIDARI, F. & KHAFI, M. S. A. 2016. Evaluation of the changes of P1NP and CTX in synovial fluid and blood serum of dogs with experimental osteoarthritis. *Comparative Clinical Pathology,* 25**,** 559-563.

ODGREN, P. R., KIM, N., MACKAY, C. A., MASON-SAVAS, A., CHOI, Y. & MARKS, S. C., JR. 2003. The role of RANKL (TRANCE/TNFSF11), a tumor necrosis factor family member, in skeletal development: effects of gene knockout and transgenic rescue. *Connect Tissue Res,* 44 Suppl 1**,** 264-71.

OLKKU, A. & MAHONEN, A. 2008. Wnt and steroid pathways control glutamate signalling by regulating glutamine synthetase activity in osteoblastic cells. *Bone,* 43**,** 483-93.

ONOE, Y., MIYAURA, C., KAMINAKAYASHIKI, T., NAGAI, Y., NOGUCHI, K., CHEN, Q. R., SEO, H., OHTA, H., NOZAWA, S., KUDO, I. & SUDA, T. 1996. IL-13 and IL-4 inhibit bone resorption by suppressing cyclooxygenase-2-dependent prostaglandin synthesis in osteoblasts. *Journal of Immunology,* 156**,** 758-764.

OSTA, B., BENEDETTI, G. & MIOSSEC, P. 2014. Classical and paradoxical effects of TNF-alpha on bone homeostasis. *Frontiers in Immunology,* 5.

PASCUAL-GARRIDO, C., DALEY, E., VERMA, N. N. & COLE, B. J. 2017. A Comparison of the Outcomes for Cartilage Defects of the Knee Treated With Biologic Resurfacing Versus Focal Metallic Implants. *Arthroscopy-the Journal of Arthroscopic and Related Surgery,* 33**,** 364-373.

PEET, N. M., GRABOWSKI, P. S., LAKETIC-LJUBOJEVIC, I. & SKERRY, T. M. 1999. The glutamate receptor antagonist MK801 modulates bone resorption in vitro by a mechanism predominantly involving osteoclast differentiation. *Faseb Journal,* 13**,** 2179-2185.

PELLETIER, J. P., MARTEL-PELLETIER, J. & ABRAMSON, S. B. 2001. Osteoarthritis, an inflammatory disease - Potential implication for the selection of new therapeutic targets. *Arthritis and Rheumatism,* 44**,** 1237-1247.

PERS, Y. M., RUIZ, M., NOEL, D. & JORGENSEN, C. 2015. Mesenchymal stem cells for the management of inflammation in osteoarthritis: state of the art and perspectives. *Osteoarthritis Cartilage,* 23**,** 2027-35.

PIEPOLI, T., MENNUNI, L., ZERBI, S., LANZA, M., ROVATI, L. C. & CASELLI, G. 2009. Glutamate signaling in chondrocytes and the potential involvement of NMDA receptors in cell proliferation and inflammatory gene expression. *Osteoarthritis Cartilage,* 17**,** 1076-83.

PIETROSIMONE, B., LOESER, R. F., BLACKBURN, J. T., PADUA, D. A., HARKEY, M. S., STANLEY, L. E., LUC-HARKEY, B. A., ULICI, V., MARSHALL, S. W., JORDAN, J. M. & SPANG, J. T. 2017. Biochemical Markers of Cartilage Metabolism Are Associated With Walking Biomechanics 6-Months Following Anterior Cruciate Ligament Reconstruction. *Journal of Orthopaedic Research,* 35**,** 2288-2297.

PLUNKETT, J. A., YU, C. G., EASTON, J. M., BETHEA, J. R. & YEZIERSKI, R. P. 2001. Effects of interleukin-10 (IL-10) on pain behavior and gene expression following excitotoxic spinal cord injury in the rat. *Experimental Neurology,* 168**,** 144-154.

POOLE, A. R., MATSUI, Y., HINEK, A. & LEE, E. R. 1989. Cartilage macromolecules and the calcification of cartilage matrix. *Anat Rec,* 224**,** 167-79.

PRIDIE, K. H. & GORDON, G. 1959. A METHOD OF RESURFACING OSTEOARTHRITIC KNEE JOINTS. *Journal of Bone and Joint Surgery-British Volume,* 41**,** 618-619.

QUATMAN, C. E., HARRIS, J. D. & HEWETT, T. E. 2012. Biomechanical outcomes of cartilage repair of the knee. *J Knee Surg,* 25**,** 197-206.

RADIN, E. L. & ROSE, R. M. 1986. Role of Subchondral Bone in the Initiation and Progression of Cartilage Damage. *Clinical Orthopaedics and Related Research***,** 34-40.

RADZIMSKI, A. O., MUNDERMANN, A. & SOLE, G. 2012. Effect of footwear on the external knee adduction moment - A systematic review. *Knee,* 19**,** 163-175.

RAGGATT, L. J. & PARTRIDGE, N. C. 2010. Cellular and molecular mechanisms of bone remodeling. *J Biol Chem,* 285**,** 25103-8.

RANDSBORG, P. H., BRINCHMANN, J., LOKEN, S., HANVOLD, H. A., AAE, T. F. & AROEN, A. 2016. Focal cartilage defects in the knee - a randomized controlled trial comparing autologous chondrocyte implantation with arthroscopic debridement. *BMC Musculoskelet Disord,* 17**,** 117.

RECKLIES, A. D., BAILLARGEON, L. & WHITE, C. 1998. Regulation of cartilage oligomeric matrix protein synthesis in human synovial cells and articular chondrocytes. *Arthritis Rheum,* 41**,** 997-1006.

RIGOGLOU, S. & PAPAVASSILIOU, A. G. 2013. The NF-kappa B signalling pathway in osteoarthritis. *International Journal of Biochemistry & Cell Biology,* 45**,** 2580-2584.

ROBBINS, S. M. & MALY, M. R. 2009. The effect of gait speed on the knee adduction moment depends on waveform summary measures. *Gait Posture,* 30**,** 543-6.

ROBERTSON, D. G. E., CALDWELL, G. E., HAMILL, J., KAMEN, G. & WHITTLESEY, S. N. 2013. *Research Methods in Biomechanics*.

ROBLING, A. G., NIZIOLEK, P. J., BALDRIDGE, L. A., CONDON, K. W., ALLEN, M. R., ALAM, I., MANTILA, S. M., GLUHAK-HEINRICH, J., BELLIDO, T. M., HARRIS, S. E. & TURNER, C. H. 2008. Mechanical stimulation of bone in vivo reduces osteocyte expression of Sost/sclerostin. *J Biol Chem,* 283**,** 5866-75.

ROBLING, A. G. & TURNER, C. H. 2009. Mechanical signaling for bone modeling and remodeling. *Crit Rev Eukaryot Gene Expr,* 19**,** 319-38.

RODRIGUEZ-MERCHAN, E. C. 2012. Knee instruments and rating scales designed to measure outcomes. *J Orthop Traumatol,* 13**,** 1-6.

ROE, J., SALMON, L., WALLER, A. & SCANELLI, J. 2012. 10 year outcome of high tibial osteotomy for medial compartment osteoarthritis of the knee. *Journal of Science and Medicine in Sport,* 15**,** 244-245.

ROEMER, F. W., GUERMAZI, A., HUNTER, D. J., NIU, J., ZHANG, Y., ENGLUND, M., JAVAID, M. K., LYNCH, J. A., MOHR, A., TORNER, J., LEWIS, C. E., NEVITT, M. C. & FELSON, D. T. 2009. The association of meniscal damage with joint effusion in persons without radiographic osteoarthritis: the Framingham and MOST osteoarthritis studies. *Osteoarthritis Cartilage,* 17**,** 748-53.

ROOS, E. M. 2005. Joint injury causes knee osteoarthritis in young adults. *Curr Opin Rheumatol,* 17**,** 195-200.

ROOS, E. M. & LOHMANDER, L. S. 2003. The Knee injury and Osteoarthritis Outcome Score (KOOS): from joint injury to osteoarthritis. *Health Qual Life Outcomes,* 1**,** 64.

ROOS, E. M., ROOS, H. P., LOHMANDER, L. S., EKDAHL, C. & BEYNNON, B. D. 1998. Knee injury and osteoarthritis outcome score (KOOS) - Development of a self-administered outcome measure. *Journal of Orthopaedic & Sports Physical Therapy,* 28**,** 88-96.

SABOKBAR, A., MAHONEY, D. J., HEMINGWAY, F. & ATHANASOU, N. A. 2016. Non-Canonical (RANKL-Independent) Pathways of Osteoclast Differentiation and Their Role in Musculoskeletal Diseases. *Clin Rev Allergy Immunol,* 51**,** 16-26.

SAH, R. L. Y., KIM, Y. J., DOONG J-Y, H., GRODZINSKY, A. J., PLAAS, A. H. K. & SANDY, J. D. 1989. BIOSYNTHETIC RESPONSE OF CARTILAGE EXPLANTS TO DYNAMIC COMPRESSION. *Journal of Orthopaedic Research,* 7**,** 619-636.

SALTER, D. M., MILLWARD-SADLER, S. J., NUKI, G. & WRIGHT, M. O. 2001. Integrin-interleukin-4 mechanotransduction pathways in human chondrocytes. *Clinical Orthopaedics and Related Research***,** S49-S60.

SALTER, D. M., MILLWARD-SADLER, S. J., NUKI, G. & WRIGHT, M. O. 2002. Differential responses of chondrocytes from normal and osteoarthritic human articular cartilage to mechanical stimulation. *Biorheology,* 39**,** 97-108.

SANCHEZ, C., GABAY, O., SALVAT, C., HENROTIN, Y. E. & BERENBAUM, F. 2009. Mechanical loading highly increases IL-6 production and decreases OPG expression by osteoblasts. *Osteoarthritis and Cartilage,* 17**,** 473-481.

SANCHEZ-ADAMS, J., LEDDY, H. A., MCNULTY, A. L., O'CONOR, C. J. & GUILAK, F. 2014. The Mechanobiology of Articular Cartilage: Bearing the Burden of Osteoarthritis. *Current Rheumatology Reports,* 16**,** 9.

SCANZELLO, C. R. 2017. Chemokines and Inflammation in Osteoarthritis: Insights From Patients and Animal Models. *Journal of Orthopaedic Research,* 35**,** 735-739.

SCANZELLO, C. R. & GOLDRING, S. R. 2012. The role of synovitis in osteoarthritis pathogenesis. *Bone,* 51**,** 249-257.

SCANZELLO, C. R., PLAAS, A. & CROW, M. K. 2008. Innate immune system activation in osteoarthritis: is osteoarthritis a chronic wound? *Current Opinion in Rheumatology,* 20**,** 565-572.

SCHIPPLEIN, O. D. & ANDRIACCHI, T. P. 1991. Interaction between Active and Passive Knee Stabilizers during Levelwalking. *Journal of Orthopaedic Research,* 9**,** 113-119.

SCHMITT, L. C. & RUDOLPH, K. S. 2008. Muscle stabilization strategies in people with medial knee osteoarthritis: The effect of instability. *Journal of Orthopaedic Research,* 26**,** 1180-1185.

SEBASTIAN, A. & LOOTS, G. G. 2017. Transcriptional control of Sost in bone. *Bone,* 96**,** 76-84.

SEEDHOM, B. B. 2006. Conditioning of cartilage during normal activities is an important factor in the development of osteoarthritis. *Rheumatology (Oxford),* 45**,** 146-9.

SEO, S. S., KIM, C. W. & JUNG, D. W. 2011. Management of focal chondral lesion in the knee joint. *Knee Surg Relat Res,* 23**,** 185-96.

SHAO, Q. D., LI, Y. F., WANG, Q. & ZHAO, J. N. 2015. IL-10 and IL-1 beta Mediate Neuropathic-Pain Like Behavior in the Ventrolateral Orbital Cortex. *Neurochemical Research,* 40**,** 733-739.

SHARMA, L., HURWITZ, D. E., THONAR, E., SUM, J. A., LENZ, M. E., DUNLOP, D. D., SCHNITZER, T. J., KIRWAN-MELLIS, G. & ANDRIACCHI, T. P. 1998. Knee adduction moment, serum hyaluronan level, and disease severity in medial tibiofemoral osteoarthritis. *Arthritis and Rheumatism,* 41**,** 1233-1240.

SHARMA, L., SONG, J., FELSON, D. T., CAHUE, S., SHAMIYEH, E. & DUNLOP, D. D. 2001. The role of knee alignment in disease progression and functional decline in knee osteoarthritis. *Jama-Journal of the American Medical Association,* 286**,** 188-195.

SHEN, K. F., ZHU, H. Q., WEI, X. H., WANG, J., LI, Y. Y., PANG, R. P. & LIU, X. G. 2013. Interleukin-10 down-regulates voltage gated sodium channels in rat dorsal root ganglion neurons. *Experimental Neurology,* 247**,** 466-475.

SHRADER, M. W., DRAGANICH, L. F., POTTENGER, L. A. & PIOTROWSKI, G. A. 2004. Effects of knee pain relief in osteoarthritis on gait and stair-stepping. *Clinical Orthopaedics and Related Research***,** 188-193.

SIMIC, M., HINMAN, R. S., WRIGLEY, T. V., BENNELL, K. L. & HUNT, M. A. 2011. Gait Modification Strategies for Altering Medial Knee Joint Load: A Systematic Review. *Arthritis Care & Research,* 63**,** 405-426.

SLATTERY, C. & KWEON, C. Y. 2018. Classifications in Brief: Outerbridge Classification of Chondral Lesions. *Clin Orthop Relat Res,* 476**,** 2101-2104.

SOLHEIM, E., HEGNA, J., INDERHAUG, E., OYEN, J., HARLEM, T. & STRAND, T. 2016. Results at 10-14 years after microfracture treatment of articular cartilage defects in the knee. *Knee Surgery Sports Traumatology Arthroscopy,* 24**,** 1587-1593.

SONEKATSU, M., TANIGUCHI, W., YAMANAKA, M., NISHIO, N., TSUTSUI, S., YAMADA, H., YOSHIDA, M. & NAKATSUKA, T. 2016. Interferon-gamma potentiates NMDA receptor signaling in spinal dorsal horn neurons via microglia-neuron interaction. *Mol Pain,* 12.

SOWERS, M. F., KARVONEN-GUTIERREZ, C. A., YOSEF, M., JANNAUSCH, M., JIANG, Y., GARNERO, P. & JACOBSON, J. 2009. Longitudinal changes of serum COMP and urinary CTX-II predict X-ray defined knee osteoarthritis severity and stiffness in women. *Osteoarthritis and Cartilage,* 17**,** 1609-1614.

SPAHN, G. & HOFMANN, G. O. 2014. Focal Cartilage Defects within the Medial Knee Compartment. Predictors for Osteoarthritis Progression. *Zeitschrift Fur Orthopadie Und Unfallchirurgie,* 152**,** 480-488.

STANTON, H., UNG, L. & FOSANG, A. J. 2002. The 45 kDa collagen-binding fragment of fibronectin induces matrix metalloproteinase-13 synthesis by chondrocytes and aggrecan degradation by aggrecanases. *Biochem J,* 364**,** 181-90.

STEEVE, K. T., MARC, P., SANDRINE, T., DOMINIQUE, H. & YANNICK, F. 2004. IL-6, RANKL, TNF-alpha/IL-1: interrelations in bone resorption pathophysiology. *Cytokine & Growth Factor Reviews,* 15**,** 49-60.

STREICH, N. A., ZIMMERMANN, D., SCHMITT, H. & BODE, G. 2011. Biochemical markers in the diagnosis of chondral defects following anterior cruciate ligament insufficiency. *International Orthopaedics,* 35**,** 1633-1637.

STRUGLICS, A., LARSSON, S., KUMAHASHI, N., FROBELL, R. & LOHMANDER, L. S. 2015. Changes in Cytokines and Aggrecan ARGS Neoepitope in Synovial Fluid and Serum and in C-Terminal Crosslinking Telopeptide of Type II Collagen and N-Terminal Crosslinking Telopeptide of Type I Collagen in Urine Over Five Years After Anterior Cruciate Ligament Rupture: An Exploratory Analysis in the Knee Anterior Cruciate Ligament, Nonsurgical Versus Surgical Treatment Trial. *Arthritis & Rheumatology,* 67**,** 1816-1825.

SZCZESNIAK, A. M., GILBERT, R. W., MUKHIDA, M. & ANDERSON, G. I. 2005. Mechanical loading modulates glutamate receptor subunit expression in bone. *Bone,* 37**,** 63-73.

TAKACS, J., CARPENTER, M. G., GARLAND, S. J. & HUNT, M. A. 2013. The Role of Neuromuscular Changes in Aging and Knee Osteoarthritis on Dynamic Postural Control. *Aging and Disease,* 4**,** 84-99.

TANDOGAN, R. N., TASER, O., KAYAALP, A., TASKIRAN, E., PINAR, H., ALPARSLAN, B. & ALTURFAN, A. 2004. Analysis of meniscal and chondral lesions accompanying anterior cruciate ligament tears: relationship with age, time from injury, and level of sport. *Knee Surgery Sports Traumatology Arthroscopy,* 12**,** 262-+.

TAT, S. K., PELLETIER, J. P., LAJEUNESSE, D., FAHMI, H., DUVAL, N. & MARTEL-PELLETIER, J. 2008a. Differential modulation of RANKL isoforms by human osteoarthritic subchondral bone osteoblasts: Influence of osteotropic factors. *Bone,* 43**,** 284-291.

TAT, S. K., PELLETIER, J. P., LAJEUNESSE, D., FAHMI, H., LAVIGNE, M. & MARTEL-PELLETIER, J. 2008b. The differential expression of osteoprotegerin (OPG) and receptor activator of nuclear factor kappa B ligand (RANKL) in human osteoarthritic subchondral bone osteoblasts is an indicator of the metabolic state of these disease cells. *Clinical and Experimental Rheumatology,* 26**,** 295-304.

TAT, S. K., PELLETIER, J. P., VELASCO, C. R., PADRINES, M. & MARTEL-PELLETIER, J. 2009. New perspective in osteoarthritis: the OPG and RANKL system as a potential therapeutic target? *Keio J Med,* 58**,** 29-40.

TEICHTAHL, A., WLUKA, A. & CICUTTINI, F. M. 2003. Abnormal biomechanics: a precursor or result of knee osteoarthritis? *British Journal of Sports Medicine,* 37**,** 289-290.

TETTEH, E. S., BAJAJ, S., GHODADRA, N. S. & COLE, B. J. 2012. Basic Science and Surgical Treatment Options for Articular Cartilage Injuries of the Knee. *Journal of Orthopaedic & Sports Physical Therapy,* 42**,** 243-253.

THEOLOGIS, A. A., SCHAIRER, W. W., CARBALLIDO-GAMIO, J., MAJUMDAR, S., LI, X. & MA, C. B. 2012. Longitudinal analysis of T1rho and T2 quantitative MRI of knee cartilage laminar organization following microfracture surgery. *Knee,* 19**,** 652-7.

THOMA, L. M., MCNALLY, M. P., CHAUDHARI, A. M., BEST, T. M., FLANIGAN, D. C., SISTON, R. A. & SCHMITT, L. C. 2017. Differential knee joint loading patterns during gait for individuals with tibiofemoral and patellofemoral articular cartilage defects in the knee. *Osteoarthritis and Cartilage,* 25**,** 1046-1054.

THOMAS, R. S., CLARKE, A. R., DUANCE, V. C. & BLAIN, E. J. 2011. Effects of Wnt3A and mechanical load on cartilage chondrocyte homeostasis. *Arthritis Research & Therapy,* 13**,** 10.

TSUCHIDA, A. I., BEEKHUIZEN, M., RUTGERS, M., VAN OSCH, G., BEKKERS, J. E. J., BOT, A. G. J., GEURTS, B., DHERT, W. J. A., SARIS, D. B. F. & CREEMERS, L. B. 2012. Interleukin-6 is elevated in synovial fluid of patients with focal cartilage defects and stimulates cartilage matrix production in an in vitro regeneration model. *Arthritis Research & Therapy,* 14.

ULRICH-VINTHER, M., MALONEY, M. D., SCHWARZ, E. M., ROSIER, R. & O'KEEFE, R. J. 2003. Articular cartilage biology. *The Journal of the American Academy of Orthopaedic Surgeons,* 11**,** 421-30.

UNO, K., TAKARADA, T., HINOI, E. & YONEDA, Y. 2007. Glutamate is a determinant of cellular proliferation through modulation of nuclear factor E2 p45-related factor-2 expression in osteoblastic MC3T3-E1 cells. *J Cell Physiol,* 213**,** 105-14.

VAN DER KRAAN, P. M. & VAN DEN BERG, W. B. 2007. Osteophytes: relevance and biology. *Osteoarthritis and Cartilage,* 15**,** 237-244.

VAN ROSSOM, S., SMITH, C. R., ZEVENBERGEN, L., THELEN, D. G., VANWANSEELE, B., VAN ASSCHE, D. & JONKERS, I. 2017. Knee Cartilage Thickness, T1 rho and T2 Relaxation Time Are Related to Articular Cartilage Loading in Healthy Adults. *Plos One,* 12.

VAN SPIL, W. E., DROSSAERS-BAKKER, K. W. & LAFEBER, F. P. 2013. Associations of CTX-II with biochemical markers of bone turnover raise questions on its tissue origin: data from CHECK, a cohort study of early osteoarthritis. *Ann Rheum Dis,* 72**,** 29-36.

VANWANSEELE, B., ECKSTEIN, F., SMITH, R. M., LANGE, A. K., FOROUGHI, N., BAKER, M. K., SHNIER, R. & SINGH, M. A. F. 2010. The relationship between knee adduction moment and cartilage and meniscus morphology in women with osteoarthritis. *Osteoarthritis and Cartilage,* 18**,** 894-901.

VIKMAN, K. S., DUGGAN, A. W. & SIDDALL, P. J. 2007. Interferon-gamma induced disruption of GABAergic inhibition in the spinal dorsal horn in vivo. *Pain,* 133**,** 18-28.

WALTER, J. P., D'LIMA, D. D., COLWELL, C. W. & FREGLY, B. J. 2010. Decreased Knee Adduction Moment Does Not Guarantee Decreased Medial Contact Force during Gait. *Journal of Orthopaedic Research,* 28**,** 1348-1354.

WANG, L., WALIA, B., EVANS, J., GEWIRTZ, A. T., MERLIN, D. & SITARAMAN, S. V. 2003. IL-6 induces NF-kappa B activation in the intestinal epithelia. *J Immunol,* 171**,** 3194-201.

WANG, Y., DING, C., WLUKA, A. E., DAVIS, S., EBELING, P. R., JONES, G. & CICUTTINI, F. M. 2006. Factors affecting progression of knee cartilage defects in normal subjects over 2 years. *Rheumatology (Oxford),* 45**,** 79-84.

WATLING, D. 2014. *Development of novel methodologies to quantify, analyse and classify*

in-vivo knee function affected by aging, osteoarthritis and total knee replacement.

WATT, F. E. 2018. Osteoarthritis biomarkers: year in review. *Osteoarthritis and Cartilage,* 26**,** 312-318.

WATT, F. E., PATERSON, E., FREIDIN, A., KENNY, M., JUDGE, A., SAKLATVALA, J., WILLIAMS, A. & VINCENT, T. L. 2016. Acute Molecular Changes in Synovial Fluid Following Human Knee Injury: Association With Early Clinical Outcomes. *Arthritis & Rheumatology,* 68**,** 2129-2140.

WEN, Z. H., CHANG, Y. C. & JEAN, Y. H. 2015. Excitatory amino acid glutamate: role in peripheral nociceptive transduction and inflammation in experimental and clinical osteoarthritis. *Osteoarthritis Cartilage,* 23**,** 2009-16.

WHATLING, G. 2009. *A contribution to the clinical validation of a generic method for the*

classification of osteoarthritic and non-pathological knee function.

WIJENAYAKA, A. R., KOGAWA, M., LIM, H. P., BONEWALD, L. F., FINDLAY, D. M. & ATKINS, G. J. 2011. Sclerostin Stimulates Osteocyte Support of Osteoclast Activity by a RANKL-Dependent Pathway. *Plos One,* 6.

WOJDASIEWICZ, P., PONIATOWSKI, L. A. & SZUKIEWICZ, D. 2014. The role of inflammatory and anti-inflammatory cytokines in the pathogenesis of osteoarthritis. *Mediators of inflammation,* 2014**,** 561459-561459.

WONG, M. & CARTER, D. R. 2003. Articular cartilage functional histomorphology and mechanobiology: a research perspective. *Bone,* 33**,** 1-13.

WU, L. Z., DUAN, D. M., LIU, Y. F., GE, X., ZHOU, Z. F. & WANG, X. J. 2013. Nicotine favors osteoclastogenesis in human periodontal ligament cells co-cultured with CD4(+) T cells by upregulating IL-1beta. *Int J Mol Med,* 31**,** 938-42.

XU, L., HAYASHI, D., ROEMER, F. W., FELSON, D. T. & GUERMAZI, A. 2012. Magnetic Resonance Imaging of Subchondral Bone Marrow Lesions in Association with Osteoarthritis. *Seminars in Arthritis and Rheumatism,* 42**,** 105-118.

YAMAZAKI, M., FUKUSHIMA, H., SHIN, M., KATAGIRI, T., DOI, T., TAKAHASHI, T. & JIMI, E. 2009. Tumor necrosis factor alpha represses bone morphogenetic protein (BMP) signaling by interfering with the DNA binding of Smads through the activation of NF-kappaB. *J Biol Chem,* 284**,** 35987-95.

YANG, N. & MENG, Q. J. 2016. Circadian Clocks in Articular Cartilage and Bone: A Compass in the Sea of Matrices. *J Biol Rhythms,* 31**,** 415-27.

YOO, Y. M., KWAG, J. H., KIM, K. H. & KIM, C. H. 2014. Effects of neuropeptides and mechanical loading on bone cell resorption in vitro. *Int J Mol Sci,* 15**,** 5874-83.

YOSHITAKE, F., ITOH, S., NARITA, H., ISHIHARA, K. & EBISU, S. 2008. Interleukin-6 directly inhibits osteoclast differentiation by suppressing receptor activator of NF-kappa B signaling pathways. *Journal of Biological Chemistry,* 283**,** 11535-11540.

YUAN, G. H., MASUKO-HONGO, K., SAKATA, M., TSURUHA, J. I., ONUMA, H., NAKAMURA, H., AOKI, H., KATO, T. & NISHIOKA, K. 2001. The role of C-C chemokines and their receptors in osteoarthritis. *Arthritis and Rheumatism,* 44**,** 1056-1070.

YUAN, X. L., LIU, H. Q., HUANG, H., LIU, H., LI, L. F., YANG, J. Q., SHI, W. M., LIU, W. Y. & WU, L. H. 2016. The Key Role of Canonical Wnt/beta-catenin Signaling in Cartilage Chondrocytes. *Current Drug Targets,* 17**,** 475-484.

ZHANG, J. W. 2007. Yin and yang interplay of IFN-gamma in inflammation and autoimmune disease. *Journal of Clinical Investigation,* 117**,** 871-873.

ZHANG, L., DING, Y., RAO, G. Z. & MIAO, D. 2016. Effects of IL-10 and glucose on expression of OPG and RANKL in human periodontal ligament fibroblasts. *Brazilian Journal of Medical and Biological Research,* 49.

ZHAO, D., BANKS, S. A., MITCHELL, K. H., D'LIMA, D. D., COLWELL, C. W., JR. & FREGLY, B. J. 2007. Correlation between the knee adduction torque and medial contact force for a variety of gait patterns. *Journal of Orthopaedic Research,* 25**,** 789-797.

ZHOU, X., FRAGALA, M. S., MCELHANEY, J. E. & KUCHEL, G. A. 2010. Conceptual and methodological issues relevant to cytokine and inflammatory marker measurements in clinical research. *Curr Opin Clin Nutr Metab Care,* 13**,** 541-7.

ZHU, M., CHEN, M., ZUSCIK, M., WU, Q., WANG, Y. J., ROSIER, R. N., O'KEEFE, R. J. & CHEN, D. 2008. Inhibition of beta-catenin signaling in articular chondrocytes results in articular cartilage destruction. *Arthritis Rheum,* 58**,** 2053-64.

ZHU, M., TANG, D., WU, Q., HAO, S., CHEN, M., XIE, C., ROSIER, R. N., O'KEEFE, R. J., ZUSCIK, M. & CHEN, D. 2009. Activation of beta-catenin signaling in articular chondrocytes leads to osteoarthritis-like phenotype in adult beta-catenin conditional activation mice. *J Bone Miner Res,* 24**,** 12-21.

ZHU, Z., OTAHAL, P., WANG, B., JIN, X., LASLETT, L. L., WLUKA, A. E., ANTONY, B., HAN, W., WANG, X., WINZENBERG, T., CICUTTINI, F., JONES, G. & DING, C. 2017. Cross-sectional and longitudinal associations between serum inflammatory cytokines and knee bone marrow lesions in patients with knee osteoarthritis. *Osteoarthritis and Cartilage,* 25**,** 499-505.

Research contributions and awards

Peer-reviewed research articles:

Van Rossom, S., Khatib, N., Holt, C., Van Assche, D. and Jonkers, I. (2018). "Subjects with medial and lateral tibiofemoral articular cartilage defects do not alter compartmental loading during walking". Clinical Biomechanics 60:149-156. Doi: https://doi.org/10.1016/j.clinbiomech.2018.10.015.

Selected conference abstracts for Oral Presentation:

Khatib, N., Whatling, G., Wilson, C., Mason, D.J., Holt, C.A. (2017). "The functional characterisation of a knee focal cartilage defect cohort". Podium presentation. International Society of Biomechanics, Brisbane, Australia.

Khatib, N., Papageorgiou, A., Fairhurst, S., Holt, C.A., Mason, D.J. (2017). "Biological profiling of early and severe osteoarthritic knee synovial fluid" Podium presentation. International Cartilage Repair Society, Gothenburg, Sweden.

Khatib, N., Biggs, P., Wilson, C., Williams., R., Holt, C.A., Mason, D.J. (2019) "Dynamic medial knee overloading influences inflammation and bone remodelling in the degenerative knee" Podium presentation. Orthopaedic Research Society International, Texas, USA.

Prizes:

2017: Travel Bursary Award (£1000 towards international conference) towards presenting winning abstract at the International Society of Biomechanics conference in Brisbane, Australia

2016: Runner-up Best podium presentation in the free paper sessions (€250 cash prize), International Cartilage Repair Society (ICRS) conference, Gothenburg, Sweden.

2014: Arthritis Research UK Bursary Prize (£500 towards conference registration fee) for notable accepted abstract at the Medical Engineering Centres Annual Meeting and Bioengineering (MECbioEng) 2014, London, UK

Appendix A

7.1 Disease cohort demographics and clinical factors

Subject Type	Patient codes	Sex	Age	BMI	Outerbridge grade	KL grade	Compartment affected	Static Knee alignment	Pivot-shift (ACL-laxity)	Meniscal damage	ACL damage
FCD	AH	Male	48	24.7	2	n/a	medial	normal	equal	medial tear	normal
FCD	DL	Female	67	25.4	2	n/a	lateral	normal	equal	normal	normal
FCD	FA	Male	35	27.6	2	n/a	lateral	normal	equal	lateral tear	normal
FCD	JBH	Male	24	27.9	2	n/a	lateral	normal	equal	lateral partial removal	normal
FCD	JD	Male	20	24.5	2	n/a	lateral	normal	+Glide	lateral tear	intact, but lax
FCD	KM	Male	33	36.9	2	n/a	lateral	normal	equal	lateral tear	normal
FCD	LP	Male	46	23.1	2	n/a	medial	normal	+Glide	medial tear	torn
FCD	MT	Male	75	26	2	n/a	medial	normal	equal	50% medial transected	normal
FCD	RP	Male	46	34.6	2	n/a	lateral	normal	equal	lateral tear	normal
FCD	SA	Male	43	26.8	2	n/a	medial	normal	equal	normal	normal
FCD	TR	Male	31	22.8	2	n/a	medial	normal	+Glide	medial partial removal	torn
OA	15	Male	57	33.6	n/a	3	medial	5° varus			
OA	16	Male	48	25.2	n/a	3	medial	15.4° varus			
OA	505	Male	48	30.8	n/a	3	medial	4.6° varus			
OA	700	Male	44	32	n/a	4	medial	11.6° varus			
OA	742	Male	46	23.6	n/a	3	medial	4.7° varus			
OA	975	Male	61	25.2	n/a	2	medial	7.2° varus			
OA	1271	Male	48	30.8	n/a	2	medial	1.9° varus			
OA	1300	Female	56	24.4	n/a	3	medial				
OA	2219	Male	57	25.1	n/a	3	medial				
OA	2234	Female	49	30.5	n/a	3	medial				
OA	2293	Female	53	26	n/a	3	medial				

7.2 Knee Osteoarthritis Outcome Survey Scores

Subject Type	Patient codes	KOOS Pain (t1)	KOOS Pain (t2)	KOOS Symptoms (t1)	KOOS Symptoms (t2)	KOOS Function (t1)	KOOS Function (t2)
FCD	AH	72.2	91.7	71.4	75	79.4	97.1
FCD	DL	66.7		78.6		79.4	
FCD	FA	72.2		60.7		89.7	
FCD	JBH	61.1	100	64.3	96.4	63.2	100
FCD	JD	86.1	97.2	78.6	89.3	94.1	95.6
FCD	KM	38.9		42.9		39.7	
FCD	LP	61.1		53.6		70.6	
FCD	MT	52.8	63.9	67.9	85.7	41.2	72.1
FCD	RP	100	88.9	75	67.9	85.3	79.4
FCD	SA	80.6	94.4	82.1	96.4	88.2	97.1
FCD	TR	63.9		21.4		41.2	
OA	15	86.1		71.4		77.9	
OA	16	94.4		85.7		95.6	
OA	505	72.2		53.6		88.2	
OA	700	72.2		64.3		77.9	
OA	742	80.6		96.4		98.5	
OA	975						
OA	1271	94.4		92.9		98.5	
OA	1300						
OA	2219						
OA	2234						
OA	2293						

Appendix B

7.3 ARUK Patient Consent Form (Motion Analysis)

Assessment of joint function in patients with joint problems using three-dimensional motion analysis techniques

Study Number
Patient Identification Number for this research:

You DO NOT have to sign this document. Please DO NOT sign this document unless you fully understand it. If there is ANYTHING which you do not understand please do not hesitate to ask for a full explanation.

To confirm agreement with each of the statements below, please initial each box and delete where applicable:

1. I confirm that I have read and understand the information sheet dated 14 April 2017 (Version 10.2) for the above study and have had the opportunity to ask questions. ☐

2. I understand that my participation in the study is voluntary and that I am free to withdraw at any time, without giving any reason, and without my medical care or legal rights being affected but any data collected up to the point of my withdrawal will be kept. ☐

3. I understand that my details will be linked to a unique identifier to allow you to follow me through course of the study ☐

4. You may / may not (please delete as appropriate) contact me in the future to ask if I would be interested in participating in a future research project/survey ☐

5. I do / do not (please delete as appropriate) agree for you to share my anonymised data with external collaborators in the UK and abroad, including commercial companies ☐

6. I agree to you accessing appropriate related medical information (such as radiological images) for the purposes of this study. ☐

7. I agree for you to video my movements on a video-camera. I understand that if the video is used for research presentations that my anonymity will be ensured using digital masking. ☐

8. I agree to my GP being informed of my participation in the study. ☐

9.- I agree to take part in the above study. ☐

Name of Patient: _____
(Please print)

Signature: _____ Date: _____

I confirm that I have fully explained the experimental protocol and purpose of the study

Name of Researcher: _____

Signature: _____ Date: _____

Name of person taking consent: _____
(If different from researcher)

Signature: _____ Date: _____

GP Details

GP Name:

GP Address:

GP Telephone Number:

7.4 ARUK Patient Consent Form (Samples)

The collection, storage and analysis of Clinical Waste, Blood & Urine Samples

PATIENT CONSENT FORM

You DO NOT have to sign this document. Please DO NOT sign this document unless you fully understand it. If there is ANYTHING which you do not understand please do not hesitate to ask for a full explanation.

To confirm agreement with each of the statements below, please initial each box and delete where applicable:

1. I confirm that I have read and understand the information sheet dated 30 Novembe 2016 (Version 10.1) for the above study and have had the opportunity to ask questions ☐

2. I understand that my participation in the study is voluntary and that I am free t withdraw at any time, without giving any reason, and without my medical care or lega rights being affected. ☐

3. I understand that my details will be linked to a unique identifier to allow you to follo me through course of the study ☐

4. I do / do not (please delete as appropriate) give permission for up to a 40 ml (teaspoons) sample of my bloo to be collected. ☐

5. I do / do not (please delete as appropriate) give permission for one or more sample of my urine to be collected ☐

6. I do / do not (please delete as appropriate) give permission for my clinical wast collected during surgery to be collected ☐

7. I understand that researchers from other organisations in the UK and abroad including commercial companies, may access my samples, that research may take man years and the information gained will not benefit me or my family directly. ☐

8. I do / do not (please delete as appropriate) give permission for genetic analysis to be carried out using my samples ☐

☐

9. I would / would not (please delete as appropriate) like to be contacted if genetic information is found that may have implications for me or my family.

10. I understand I can withdraw my consent for the storage and future use of my samples at any point and that any unused samples will be destroyed immediately. I understand that any samples used in research prior to the withdrawal of consent may not be destroyed until the end of the study. ☐

11. You may / may not (please delete as appropriate) contact me in the future to ask if I would be interested in participating in a follow up study. ☐

12. I give permission for my consent to cover the collection of any additional samples over the next 2 years for this study and I understand that by signing this form I am not obliged to give these additional samples. ☐

13. I agree to my GP being contacted ☐

14. I understand that you may access my Medical notes. ☐

15. I agree to take part in the above study. ☐

Name of Patient: _____

Signature: _____ Date: _____

I confirm that I have fully explained the experimental protocol and purpose of the study

Name of person taking consent: _____
(If different from researcher)

Signature: _____ Date: _____

GP Details

GP Name:

GP Address:

7.5 Healthy Volunteer Consent Form (Motion analysis)

Assessment of joint function in healthy volunteers using three dimensional motion analysis techniques

Study Number:
Volunteer Identification Number for this trial:

You DO NOT have to sign this document. Please DO NOT sign this document unless you fully understand it. If there is ANYTHING which you do not understand please do not hesitate to ask for a full explanation.

To confirm agreement with each of the statements below, please initial the box and amend as necessary:

1. I confirm that I have read and understand the information sheet dated 14 April 2017 (Version 10.2) for the above study and have had the opportunity to ask questions. ☐

2. I understand that my participation in the study is voluntary and that I am free to withdraw at any time, without giving any reason, and without my legal rights being affected but any data collected up to the point of my withdrawal will be kept. ☐

3. I understand that my details will be linked to a unique identifier to allow you to follow me through course of the study ☐

4. You may / may not (please delete as appropriate) contact me in the future to ask if I would be interested in participating in a future research project/survey ☐

5. I do / do not (please delete as appropriate) agree for you to share anonymised data with external collaborators in the UK and aboard, including commercial companies.. ☐

6. I agree for you to video my movements on a video-camera. I understand that if the video is used for research presentations that my anonymity will be ensured using digital masking. ☐

7. I agree to my GP being contacted ☐

8. I agree to take part in the above study. ☐

Name of Volunteer: _____

Signature: _____ Date: _____

I confirm that I have fully explained the experimental protocol and purpose of the study

Name of Researcher: _____

Signature: _____ Date: _____

Name of person taking consent: _____
(If different from researcher)

Signature: _____ Date: _____

GP Details

GP Name:

GP Address:

GP Telephone Number:

Original Centre file, 1 copy for the volunteer, 1 copy for the researcher

7.6 Healthy Volunteer Consent Form (Samples)

The collection, storage and analysis of blood and urine samples

Study Number:

Participant Identification Number for this trial:

You DO NOT have to sign this document. Please DO NOT sign this document unless you fully understand it. If there is ANYTHING which you do not understand please do not hesitate to ask for a full explanation.

To confirm agreement with each of the statements below, please initial each box and delete where applicable:

1. I confirm that I have read and understand the information sheet dated 30 November 2016 (Version 10.1) for the above study and have had the opportunity to ask questions ☐

2. I understand that my participation in the study is voluntary and that I am free to withdraw at any time, without giving any reason, and without my legal rights being affected. ☐

3. I understand that my details will be linked to a unique identifier to allow you to follow me through course of the study ☐

4. I do / do not (please delete as appropriate) give permission for up to a 40 ml (8 teaspoons) sample of my blood to be collected. ☐

5. I do / do not (please delete as appropriate) give permission for one or more samples of my urine to be collected. ☐

6. I understand that researchers from other organisations in the UK and abroad, including commercial companies, may access my samples, that research may take many years and the information gained will not benefit me or my family directly. ☐

7. I do / do not (please delete as appropriate) give permission for genetic analysis to be carried out using my samples ☐

8. I would / would not (please delete as appropriate) like to be contacted if genetic information is found that may have implications for me or my family. ☐

9. I do / do not (please delete as appropriate) give permission for my samples to be stored and used in future research in the UK and abroad, including use by commercial companies ☐

10. I understand I can withdraw my consent for the storage and future use of my samples at any point and that any unused samples will be destroyed immediately. I understand that any samples used in research prior to the withdrawal of consent may not be destroyed until the end of the study. ☐

11. You may / may not (please delete as appropriate) contact me in the future to ask if I would be interested in participating in a future research project/survey. Yes ☐

12. I give permission for my consent to cover the collection of any additional samples over the next 2 years for this study and I understand that by signing this form I am not obliged to give these additional samples. ☐

13. I do agree to my GP being contacted. ☐

14. I agree to take part in the above study. ☐

Name of Particpant:_____

Signature: _____ Date: _____

I confirm that I have fully explained the experimental protocol and purpose of the study

Name of Researcher: _____

Signature: _____ Date: _____

Name of person taking consent: _____
(If different from researcher)

Signature: _____ Date: _____

Appendix C

7.7 Knee Osteoarthritis Outcome Survey

KOOS KNEE SURVEY

Today's date: _____/_____/_____ Date of birth: _____/_____/_____

Name: _____

INSTRUCTIONS: This survey asks for your view about your knee. This information will help us keep track of how you feel about your knee and how well you are able to perform your usual activities.
Answer every question by ticking the appropriate box, only one box for each question. If you are unsure about how to answer a question, please give the best answer you can.

Symptoms
These questions should be answered thinking of your knee symptoms during the **last week**.

S1. Do you have swelling in your knee?

Never	Rarely	Sometimes	Often	Always
☐	☐	☐	☐	☐

S2. Do you feel grinding, hear clicking or any other type of noise when your knee moves?

Never	Rarely	Sometimes	Often	Always
☐	☐	☐	☐	☐

S3. Does your knee catch or hang up when moving?

Never	Rarely	Sometimes	Often	Always
☐	☐	☐	☐	☐

S4. Can you straighten your knee fully?

Always	Often	Sometimes	Rarely	Never
☐	☐	☐	☐	☐

S5. Can you bend your knee fully?

Always	Often	Sometimes	Rarely	Never
☐	☐	☐	☐	☐

Stiffness
The following questions concern the amount of joint stiffness you have experienced during the **last week** in your knee. Stiffness is a sensation of restriction or slowness in the ease with which you move your knee joint.

S6. How severe is your knee joint stiffness after first wakening in the morning?

None	Mild	Moderate	Severe	Extreme
☐	☐	☐	☐	☐

S7. How severe is your knee stiffness after sitting, lying or resting **later in the day**?

None	Mild	Moderate	Severe	Extreme
☐	☐	☐	☐	☐

Pain

P1. How often do you experience knee pain?

Never	Monthly	Weekly	Daily	Always
☐	☐	☐	☐	☐

What amount of knee pain have you experienced the **last week** during the following activities?

P2. Twisting/pivoting on your knee

None	Mild	Moderate	Severe	Extreme
☐	☐	☐	☐	☐

P3. Straightening knee fully

None	Mild	Moderate	Severe	Extreme
☐	☐	☐	☐	☐

P4. Bending knee fully

None	Mild	Moderate	Severe	Extreme
☐	☐	☐	☐	☐

P5. Walking on flat surface

None	Mild	Moderate	Severe	Extreme
☐	☐	☐	☐	☐

P6. Going up or down stairs

None	Mild	Moderate	Severe	Extreme
☐	☐	☐	☐	☐

P7. At night while in bed

None	Mild	Moderate	Severe	Extreme
☐	☐	☐	☐	☐

P8. Sitting or lying

None	Mild	Moderate	Severe	Extreme
☐	☐	☐	☐	☐

P9. Standing upright

None	Mild	Moderate	Severe	Extreme
☐	☐	☐	☐	☐

Function, daily living

The following questions concern your physical function. By this we mean your ability to move around and to look after yourself. For each of the following activities please indicate the degree of difficulty you have experienced in the **last week** due to your knee.

A1. Descending stairs

None	Mild	Moderate	Severe	Extreme
☐	☐	☐	☐	☐

A2. Ascending stairs

None	Mild	Moderate	Severe	Extreme
☐	☐	☐	☐	☐

For each of the following activities please indicate the degree of difficulty you have experienced in the **last week** due to your knee.

A3. Rising from sitting

None	Mild	Moderate	Severe	Extreme
☐	☐	☐	☐	☐

A4. Standing

None	Mild	Moderate	Severe	Extreme
☐	☐	☐	☐	☐

A5. Bending to floor/pick up an object

None	Mild	Moderate	Severe	Extreme
☐	☐	☐	☐	☐

A6. Walking on flat surface

None	Mild	Moderate	Severe	Extreme
☐	☐	☐	☐	☐

A7. Getting in/out of car

None	Mild	Moderate	Severe	Extreme
☐	☐	☐	☐	☐

A8. Going shopping

None	Mild	Moderate	Severe	Extreme
☐	☐	☐	☐	☐

A9. Putting on socks/stockings

None	Mild	Moderate	Severe	Extreme
☐	☐	☐	☐	☐

A10. Rising from bed

None	Mild	Moderate	Severe	Extreme
☐	☐	☐	☐	☐

A11. Taking off socks/stockings

None	Mild	Moderate	Severe	Extreme
☐	☐	☐	☐	☐

A12. Lying in bed (turning over, maintaining knee position)

None	Mild	Moderate	Severe	Extreme
☐	☐	☐	☐	☐

A13. Getting in/out of bath

None	Mild	Moderate	Severe	Extreme
☐	☐	☐	☐	☐

A14. Sitting

None	Mild	Moderate	Severe	Extreme
☐	☐	☐	☐	☐

A15. Getting on/off toilet

None	Mild	Moderate	Severe	Extreme
☐	☐	☐	☐	☐

For each of the following activities please indicate the degree of difficulty you have experienced in the **last week** due to your knee.

A16. Heavy domestic duties (moving heavy boxes, scrubbing floors, etc)

None	Mild	Moderate	Severe	Extreme
☐	☐	☐	☐	☐

A17. Light domestic duties (cooking, dusting, etc)

None	Mild	Moderate	Severe	Extreme
☐	☐	☐	☐	☐

Function, sports and recreational activities

The following questions concern your physical function when being active on a higher level. The questions should be answered thinking of what degree of difficulty you have experienced during the **last week** due to your knee.

SP1. Squatting

None	Mild	Moderate	Severe	Extreme
☐	☐	☐	☐	☐

SP2. Running

None	Mild	Moderate	Severe	Extreme
☐	☐	☐	☐	☐

SP3. Jumping

None	Mild	Moderate	Severe	Extreme
☐	☐	☐	☐	☐

SP4. Twisting/pivoting on your injured knee

None	Mild	Moderate	Severe	Extreme
☐	☐	☐	☐	☐

SP5. Kneeling

None	Mild	Moderate	Severe	Extreme
☐	☐	☐	☐	☐

Quality of Life

Q1. How often are you aware of your knee problem?

Never	Monthly	Weekly	Daily	Constantly
☐	☐	☐	☐	☐

Q2. Have you modified your life style to avoid potentially damaging activities to your knee?

Not at all	Mildly	Moderately	Severely	Totally
☐	☐	☐	☐	☐

Q3. How much are you troubled with lack of confidence in your knee?

Not at all	Mildly	Moderately	Severely	Extremely
☐	☐	☐	☐	☐

Q4. In general, how much difficulty do you have with your knee?

None	Mild	Moderate	Severe	Extreme
☐	☐	☐	☐	☐

Thank you very much for completing all the questions in this questionnaire.